Spatial organisation of the cells in the mammalian lens epithelium and its role in lens growth

WU, WEIJU

Spatial organisation of the cells in the mammalian lens epithelium and its role in lens growth

Weiju Wu

A thesis submitted to the university of Durham for the degree of Doctor of Philosophy

Department of Biological and Biomedical Sciences

University of Durham, January 2012

Table of Contents

1 Introduction 1

1.1 Lens embryology 2

1.1.1 Lens induction 2

1.1.2 Secondary fibre formation 5

1.2 Lens epithelial cell proliferation 6

1.2.1 Lens epithelium partition 6

1.2.1.1 Central zone (CZ) 6

1.2.1.2 Germinative zone (GZ) 8

1.2.1.3 Transitional zone (TZ) 9

1.2.2 Lens epithelial cell proliferation 10

1.2.2.1 Lens epithelial cell proliferation in the CZ 10

1.2.2.2 Lens epithelial cell proliferation in the GZ 11

1.2.3 Stem cells in the lens epithelium 12

1.2.3.1 Stem cell properties 12

1.2.3.2 Stem cell detection 13

1.2.3.3 Stem cells in the lens epithelium 13

1.3 Lens fibre cell differentiation 15

1.3.1 Fibre cell organisation and morphology during differentiation 15

1.3.2 Fibre cell organelle degradation during terminal differentiation 16

1.3.3 The expression of fibre-cell specific proteins during differentiation 18

1.4 Regulation of lens epithelial cell proliferation and differentiation 19

1.4.1 Growth factors 19

1.4.1.1 Fibroblast growth factors (FGFs) 19

1.4.1.2 Other growth factors 22

1.4.2 Downstream signalling pathways 24

1.4.2.1 Ras/Raf/MEK/MAPK pathway 24

1.4.2.2 PI3-K/AKT pathway 27
1.5 Lens ageing 28
1.5.1 Lens growth 28
1.5.1.1 Lens weight 28
1.5.1.2 Lens dimensions 29
1.5.2 Compaction 31
1.5.2.1 Water loss 31
1.5.2.2 Lens refractive index gradient 32
1.5.3 Lens stiffness 33
1.5.4 Presbyopia 34
1.6 Lens pathology: cataract 35
1.6.1 Cataract classification 35
1.6.2 Age-related cataract 36
1.6.2.1 Causes 36
1.6.2.2 Pathogenesis 37
1.6.2.2.1 Increased protein damage and loss of chaperone activity 37
1.6.2.2.2 Development of lens barrier and increasing oxidation in the nucleus 38
1.6.2.2.3 UV filter changes with age 38
1.6.2.3 Signs and symptoms 39
1.6.2.4 Treatment 40
1.7 Summary 41
2 Spatial organisation of the cells in the mammalian lens epithelium 43
2.1 Introduction 43
2.1.1 Lens epithelial cell proliferation 43
2.1.2 Lens epithelial cell apoptosis 44
2.1.3 Lens epithelial cell density 45
2.1.4 Lens epithelial cell morphology and size 48
2.1.5 Lens epithelial cell polarity 50
2.2 Aims 51
2.3 Materials and methods 52
2.3.1 Eye lens materials 52
2.3.2 Eye lens dissection 53

2.3.3 Immunofluorescence microscopy 53
2.3.3.1 Antibodies 53
2.3.3.2 Immunofluorescence microscopy 55
2.3.3.3 Cell profile determination 55
2.3.3.4 Detection of apoptotic cells.....56
2.3.3.4.1 Annexin-V-affinity assay.....56
2.3.3.4.2 TUNEL assay.....57
2.3.4 Data analysis 57
2.3.4.1 Calculation of lens epithelial cell density 57
2.3.4.2 Calculation of the total lens epithelial cell number.....61
2.3.4.3 Calculation of the total proliferating epithelial cell number 64
2.3.4.4 Calculation of the number of the meridional lines in the TZ.....66
2.3.4.5 Analysing the influence of delivery time on the human lens epithelial cell apoptosis.....67
2.3.4.6 Human lens epithelial cell apoptosis change with age.....67
2.3.4.7 Measurements of the lens epithelial cell height, cross-sectional area and volume.....67
2.3.4.8 Measurement of the lens epithelial cell nuclear volume.....68
2.4 Results.....69
2.4.1 Lens epithelial cell turnover.....69
2.4.1.1 Lens epithelial cell proliferation 69
2.4.1.1.1 Lens epithelial cell proliferation in the GZ.....69
2.4.1.1.2 Lens epithelial cell proliferation in the CZ.....71
2.4.1.2 Lens epithelial cell apoptosis 87
2.4.1.2.1 Lens epithelial cell apoptosis analysed by Annexin-V-Fluorescein.....87
2.4.1.2.2 Lens epithelial cell apoptosis analysed by TUNEL assay 89
2.4.1.2.2.1 Cell apoptosis in the bovine, mouse and rat lens epithelia.....89
2.4.1.2.2.2 Cell apoptosis in the human lens epithelium.....93
2.4.1.3 Lens epithelium homeostasis 99
2.4.2 Lens epithelial cell density.....100
2.4.2.1 Lens epithelial cell density in different mammals 100
2.4.2.2 Human lens epithelial cell density changes with age.....106
2.4.2.3 Difference of lens epithelial cell density in males and females.....108
2.4.3 Lens epithelial cell morphology and size.....110

2.4.3.1 Changes of lens epithelial cell morphology and size in different mammals 110
2.4.3.2 Changes of human lens epithelial cell size with age....121
2.4.3.3 Changes of human lens cell morphology in the capsular bags with IOLs 124
2.4.3.4 Changes of nuclear morphology and volume in the bovine and human lens epithelial cells 131
2.4.4 Lens epithelial cell centrosome....134
2.4.4.1 Loss of γ-tubulin and pericentin and the cytoskeleton change of the epithelial cells in the further half of the meridional lines 134
2.4.4.2 Cell centrosome in the human donor capsular bags with IOLs 144
2.5 Discussion 146
2.5.1 Lens epithelial cell proliferation 146
2.5.1.1 The lens epithelial cell proliferation in the GZ 146
2.5.1.2 Are there stem cells in the lens epithelium?....148
2.5.2 Lens epithelial cell apoptosis 149
2.5.3 Homeostasis of the lens epithelium 152
2.5.4 Cell density change across the lens epithelium....154
2.5.5 Changes of cell morphology and size across the lens epithelium....156
2.5.5.1 The consistency of the epithelial cell morphology and size change in different mammalian lenses 156
2.5.5.2 Lens epithelial cell nuclear volume change 157
2.5.6 Lens epithelial cell centrosome....158
2.5.7 The cells in the periphery of the human capsular bags with IOLs retain many characteristics of the epithelial cell organisation 161
2.6 Summary 162
3 FGF-2 and perlecan distribution in the inner surface of the bovine lens capsule and the capsule structure 163
3.1 Introduction....163
3.2 Aims 164
3.3 Materials and methods 164
3.3.1 The lens capsules 164

3.3.2 Lens capsule cleaning 165
3.3.3 Lens capsule fixing 167
3.3.4 Immunogold labelling 169
3.3.5 SEM 169
3.3.5.1 Specimen preparation for SEM 169
3.3.5.1.1 Specimen post-fixation and dehydration 169
3.3.5.1.2 Specimen drying 169
3.3.5.1.3 Specimen coating for conductivity 170
3.3.5.1.4 Specimen imaging 170
3.4 Results 173
3.4.1 FGF-2 and perlecan had a gradient distribution on the inner surface of the bovine lens capsule 173
3.4.2 The morphology was different on the two surfaces of the lens capsule 178
3.5 Discussion 184
3.6 Summary 186
4 Regulation of lens epithelial cell proliferation by MAPK signalling pathways 187
4.1 Introduction 187
4.2 Aims 189
4.3 Materials and methods 190
4.3.1 Protein extraction 190
4.3.2 SDS- polyacrylamide gel electrophoresis (SDS-PAGE) and immunoblotting 193
4.3.3 Immunofluorescence 195
4.3.3.1 FGF-2 treatment 195
4.3.3.2 Immunofluorescence 196
4.4 Results 197
4.4.1 The levels of phosphorylated MAPK and PI3-K signalling proteins were higher in the GZ+TZ than in the CZ of the bovine lens epithelium 197
4.4.2 FGF-2 increased the phosphorylated ERK1/2 level and cell proliferation index 201
4.4.3 Phosphorylated ERK1/2 was associated with spindle poles and the spindle during the M phase of the cell cycle 209

4.5 Discussion 214
4.5.1 The levels of phosphorylated MAPK and PI3-K signalling proteins are consistent with the FGF-2 gradient 214
4.5.2 FGF-2 initiates cell proliferation by activating ERK1/2 215
4.5.3 Phosphorylated ERK1/2 was correlative with the spindle formation in the M phase 216
4.6 Summary 217
5 Conclusions and future experiments 219
5.1 Summary of this study's main results 219
5.2 Cell organisation in the mammalian lens epithelium is specific to their functions 224
5.3 Ageing, cataract and PCO influences cell organisation in the mammalian lens epithelium 225
5.4 A Single model could explain the cell organisation in the mammalian lens epithelium 226
5.5 Future work 226
6 References 229

List of Figures

Figure 1.1 Schematic diagrams of the lens induction and secondary fibre cell formation.....3
Figure 1.2 A diagram of the lens epithelium partition.....7
Figure 1.3 FGF-2 passes through the lens capsule and activates MAPK and PI3-K signalling pathways inside the epithelial cells.....21
Figure 2.1. Calculation of the lens epithelial cell density.....59
Figure 2.2. Calculation of the total lens epithelial cell number.....62
Figure 2.3. Calculation of the total proliferating cell number in the lens epithelium..65
Figure 2.4. Calculation of the meridional line number in the TZ of the lens epithelium. 66
Figure 2.5. Cell proliferation in the GZ of the bovine lens epithelium.....72
Figure 2.6. Cell proliferation in the CZ of the bovine lens epithelium.....74
Figure 2.7. Cells proliferated in the GZ of the rabbit lens epithelium.....75
Figure 2.8. Cell proliferation in the CZ of the rabbit lens epithelium.....77
Figure 2.9. Cell proliferation in the GZ and the CZ of the rat lens epithelium.....79
Figure 2.10. Cell proliferation in the GZ of the human lens epithelium.....81
Figure 2.11. The proliferating cells in the GZ of the human lens epithelium are in different phases of the cell cycle.....83
Figure 2.12. Cell proliferation in the human lens capsular bag implanted with an IOL. 85
Figure 2.13. The Annexin-V-Fluorescein staining of the bovine lens epithelial cells.88
Figure 2.14. Cell apoptosis in the bovine lens epithelium.....90
Figure 2.15. Cell apoptosis in the mouse lens epithelium.....91
Figure 2.16. Cell apoptosis in the rat lens epithelium.....92
Figure 2.17. Morphological changes of the apoptotic nuclei in the human lens epithelium.....95
Figure 2.18. The negative and positive controls of the TUNEL assay performed on the human lens epithelial cells.....97
Figure 2.19. Cell apoptosis in a human lens capsular bag implanted with an IOL.....98
Figure 2.20. Epithelial cell density in different mammalian lenses.....101

Figure 2.21. The cell density change in the periphery of the bovine lens epithelium. 103
Figure 2.22. Nucleus arrangement in the TZ of the lens epithelium of different mammals. 104
Figure 2.23. The changes of the human lens cell density with age. 107
Figure 2.24. Difference of the lens epithelial cell density in women and men. 109
Figure 2.25. The changes of the cell cross-sectional area and height across the bovine lens epithelium. 111
Figure 2.26. The changes of the cell cross-sectional area and height across the mouse and rat lens epithelia. 113
Figure 2.27. The changes of the cell cross-sectional area across the rabbit lens epithelium. 115
Figure 2.28. The changes of cell cross-sectional area and cell height in the human lens epithelium. 116
Figure 2.29. The changes of cell height in the bovine lens epithelium. 117
Figure 2.30. The changes of the cell height and cross-sectional area across the bovine lens epithelium. 119
Figure 2.31. The changes of cell volume and density across the bovine lens epithelium. 120
Figure 2.32. The changes of cell height, cross-sectional area and volume across the lens epithelia of different ages of people. 122
Figure 2.33. The multilayer of elongated cells along the rhexis of the human donor capsular bag. 125
Figure 2.34. The cells on the anterior capsular bag. 127
Figure 2.35. The cells at the equator and on the posterior lens capsular bag. 129
Figure 2.36. The changes of nuclear volume across the bovine lens epithelium. 132
Figure 2.37. The changes of nuclear volume across the human lens epithelium. 133
Figure 2.38. The location of γ-tubulin in the bovine lens epithelial cells. 136
Figure 2.39. The location of γ-tubulin and ZO-1 in the bovine lens epithelial cells. 138
Figure 2.40. The γ-tubulin structure in the peripheral TZ of the bovine lens epithelium. 139
Figure 2.41. The location of γ-tubulin in the human lens epithelial cells. 140
Figure 2.42. The γ-tubulin staining in the meridional lines of the human lens epithelium. 141

Figure 2.43. The α-tubulin structure changes with the loss of γ-tubulin in the further half of the meridional lines in the bovine lens epithelium.....142
Figure 2.44. The F-actin structure changes with the loss of pericentrin in the further half of the meridional lines in the human lens epithelium.....143
Figure 2.45. The γ-tubulin staining in the human donor lens capsular bag. 145
Figure 2.46. Morphological characteristics of the modiolus. 160
Figure 3.1. The structural changes in the inner surface of the bovine lens capsule with different kinds of cleaning. 166
Figure 3.2. The SEM images of the inner surface of the bovine lens capsule fixed with glutaraldehyde and PFA. 168
Figure 3.3. A montage of the lens capsule prepared for SEM. 172
Figure 3.4. The collagen IV distribution in the inner surface of the bovine lens capsule. 174
Figure 3.5. The distribution of matrix-bounded FGF-2 and perlecan in the inner surface of the bovine lens capsule. 176
Figure 3.6. The bovine lens capsule morphology in the cross-sectional side. 179
Figure 3.7. The SEM images of the inner and outer surfaces of the bovine lens capsule. 180
Figure 3.8. The SEM images of the inner and outer surfaces of the human lens capsule. 182
Figure 4.1. The pictures showing the cutting line between the CZ and the GZ+TZ zones of the bovine lens epithelium.....191
Figure 4.2. The expression of MAPK and PI3K/Akt signalling proteins in the central and peripheral regions of the bovine lens epithelium. 198
Figure 4.3. The phosphorylated ERK1/2 staining is only present in the proliferating bovine lens epithelial cells in the M phase. 200
Figure 4.4. The changes of the total and phosphorylated ERK1/2 levels in the bovine lens epithelial cells with or without FGF-2 treatment. 203
Figure 4.5. Representative immunoblotting results of primary bovine lens epithelial cells exposed to FGF-2 and/or U0126. 204
Figure 4.6. Representative immunoblotting results of FHL124 cells exposed to FGF-2 and/or U0126. 205
Figure 4.7. Cell proliferation in the bovine lens epithelium with or without the presence of FGF-2 and U0126.....205

Figure 4.8. Association of phosphorylated ERK1/2 with the spindle poles and the spindle in the cells in the M phase. 210
Figure 4.9. Colocalisation of phosphorylated ERK1/2 with γ-tubulin at the centrosomes in the cells in the M phase. 212
Figure 5.1 The summary diagram of this thesis's main results. 223

List of Tables

Table 1.1. The GZ length in different ages of rats and mice 8
Table 2.1 Human lens epithelial cell density in the normal and cataractous lenses 47
Table 2.2. Epithelial cell size in different species of lenses.....49
Table 2.3. Primary antibodies used for immunofluorescence.....54
Table 2.4. Secondary antibodies used for immunofluorescence.....54
Table 2.5. Characteristics of the lens epithelium whole-mounts in different species (mean ± SD).....70
Table 2.6. Cell proliferation in the CZ of the different mammalian lens epithelia.....71
Table 2.7. TUNEL-positive cell numbers in the fixed-immediately group and fixed-later group.....93
Table 2.8. The TUNEL-positive epithelial cell number in each human lens.....94
Table 2.9. Numbers of the proliferating cells, apoptotic cells and meridional lines....99
Table 2.10. Cell density and proliferation index with respect to age.....100
Table 2.11. The *p* values of Student's t-Test in the comparison of cell density in the lens periphery of the four human age groups 106
Table 4.1. List of the solutions used in making SDS-PAGE gels.....194
Table 4.2. Primary antibodies used for immunoblotting and immunofluorescence ..195
Table 4.3. The *p* values of χ^2 test in the comparisons of proliferation indexes of the primary bovine lens epithelial cells treated with FGF-2 and/or U0126 202

List of abbreviation

^{3}H-thymidine: tritiated thymidine

3OHKG: 3-hydroxykynurenine O-β-d-glucoside

AKT: protein kinase identified in the AKT virus. AK was a temporary classification name for a mouse strain developing spontaneous thymic lymphomas. The "t" stands for “transforming”

APS: ammonium persulphate

AQP0: aquaporin 0

BFSP: beaded filament structural protein

BMP: bone morphogenetic protein

BrdU: bromodeoxyuridine

BSA: bovine serum albumin

CP115: cytoskeletal protein 115

CP49: cytoskeletal protein 49

CREB: cAMP-responsive element binding protein

CZ: central zone

DAPI: 4,6-diamidino-2-phenylindole

DMEM: Dulbecco’s modified Eagle’s medium

ECCE: extracapsular cataract extraction

ECL: enhanced chemiluminescence

ECM: extracellular matrix

EDTA: ethylene diamine tetra acetate

EGF: epidermal growth factor

EGFR: epidermal growth factor receptor

EMT: epithelial-mesenchymal transition

ERK: extracellular signal-regulated kinase

FACS: fluorescence-activated cell sorting

FCS: feotal calf serum

FGF: fibroblast growth factor

FGFR: fibroblast growth factor receptor

FITC: fluorescein isothiocyanate

GAG: glycosaminoglycan

GDP: guanosine diphosphate

GSH: glutathione

GSK: glycogen synthase kinase

GTP: guanosine triphosphate

GZ: germinative zone

HGF: hepatocyte growth factor

HRP: horseradish peroxidase

HS: heparan sulphate

HSPG: heparan sulphate proteoglycan

IF: immunofluorescence

Ig: immunoglogulin

IGF-1: Insulin growth factor 1

IL-1: interleukin 1

IOL: intraocular lens

JNK: c-Jun N-terminal kinase

LDL: low-density lipoprotein

LOCS: lens opacities classification system

LRC: label-retaining cell

MAPK: mitogen-activated protein kinase

MAPKK: mitogen-activated protein kinase kinase

MAPKKK: mitogen-activated protein kinase kinase kinase

MK: MAPK-activated protein kinase

MMP: matrix metalloproteinase

MP20: membrane protein 20

MSK: mitogen and stress activated kinase

MTOC: microtubule organising centre

mTOR: mammalian target of rapamycin

NADPH: nicotinamide adenine dinucleotide phosphate

Nd-YAG: neodymium-yttrium-aluminum-garnet

Nf1: neurofibromatosis type 1

NP-40: nonidet P-40

OFZ: organelle-free zone

PBS: phosphate buffered saline

PCNA: proliferating cell nuclear antigen

PCO: posterior capsule opacification

PDGF: Platelet-derived growth factor

PFA: paraformaldehyde

PI: propidium iodide

PI3-K: phosphatidylinositol-3-kinase

PIP2: phosphatidylinositol 4, 5-biphosphate

PIP3: phosphatidylinositol 3, 4, 5-triphosphate

PKB: protein kinase B

PLC: phospholipase C

RTK: receptor tyrosine kinase

RSK: ribosomal S6 kinase

SAPK: stress-activated protein kinase

SD: standard deviation

SDS-PAGE: sodium dodecyl sulphate-polyacrylamide gel electrophoresis

Sef: similar expression to FGFs

SEM: standard error of the mean

SEM: scanning electron microscopy

Spry: Sprouty

TA: transit amplifying

TBS: Tris-buffered saline

TdT: terminal deoxynucleotidyl transferase

TEMED: N, N, N′, N′-tetramethylethylenediamine

TGFβ: transforming growth factor beta

TRITC: tetramethylrhodamine isothiocyanate

TSC: tuberous sclerosis complex

TTBS: Tween 20-Tris-buffered saline

TUNEL: TdT-mediated dUTP nick end labelling

TZ: transitional zone

UV: ultraviolet light

WGA: wheat germ agglutinin

WHO: world health organisation

ZO-1: Zonula occludens-1

α-SMA: α-smooth muscle isoform of actin

γ-TuRC: γ-tubulin ring complex

Declaration:

I declare that the experiments described in this thesis were carried out by myself in the Department of Biological and Biomedical Sciences, University of Durham, under the supervision of Prof. Roy A. Quinlan. This thesis has been composed by myself and is a record of work that has not been submitted previously for a higher degree. All references have been consulted by myself unless stated otherwise.

Weiju Wu

I certify that the work reported in this thesis has been performed by Weiju Wu, who, during the period of study, has fulfilled the conditions of the Ordinance and Regulations governing the Degree of Doctor of Philosophy.

Roy A. Quinlan

Statement of copyright

Acknowledgements

I owe my deepest gratitude to my supervisor Prof. Roy Quinlan for providing me such a good opportunity to study in the University of Durham, and all the advice, support and encouragement in the past four years. I also want to thank Durham University Doctoral Fellowship for funding my PhD study.

A huge thank you to Dr. Frederique Tholozan, for all the technical help since my first day in the lab, collecting cows' eyes for me in the past three years, suggestions about my research and the corrections of my thesis writing.

A big thank you to Dr. Martin Goldberg, Christine Richardson, Leon Bowen and Helen Grindley for all the help with the scanning electron microscope and the confocal microscope. Many thanks to Terry Gibbons, Dr. Antal Tapodi, Jayne Elliott, Andrew Landsbury, Dr. Ming-Der Perng, Dr. Shu-fang Wen, Pam Ritchie, Bo Qu and Dr. Junjie Wu for all the technical assistance. Special thanks to Dr. Alan Prescott for taking some beautiful microscope images for me and sending me some antibodies. Many thanks to Dr. Iakowos Karakesisoglou, Dr. Maria Schneider, Dr. Ewa Markiewicz, Dr. Andrin Smertenko and the people in Dr. Chris J. Hutchison and Dr. Arto Määtä's lab for lending me antibodies. A special thank you to Dr. Christopher Saunter for writing software to help me easily count the nuclei numbers. Thanks to Andrew Hardisty for all the IT help.

A very big thanks must go to Whitley Bay Meat Supply Co. Ltd of Northumberland and Coast and Country Meat Supplies of Gateshead, Newcastle, for their continuous supply of thirty bovine eyes every week. I also thank Colin Chidzey and John Simpson for driving to the slaughterhouses to take the eyes for me. A special thank you to Dr. Val Smith in Bristol Eye Hospital for sending me all the human eyes. I also want to thank the animal laboratory of Durham University, Simon Cork, Graeme Watson, Dr. Carrie Ambler and Zhi Li for giving me the rat, rabbit and mouse eyes. I also would like to thank the School of Biological and Biomedical Sciences for providing the excellent facilities, and my thesis committee members, Dr. Paul Chazot, Dr. Rumaisa Bashir and Professor Stefan Przyborski for all their suggestions and encouragement.

A very special thank you to Jeffrey Rackham for patiently reading and carefully correcting my thesis writing. I also want to thank Marie-therese Pinder for continuously encourageing me in the past four years.

I am deeply indebted to my parents, Shaosheng Wu and Zailian Zhang, for their love, generosity, and complete support throughout my entire life. I am also grateful to my sister, Yuai Wu, and my brother, Weiguo Wu for their encouragement and unconditional support during my PhD study.

Abstract

The eye lens consists of epithelial cells, fibre cells and an outer capsule. The epithelium plays a crucial role in maintaining lens growth by continuous cell proliferation and differentiation into fibre cells throughout life. Many studies make or support the assumption that cell organisation within the epithelia of different mammalian lenses follows a common plan, while this has not been studied in detail. To better understand this and how it is associated with the development of posterior capsule opacification (PCO) in the human capsular bag after cataract surgery, I studied some basic cell characteristics in five kinds of mammalian lenses and in human donor capsular bags. The apoptotic cell number was very low in the lens epithelium. Cell density, height, cross-sectional area and volume were different in the three zones of the epithelium, and changed with age in the human lens epithelium. The majority of the cells in the peripheral capsular bag retained their polygonal morphology and were as a single layer. Cell proliferation was mainly restricted to the germinative zone (GZ) in the normal lenses and capsular bags. The proliferation index decreased with age in the human lens epithelium. FGF-2 could initiate cell proliferation by activating the extracellular signal-regulated kinase 1 and 2 (ERK1/2) signalling pathway. An FGF-2 gradient was detected in the inner surface of the bovine lens capsule and its level was statistically higher at the equator where cell proliferation and differentiation occurred. Cell proliferation, cell apoptosis and cell density and size in each zone were all consistent in the young lenses from bovine, mice, rats, rabbits and humans. This suggests that a single model may explain cell organisation in the mammalian lens epithelium and age will be one of its important parameters. Moreover, destroying the residual cell organisation in the peripheral capsular bags might prevent PCO.

1 Introduction

The eye lens consists of two types of cells, the epithelial cells and fibre cells; in addition there is a thick basement membrane surrounding these called the lens capsule. The monolayer of epithelial cells covers the inner surface of the anterior and equatorial lens capsule. They proliferate in a region called the germinative zone (GZ), which is just anterior to the lens equator. The proliferated epithelial cells migrate to an area posterior to the equator called the transitional zone (TZ) to differentiate into fibre cells, which make up the bulk of the lens. It is the epithelium that maintains the lens growth by consistent cell proliferation and differentiation throughout life. The cell organisation within the epithelia of different mammalian lenses is assumed to follow a common plan. Although previous studies would support this concept, it has not been investigated in detail. In this thesis, I studied some basic characteristics, including cell proliferation, apoptosis, density, size and centrosome location, of the lens epithelium in five kinds of mammalian lenses in order to test this assumption. Since ageing is an important factor that influences the cell organisation in the lens epithelium and can lead to cataract, those characteristics were also studied in different ages of human normal lenses and capsular bags after cataract surgery. Growth factors, especially fibroblast growth factor 2 (FGF-2), regulate lens epithelial cell proliferation and differentiation through mitogen-activated protein kinase (MAPK) and phosphatidylinositol-3-kinase (PI3-K) signalling pathways. Therefore, the FGF-2 distribution in the lens capsule and the activated MAPK and PI3-K signalling protein levels in the lens epithelium were also included in this study. All the studies were mainly to answer the following questions: (1) Where does cell proliferation occur in the young mammalian lenses? Is it only in the GZ or in the GZ and the CZ? (2) How does epithelial cell proliferation change with age? (3) How many cells undergo apoptosis in the lens epithelium? (4) Is there a cell number balance existing between epithelial cell production (cell proliferation in the GZ) and epithelial cell loss (cell apoptosis and fibre cell differentiation at the end of the TZ)? (5) How does the cell density and size change across the epithelium with age? (6) Where is the epithelial cell centrosome located? (7) How do the cell characteristics above change in the human lens capsular bags after cataract surgery? (8) Does a gradient of matrix-bounded FGF-2 exist in the capsule? (9) Are higher levels of MAPK and PI3-K signalling phosphorylation present in the GZ and the TZ compared to the central zone

(CZ)? (10) How does MAPK signalling pathway regulate lens epithelial cell proliferation?

1.1 Lens embryology

1.1.1 Lens induction

Lens induction occurs very early in gestation. In mammals and avian, the cells that form the lens originally come from the surface ectoderm in the head of the embryo (Figure 1.1). The neural epithelial cells of the diencephalon in the embryonic forebrain protrude to form the optic vesicle, which contacts with the nearby surface of the ectoderm called presumptive lens ectoderm (Lovicu and McAvoy, 2005). After they make contact, both of them start to secrete an extracellular matrix that makes them adhere tightly to each other. The surface lens ectoderm elongates to form the thickened lens placode. As the distal optic vesicle folds inward to form the optic cup, the lens placode invaginates toward the developing optic cup to form the lens pit. The lens pit enlarges, finally closes off and separates from the surface ectoderm to form the lens vesicle, which is an enclosed spherical bag with ectodermal cells lined on the inside. The ectodermal cells in the anterior portion of the lens vesicle differentiate into a monolayer of epithelial cells. Those in the posterior half of the lens vesicle differentiate into the primary fibre cells, which elongate towards the anterior side until they contact with the epithelial cells and fill the vesicle lumen (Augusteyn, 2008; Lovicu and McAvoy, 2005; McAvoy, 1980b). Meanwhile, the lens capsule is formed during lens development. The basement membrane is first detected at the basal surface of the head ectoderm (Center and Polizotto, 1992; Csato, 1989). It continually thickens due to matrix molecule secretion by the pit cells as the lens pit deepens (Csato, 1989) and finally fuses with the opposite pit when the pit pinches off to form the lens vesicle (Parmigiani and McAvoy, 1989). Later the lens epithelial cells and fibre cells continually synthesize and secrete basement membrane molecules to facilitate the growth of the lens capsule. Pulse labelling studies show that the embryonic lens capsule is made up of successive layers of matrix that are continually formed by the lens cells (Parmigiani and McAvoy, 1991; Young and Ocumpaugh, 1966).

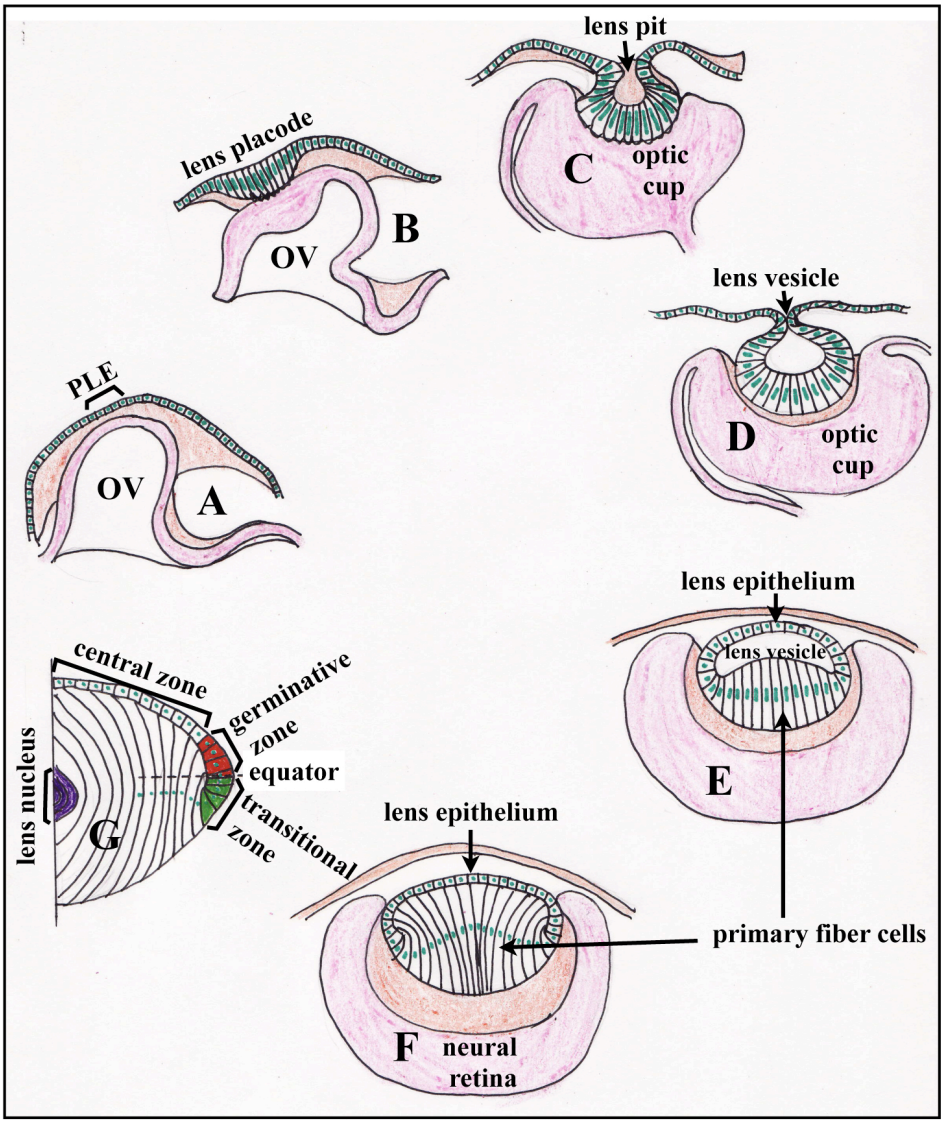

Figure 1.1. Schematic diagrams of the lens induction and secondary fiber cell formation.

A: Lens development begins as the optic vesicle (OV) approaches the presumptive lens ectoderm (PLE).
B: Upon physical contact of the OV with the PLE, cells within the PLE elongate to form the lens placode.
C: The lens placode invaginates to form the lens pit.
D: The lens pit deepens and closes off to form the lens vesicle.
E: The cells at the anterior of the lens vesicle form the lens epithelium and the cells at the posterior elongate to form the primary fibre cells.
F: The primary fiber cells fill the lumen of the lens vesicle as they reach the anterior lens epithelium.
G: The mature lens consists of an anterior epithelial layer composed of non-proliferating central lens epithelial cells (central zone), a narrow band of proliferating cells located anterior to the equator (germinative zone), and the elongating cells located posterior to the equator (transitional zone) to differentiate into the secondary fibre cells. The lens nucleus (purple) is composed of fiber cells that were present in the embryonic lens.

In contrast to mammals or avian, the zebrafish lens induction occurs without the formation of a lens vesicle (Easter and Nicola, 1996; Schmitt and Dowling, 1994; Soules and Link, 2005). The cells in the zebrafish placode thicken and undergo progressive delamination to form a solid, multilayered lens cell mass. This cell mass is reorganised into a spherical structure that undergoes cell differentiation to form a lens similar to the mammalian lens, with the epithelium in the anterior side and primary fibres in the posterior (Dahm *et al.*, 2007b; Greiling *et al.*, 2010; Greiling and Clark, 2009).

Besides the difference of lens induction in different species, some studies report that the lens induction is not a simple one-step progress dependent upon the close association of the surface ectoderm with the optic vesicle, but a multi-step process that involves a series of inductive interactions. Fisher and Grainger have proposed a critical evaluation model for lens determination that includes at least four stages: (1) a period of lens-forming competence in the mid/late gastrula ectoderm, (2) the acquisition of a lens-forming bias throughout the head ectoderm during neurulation, (3) specification of lens during optic vesicle formation and its apposition to the presumptive lens towards the end of neurulation, and (4) lens differentiation by forming placode, lens pit, and lens vesicle at subsequent stages (Fisher and Grainger, 2004). Each stage is regulated by different signalling proteins (Donner *et al.*, 2006). This model indicates that one of the current challenges is to make clear the embryological and molecular genetic definitions of lens induction.

Lens induction is regulated by a series of transcription factors (e.g. Pax6, Sox2, the Meis transcription factors, Six3, Mab21l1, FoxE3, and Prox1) and different signalling pathways [e.g. bone morphogenetic protein (BMP) and FGF signalling pathways]. Among them, Pax6 is necessary and sufficient for lens development in both invertebrates and vertebrates (Lang, 2004a). Pax6 is expressed in the region of the head surface ectoderm that will give rise to the lens, and its expression is restricted to a region that includes the lens placode and the surface ectoderm during lens development (Ashery-Padan *et al.*, 2000). The expression level of Pax6 rises in the lens placode after the lens placode contacts with the optic vesicle (Grindley *et al.*, 1995). The misexpression of Pax6 could induce ectopic eye formation in multiple locations in Drosophila (Halder G, 1995) and Xenopus (Chow *et al.*, 1999), which suggests that Pax6 occupies the apex of a genetic hierarchy that controls eye development. Group B1 Sox proteins (Sox1, Sox2 and Sox3. Sox2 is the major

component) were first found to be an activator of δ1-crystallin, which is the earliest lens-specific gene to be turned on after lens induction. As the optic vesicle makes contact with the head ectoderm, Sox2/3 are expressed only in the contacted area of the head ectoderm and meet Pax6 in the same cell nucleus. This interaction initiates the formation of the lens placode and the activation of δ1-crystallin (Kondoh *et al.*, 2004). The Meis transcription factors are expressed independently of Pax6. They regulate the expression of Pax6 by binding to EE and SIMO (Lang, 2004b). Other transcription factors such as Six3, Mab21l1, FoxE3, and Prox1 are found downstream of Pax6 and regulate late stages of lens development (Lang, 2004a). The BMP-7 is also proposed to play important roles in lens induction. It is expressed in the presumptive lens ectoderm and the dorsal optic vesicle. Deletion of BMP-7 results in a failure to form the lens placode and the lost expression of Pax6 (Wawersik *et al.*, 1999), which indicates BMP-7 is genetically upstream of the enhancers of Pax6. Although no essential ligands of FGFs have so far been documented (Smith *et al.*, 2010), the inhibition of FGF receptor kinase results in reduced levels of Pax6 in the presumptive lens ectoderm; and the expression of dominant-negative FGF receptors in transgenic mice causes a failure to form the lens placode (Faber *et al.*, 2001). These findings indicate that FGF receptor signalling converges upstream and controls Pax6 expression in the lens induction.

1.1.2 Secondary fibre formation

Once the primary fibre cells contact with the epithelial cells, the lens polarity is established. The lens then grows rapidly by lens epithelial proliferation and fibre cell differentiation. Lens epithelial proliferation takes place in the GZ, which is just anterior to the lens equator (Figure 1.1G) (Harding *et al.*, 1971; McAvoy, 1978a; McAvoy, 1978b). The new cells migrate along the capsule to the posterior of the equator known as the TZ, where they elongate, and rotate 180 degrees through their polar axis to differentiate into the fibre cells. These fibre cells are called the secondary fibres cells. Their apical plasma membranes make contacts with the apical membranes of the lens epithelial cells (Kuszak *et al.*, 1995). Their basal plasma membranes make contacts with the posterior lens capsule and face the vitreous humour (Bassnett *et al.*, 1999). The differentiated fibre cells bi-directionally elongate along the posterior lens capsule and the lens epithelium until they meet the cells from the other side at the

midpoints of the anterior and posterior sides where they form sutures and detach from the capsule. In this way, the lens continues to grow throughout life with new fibre cells continuously added on top of the older fibre cells to form an "onion-like" structure. The primary fibre cells wrapped in the centre are termed the embryonic nucleus. The embryonic nucleus only represents two to three percent of the adult lens thickness (Al-Ghoul *et al.*, 2001).

1.2 Lens epithelial cell proliferation

1.2.1 Lens epithelium partition

The monolayer of the lens epithelium covers the anterior surface of the lens. Depending on the difference in proliferative status, the lens epithelium is divided into three zones: central zone (CZ), GZ and TZ (Augusteyn, 2008; Bhat, 2001; Kuszak, 1997; McAvoy, 1978a; McAvoy *et al.*, 1999; Ong *et al.*, 2003) (Figure 1.2).

1.2.1.1 Central zone (CZ)

The CZ is the region medial to the iris rim (McAvoy, 1978a; Ong *et al.*, 2003). This is the pupillary area of the lens epithelium, where light passes as it comes into the eye. The cells here are characterised by a low proliferation index with most cells in a quiescent state.

They are cuboidal or flat and show varying morphology in the apical side and basal side (Bassnett, 2005; Zampighi *et al.*, 2000). Their apical membranes, which are associated with the apical membranes of the fibre cells, have relatively uniform polygonal shapes. The basal membranes, which contact with the lens capsule, possess elaborate invaginations or lamellipodia- and filopodia-like protrusions. Because of the regularity of the apical membranes in different conventional optics, the lens epithelial cells are usually described as exhibiting a regular polygonal morphology.

The diameter and volume of the cells at the anterior pole are proportionately bigger than those located in the periphery of the CZ, but the cell height at the anterior pole is less than those in the periphery. The cell size (including cell height, cross-sectional area and volume) in the CZ progressively increases with age (Hendrix and Rubinson, 1996; Kuszak, 1997).

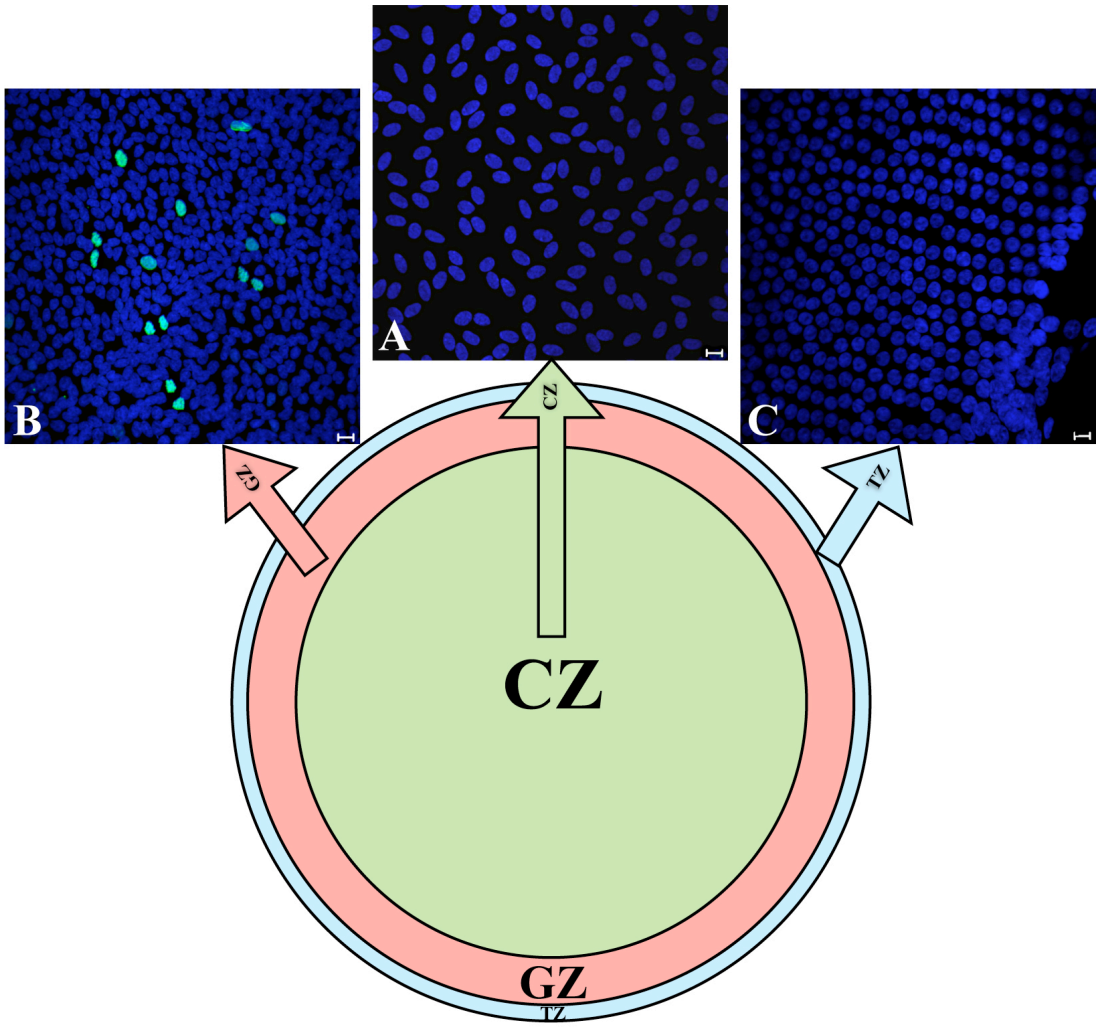

Figure 1.2. A diagram of the lens epithelium partition.

The diagram shows the location of the three zones in the lens epithelium. The bovine lens epithelial cells were stained with DNA indicator DAPI (blue) and proliferation marker Ki-67 (green) in order to study the location of the dividing cells.

A: The cells in the central zone (CZ) are in a quiescent state.

B: Many dividing cells are detected in the germinative zone (GZ).

C: In the TZ, the cells rearrange into ordered columns and no cell proliferation occurs.

1.2.1.2 Germinative zone (GZ)

The GZ is a narrow band of the epithelium just anterior to the lens equator and characterised by a high proliferation index (Harding *et al.*, 1971; McAvoy, 1978a; McAvoy *et al.*, 1999; Mikulicich and Young, 1963; Ong *et al.*, 2003; Persons and Modak, 1970; Wiley *et al.*). It faces the anterior part of the ciliary body (McAvoy, 1978a). The length of the GZ in different vertebrate lenses is different. Its length also changes with age. The cell number from the outer edge (the location of the last dividing cell on the outside) of the GZ directly to the inner edge (the location of the first dividing cell on the inside) is often used to record its length and position. The GZ is located in between cell positions 5 and 45 (the cell at the equator is numbered 1) in 1-day-old rats (the total cell number from equator to the centre of the epithelium is 140), and in between cell positions 17 and 68 in the 6- to 7-week-old rats (the total cell number from equator to the centre of the epithelium is 200) (McAvoy, 1978a). In mice, it is in cell position 5 to 30 at age two weeks and in cell position 5 to 15 at age four weeks (the lens epithelial cell number from the anterior pole to equator is about 190 in the 2- and 4-week-old mice) (Yamamoto *et al.*, 2008). Apart from the GZ length decreases with age, the number of the dividing cells in the GZ also decreases with age (McAvoy, 1978a; McAvoy, 1978b; Mikulicich and Young, 1963; Wiley *et al.*, 2010).

Table 1.1. The GZ length in different ages of rats and mice

Species	Age	GZ length (cell positions)	Total cell number (from the CZ to the GZ)	Literature
Rat	1 day	5-45	140	McAvoy, 1978
Rat	6-7 weeks	17-68	200	McAvoy, 1978
Mouse	2 weeks	5-30	190	Yamamoto *et al.*, 2008
Mouse	4 weeks	5-15	190	Yamamoto *et al.*, 2008

The boundary of the CZ and GZ is not clearly defined yet. Hendrix and Rubinson defined the boundary as the position where cell height started to increase. They also measured the GZ length in the lamprey lens was about 200 μm (the total length from the anterior pole to the equator was about 800 μm in the 3-year-old lamprey lens) (Hendrix and Rubinson, 1996).

Compared with the flat cells in the CZ, the cells in the GZ are much higher and show a columnar morphology (Bassnett, 2005; Hendrix and Rubinson, 1996; Zampighi *et al.*, 2000). The cell height in the GZ increases gradually across this region, while it continuously decreases with age. It ranges from 10 to 25 μm in 1-day-old rats and 6 to 10 μm in the 6- to 7-week-old rats (McAvoy, 1978a). The average cell height in the GZ was reported to be about 31 μm in the 1.5- to 2-year-old lamprey and 12 μm in the 4- to 5-year-old lamprey (Hendrix and Rubinson, 1996).

As in the central epithelium, the cells in the GZ are also polygonal. Their diameter and volume are much smaller than the cells in the CZ. In the sea lamprey lenses, the average cell area and volume in the GZ were about 23.4 μm^2 and 300 μm^3 while they were 439 μm^2 and 1000 μm^3 in the cells at the centre of the CZ (Hendrix and Rubinson, 1996). The GZ cell cross-sectional area continuously increases with age. The average GZ cell cross-sectional area was respectively 83.76 μm^2 and 99.58 μm^2 in the lenses of 7-year-old monkeys and 24-year-old monkeys (Kuszak, 1997).

1.2.1.3 Transitional zone (TZ)

The TZ lies just posterior to the lens equator (Kuszak, 1997; McAvoy *et al.*, 1999; Ong *et al.*, 2003). This zone is called the annular pad in the chicken lens (Zwaan and Kenyon, 1984). The progeny of epithelial cell divisions in the GZ migrate to this zone and rearrange into ordered columns called meridional lines (Worgul and Rothstein, 1975). All the epithelial cells continuously elongate across the TZ. Those at the end of the TZ are about five times longer than the cells in the CZ in the rat lenses (Zampighi *et al.*, 2000). The cell height is found to increase immediately at the beginning of the TZ in the sea lamprey lenses (Hendrix and Rubinson, 1996) and keeps constant increase across the TZ. Interestingly, although the cell height increases dramatically in the TZ, the average cell volume is still similar to those cells in the CZ (Bassnett, 2005; Hendrix and Rubinson, 1996). This is because the cell diameter is

much smaller in the TZ than in the CZ. With cell elongation, the nuclei move close to the lens capsule and take up a basal position in the cells (Zwaan and Kenyon, 1984).

1.2.2 Lens epithelial cell proliferation

1.2.2.1 Lens epithelial cell proliferation in the CZ

In newborn or young animals, many cells still divide in the CZ (Gloor *et al.*, 1985; McAvoy, 1978a; Pe'er *et al.*, 1996; Rafferty and Rafferty, 1981b). It was reported that the mitotic index of lens epithelium in one-day-old rats was about 1% at the centre and was near 5% in the periphery of the CZ. In the 6- to 7-week-old rats, it decreased to 0.02% at the centre and to about 0.1% in the periphery (McAvoy, 1978a). In the adult lens, cell division does not occur often in the CZ (Zwaan and Kenyon, 1984).

The period between one mitosis and the next is known as the cell cycle time (Gloor *et al.*, 1985). It is quite variable in the cells of the CZ in different ages and species of animals. Gloor and colleagues observed that the cell cycle time of the mouse CZ epithelial cells increased with lens development (Gloor *et al.*, 1985). It was three days in the mice immediately after birth, 9-10 days in the 10-day-old mice, and 285.5 days in the 2- to 3-month-old mice. Riley and Devi found the cell cycle time was 198 days in the 3- to 4-month-old rats (Riley and Devi, 1967). Sallmann and colleagues reported it was 250 days in the anterior pole of the adult rat lens (Von Sallmann *et al.*, 1962). In conclusion, the cells in the CZ have a very long cell cycle time and divide very slowly in adult lenses.

Although the CZ cells exhibit a generally quiescent state in mature lenses, they do retain the proliferative potential and will divide again after injury (Harding *et al.*, 1959; Kojima *et al.*, 2009; Rafferty, 1973; Rafferty and Smith, 1976; Saika *et al.*, 2007; Tanaka *et al.*, 2004; Zhou *et al.*, 2006) or irradiation (Kojima *et al.*, 2009). Tanaka and colleagues reported that the lens epithelial proliferation around the injured area increased dramatically five days after a small incision in the rat central anterior capsule (Tanaka *et al.*, 2004). In the same study, they found the cells in this area became multilayered and underwent epithelial-mesenchymal transition (EMT) (Tanaka *et al.*, 2004). Osteopontin (a matrix structural glycophosphoprotein) (Saika *et al.*, 2007) and tenascin-C (an extracellular matrix protein) (Tanaka *et al.*, 2010) are found to influence EMT by activating or inhibiting Smad2/3 signal after the injury.

Moreover, these injury-stimulated dividing cells in the CZ are found to have a similar cell cycle time with those normal cells in the GZ (Rafferty and Smith, 1976). This indicates the cell cycle time of these cells is shortened compared with that of the normal central epithelial cells.

1.2.2.2 Lens epithelial cell proliferation in the GZ

Different DNA precursors [e.g. tritiated thymidine (^{3}H-thymidine) and bromodeoxyuridine (BrdU)] and cell proliferation markers [e.g. proliferating cell nuclear antigen (PCNA) and Ki-67] have shown that lens epithelial cell proliferation mainly occurs in the GZ, and the proliferation index decreases with age (Mikulicich and Young, 1963; Tseng *et al.*, 1999; Yamamoto *et al.*, 2008a). The proliferation rate in the GZ of the mouse lenses is observed to have a circadian rhythm, rising in the late evening through the early morning hours and diminishing during the late morning and afternoon hours (Rafferty, 1972). Furthermore, similar to the cells in the CZ, the cells in the GZ can also be activated to proliferate after injury. Zhou and colleagues found many GZ cells came into cell cycle after a needle perturbation in the GZ, and some cells divided within 24 hours after the injury (Zhou *et al.*, 2006).

The cell cycle time in the GZ is much shorter than that in the CZ. It is two days in the neonatal mice, 3.4 days in 10-day-old mice, and 16 days in 2- to 3-month-old mice (Gloor *et al.*, 1985). The cell cycle time is about 3 days in rats aged 6-30 days (Mikulicich and Young, 1963) and 23 days in 3- to 4-month-old rats (Riley and Devi, 1967). It is also reported to be 19 days in the adult rat lens (Von Sallmann *et al.*, 1962). Rafferty and Smith found that in the lens epithelial cells of mice it took 55-61 hours (G1: 38-44 hours; S: 11-12 hours; G2: 1.5-2 hours; M: 4.2-5 hours) from the start of cell division to the end (Rafferty and Smith, 1976). Unlike Gloor's definition about cell cycle time (Gloor *et al.*, 1985), Rafferty and Smith did not include the quiescent state of the cells, G0 phase, in their study. Therefore, the value is much smaller than those including G0 phase.

1.2.3 Stem cells in the lens epithelium

1.2.3.1 Stem cell properties

According to their different proliferative capacities, cells are divided into stem cells, young transit amplifying (TA) cells and mature TA cells (Lavker and Sun, 2003; Zhou *et al.*, 2006). Stem cells have unlimited proliferative capacity, while young TA cells have a large proliferative ability and can divide many times, and mature TA cells have limited proliferative ability and can only divide a few times (Zhou *et al.*, 2006). Stem cells are a subpopulation of cells that can divide through mitosis, and differentiate into diverse specialized cell types or can self-renew to produce more stem cells. According to their differentiation potential (the potential to differentiate into different cell types), they are subdivided into totipotent stem cells, pluripotent stem cells, multipotent stem cells, oligopotent stem cells and unipotent stem cells (Mitalipov and Wolf, 2009; Ulloa-Montoya *et al.*, 2005). In mammals, there are two broad types of stem cells: embryonic stem cells and adult stem cells. The embryonic stem cells, which are isolated from the inner cell mass of blastocysts, can not only differentiate into all the specialized cells but also maintain the normal turnover of regenerative organs such as blood, skin, or intestinal tissue. The adult stem cells can be found in many self-renewing tissues such as the corneal epithelium (Sun and Lavker, 2004), the hair follicle epithelium (Fujiwara H, 2011), epidermis (Williams *et al.*, 2011), the intestinal epithelium (van der Flier and Clevers, 2009) and the cells of the haematopoietic system (Varma *et al.*, 2011). They mainly act as a repair system to maintain the organ homeostasis.

Stem cells reside in a special microenvironment called niche. The stem cell niche is a specific anatomic location that regulates how stem cells participate in tissue generation, maintenance and repair (Scadden, 2006). It varies in nature and location depending on the tissue type. The niche consists of the cellular components of the microenvironment surrounding the stem cells and the signals emanating from the support cells (Li and Xie, 2005). It protects stem cells from depletion and regulates stem cell proliferation in case excessive stem cell production causes cancer (Scadden, 2006). As stem cells must activate periodically to produce TA cells in order to maintain the normal tissue, maintaining a balance of stem cell quiescence and activity is a typical characteristic of a functional niche (Moore and Lemischka, 2006).

1.2.3.2 Stem cell detection

As stem cells and their neighbouring cells within tissues can rarely be separated by histological methods, it is very difficult to identify stem cells *in vivo*. The methods used to detect stem cells now are mainly based on their properties. One important method is by some specific stem cell markers, which are the genes and their proteins expressed by stem cells. For example, Lgr5 is found to be a pluripotent stem cell marker in both the small intestine and the colon (Barker *et al.*, 2007). The intermediate filament protein nestin is a marker of neural stem cells (Azan *et al.*, 2011; Stemple and Anderson, 1992). Another intermediate filament protein keratin 15 is an epidermal stem cell marker (Troy TC, 2011). Since these specific stem cell markers are only found in a small number of tissue types and are not reliable for detecting stem cells in other types of tissues, the label retention method based on the slow-cycling feature of stem cells is widely used. In this procedure, all the epithelial cells are repeatedly or continuously labelled with ^{3}H-thymidine and/or BrdU, followed by a long chase period during which the label is lost or decrease from all the rapidly-cycling TA cells, so that only the slowly-cycling stem cells have the heaviest labelling and are designated as label-retaining cells (LRCs) (Lavker and Sun, 2003). Using this method, hair follicular epithelial stem cells are found to reside in the upper follicle in an area called the bulge (Oshima *et al.*, 2001; Taylor *et al.*, 2000); prostate epithelial stem cells are located in the proximal region of prostatic ducts (Tsujimura *et al.*, 2002); and corneal epithelial stem cells reside in the peripheral cornea in the limbal region (Sun *et al.*, 2010; Zhao *et al.*, 2009).

1.2.3.3 Stem cells in the lens epithelium

Although the existence of stem cells in the lens epithelium has been proposed and many studies have been carried out, their exact location is still controversial and no specific stem cell marker or niche has been found in the lens epithelium (Oka *et al.*, 2010; Rafferty and Rafferty, 1981a; Yamamoto *et al.*, 2008b; Zhou *et al.*, 2006). Using different methods, the stem cells of the lens epithelium have been reported to locate in the CZ (Zhou *et al.*, 2006) or in the GZ (Oka *et al.*, 2010; Yamamoto *et al.*, 2008a).

Zhou and colleagues repeatedly injected pregnant female mice and utero-labelled neonatal mice with ^{3}H-thymidine and detected the LRCs in the lens

epithelium after a long-term chase (Zhou *et al.*, 2006). They observed the heavily-labelled cells only in the CZ and suggested they were lens epithelial stem cells that divided very infrequently during homeostasis. After wounding, these cells could proliferate. Interestingly, they detected the lightly-labelled cells, presumably the progeny of the heavily-labelled cells, in both the CZ and GZ and non-labelled actively cycling cells in the GZ. Therefore, they suggested the hierarchy of the proliferative lens epithelial cells included the stem cells (heavily-labelled LRCs), the young TA cells (lightly-labelled LRCs), the adult TA cells (non-labelled actively cycling cells), and the postmitotic cells (lens fibre cells). Yamamoto and colleagues used BrdU to label mouse lens epithelium and found the BrdU-labelled cells located just anterior to the GZ did not move in 48 hours (Yamamoto *et al.*, 2008b). Considering that the lens epithelial cells proliferated in the GZ and migrated to the TZ to differentiate, they suggested these unmoved BrdU-positive cells were stem cells. Since it is not clear whether the divided daughter cells have to move towards the TZ or will temporarily stay in the GZ for the next division, the conclusion made by Yamamoto and colleagues still needs to be confirmed. Oka and colleagues stained the mouse lens epithelial cells with Hoechst 33342 and sorted them by fluorescence-activated cell sorting (FACS) (Oka *et al.*, 2010). They found the sorted cells contained side population cells, which were no longer separable by FACS following treatment with verapamil. These side population cells were located in the GZ and expressed higher levels of the stem cell markers such as ATP-binding cassette transporter G2, p75 neurotrophin receptor, nestin, B-cell lymphoma 2, and cell surface antigen Sca-1 mRNA than the main population cells. Thus, they suggested that the side population cells contained a high proportion of stem cells.

Since no stem cell niche has been found in the CZ and GZ and these suggested stem cells are not proved to have unlimited proliferative capacity, it is not possible to define that they are the stem cells of the lens epithelium. However, the success of lens regeneration (Huang and Xie, 2010; Liu *et al.*, 2008; Lois *et al.*, 2010) indicates the presence of stem cells in the lens. Therefore, lens regeneration is possibly a good model to study the position of stem cells in the lens epithelium.

1.3 Lens fibre cell differentiation

1.3.1 Fibre cell organisation and morphology during differentiation

Before fibre cell differentiation, the epithelial cells in the TZ migrate along the capsule to the posterior side and rotate from 90° to 180° along the curvature of the equator lens capsule. The cells stop rotating when the long axis of a nascent fibre cell is aligned parallel to the antero-posterior axis of the lens. Then the nascent fibre cells elongate and migrate bi-directionally along the epithelium and posterior lens capsule. The elongation is complete when they abut with the fibre cells from opposite sides at their apical and basal ends to form sutures (Beebe *et al.*, 1982). Meanwhile they complete a growth shell. According to the pattern difference, four kinds of sutures are defined: umbilical sutures, line sutures, Y sutures, and star sutures (Kuszak *et al.*, 2004b). Umbilical sutures are branchless sutures while the other three are branched sutures. Umbilical sutures are mainly formed in the avian (e.g., chicken) and reptilian lenses. Their fibre cells are meridians and the apical and basal ends meet at the anterior and posterior poles to form umbilical sutures (Kuszak *et al.*, 2004a). Line sutures occur in the amphibian (e.g., frog) and rabbit lenses. Y sutures happen in the rodent (e.g., mouse and rat), canine (e.g., dog), feline (e.g., cat), porcine (e.g., pig), ovine (e.g., sheep) and bovine lenses. Star sutures can be found in the human and primate lenses (Kuszak *et al.*, 2004b). The fibre cell arrangement in each growth shell of the branched sutures is more complex than in the umbilical sutures. The increasing geometric complexity of suture patterns exerts a quantifiable negative influence on lens optical quality and reflects species difference in visual needs and visual capabilities (Kuszak *et al.*, 1994).

The vast majority of fibre cells are hexagonal in cross-sectional. They have two broad sides oriented parallel to the lens surface and four narrow sides oriented at acute angles to the lens surface (Bassnett and Winzenburger, 2003; Kuszak and Rae, 1982; Kuszak *et al.*, 2000). Their width at the equator (a span of a fibre between the two acute angles formed by the opposite, paired narrow faces) is relatively constant in the cortical or lens nucleus region. The fibre width at the basal and apical ends is less than that at the equator and is found to be variable in different kinds of lenses. In lenses with umbilical sutures, the fibre ends taper to a point. In lenses with line sutures, the fibre ends taper to about 1/3-1/2 of their width at the equator. In lenses with Y sutures, the fibre ends taper to about 1/2-2/3 of their width at the equator. Besides hexagonal

fibres, a very small number of pentagonal fibre cells are also detected in cross-sectional. Their width is half or one and a half times the width of hexagonal fibres. Since the circumference increase of successive growth shells is possibly less than the width of hexagonal fibres, these pentagonal fibres are necessary (Kuszak *et al.*, 2004a).

Some diseases can influence or are related to the suture formation. For example, diabetes has a cumulative negative effect on lens structure and can result in asymmetrical star sutures (Kuszak *et al.*, 2004b); The characteristic cuneiform opacities in cortical cataract are reported to be the manifestation of sutural malformation during adolescence and adulthood (Kuszak J.R., 1998); Some congenital cataracts caused by gene mutation are located at the suture and form characteristic Y-shaped cataracts (Zhang *et al.*, 2006). Furthermore, some ocular surgeries such as vitrectomy can lead to post-surgical change in lens sutures that precedes cataract formation (Kuszak *et al.*, 2000).

1.3.2 Fibre cell organelle degradation during terminal differentiation

The organelles and cytoplasm of the lens fibre cells have different refractive indexes, which can cause light scatter and influence lens transparency (Bassnett, 2009). In order to minimize potential light scatter, the organelles are degraded in the fibre cells located in the lens core, leading to the formation of an organelle-free zone (OFZ) (Bassnett, 2002). Therefore, the lens contains organelle-containing fibre cells in the periphery, which lie in the shadow of the iris, and organelle-degraded fibres in the core situated in the light path. The failure of organelle degradation in the core fibres can result in cataract (Bassnett, 2009).

The lost organelles include nucleus, mitochondria, endoplamic reticulum and Golgi apparatus (Wride, 2011). Among them, the nuclear loss is first noticed (Rabl, 1899) and extensively studied. During the denucleation process, the fibre cell nuclei experience some distinct morphological change. At the beginning, transcription is shut down (Dahm *et al.*, 1998). The elongated nuclei become irregular with marginalisation of the chromatin to the nuclear periphery. Meanwhile, the nuclear pores in the nuclear envelope progressively cluster into large aggregates that are associated with the condensed chromatin (Dahm and Prescott, 2002), and A- and B-type nuclear lamins are rearranged (Dahm *et al.*, 1998). Then holes appear in the

nuclear envelope and underlying lamina and the nuclei collapse into spherical structures (Bassnett and Mataic, 1997). In the meantime, the homogeneous nucleoli condense to a spoke-like configuration (Kuwabara and Imaizumi, 1974). Finally, the nuclear envelopes disintegrate into chains of vesicles, and nuclear and cytoplasmic substances become indistinguishable (Kuwabara and Imaizumi, 1974). The residual bodies, composed of condensed chromatin, remain in the cytoplasm for a period before finally disappearing. Once nuclei degradation is complete, their transcriptional capacity is lost (Gribbon *et al.*, 2002). At the same time as the nuclear degradation, mitochondria, endoplamic reticulum and Golgi apparatus also break down and lose their potentials (Sanders and Parker, 2002; Wride, 2011). The whole process takes place over several days.

What triggers lens fibre organelle degradation is not clear at present. Bassnett hypothesises that probably a gradient of a diffusible substance such as oxygen triggers this process (Bassnett, 2002; Bassnett and Mataic, 1997), although there is currently little experimental evidence to support this. The biochemical mechanisms underlying organelle degradation are not fully understood. The nuclease DNase IIβ is found to play an important role in lens denucleation (De Maria and Bassnett, 2007; Ivanov *et al.*, 2005; Nishimoto *et al.*, 2003). Some studies suggest that DNase IIβ is a lysosomal enzyme in the lens and probably is delivered to the nucleus when lysosomes fuse with the nuclear envelope (Bassnett, 2009; Nakahara *et al.*, 2007).

The morphological changes during nuclear degradation are similar to cell apoptosis. For example, chromatin condenses and marginalises, and DNA is fragmented to produce the characteristic laddering pattern of apoptosis seen in agarose gel electrophoresis (Bassnett and Mataic, 1997; Nagata, 2005). However, some clear differences are present between them. The process of organelle loss happens over several days while cell apoptosis just takes several hours (Bassnett, 2009). The cytoskeleton is still maintained in the fibres after the organelle loss, but in the apoptotic cells the cytoskeleton is completely degraded (Dahm, 1999). Phosphatidylserine does not flip to the outer leaflet of the fibre cell membrane in the organelle loss as it usually does during apoptosis (Wride and Sanders, 1998). Moreover, the fibres without organelles still remain in the lens while the apoptotic cells are usually engulfed and digested by invading macrophages (Wride, 2011). Despite these differences, some apoptosis-related molecules are still found to

associate with fibre cell organelle degradation. It is reported that in the chicken lens over-expression of Bcl-2, an anti-apoptotic molecule, leads to the failure of the nuclear chromatin condensation in the fibres of the core and the disruption of cell denucleation (Sanders and Parker, 2003). Some caspases, which cleave critical regulatory or structural proteins during cell apoptosis, especially caspase-3, are directly involved in organelle degradation (Ishizaki *et al.*, 1998).

1.3.3 The expression of fibre-cell specific proteins during differentiation

One important characteristic of lens fibre cell differentiation is the expression of fibre-cell specific proteins. They mainly include β-crystallin, γ-crystallin, cytoskeletal protein 49 (CP49), filensin, aquaporin 0 (AQP0), membrane protein 20 (MP20) and connexin46.

β-crystallin is expressed earlier than γ-crystallin during lens fibre cell differentiation. They are thought to bind to α-crystallin in order to maintain lens transparency (Rao *et al.*, 1995) and regulate lens refractive index (Cui *et al.*, 2004). Mutations of βA1/A3, βB2 and βB1 lead to nuclear autosomal dominant congenital cataract in humans (Devi *et al.*, 2008; Ferrini *et al.*, 2004; Gu *et al.*, 2010; Lu *et al.*, 2007; Pauli *et al.*, 2007; Wang *et al.*, 2011; Zhu *et al.*, 2010). Nuclear congenital cataract caused by γD-crystllin has also been reported (Banerjee *et al.*, 2011; Messina-Baas *et al.*, 2006). These gene mutations change the solubility of β- and γ-crystallins and cause them to easily precipitate or aggregate and form light-scattering particles (Vendra and Balasubramanian, 2010).

CP49 and filensin are the intermediate filaments. Since they show a special beaded feature with a 5-6 nm filament backbone and 15-20 nm beads decorating the filament, CP49 is also called beaded filament structural protein 2 (BFSP2) and filensin is called beaded filament structural protein 1 (BFSP1). Both are important in making up the cytoskeletal network and providing internal support and structure for the fibre cells. Mutations of CP49 in humans result in a characteristic Y-shaped cataract at the lens suture (Cui *et al.*, 2007; Jakobs *et al.*, 2000; Zhang *et al.*, 2006; Zhang *et al.*, 2004), or juvenile-onset, progressive cataract (Conley *et al.*, 2000), or congenital lamellar cataract (Ma *et al.*, 2008). The cataracts caused by these three CP49 mutations are all autosomal dominant. Filensin mutation leads to inherited recessive juvenile-onset cataract (Ramachandran *et al.*, 2007). Furthermore, studies of

CP49 and filensin knockouts show that beaded filaments do not contribute to the generation of cellular and tissue level phenotypes in lens, but are required to maintain the structural phenotype of the fibre cells with age (Alizadeh *et al.*, 2003; Alizadeh *et al.*, 2002; Sandilands *et al.*, 2003; Sandilands *et al.*, 2004).

1.4 Regulation of lens epithelial cell proliferation and differentiation

1.4.1 Growth factors

1.4.1.1 Fibroblast growth factors (FGFs)

Growth factors, especially FGFs, play an essential role in lens epithelial cell proliferation and differentiation. The FGF family currently includes 22 distinct genes named FGF1-23 in mammals. FGF-1, FGF-2 (McAvoy and Chamberlain, 1989), transcriptions and/or protein for FGF-3 (Wilkinson *et al.*, 1989), FGF-5 (Kitaoka *et al.*, 1994), FGF-7 (Finch *et al.*, 1995), FGF-8 (Vogel-Hopker *et al.*, 2000), FGF-9 (Zhao *et al.*, 2001), FGF-10 (Makarenkova *et al.*, 2000), FGF-11-13 (Smallwood *et al.*, 1996), and FGF15/19 (Kurose *et al.*, 2004) are present in the developing or mature eye.

FGF-1 and FGF-2 are the most important growth factors in inducing lens epithelial cell proliferation and differentiation. They were first isolated and purified from eyes by the McAvoy lab in the 1980s (Chamberlain and McAvoy, 1987; McAvoy, 1980a). FGF-2 is found to initiate lens epithelial cell proliferation and differentiation in a dose-dependent manner: for example, a low dose of FGF-2 only induces cell proliferation, while a high dose can induce cell differentiation (McAvoy and Chamberlain, 1989). The early classical lens inversion experiments of Coulombre showed that the lens epithelial cells, which initially faced the aqueous humour, elongated into fibre cells when they faced the vitreous humour, while the lens fibre cells that initially faced the vitreous humour stopped elongation when they faced the aqueous humour (Coulombre and Coulombre, 1963). Based on these findings, a hypothesis is proposed that normal lens morphology with its antero-posterior patterns of cellular behaviour is determined by an antero-posterior gradient of FGFs stimulation. This means that the aqueous humour has a low level of FGFs while the vitreous humour has a high level of FGFs. Further studies show that the aqueous humour or a low level of FGF-2 can only induce epithelial cell proliferation but the

vitreous humour or a high level of FGF-2 induces the epithelial cell to elongate and express fibre-specific proteins (Iyengar *et al.*, 2006; Lovicu *et al.*, 1995; Wang *et al.*, 2009b). If FGF-1 and FGF-2 of the vitreous humour are blocked, about 70% of the fibre cell differentiation activity in the cultured epithelial explants will be inhibited (Schulz *et al.*, 1993). Immunoblotting also shows that vitreous humour contains substantially more FGFs than aqueous humour (Chamberlain and McAvoy, 1997; Schulz *et al.*, 1993). To date, FGFs have been reported to be the only growth factor that is able to initiate fibre differentiation in mammals (Wang *et al.*, 2009b). Moreover, FGF-2 is found to be five times more potent than FGF-1 in inducing fibre differentiation (Chamberlain and McAvoy, 1987; Chamberlain and McAvoy, 1989).

FGFs are synthesised in the retina and the ciliary body. They are then secreted to the vitreous and aqueous humours and diffuse to the lens capsule (Figure 1.3). Later they come inside the lens capsule and bind to heparan sulphate proteoglycans (HSPGs) such as perlecan (Iozzo, 1998; Tholozan *et al.*, 2007). The binding between perlecan and FGFs can help to form a FGF reservoir in the lens capsule and protect it from degradation as well as regulate its function. A conditional ablation of heparan sulphate modification genes, Ndst1 and Ndst2, results in reduced lens cell proliferation, increased cell death and defective fibre cell differentiation in later lens development (Qu *et al.*, 2011). FGFs regulate lens cell activity by binding to FGF receptors (FGFRs), which are located in the cell membrane. The lenses of chickens and mammals express four FGFR tyrosine kinase genes (FGFR1-4). FGFR molecules include three extracellular immunoglogulin-like (Ig) domains, a single transmembrane domain and a split intracellular tyrosine kinase domain. An FGF ligand binds to the extracellular Ig domains and induces the dimerisation of the FGFR monomers. This then leads to transphosphorylation and activation of tyrosine kinase in the intracellular domain. The FGFR distribution in the lens supports the hypothesis of FGF regulating lens growth by an antero-posterior FGF gradient. For example, in embryonic and neonatal rats, the FGFR3 expression shows an antero-posterior increase and is strongest in the outer cortical fibres; one pattern of FGFR2, keratinocyte growth factor receptor, shows stronger expression in the TZ than in the GZ; FGFR4 is also mainly expressed in the cells of the TZ and the fibre cells (de Iongh *et al.*, 1997; Robinson, 2006) Overexpression of a truncated FGFR (Stolen and Griep, 2000) or a

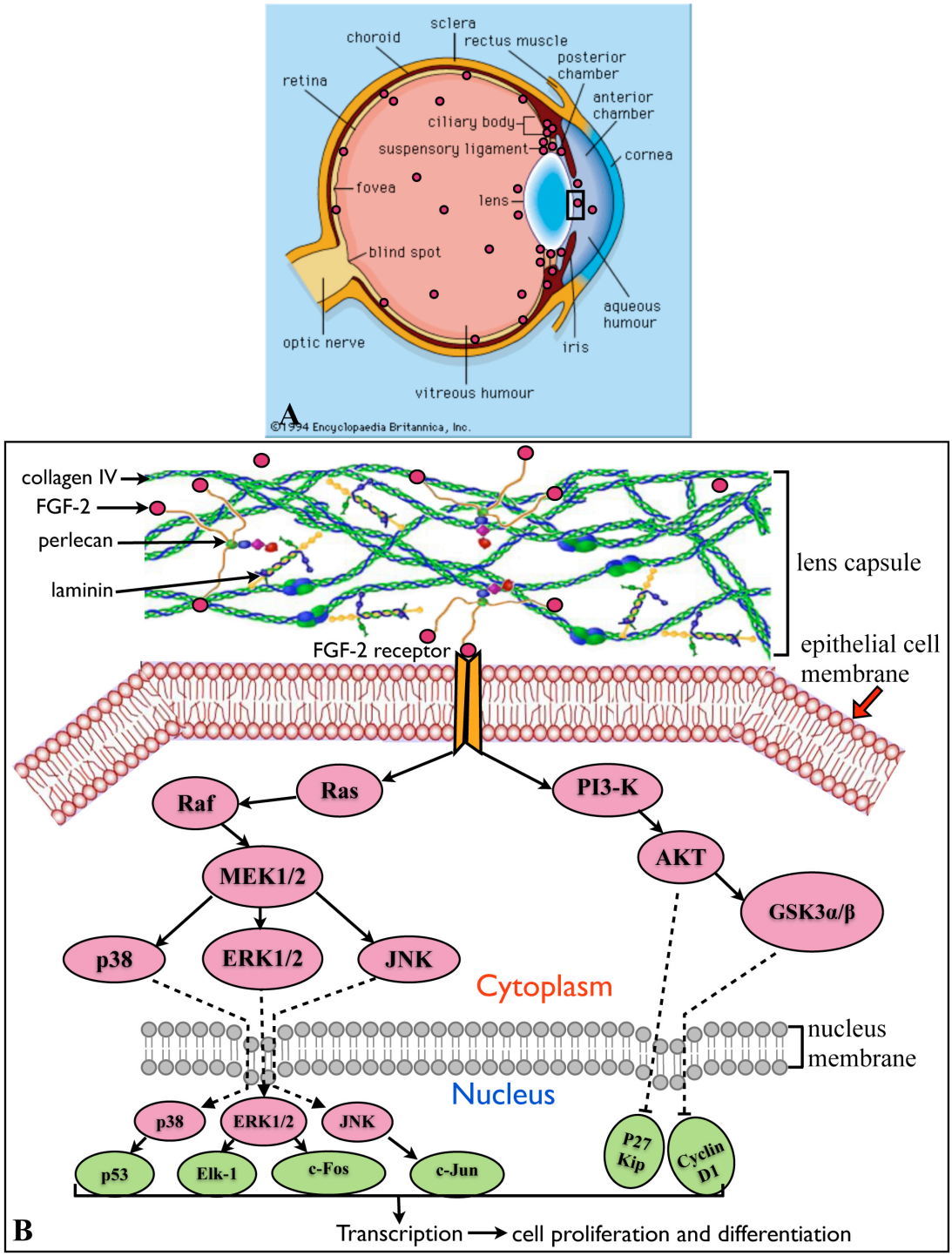

Figure 1.3. FGF-2 passes through the lens capsule and activates the signalling pathways inside the epithelial cells.

A: FGF-2 is synthesized in the ciliary body and retina, and secreted to the aqueous and vitreous humours.

B: FGF-2 is restored in the lens capsule by binding to perlecan. After they bind to their receptors, they activate the intracellular receptor tyrosin kinases (RTKs). RTKs consequently active Ras/Raf/MEK/MAPK and PI3-K/AKT/GSK3α/β. The activated signalling proteins translocate into the nucleus to regulate the expression of transcription factors, which then regulate cell proliferation and differentiation.

. specific secreted FGFR (sFGFR3 but not sFGFR1) (Govindarajan and Overbeek, 2001) results in the inhibition of mouse fibre cell differentiation *in vivo*. The mouse lenses with triple knockouts of FGFR1, FGFR2 and FGFR3 undergo no fibre differentiation (Zhao 2003). FGFR inhibitors can effectively block FGF-induced fibre differentiation (Wang *et al.*, 2010). All these results indicate the importance of FGFRs in the lens.

Besides FGFRs, FGFs temporally and spatially regulate lens fibre differentiation by specific growth-factor signalling-pathway antagonists. Sprouty (Spry) and Sef (similar expression to FGFs) are the main antagonists that have been studied in lens (Boros *et al.*, 2006; Newitt *et al.*, 2010). Spry was initially discovered through a genetic screen in *Drosophila* and later found to act as an FGF antagonist in FGF-induced tracheal branching in this species (Hacohen *et al.*, 1998). Up to four members of Spry have been identified in mammals (Spry1-4). Only Spry1 and Spry2 are detected in mouse lenses. They are expressed both in the epithelial cells and fibre cells in the early lens development, and restricted to lens epithelial cells after birth (Boros *et al.*, 2006). Spry2 is also detected in the early differentiating fibre cells in the early postnatal stage (Boros *et al.*, 2006). Sef is a transmembrane protein and its expression is restricted to vertebrates. As with Spry1 and Spry2, it is expressed in the lens epithelial cells and primary fibre cells during early lens development but is restricted to the lens epithelial cells later in mice (Boros *et al.*, 2006). Since the strongest expressions of Spry and Sef in the anterior lens epithelium are consistent with an inverse FGF gradient and bioactivity, this is possibly important for the lens epithelial cell maintenance and fibre cell differentiation. Overexpression of Sef in the lenses of transgenic mice results in the inhibition of primary fibre cell elongation and differentiation, as well as the increase of apoptosis, which impairs lens and eye development and leads to microphthalmia (Newitt *et al.*, 2010). The inhibition is reported to be associated with the disruption of ERK1/2 signalling (Newitt *et al.*, 2010; Ron *et al.*, 2008).

1.4.1.2 Other growth factors

Platelet-derived growth factor (PDGF) is strongly expressed in the iris and ciliary body, and regulates lens epithelial cell proliferation by inducing a dose and time dependent increase in lens cell DNA synthesis (Kok *et al.*, 2002). The PDGF

family includes four gene products that form five dimeric isoforms: αα, ββ, αβ, CC and DD (Fredriksson *et al.*, 2004). The expression of PDGFα receptor, which binds to both PDGF-A and PDGF-B, is detected in the lens epithelium throughout life. Overexpression of PDGF-A in the transgenic lenses results in abnormally high levels of Cyclin A and Cyclin D2 expression and an increased percentage of epithelial cells in S-phase (Reneker L.W., 1996). However, the deletion of PDGFα receptor does not influence lens shape or epithelial cell proliferation (Soriano, 1997). PDGF-D also induces lens epithelial cell proliferation and this ability can be strongly inhibited by anti-PDGF-D (Ray *et al.*, 2005).

Insulin growth factor 1 (IGF-1) has been detected in the aqueous and vitreous humours (Arnold *et al.*, 1993; Beebe *et al.*, 1987). The receptors of IGF-1 and insulin are present in the lens epithelial and fibre cells (Bassnett and Beebe, 1990; Palmade *et al.*, 1994). Overexpression of IGF-1 in mouse lenses not only increases lens epithelial proliferation but also extends the GZ and TZ to the posterior lens pole (Shirke *et al.*, 2001). This indicates that endogeous IGF-1 probably also provides a spatial cue that helps to control the normal location of the GZ and TZ. Interestingly, the overexpression of IGF-1 in chick lens epithelial cells is reported to be different from that in mice and it causes fibre cell differentiation (Beebe *et al.*, 1987).

The epidermal growth factor (EGF) family consists of at least eight different hormones, including EGF and transforming growth factor alpha (TGFα). All of them can act as ligands for EGF receptors (EGFRs) (Riese and Stern, 1998). Traces of EGF have been detected in the human aqueous humour (Tripathi *et al.*, 1991) and its receptor, EGFR, is evenly distributed in the human lens epithelium (Maidment *et al.*, 2004). EGF can trigger lens epithelial cell proliferation and increase DNA synthesis *in vitro* (Reddan and Wilson-Dziedzic, 1983). By incubating EGF with the central and peripheral human lens epithelial cells, Maidment and colleagues found that EGF activated a higher level of extracellular signal-regulated kinase (ERK) and phospholipase C (PLC)-γ in the periphery than at the centre of the lens epithelium (Maidment *et al.*, 2004). This suggests that EGF may play a role in GZ cell proliferation.

In vitro and *in vivo* experiments show that IGF-1, PDGF and EGF cannot induce fibre differentiation independently, while they can potentiate FGF-induced fibre differentiation when combined with FGF-2 (Chandrasekher and Sailaja, 2003;

Kok *et al.*, 2002; Liu *et al.*, 1996; Richardson *et al.*, 1993; Wang *et al.*, 2010). Inhibition of their receptors partially blocks vitreous-induced fibre differentiation in the rat lens epithelial explants (Wang *et al.*, 2010).

Members of the TGFβ superfamily, especially TGFβ2, are abundant in the aqueous humour (Chowdhury *et al.*, 2010; Jampel *et al.*, 1990). TGFβ has been implicated in various stages of lens development and functions by binding to and activating the type I and type II receptors (de Iongh *et al.*, 2001b), which have been found in lens epithelial cells (de Iongh *et al.*, 2001a). Unlike other growth factors, TGFβ2 is shown to inhibit lens epithelial cell proliferation *in vitro* (Wormstone *et al.*, 2004). This is possibly because TGFβ2 can block the late G1 activation of the cyclin-dependent kinases, thereby preventing pRb phosphorylation and S phase entry (Hocevar and Howe, 1998). Overexpression of dominant-negative type II receptors does not significantly influence lens epithelial cell proliferation (de Iongh *et al.*, 2001b), which suggests other factors inhibiting cell proliferation are probably present in the lens.

BMPs also play a role in regulating fibre differentiation. They appear to be important for the promotion of fibre cell elongation. Inhibition of BMPs by noggin can block vitreous-induced cell elongation in the chick lens epithelial explants, and this can be restored by adding BMPs to the vitreous humour (Belecky-Adams *et al.*, 2002). In the mouse lens epithelial explants, both noggin and a dominant-negative form of type 1 BMP family receptor Alk6 suppress the differentiation of primary lens fibre cells (Faber *et al.*, 2002).

1.4.2 Downstream signalling pathways

The pathways activated by growth factors include the Ras/Raf/MEK/MAPK pathway, the PI3-K/AKT pathway (Iyengar *et al.*, 2006), the PLCγ pathway (responsible for intracellular calcium release and PKC activation) (Sa and Das, 1999), and the Src family kinases (Hunter, 2000). By now the well-characterised downstream pathways are the first two, especially the Ras/Raf/MEK/MAPK pathway.

1.4.2.1 Ras/Raf/MEK/MAPK pathway

After receptor tyrosine kinase (RTK) is activated by growth factors, it then activates Ras from the GDP (guanosine diphosphate)-bound inactive state to the GTP

(guanosine triphosphate)-bound active state (Xie *et al.*, 2006). Ras is a small guanine nucleotide-binding protein. It in turn activates the downstream mitogen-activated protein kinase (MAPK) signalling pathway, which is organised hierarchically into three-tiered modules. Ras first activates the first module called MAPK kinase kinases (MAPKKKs), which mainly consist of the isoforms of the serine/threonine kinase Raf (e.g. A-Raf, B-Raf, C-Raf and Tpi2/cot1). The activated MAPKKKs in turn phosphorylate MAPK kinases (MAPKKs), which in turn stimulate MAPK activity through dual phosphorylation on threonine and tyrosine residues located in the activation loop of kinase subdomain VIII. The activated MAPKs then phosphorylate target substrates on serine or threonine residues followed by a proline (Krishna and Narang, 2008).

To date, six distinct groups of MAPKs have been characterised in mammals: ERK1/2 (also called p44/42), c-Jun amino-terminal kinases/stress-activated protein kinases (JNKs/SAPKs) 1, 2, and 3, p38 isoforms α, β, γ, and δ, ERK7/8, ERKs 3 and 4, and ERK5 (Chen *et al.*, 2001; Krishna and Narang, 2008; Kyriakis and Avruch, 2001). The most extensively studied groups of vertebrate MAPKs are the ERK1/2, JNKs/SAPKs and p38 kinases. JNK/SAPK and p38 are mainly activated by stress stimuli (e.g. osmotic shock, ionizing radiation and cytokine stimulation), while ERK1/2 is preferentially activated by growth factors, serum and phorbol esters, and is a key regulator of cell proliferation and differentiation (Lovicu and McAvoy, 2001; Roux and Blenis, 2004).

Some ERK1/2 is distributed throughout quiescent cells, especially in the cytoplasm. Once it is activated by MAPKK1 and 2 (MEK1/2), a significant amount of ERK1/2 accumulates in the nucleus (Lenormand *et al.*, 1993). The mechanism involved in this nuclear accumulation is still unclear yet. The activated ERK1/2 phosphorylates numerous substrates in all cellular compartments, including various cytosolic and membrane proteins (PLA2, CD120a, Syk and calnexin), nuclear substrates (Elk-1, c-Fos, c-Myc, SRC-1, Pax6, NF-AT and STAT3), cytoskeletal proteins and other MAPK-activated protein kinases (MKs) [e.g. the p90 ribosomal S6 kinases (RSK 1-4), the MAPK-interacting kinases (MNK1 and 2), mitogen and stress activated kinases (MSK1 and 2)] (Krishna and Narang, 2008). ERK1/2 regulates cell proliferation and differentiation mainly by activating or up-regulating the transcription factors in the nucleus. For example, the phosphorylation of Elk-1 can induce the transactivation of genes; *c-Fos*, *c-Myc and c-Jun* that can be activated by

ERK1/2 are all important regulators of downstream gene expression. Furthermore, ERK1/2 regulates cell proliferation by activating important transcription factors in the cell cycle such as cyclin D (Lavoie *et al.*, 1996), p21 (Coller *et al.*, 2000), and cdc25 (Galaktionov *et al.*, 1996). The inhibitors of MEK1/2/5 (U0126 and PD98059) prevent the activation of ERK1/2 and block the growth factor-stimulated global protein synthesis and pyrimidine synthesis (Servant *et al.*, 1996).

Duration and levels of phosphorylated ERK1/2 determines lens cells fate. A lower dose of FGF and aqueous humour can only stimulate a low level of ERK1/2 phosphorylation for a short time and induce lens epithelial proliferation. However, a high dose of FGF and vitreous humour stimulate and maintain a prolonged and higher level of ERK1/2 phosphorylation, which results in lens fibre differentiation (Iyengar *et al.*, 2007; Lovicu and McAvoy, 2001). This phenomenon is also found in other cells such as PC12 cells, a cell line derived from a pheochromocytoma of the rat adrenal medulla (Dailey *et al.*, 2005). How the duration of ERK1/2 results in different cellular responses is proposed to be due to its stimulatory effects on its downstream targets (e.g., Elk-1) and the expression of immediate-early genes (e.g., *c-Fos* and *Egr-1*). For example, EGF only induces a transient ERK1/2 phosphorylation, which leads to a weaker effect of Elk-1 during EGF-induced PC12 cell proliferation, while the sustained ERK1/2 phosphorylation possibly has a greater stimulatory effect on Elk-1 in nerve growth factor-induced PC12 cell differentiation (York *et al.*, 1998). The immediate-early genes can normally be induced by any activated ERK1/2 but their subsequent phosphorylation and stability, which may permit different gene expression governing the specificity of the cellular response, require a prolonged, sustained activation status of ERK1/2 (Murphy *et al.*, 2002). If FGFR is selectively blocked, the level and sustained time of ERK1/2 phosphorylation stimulated by the vitreous humour in rat lens epithelial explants can be effectively reduced (Iyengar *et al.*, 2007). Similarly, if ERK1/2 signalling is selectively blocked by its inhibitor U0126, both FGF- and vitreous-activated ERK1/2 phosphorylation remains at basal levels (Wang *et al.*, 2009b). Interestingly, the blocking of FGFR inhibits lens epithelial cells from elongating and accumulating fibre specific β-crystallin, while the blocking of ERK1/2 just inhibits cell elongation but does not stop the β- and γ-crystallins expression (Iyengar *et al.*, 2007; Wang *et al.*, 2009b). This suggests that ERK1/2 is important to cell elongation but not to accumulation of fibre-specific proteins during lens fibre

differentiation. Therefore, there must be other signalling pathways that are related to FGF-induced fibre differentiation.

1.4.2.2 PI3-K/AKT pathway

The PI3-K/AKT pathway can be activated by mitogenic stimulus such as FGF, IGF, PDGF or EGF and regulates cell proliferation, differentiation, cell migration, tubule formation and cell apoptosis (Osaki *et al.*, 2004). The key components of the PI3K/AKT pathway are phosphatidylinositol-3-kinase (PI3K) and AKT (protein kinase identified in the AKT virus. AK was a temporary classification name for a mouse strain developing spontaneous thymic lymphomas. The "t" stands for “transforming”. AKT is also known as protein kinase B, PKB). PI3-K is a heterodimer composed of a catalytic subunit (p110) and a regulator/adapter subunit (p85), which can be activated by RTK or G protein-coupled receptors (Katso *et al.*, 2001). The activated PI3K converts the plasma membrane lipid phosphatidylinositol-4, 5-biphosphate (PIP2) into the second messenger phosphatidylinositol-3,4,5-triphosphate (PIP3). The increase of PIP3 level causes AKT to translocate to the plasma membrane and bind to the phospholipids through its pleckstrin homology domains (Osaki *et al.*, 2004). The activation of AKT requires phosphorylation of Thr 308 in the kinase domain and of Ser473 in the C-terminal regulatory domain (Brunet *et al.*, 2001). After AKT is activated, it relocates to several subcellular sites and phophorylates its substrates such as glycogen synthase kinase-3 (GSK-3) (Cross *et al.*, 1995), membrane translocation of the glucose transporter GLUT4 (Wang *et al.*, 1999), cyclin-dependent kinase inhibitors P21/Waf1/Cip1 (Diehl *et al.*, 1998), P27/Kip2 (Liang *et al.*, 2002), mammalian target of rapamycin (mTOR) (Sekulic *et al.*, 2000) and tuberous sclerosis complex 2 (TSC2) (McManus and Alessi, 2002). It is reported that AKT inhibits GSK3 (Cross *et al.*, 1995) and this inhibition further prevents the phosphorylation of the cytoplasmic signalling molecule β-catenin. Therefore, β-catenin avoids its degradation and translocates to the nucleus, where it combines with transcription factors like TCF/LEF-2 to induce the cell cycle-related gene expression such as *Cyclin D1*. The inactivated P21/Waf1/Cip1 and P27/Kip2 inhibit cell proliferation by inhibiting the activation of Cyclin/Cdk complex, especially CyclinD1/Cdk4. Once they are activated by AKT, they stay in the cytoplasm and their inhibition effect to cell proliferation is relieved (Liang *et al.*,

2002; Viglietto *et al.*, 2002). The activation of mTOR by AKT promotes the translation of Cyclin D mRNA and regulates cell proliferation (Muise-Helmericks *et al.*, 1998). Furthermore, the phosphorylation of TSC2 by AKT can inhibit its growth suppressor function (Li *et al.*, 2004).

In the lens, PI3-K/AKT pathway has been reported to regulate lens epithelial cell proliferation (Iyengar *et al.*, 2006) and fibre cell differentiation (Wang *et al.*, 2009b). If PI3-K inhibitor blocks this signalling pathway, the AKT phosphorylation will remain at its basal level and all the cells in the FGF-treated lens epithelial explants, or many cells in the vitreous-treated epithelial explants, will fail to elongate and express β-crystallin. These results also indicate that FGF cannot completely substitute for the vitreous humour. Other growth factors in the vitreous humour, especially IGF, are also able to stimulate strong and sustained AKT phosphorylation (Wang *et al.*, 2010). These growth factors cannot initiate fibre differentiation independently, but they can potentiate FGF-induced fibre differentiation by activating PI3K/AKT and ERK1/2 signalling pathways.

1.5 Lens ageing

1.5.1 Lens growth

1.5.1.1 Lens weight

The eye lens grows throughout life. New fibre cells are continuously laid down over existing fibre cells. This is unlike other stratified epithelia such as skin epithelium, in which the older uppermost strata are routinely sloughed off. The lens does not lose any cells throughout life because the cells are enclosed by the lens capsule. Therefore, it continues to grow larger with age. One of the simplest and most reliable ways to assess lens growth is lens weight (Augusteyn, 2008).

Two kinds of weights, dry weight and wet weight, are usually measured. Dry weight is often used as a measure of age when culling and monitoring animal population in the wild (Augusteyn, 2007b; Connolly *et al.*, 1969; Friend, 1967; Hagen A, 1980; Hockwin 1971). In many studies on the human lenses, wet weight is used to assess lens growth with age (Augusteyn, 2008; Rosen *et al.*, 2006). Both kinds of measurement show that the lenses grow faster at the early stage and slower but

continuously throughout the rest of the life span. By comparing primate (e.g., human) lens weight with other non-primates (e.g., kangaroo, rabbit and bovine) carefully, it is found that primates have a biphasic lens growth while the others just have one phase (Augusteyn, 2007a; Augusteyn *et al.*, 2003b; Myers and Gilbert, 1968; Pierscionek and Augusteyn, 1992; Wheeler and King, 1980). For example, human lens growth is asymptotic during prenatal life and early childhood, and becomes linear from around age three (Augusteyn, 2007a; Augusteyn, 2010; Bours and Fodisch, 1986), while the growth of non-primate lenses is asymptotic throughout life (Augusteyn, 2007a). Furthermore, the change of lens weight with age is not influenced by gender (Augusteyn, 2007a; Augusteyn *et al.*, 2003a; Catling *et al.*, 1991), environment (Augusteyn, 2008), diet (Kauffman and Norton, 1966; Priolo *et al.*, 2000; Teska and Pinder, 1986) or body size (Augusteyn, 2008). It is not clear why the primate lens growth has two phases while other species have just one. Possibly it indicates that the prenatal and postnatal growth of primate lenses have different regulatory mechanisms.

1.5.1.2 Lens dimensions

Lens dimensions are another important indicator of lens growth with age. They consist of lens equatorial diameter (D) and anterior and posterior sagittal thickness (T). Studies on the changes of lens dimensions with age have so far mainly involved in the human lenses.

Although the primary fibre cells fill in the lumen of the lens vesicle during about 54 to 56 days' gestation in human, most measurements of the lens size are taken from 14 or 15 weeks' gestation when the lenses are big enough to be recognized in ultrasonography. The lens equatorial diameter is about 2.5 mm in the fourteenth week and shows a linear increase with gestational age (Dilmen *et al.*, 2002; Goldstein *et al.*, 1998; Sukonpan and Phupong, 2009). In the fortieth week, it is about 6.28 mm. No report is found about the lens sagittal thickness change during gestation.

After birth, lens equatorial diameter increases fast in the early childhood and slowly later (Augusteyn, 2008; Augusteyn, 2010; Kasthurirangan *et al.*, 2008; Rosen *et al.*, 2006). At birth, the lens is more spherical than in adult life. Its sagittal thickness is about 4 mm. This thickness is found to continuously decrease to around 3.3 mm at age 10 years (Augusteyn, 2010; Mutti *et al.*, 1998). With the lens becoming more elliptical, its refractive power also decreases from about 43.5D (Wood *et al.*, 1996) in

infancy to 22.9D at age 10 years (Mutti *et al.*, 1998). The lens equatorial diameter continuously increases during this period. Therefore, the change of the ratio between lens equatorial diameter and sagittal thickness (D/T) directly reflects the lens flattening. The ratio is about 1.5 at birth and increases to 2.2 in early adult life (Augusteyn, 2008). Since there is no turnover of protein, the lens thinning must involve water loss and redistribution of cytoplasm and proteins in the fibre cells. Moreover, it is possibly due in part to the increased zonular tension in the anterior side (Hiraoka *et al.*, 2010).

In adults, the lens equatorial diameter shows a linear increase with age, about 0.0138 mm per year (Rosen *et al.*, 2006). Both the anterior and posterior sagittal thicknesses also increase at a linear rate but their ratio (anterior sagittal thickness/posterior sagittal thickness) is constant at 0.7 (Rosen *et al.*, 2006). A similar sagittal thickness increase with age is detected in bovine lenses and the ratio is constant at 0.84 (Pierscionek and Augusteyn, 1992).

The orbit does not change any more once fully developed and its cavity size is limited. How can lens dimension continue to increase with accommodation and age without influencing other tissues inside the eye? *In vivo* studies show that anterior chamber depth decreases with accommodation and age while the lens thickness increases with accommodation and age (Atchison *et al.*, 2008; Kasthurirangan *et al.*, 2008; Tsorbatzoglou *et al.*, 2007). Furthermore, the decrease in anterior chamber depth is similar to the increase in lens thickness during accommodation (Kasthurirangan *et al.*, 2011). The space between the lens equatorial edge and the ciliary body tip decreases with age (Strenk *et al.*, 2006). Whether the posterior lens surface will move toward the vitreous humour is still controversial. Koretz and colleagues found that the posterior lens surface remains fixed in position relative to both the cornea and retina (Koretz *et al.*, 1989). However, others have observed that the distance between the anterior cornea and posterior lens surface increased with age, which means that the lens moves towards the vitreous humour with age (Brown, 1973; Kasthurirangan *et al.*, 2011)

1.5.2 Compaction

1.5.2.1 Water loss

In order to cater for the limited intraocular space and produce a high refractive index, the lens fibre cells are compacted. If no compaction occurred, human lenses would be probably two or three times larger, and rodent lenses would be up to five times larger (Augusteyn, 2010). Once fibre cells lose their organelles in the cortex, no further protein synthesis or degradation will occur. Therefore, the compaction is possibly obtained by water loss, which in turn results in the loss of cell volume without reduction in cell surface area (Augusteyn, 2010).

It has been difficult to correctly measure the water content in the nucleus. The values that have been reported vary from 50% to 85% in the human lenses (Bours *et al.*, 1990; Heys *et al.*, 2004; Huizinga *et al.*, 1989; Siebinga *et al.*, 1991). The differences in these findings are mainly due to the prolonged storage of the lenses in eye banks and the methods used for tissue preparation and assessment. Therefore, the water loss can be indirectly shown by the fibre size change with age. The results of scanning electron microscope studies show that the fibre thickness in the foetal nucleus decreases with age from 2.35 μm in 15-25-year-old (young) lenses to 1.82 μm in 36-46-year-old (middle-aged) lenses and 1.73 μm in 59-81-year-old (old) lenses (Al-Ghoul *et al.*, 2001). The posterior fibre end thickness also decreased from 2.49 μm in the young lenses to 1.97 μm in middle-aged lenses and 1.96 μm in the old lenses (Al-Ghoul *et al.*, 2001). The decrease of fibre cell thickness is mainly attributed to water loss with age. Furthermore, the anterior-posterior axis length of the embryonic nucleus, which is encircled by the foetal fibre cells, is 35% shorter in the old lenses as compared with the young lenses. This also indicates fibre cell compaction and water loss.

The driving force for the loss of water is not very clear. It is possibly because the γ-crystallins tend to self-associate into larger aggregates with age, which decreases their requirement for interaction with water, then causes the nuclear cytoplasm to have a reduced osmolarity (Kenworthy *et al.*, 1994; Tardieu *et al.*, 1992). The decrease of osmolarity is necessary for the water exit from the nuclear fibre cells with high concentrations of proteins to adjacent cortical fibre cells with relatively high water content. The synthesis of γ-crystallins stops after birth in the primate lenses while it continues throughout life in the rodent lenses. Therefore, the rodent lenses are

found to lose more water than primate lenses, which results in higher refractive index levels and harder tissues. In contrast, bird and reptile lenses, which do not contain γ-crystallins, do not appear to compress at all throughout life (Augusteyn, 2008).

1.5.2.2 Lens refractive index gradient

As the lens growth speed is different throughout life in humans, the fibre cells are compacted into the nucleus at different speeds. It is observed by slit-lamp examination that adult human lenses show a layered structure with zones of discontinuity (Berliner, 1949; Duke-Elder and Cook, 1963). From outside to inside, the lens consists of the cortex, adult nucleus, juvenile nucleus (also called infantile nucleus), foetal nucleus and embryonic nucleus. The combined nuclear layers represent about 60-70% of the total lens thickness (Augusteyn, 2010). With the increase of water loss from the cortex to the embryonic nucleus, the protein concentration continues to rise, which results in the increase of the refractive index and the generation of a refractive index gradient (Augusteyn, 2008). A refractive index gradient is necessary for a short focal length and for reducing spherical aberration. As well as human lenses, other mammal lenses (e.g., rat, cow, guinea pig, gibbon and baboon lenses) and fish lenses also have a refractive index gradient (Campbell and Hughes, 1981; Pierscionek, 2005; Pierscionek *et al.*, 1988). In most species studied, the refractive index at the centre increases with age (Pierscionek and Augusteyn, 1993). However, the human lens is different. Its refractive index does not increase beyond 1.418. The refractive index gradient becomes a sharper increase in the periphery while it becomes much flatter at the centre, with the appearance of a much wider plateau with increasing age (Augusteyn *et al.*, 2008). Similar characteristics are also found in gibbons (Pierscionek, 2005). By studying the human lenses in different ages *in vitro*, it is found that the refractive index plateau is very small at age seven years while it gradually increases in both sagittal and equatorial directions until about age 60 years. Thereafter, no further increases are observed although the lens dimension still increases (Augusteyn *et al.*, 2008; Jones *et al.*, 2005). Furthermore, the refractive index gradient is shallower in the outer 0-1 mm in the youngest eyes than that in the 60-year-old lenses (Pierscionek and Chan, 1989).

The maximum dimension of the plateau is about 7.0 (equatorial) × 3.05 (sagittal) mm, which is very similar to the isolated nucleus (7.0 × 3.05 mm) obtained

by hydrodissection (Gullapalli *et al.*, 1995) and to the location of the diffusion barrier (7.2 × 2.8 mm from the centre) (Sweeney and Truscott, 1998). Compared with the continuous water loss and fibre cell compaction, the result of the constant refractive index at the centre looks contradictory. In fact, fibre cell compaction and water loss are very slow after 60 years old. Compared with 0.53 μm from young (15-25-year-old) lenses to middle-aged (36-46-year-old) lenses, the fibre thickness only increases 0.09 μm from middle-aged lenses to old lenses (Al-Ghoul *et al.*, 2001). Therefore, the presence of a plateau with a stable dimension in the human lenses is reasonable.

1.5.3 Lens stiffness

Lens stiffness is considered as the main reason for the development of presbyopia, which involves in a loss of accommodative ability by the age of 50 in humans, and renders people unable to focus on near objects (Augusteyn, 2010). Heys and colleagues found that lens stiffness increased almost 1000-fold in the nucleus and about 20-fold in the cortex over the age range from 14 to 78, with the largest change observed in the lenses between the ages of 20 and 60 (Heys *et al.*, 2004). While Weeber and colleagues even reported stiffness changes of as much as 10000-fold in the nucleus and 100-fold in the cortex of lenses ranging from age 19 years to age 78 years (Weeber *et al.*, 2007). Both studies detect that the cortex (that is at 3.0 to 3.5 mm to the centre) is stiffer than the nucleus in the lenses younger than 30 years. How the cortex could be stiffer is very difficult to explain. Possibly it is because the prenatal and postnatal tissues, which are separated at about 3 mm from the centre, have different properties before the stiffening process commences (Augusteyn, 2007a).

Surprisingly, there appears to be no relationship between compaction judged by refractive index and stiffness. For example, the refractive index at the nuclear centre remains consistent from age 20 years to age 80 years while lens stiffness increases nearly 1000-fold (Heys *et al.*, 2004). This indicates that lens stiffness is not caused by compaction. The exact reason for the lens stiffness change with age is still unclear. Three possible assumptions have been proposed to explain it. First, the progressive decrease of soluble α-crystallin with age, which results from its modification into high molecular weight aggregates and insoluble protein, probably increases lens stiffness (Heys *et al.*, 2007; Wilmarth *et al.*, 2006). Second, the age-related changes of

the phospholipids in the lens fibre membrane may increase membrane stiffness, which then results in the increase of lens stiffness (Huang *et al.*, 2005). Third, the cell-cell interactions probably change with age and this may influence lens stiffness. This is suggested by the observation that the nucleus remains intact while the cortex and young lenses disintegrate when old human lenses are lyophilised (Truscott and Augusteyn, 1977)

1.5.4 Presbyopia

Presbyopia is the loss of ability to focus for near vision that occurs universally with increasing age (Bron *et al.*, 2000). The word comes from the Greek word presbys*,* meaning old man or elder, and the Latin suffix -opia, meaning sightedness. It is usually first symptomatic in the fourth and fifth decades.

To understand presbyopia, it is necessary to understand accommodation first. Accommodation is defined as a dioptric change in the power of the eye (Keeney *et al.*, 1995; Millodot, 1997). Mammals, birds and reptiles change their optical power by varying the form of their elastic lens. Fish and amphibians change power by changing the distance between the rigid lens and the retina. Here it is mainly human accommodation that is described. The anatomical structures that participate in accommodation include the ciliary muscle, the zonular fibres and the lens. When the eye is at rest and focuses for distance, the ciliary muscle is relaxed but the anterior zonular fibres around the lens equator are in tension, which causes the surface of the lens to flatten and the optical power of the lens to decrease (Glasser, 2008). The lens is held in an unaccommodated state. When the eye focuses for near objects, the ciliary muscle contracts and the anterior ciliary body moves forward and towards the axis of the eye (Bacskulin *et al.*, 1995; Bacskulin *et al.*, 1996; Glasser and Kaufman, 1999; Strenk *et al.*, 1999), which decreases the equatorial circumlenticular space and releases zonular fibre tension. The soft lens is then able to round up to increase the optical power and stay in an accommodated state (Glasser, 2008). During accommodation, the sagittal thickness increases and this is mainly attributed to the lens nucleus shape change, with the cortical thickness remaining unaltered (Bron *et al.*, 2000). In fact, the accommodation ability in humans continuously declines throughout life, from an accommodation of about 20 dioptres (ability to focus at

50 mm away) in a child, to 10 dioptres at age 25 (100 mm), and levels off at 0.5 to 1 dioptre at age 60 (ability to focus down to 1-2 m).

The first signs of presbyopia such as eyestrain, difficulty seeing in dim light, problems focusing on small objects and/or fine print, usually become apparent between the ages of 40 and 50. The real aetiology of presbyopia still remains unclear. Since it affects people at the age of around 50, the changes of accommodative structure with age are considered as the causes of presbyopia, which include the configurational change in the ciliary body (Strenk *et al.*, 1999; Strenk *et al.*, 2006), anterior shift of the zonular insertion onto the lens (Farnsworth and Shyne, 1979), lens capsule elasticity and thickness changes (Krag and Andreassen, 2003a; Krag and Andreassen, 2003b; Krag *et al.*, 1997) and lens growth with age (Augusteyn, 2010). Glass and Campbell found that intact lenses extracted from donor eyes older than 60 could not change shape when forces were applied to them (Glasser and Campbell, 1998). Based on this evidence, they suggest that the increasing lens stiffness and the decreasing elasticity with age may account for the loss of accommodation and the development of presbyopia (Glasser and Campbell, 1999).

The most common correction from presbyopia is by reading glasses and bifocal or progressive addition lenses (Evans, 2007). Another kind of correction is monovision, in which one eye is focussed for distance vision and the other for near (Evans, 2007). Some surgical approaches, such as near vision conductive keratoplasty, multifocal corneal refractive surgical procedures and monovision through corneal refractive surgery, implanting multifocal intraocular lenses (IOLs) or accommodative IOLs during standard cataract surgery (Glasser, 2008), are also used to treat presbyopia.

1.6 Lens pathology: cataract

1.6.1 Cataract classification

Cataract is defined as lens opacities or loss of lens optical clarity for any reason (Asbell *et al.*, 2005). It is the most common reason of reversible loss of useful vision worldwide, especially in middle and low-income countries. Several systems have been developed to classify cataract. Here three most common clinical classifications used in clinical are described. (1) According to aetiology, cataract can be classified

into four types: age-related cataract, congenital cataract, traumatic cataract and secondary cataract. (2) According to anatomic location and clinical appearance, cataract is mainly divided into nuclear cataract, cortical cataract, and posterior subcapsular cataract (Asbell *et al.*, 2005; Delcourt *et al.*, 2000). These three types of cataract can present alone or in combination. (3) Based on the degree of nuclear colour, cataract is classified into four types (Pirie, 1968). Type I lenses are uniform pale yellow. Type II lenses have pale cortex with visible nucleus. Type III lenses have pale cortex with hazel brown nucleus. Type IV lenses have pale cortex with deep brown nucleus. The darker the nucleus colour is, the much harder the nucleus is and the more difficult it is to remove during surgery.

1.6.2 Age-related cataract

Age-related cataract means that cataract is caused by ageing. It is the most common type of cataract and responsible for 48% of world blindness, which represents about 18 million people, according to the latest world health organisation (WHO) assessment. It happens not only in humans, but also in other mammals such as mice (Graw, 2009; Wolf *et al.*, 2005), rats (Wolf *et al.*, 2000), and dogs (Urfer *et al.*, 2010; Williams *et al.*, 2004), as well as in birds (Slatter *et al.*, 1983). However, the human lenses are quite different from the lenses of other species in terms of ultraviolet (UV) filter, protein and crystallin contents, antioxidant enzyme, oxidation degree with age and other factors (Truscott, 2005). Although some animal models are used to study the reasons of age-related cataract, they cannot fully display the mechanisms of human age-related cataract. Therefore, here mainly the causes, lens pathogenesis, symptoms and signs, and treatment of human age-related cataract are described.

1.6.2.1 Causes

The exact causes of age-related cataract are unknown. Some risk factors are proposed to lead to age-related cataract. Age is the major risk factor for cortical and nuclear age-related cataracts. It is reported that 10.1%-12.3% of people below age 70 years developed cataract while 62.4-73.7% of people over age 80 years had cataract (Delcourt *et al.*, 2000). Genetic factors also account for as much as 50% of the severity of nuclear age-related cataract in the study of monozygotic and dizygotic

twins (Hammond *et al.*, 2000). Some studies suggest that the prevalence of cataract in women is slightly higher than in men (Delcourt *et al.*, 2000). Smoking is significantly associated with nuclear age-related cataract development (Delcourt *et al.*, 2000; Klein *et al.*, 2003). The higher total cumulative dose of smoking results in a more serious nuclear opacity (Christen *et al.*, 2000; Klein *et al.*, 1999; West *et al.*, 1989). Cumulative UV light exposure is also linked to the development of cataract, especially cortical cataract in men (Cruickshanks *et al.*, 1992; McCarty and Taylor, 2002; Taylor *et al.*, 1988). Lower socioeconomic nutrition status increases the prevalence of cortical and nuclear age-related cataract (Asbell *et al.*, 2005; Delcourt *et al.*, 2005). Diabetes shows a robust correlation with cortical and posterior subcapsular cataracts (Sabanayagam *et al.*, 2011; Tan *et al.*, 2008b). The use of long-term and high doses of systemic corticosteroid has been strongly related to posterior subcapsular cataract and nuclear cataract (Praveen *et al.*, 2011; Wang *et al.*, 2009a). Topical, peri-ocular and introcular injections of corticosteroids or inhaled corticosteroids can also result in cataract (Kiernan and Mieler, 2009; Wang *et al.*, 2009a). Other diseases such as hypertension are also found to be associated with cataract development (Sabanayagam *et al.*, 2011).

1.6.2.2 Pathogenesis

1.6.2.2.1 Increased protein damage and loss of chaperone activity

α-crystallin is the major lens protein and functions like a chaperone to prevent cellular aggregation and maintain lens transparency. It undergoes many age-related post-translational modifications including truncation, deamidation, glycation, carbamylation, cys-methylation, phosphorylation and acetylation (Grey and Schey, 2009; Michael and Bron, 2011; Sharma and Santhoshkumar, 2009). The intact, soluble, non-cross-linked α-crystallin products, which are found in both the cortex and nucleus of young lenses, can be detected in only the cortex of the old lenses (Grey and Schey, 2009). The modifications reduce the chaperone activity of α-crystallin, and the modified crystallins easily aggregate, which causes the lens to lose its transparency gradually and become opaque (Sharma and Santhoshkumar, 2009). Moreover, the membrane proteins, connexins and AQP0, are also cleaved in the old lenses (Ball *et al.*, 2003; Kistler *et al.*, 1986). These truncations may lead to

alterations to the functional properties of these channel proteins and contribute to the development of the small molecular barrier.

1.6.2.2.2 Development of lens barrier and increasing oxidation in the nucleus

At middle age, an internal barrier to the diffusion of small molecules develops at the nucleus/cortex interface (Moffat *et al.*, 1999; Sweeney and Truscott, 1998). This barrier limits the flow of antioxidants into the nucleus and thus inclines the lens centre towards oxidation (Truscott, 2005; Truscott and Zhu, 2010). Its formation is possibly related to the large-scale binding of protein aggregates to the cell membrane at middle age (Truscott and Zhu, 2010).

Glutathione (GSH) is the most important antioxidant in the lens (Giblin, 2000). Its precursor, cysteine, enters the lens at the GZ and is synthesised into GSH in the cortex. Any oxidized glutathione can be rapidly reduced to GSH by glutathione reductase in the presence of nicotinamide adenine dinucleotide phosphate (NADPH). GSH protects exposed protein thiols from oxidation by scavenging reactive molecules directly (Michael and Bron, 2011). The synthesis and recycling of GSH decrease with age. Furthermore, the formation of the lens barrier at middle age impedes inward diffusion of GSH into the lens nucleus (Sweeney and Truscott, 1998). This results in the low level of GSH in the nucleus and makes the nucleus especially vulnerable to oxidative stress.

1.6.2.2.3 UV filter changes with age

The human lens contains several UV filter compounds that absorb UV light, especially UVA, in the 300-400 nm region of the spectrum, and protect the lens and retina from UV-induced photodamage. It is found that the concentration of some UV filters, including 3-hydroxykynurenine O-β-d-glucoside (3OHKG), kynurenine and 3-hydroxykynurenine, decays by approximately 12% per decade (Bova *et al.*, 2001). Therefore, more UVA may reach the nuclear proteins of the old lenses and cause protein modification (Truscott, 2005). The delaminated 3OHKG, a major UV filter, is present in the cataractous human lens in a relatively high concentration (Snytnikova *et*

al., 2008). This is mainly caused by the low concentration of GSH, which normally changes the delaminated 3OHKG into GSH-3OHKG.

1.6.2.3 Signs and symptoms

Age-related cataract develops slowly over time. Lens opacity can exist without any vision problems and be discovered incidentally. Many age-related cataracts at the early stage are diagnosed during routine comprehensive eye examination. When the wedge-shaped cortical opacity extends into the papillary zone or the nucleus or subcapsular opacity becomes more serious, the patients have gradual painless decrease of vision at distance, near, in one or both eyes. The vision decrease is more obvious at night and patients may see halos around lights (Michael and Bron, 2011). This is because the pupils dilate at night and the radial, circular and band opacities in the periphery affect vision. Some patients also complain of glare, sensitivity to light, double vision or multiple visions in one eye (Asbell *et al.*, 2005). As the age-related nuclear cataract often accompanies an exaggeration of lens volume, the refractive index increases and symptoms of myopia appear. The patients with hyperopia can see near and far things clearly without spectacles. This phenomenon is called second sight of the aged. With the continuous development of cataract, the patients possibly lose vision finally.

The opacity degree and characteristics are different in different kinds of age-related cataract. In the early stage of cortical cataract, some small, dot-like opacity measuring several micrometres in diameter first appear in the lens periphery. Then some radical and circular lens opacities appear in the periphery. Radial opacities run perpendicular and circular opacities run parallel to the equatorial circumference of the lens. Later these small opacities merge and show a typical spoke-shaped cataract, also referred to as cuneiform or wedge-shaped cataract (Michael and Bron, 2011). The spoke-shaped opacities can merge together finally and involve in the whole lens cortex. Subcapsular cataract usually shows a discoid opacity subjacent to the lens capsule at the anterior or posterior pole. In the clinical context, posterior subcapsular cataract occurs more common than anterior subcapsular cataract. Due to its location at the nodal point of the lens, subcapsular opacity has a more profound effect on vision than a comparable cortical or nuclear cataract. Both cortical and subcapsular opacities appear white on oblique illumination in slit-lamp examination. At the early stage of

age-related nuclear cataract, the nucleus is yellow. With the accumulation of fluorescent chromophores during cataract development, the nucleus becomes brown and/or dark brunescent in late stage.

The lens opacities classification system (LOCS) III is widely used for grading the features of age-related cataract for clinical practice (Bencic *et al.*, 2005; Chylack *et al.*, 1993; Davison and Chylack, 2003; Grewal *et al.*, 2009; Karbassi *et al.*, 1993; Pei *et al.*, 2008; Tan *et al.*, 2008a). It reflects the cataract severity by scoring the nuclear opalescence, nuclear colour, cortical cataract and posterior subcapsular cataract. As LOCS III helps to estimate the severity of cataract, it becomes very important in making decisions for surgical intervention.

1.6.2.4 Treatment

Cataract at the early stage does not need to be treated. Only when vision decline influences patients' normal life, is cataract surgery performed. There is no drug or other methods to reverse or delay cataract development.

The widely used cataract surgeries are phacoemulsification and conventional extracapsular cataract extraction (ECCE). Both require making a limbal incision and removing central anterior lens capsule with epithelial cells. Conventional ECCE needs a relatively large circumferential limbal incision (8-10 mm) through which the lens nucleus is extracted and the residual cortical lens materials are aspirated (Asbell *et al.*, 2005). This procedure leaves behind an intact posterior lens capsule. An IOL is then implanted into the lens capsular bag. Since the large limbal incision can result in collapse of the eye contents during surgery and suture-induced corneal astigmatism, it is replaced by phacoemulsification that requires a small incision (2.5-3 mm). Phacoemulsification was first developed by Kelman in 1967 (Kelman, 1967). It uses high-frequency ultrasound to emulsify the lens nucleus first before the fragments are aspirated. This process only needs a small incision to insert the probe into the eye. The small limbal incision allows for the maintenance of a near-normal anterior chamber during surgery and decreases corneal astigmatism and complications. Another challenge that may be encountered is that many replacement IOLs exceed the size of the incision. The development of foldable IOLs resolves this problem. They have a diameter of 5.5-6 mm but can be folded and inserted through a 2.5-3 mm incision.

Although cataract surgery is usually very successful these days, no procedure is without risk and some complications still happen. The intraoperative complications include iris damage and haemorrhage, posterior capsule rupture, zonule damage, or prolapse of vitreous into the anterior chamber. The postoperative complications mainly consist of endophthalmitis, cystoid macular oedema, retinal detachment, vitreous haemorrhage, and posterior capsule opacification (PCO). PCO is the most common late postoperative complication. It is reported to occur in 2% to more than 50% of patients (Asbell *et al.*, 2005). A systematic review reported that it happened in 25% of eyes in the first five years after cataract surgery (Schaumberg *et al.*, 1998). The opacification happens mainly because the residual lens epithelial cells in the periphery proliferate and undergo EMT, which leads to a capsular haze and capsule wrinkles. Postoperative inflammation, the material composition of the implanted IOLs and the quality of surgery are related to the incidence of PCO (Wormstone *et al.*, 2009). If the fibrosis appears in the papillary zone, the restored visual acuity will be influenced seriously. The most common method to treat PCO is laser capsulotomy, which uses a neodymium-yttrium-aluminum-garnet laser (Nd-YAG; wavelength 1064 nm) to open a hole in the posterior capsule, allowing improved clarity of the visual axis and therefore better vision (Asbell *et al.*, 2005).

1.7 Summary

The eye lens comprises the epithelial cells, the fibre cells and the outer capsule. The single layer of epithelium is located on the anterior and part of the equatorial lens capsule. It is separated into the CZ, the GZ and the TZ depending on the cell location and proliferation ability in literature. The cells in the CZ are usually quiescent, and cell proliferation is mainly restricted to the GZ in mature lenses. The changes of proliferation index, which can correctly reflect cell proliferation, have been mainly studied on mouse or rat lens sections. However, it is very difficult to obtain the correct values because not every proliferating cell can be sectioned. The cells in the CZ have been found to be flatter and bigger than those in the GZ. How do cell height, cross-sectional area and volume change from the CZ to the GZ? Moreover, the lens is growing bigger with age and the area of the lens epithelium also increases simultaneously. How do the cells within the epithelium adapt to this change, by increase the total cell number or by increase the cross-sectional area of each cell? In

the TZ, the cells align into meridional lines and prepare for fibre cell differentiation. How many cells undergo apoptosis? Is the number of cells that will differentiate into fibre cells and die of apoptosis equal to the number of cells that are proliferated in the GZ? All these questions are very important to the cell organisation in the lens epithelium but have not been studied very well. They will be studied in chapter 2. Furthermore, since PCO is one of the most common complications in the cataract surgery, what does the cell look like in those capsular bags with PCO? Where does cell proliferation and apoptosis happen? These questions will also investigated in chapter 2.

FGF-2 is secreted from the retina and ciliary body to the aqueous and vitreous humours and regulates lens epithelial cell proliferation and fibre cell differentiation. It binds to HSPGs such as perlecan and are temporally stored there. As epithelial cell proliferation and fibre cell differentiation mainly occur at the equator and in the posterior. It is hypothesised that an antero-posterior gradient of FGF is present and there is a higher level of FGF-2 in the vitreous humour than in the aqueous humour. Previous studies have investigated the function of aqueous and vitreous humours in inducing epithelial cell proliferation and fibre cell differentiation. All the results suggest that a higher level of FGF-2 is present in the vitreous humour. FGF-2 needs to be stored in the capsule before it acts on its receptor, it is not clear whether more FGF-2 is present in the capsule which is surrounded by the vitreous humour. This is studied in chapter 3 on the bovine lens capsule by immunogold labelling.

FGF-2 regulates lens epithelial cell proliferation and fibre cell differentiation by binding to its receptors on the epithelial cell membrane and activating Ras/Raf/MEK/MAPK and PI3-K/AKT signalling pathways in the cell cytoplasm. If an FGF-2 gradient is present in the vitreous and aqueous humours, does the levels of the phosphorylated Ras/Raf/MEK/MAPK and PI3-K/AKT signalling proteins have a gradient in the lens epithelium where cell proliferation and preparation of differentiation occur in the GZ and TZ. Furthermore, it is reported that activated MAPK, especially ERK1/2, regulates cell proliferation by translocating to the nucleus and up-regulating the expression of transcription factors, while this nucleus translocation of phosphorylated ERK1/2 has not been investigated in the lens epithelial cells. The levels of Ras/Raf/MEK/MAPK and PI3-K/AKT signalling proteins and the location of phosphorylated ERK1/2 in the lens epithelial cells will be studied in chapter 4.

2 Spatial organisation of the cells in the mammalian lens epithelium

2.1 Introduction

The epithelial cells cover the anterior and equatorial lens capsule and continually provide new cells for the lens growth. A specific cell organisation is very necessary for its function. Some studies have studied the cell proliferation, cell size and cell morphology of rat, mouse, monkey and sea lamprey lens epithelia (Hendrix and Rubinson, 1996; Kuszak, 1997; McAvoy, 1978a; Yamamoto *et al.*, 2008a), and the results suggest that cell organisation within the lens epithelia of different species follow a common plan. However, some characteristics of cell organisation such as cell density have not been studied in detail, and some conclusions that have been drawn are still controversial. To better understand cell organisation in the mammalian lens epithelium and how it influences the development of PCO in the human lens capsular bags after cataract surgery, I studied the basic characteristics in five kinds of mammalian lenses and in human donor capsular bags.

2.1.1 Lens epithelial cell proliferation

Lens epithelial cell proliferation occurs in both the CZ and the GZ in the embryologic, newborn and very young lenses (McAvoy, 1978a; Rafferty and Rafferty, 1981a; Yamamoto *et al.*, 2008a). Later cell proliferation is gradually restricted to the GZ with lens growth and age. However, the epithelial cells in the CZ still retain the proliferative potential and will divide again after injury or irradiation (Kojima *et al.*, 2009; Rafferty and Smith, 1976). The method usually used to study lens epithelial cell proliferation is to sagittally section the whole fixed lenses (Mikulicich and Young, 1963; Yamamoto *et al.*, 2008a; Zhou *et al.*, 2006). It is useful for studying small lenses like mouse and rat lenses. One important limitation is that not every proliferating cell can be sectioned. This makes it difficult to count all the proliferating cells and to correctly calculate the proliferation index. Compared with lens sections, lens epithelial flat explants are much better, especially for some big lenses (Ong *et al.*, 2003). Wiley also invented a new method to use EdU to label whole mouse lenses and examine the labelled cells under the microscope (Wiley *et al.*, 2010). As the methods are different, the results about the length of the GZ and

proliferation index in those lenses are quite variable (McAvoy, 1978a; Ong *et al.*, 2003; Wiley *et al.*, 2010). Furthermore, most studies about human lens epithelial cell proliferation have been done in capsulotomy specimens (Charakidas *et al.*, 2005; Karim *et al.*, 1987; Liu *et al.*, 2000), which mainly include the cells in the CZ. Therefore, their results do not reflect cell proliferation in the GZ, and the proliferation indexes calculated in these studies are lower than the real ones.

2.1.2 Lens epithelial cell apoptosis

Apoptosis is the process of programmed cell death that happens in the course of embryonic development, in the maintenance of tissue homeostasis and in response to viral infection or toxic damage (Harocopos *et al.*, 1998; Hetts, 1998). In eye development, apoptosis plays a crucial role in separating the lens from the future corneal epithelium (Garcia-Porrero *et al.*, 1979; Schook, 1980), removing the tunica vasculosa lentis and the anterior papillary membrane (Lang *et al.*, 1994; Latker and Kuwabara, 1981). The apoptotic cells have characteristic cell changes, which include blebbing and loss of cell membrane asymmetry in the early phase, cell and nucleus shrinkage, and chromatin condensation in the later stage, and nuclear and chromosomal DNA fragmentation at the end. In most tissues, apoptotic cells are removed by macrophages. Since macrophages are excluded from the lens epithelium and cannot pass through the thick lens capsule, the apoptotic cells in the lens are phagocytosed by their neighbours (Hetts, 1998). A common method to detect apoptotic cells is terminal deoxynucleotidyl transferase (TdT)-mediated dUTP nick end labelling (TUNEL) assay, which was originally described by Garvrieli and colleagues in 1992 (Gavrieli *et al.*, 1992) and subsequently improved dramatically by Negoescu and colleagues later (Negoescu *et al.*, 1998; Negoescu *et al.*, 1996). It detects DNA fragmentation that is caused by apoptotic signalling cascades. The assay relies on the presence of nicks in the DNA, which can be recognised by terminal deoxynucleotidyl transferase, an enzyme catalysing the addition of dUTP that are secondarily labelled with a fluorecein marker. It has been used in the studies of lens epithelial cell apoptosis (Harocopos *et al.*, 1998; Lee *et al.*, 2002; Li *et al.*, 1995). An important limitation of TUNEL assay is that it may also label cells that have suffered severe DNA damage such as in necrosis.

Some gene studies about lens epithelial cell apoptosis have been done on chicken during lens development (Geatrell *et al.*, 2009; Rampalli and Zelenka, 1995; Wride and Sanders, 1993). The other studies are mainly on human lens epithelial cells and try to investigate the relationship between lens epithelial apoptosis and cataractogenesis. Li and colleagues reported that apoptotic rates of lens epithelial cells in capsulotomy specimens obtained from cataract surgery ranged from 4% to 41.8% (Li *et al.*, 1995). However, Harocopos and colleagues questioned the presence of such a high rate of apoptotic cells in cataractous lenses and repeated the study. They found that lens epithelial cell apoptosis rate was very low and suggested that the apoptotic cells observed by Li and colleagues were most likely necrotic cells damaged during or soon after cataract surgery (Harocopos *et al.*, 1998). Lee and colleagues found that epithelial cell apoptosis mainly occurred in human anterior polar cataract but was rarely detected in nuclear cataract or in the normal lenses (Lee *et al.*, 2002). Diabetic rats or rats fed a galactose diet show a higher rate of apoptosis in lens epithelial cells and these results suggest this apoptosis is associated with the accumulation of sugar alcohols (Kim *et al.*, 2010; Kim *et al.*, 2011; Takamura *et al.*, 2003). Increased cell apoptosis is also reported in cataract caused by UV radiation (Ayala *et al.*, 2007; Michael *et al.*, 1998) or TGFβ treatment (Maruno *et al.*, 2002).

2.1.3 Lens epithelial cell density

Most epithelial cells in the CZ remain quiescent, while the cells in the GZ continuously proliferate and differentiate throughout life. Nonetheless, cumulative damage and senile changes may lead to the physiological changes of the lens epithelial cells, which in turn influence cell density. Therefore, cell density of the lens epithelium is of interest for lens ageing and lens pathology, cataract. Most studies about cell density are done on human cataractous lenses, mainly on the capsulotomy specimens of those lenses obtained from patients undergoing extracapsular cataract extraction (Argento and Zarate, 1990; Charakidas *et al.*, 2005; Fagerholm and Philipson, 1981; Gao *et al.*, 1998; Hara, 1988; Harocopos *et al.*, 1998; Hass *et al.*, 1995; Karim *et al.*, 1987; Konofsky *et al.*, 1987; Kumamoto *et al.*, 2007; Oharazawa *et al.*, 2001; Saitoh *et al.*, 1990; Struck *et al.*, 1997; Tkachov *et al.*, 2006; Tseng *et al.*, 1994; Vasavada *et al.*, 1991). In some reports, the epithelial cell density of the normal lenses, which are obtained from eye banks, is used as a control (Fagerholm and

Philipson, 1981; Guggenmoos-Holzmann *et al.*, 1989; Harocopos *et al.*, 1998). Moreover, the changes of epithelial cell density with age in other mammalian lenses are also reported (Kuszak, 1997; Suzuki and Ohno, 2006; Uga *et al.*, 1983; Uga *et al.*, 1996; Wang *et al.*, 1990). All these studies principally focus on the following four questions. (1) What is the lens epithelial cell density in normal and cataractous lenses? (2) How does the cell density change with the increasing severity of cataract? (3) How does the cell density change with age? (4) Do women and men have similar cell density? The answers to these questions are quite controversial. The human lens epithelial cell density in normal people varies between 3900 cells/mm^2 and 5734 cells/mm^2 (Fagerholm and Philipson, 1981; Gao *et al.*, 1998; Guggenmoos-Holzmann *et al.*, 1989; Harocopos *et al.*, 1998; Karim *et al.*, 1987; Tkachov *et al.*, 2006) (Table 2.1). In cataractous lenses, the values are more variable, ranging from 2857 cells/mm^2 (Tseng *et al.*, 1994) to 5906 cells/mm^2 (Harocopos *et al.*, 1998), and lens epithelial cell density decreases with the development of cataract (Argento and Zarate, 1990; Harocopos *et al.*, 1998; Saitoh *et al.*, 1990; Struck *et al.*, 1997; Tkachov *et al.*, 2006; Tseng *et al.*, 1994). Some studies report a decrease of epithelial cell density with increasing age (Balaram *et al.*, 2000; Gao *et al.*, 1998; Guggenmoos-Holzmann *et al.*, 1989; Konofsky *et al.*, 1987; Oharazawa *et al.*, 2001), while others find no correlation between cell density and age (Fagerholm and Philipson, 1981; Karim *et al.*, 1987; Tseng *et al.*, 1994). It is found that lens epithelial cell density in women is slightly higher than in men in some studies (Konofsky *et al.*, 1987; Meder *et al.*, 2005; Richardson and Simmons, 1979; Saitoh *et al.*, 1990; Vasavada *et al.*, 1991; Yeaman *et al.*, 1999), but others report there is no gender difference (Nejsum and Nelson, 2009; Tseng *et al.*, 1994). Therefore, a careful study is really necessary to clarify these questions.

Table 2.1 Human lens epithelial cell density in the normal and cataractous lenses

	Normal lenses			cataractous lenses		
Literature	**Age**	**Position**	**Cell density[1]**	**Age**	**Position**	**Cell density***
Guggenmoos-Holzmann *et al.*, 1989	13-91	Centre and the middle periphery	5031 (male)			
Guggenmoos-Holzmann *et al.*, 1989	13-91	Centre and the middle periphery	5734 female)			
Fagerholm and Philipson, 1981	NA[2]	Anterior pole	3900	NA	Anterior pole	500-4000
Harocopos et al., 1998	NA	Central region	4508	NA	Central region	4521
Harocopos et al., 1998	NA	Peripheral region	5938	NA	Peripheral region	5906
Gao et al., 1998	<12	Central region	5020			
Gao et al., 1998	51-80	Central region	4340			
Struck et al., 1997	NA	Central region	5454	NA	Central region	4838
Hass et al., 1995				NA	Central region	3116
Argento and Zarate, 1990				NA	Central region	3227
Saitoh et al., 1990				NA	Central region	4701
Konofsky et al., 1987				NA	Central region	4382
Tseng et al., 1994				NA	Central region	3683
Hara, 1988				69	Central region	3574
Kumamoto et al., 2007	NA	Central region	4560	NA	Central region	4141
Tkachov et al., 2006	NA	Central region	4593	NA	Central region	3951

[1]: cell number/mm^2

[2]: not available

2.1.4 Lens epithelial cell morphology and size

Lens epithelial cells are irregularly polygonal with 5-8 sides. They are flat in the CZ and become columnar in the GZ (Table 2.2). In the TZ, they continually elongate and are much taller than those in the CZ (Bhat, 2001; Hendrix and Rubinson, 1996; Kuszak, 1997; McAvoy, 1978a). The lens epithelial cell diameter and cross-sectional area also vary in different zones. They are bigger at the centre of the CZ than in the GZ, and they increase with age across the lens epithelium (Hendrix and Rubinson, 1996; Kuszak, 1997). In the lens epithelial cells of sea lampreys, the average cell volume in the TZ is similar to that in the CZ (Hendrix and Rubinson, 1996). One limitation in previous studies is that only some lens epithelial cells in special positions such as the anterior pole and the GZ are chosen to measure. The gradual cell size in the lens epithelium change from the anterior pole to the end of the TZ is not studied. The following four questions still need to be answered: (1) how do the lens epithelial cell height, cross-sectional area and volume change from the anterior pole to the TZ? (2) Are these changes consistent in different species of mammalian lenses? (3) How do the height, cross-sectional area and volume of the epithelial cells from the CZ to the TZ change with age? (4) Does the nuclear volume change within the lens epithelium? Some of these questions have been studied before, but it is still necessary to study them in detail in order to detect the consistency of cell size in different mammalian lenses.

Table 2.2. Epithelial cell size in different species of lenses

Species	Age	Position	Cell height (μm)	Cell diameter (μm)	Cell cross-sectional area (μm^2)	Cell volume (μm^3)	Literature
Sea lamprey	NA	CZ	8	13		1000	Hendrix and Rubinson, 1996
		GZ	30	3		400	
		TZ	50	4		1050	
Rat	1 day	CZ	10				McAvoy, 1978
		GZ	25				
		TZ	40				
	6-7 weeks	CZ	4				
		GZ	8				
		TZ	35				
Monkey	At birth	CZ and GZ			77.43		Kuszak, 1997
	7 years	CZ			92.21		
		GZ			193.97		
	24.5 years	CZ			83.76		
		GZ			99.58		
Human	NA*	Anterior pole		12.5-22.5	257		Fagerholm and Philipson, 1981
	NA	NA		9-17 (mean 12.7)			Brown and Bron, 1987

*: not available

2.1.5 Lens epithelial cell polarity

Epithelial cells exhibit permanent cell polarity characterised by asymmetric distribution of proteins and lipid components in the apical and basolateral surface domains that are segregated by tight junctions (Shin *et al.*, 2006). Lens epithelial cells are polarised with their apical domain apposing the corresponding apical plasma membrane of the lens fibre cells, and the basal domain contacted with the inner surface of the lens capsule (Sugiyama *et al.*, 2009). Tight junctions, which demarcate the boundary between the apical and basolateral membrane domains of the lens epithelial cells, consist of transmembrane proteins and peripheral membrane proteins (Shin *et al.*, 2006). Transmembrane proteins such as occudin and claudins link to the actin cytoskeleton by directly interacting with peripheral membrane proteins (Gonzalez-Mariscal *et al.*, 2000). Zonula occludens (ZO)-1, ZO-2 and ZO-3 are some of the most important peripheral membrane proteins. In addition, ZO-2 and ZO-3 function by binding to ZO-1 (Shin *et al.*, 2006). Therefore, ZO-1 serves as a vital scaffolding protein among the interactions. In the lens epithelial cells, ZO-1 is localised in the apical surface and show a typical cobble-stone-like appearance of the cells (Sugiyama *et al.*, 2008).

Microtubules, consisting of α-tubulin and β-tubulin, fulfil a variety of functions in lens epithelial cells including the organisation of the cytoplasm, regulation of cell shape and maintenance of gap junctional activity (Giessmann *et al.*, 2005). They are polarised filaments with fast-growing plus-ends and slow-growing minus-ends. In the majority of animal cells, a radial array of microtubules is nucleated from a region called centrosome or microtubule organising centre (MTOC) and grows outwards towards the cell membrane (Wade, 2009). Similar to those cells, lens epithelial cells display the classical radial microtubule organisation that is centred on a centrosome (Prescott *et al.*, 1991). The centrosome is composed of a pair of centrioles surrounded by pericentriolar material. It has a subapical position in the polarised lens epithelial cells (Musch, 2004; Nigg, 2002). The pericentriolar material is a protein matrix and includes many proteins required for centrosome-associated functions (Bornens, 2002; Doxsey *et al.*, 2005). γ-tubulin and pericentrin are two key components of the pericentriolar material. γ-tubulin belongs to the tubulin superfamily. Instead of incorporating into the microtubule wall, γ-tubulin is embedded in the pericentriolar material and binds to the minus end of microtubules for microtubule nucleation

(Wiese and Zheng, 2006). It functions either as a monomer or as a large γ-tubulin ring complex (γ-TuRC) (Wade, 2009). Pericentrin is a large conserved coiled-coil protein (Doxsey *et al.*, 1994). It interacts with many proteins and protein complexes including γ-TuRC in the pericentriolar material, and serves as a molecular scaffold involved in microtubule nucleation and spindle organisation (Delaval and Doxsey, 2010). γ-tubulin and pericentrin play an important role in microtubule organisation, which is critical for the asymmetry of the polarised epithelial cells (Musch, 2004).

It is reported that γ-tubulin and other centrosomal marker protein signals are lost during late stages of lens epithelial cell differentiation and re-appear at the apical ends of early differentiating fibre cells (Dahm *et al.*, 2007a). Based on their important functions, it was hypothesised that these centrosomal proteins possibly broke into pieces in those cells. In order to test this hypothesis, the centrosomes in the TZ of the lens epithelium were re-studied by immunofluorescence in the present study.

2.2 Aims

In the present study, the lens epithelia of bovine, rat, rabbit and human were used to study the location of cell proliferation, the length of the GZ and the proliferation index. The change of the proliferation index was also investigated in different ages of human lenses. The apoptotic cell number was studied in the young bovine, rat and mouse lenses and 46-81-year-old human lenses in order to study how many cells were died of apoptosis. The lens epithelial cell height, cross-sectional area and volume were measured to detect their changes across the lens epithelium. Their changes with age were also studied in the human lenses. The position of the centrosome was studied in the lens epithelial cells in order to test the hypothesis that it was not absent from those cells in the peripheral TZ. Moreover, cell proliferation, apoptosis, morphology, and centrosome location were also studied in the human donor capsular bags with IOLs to investigate the influences of cataract surgery and PCO development to the cell organisation.

2.3 Materials and methods

2.3.1 Eye lens materials

Fresh bovine eyes were collected from Whitley Bay Meat Supply Co. Ltd (Northumberland, UK) and Coast and Country Meat Supply (Gateshead, Newcastle, UK) within 2-3 hours after the death of animals. Donor cows were up to 30 months old. Both females and males were included. Waste material was disposed according to the "Meat Hygiene Service regulations for the dispatch of serious risk material for research purposes". All the mice, rats and rabbits came from the animal laboratory in the School of Biological and Biomedical Sciences of the University of Durham. The mice were about 6 weeks old. The rats were 4 months old. The rabbits were at least 6 months old. Eyes from male and female animals were taken approximately 3 hours after the animals had died. All experiments were approved by the local ethics committee of Durham University. Human eyes came from the eye bank of Bristol Eye Hospital and were posted to Durham University about 2 to 4 days postmortem. Most donors died of cancer, hypoxia, myocardial infarction, and intracerebral hemorrhage. The donors between 20 and 60 years old did not have cataracts and some donors above 60 years old possessed mild to moderate cortical or nuclear age-related cataracts. A small number of donors had cataract surgery in the past and were implanted with IOLs. The eyes were kept in 0.9% (v/v) NaCl at 4ºC after their corneas had been removed for cornea transplantation. A total of 82 eyes from 49 donors (age range: 20-98, 58 ± 21) were used in the present study. In the study of proliferation index change with age, the lenses were divided into the 30-50 (6 eyes, 39 ± 5.7 years old) and 80-100 (12 eyes, 83 ± 5 years old) years old groups. To study the influence of age on lens epithelial cell apoptosis, the human lenses were divided into the younger group (6 eyes, 45.3 ± 0.58 years old) and the older group (8 eyes, 69.5 ± 12 years old). In the study of lens epithelial cell density change with age, the human lenses were divided into four groups: 20-30 (6 eyes, 23.7 ± 4.2 years old), 40-50 (11 eyes, 44.5 ± 1.6 years old), 60-70 (8 eyes, 61.8 ± 2.7 years old), and 80-90 (13 eyes, 83.7 ± 5.3 years old) years old. In the study of lens epithelial cell density in women and men, 26 lenses were collected from 13 females (59.6 ± 20.8 years old) and 13 males (59.7 ± 23.7 years old) whose ages were matched. All the human lens research was performed according to the tenets of the Declaration of Helsinki and was also approved by the Newcastle and North Tyneside local ethics committee.

2.3.2 Eye lens dissection

To obtain the lenses, the sclera in the posterior hemisphere was cut with a surgical blade (Swann-Morton, Sheffield, UK). The vitreous humour was gently removed to expose the posterior of the lens and the suspensory ligaments, known as zonules. The zonules were cut without damaging the lens capsule. The free lenses were placed onto Sylgard (Dow Corning, Barry, United Kingdom) -covered wells of a 6- or 12-well plate with the posterior side facing upward. Six pie-shape cuts were made from the centre of posterior lens capsule to the lens equator. The wedges of the posterior lens capsule were pinned down onto the Sylgard by steel pins. The lens fibres were then gently removed with a curved pair of tweezers. The lens capsule with the epithelial cells was left facing upward for the following experiments.

The human eyes whose donors had had cataract surgery and implanted IOLs were also dissected as above under a light microscope. After the lens capsular bag with implanted IOL was taken out from the eye, the IOL was carefully removed from the lens bag without breaking the posterior lens capsule. Some lens capsular bags were then directly pinned down on the Sylgard for cell proliferation and apoptosis study. For the other lens capsular bags, four cuts were made in the rhexis, and the anterior capsule was peeled off from the posterior capsule along the cuts and pinned down on the Sylgard in order to observe the cell morphology and cell centrosome on the anterior and posterior capsule clearly.

2.3.3 Immunofluorescence microscopy

2.3.3.1 Antibodies

The primary and secondary antibodies used for immunofluorescence are described in Tables 2.3 and 2.4.

Table 2.3. Primary antibodies used for immunofluorescence

Antigen	Source	Clone	Dilution	Supplier/Reference
Actin	mMouse[1]	AC-40	1:100	Sigma
F-actin	Phalloidin		1:20	Sigma
ZO-1	pRabbit[2]		1:200	Invitrogen™,
Ki-67	mMouse	MIB-1	1:100	Dako
pericentrin	pRabbit	Pc-4448	1:100	Abcam
pericentrin	pRabbit	Ab448-100	1:100	Abcam
γ-tubulin	mMouse	GTU-88	1:1000	Sigma
N-cadherin	mMouse	32	1:100	BD Transduction Laboratories
CP49	pRabbit	2981	1:100	Sandilands *et al*., 1995
filensin	mMouse	R2D2	1:100	Sandilands *et al*., 1995
α-tubulin	mMouse	WA3	1:100	Karakesisoglou *et al*., 2010
LaminA/C	mMouse	JoL2	1:100	Willis *et al*., 2008
PCNA	pRabbit	3009	1:100	Moravian Biotechnology Ltd.

[1]: monoclonal antibody is produced from mice
[2]: polyclonal antibody is produced from rabbits

Table 2.4. Secondary antibodies used for immunofluorescence

Name	Dilution	Supplier
Goat anti-mouse IgG FITC conjugate	1:100	Sigma
Goat anti-mouse IgG TRITC conjugate	1:100	Sigma
Goat anti-rabbit IgG FITC conjugate	1:100	Sigma
Goat anti-rabbit IgG TRITC conjugate	1:200	Sigma

2.3.3.2 Immunofluorescence microscopy

After lens dissection, the lens epithelium whole-mounts were fixed in 4% (w/v) paraformaldehyde (PFA) (Agar Scientific, Stansted, UK) at room temperature or in ice-cold methanol/acetone (1 volume: 1 volume) at -20ºC for 20 minutes. After being rinsed three times in phosphate-buffered saline (PBS), the lens epithelium whole-mounts were incubated in blocking solution [PBS containing 0.1% (v/v) goat serum, 1% (w/v) bovine serum albumin (BSA), and 0.05% (v/v) Triton X-100] for 30 minutes. Then they were incubated with the primary antibodies diluted in the blocking solution for 2 hours at room temperature or overnight at 4˚C. The negative controls were just incubated in the blocking solution for the same amount of time. After removing the primary antibodies, the whole-mounts were washed 5 times with blocking buffer for 5 minutes each time. The secondary antibodies were also diluted in blocking buffer and incubated with the lens epithelium whole-mounts for 1 hour at room temperature. 4,6-diamidino-2-phenylindole (DAPI, 1 µg/ml; Molecular Probe Inc., Eugene, Oregon, USA) was added alongside the secondary antibody for nuclear staining. After being rinsed 5 times in blocking buffer, the whole-mounts were transferred onto the microscope slides with the epithelial cells facing upward. A drop of fluorescent protecting agent, citifluor (Citifluor Labs, UK), was added onto the lens epithelial cells to retard photo bleaching. Coverslips were put on top of the whole-mounts and the slides were sealed with nail varnish.

Fluorescent signals were observed and images were taken with a Zeiss LSM 510 Meta scanning confocal microscope (Carl Zeiss Inc., Jena, Germany). DAPI, fluorescein isothiocyanate (FITC) and tetramethylrhodamine isothiocyanate (TRITC) were excited respectively at wavelengths of 358 nm, 495 nm and 547 nm. Since lens epithelium whole-mounts on the slides were not flat, a Z-stack was used to collect a series of images at different points along the Z-axis. The series of images were compressed into one image. Images were analysed with Adobe Photoshop 8.0 (Adobe system, San Jose, CA, USA) or ImageJ (Wayne Rasband, National Institute of Health, USA).

2.3.3.3 Cell profile determination

Wheat germ agglutinin (WGA) selectively binds to N-acetylglucosamine and N-acetylneuraminic acid (sialic acid) residues in the cell membrane. In the present

study, fluorescent WGA conjugate was used to stain the cell membrane to obtain a cell profile.

The bovine and human lens epithelium whole-mounts were fixed in 4% (w/v) PFA for 20 minutes. After three washes in PBS, they were incubated with WGA, Alexa Fluor® 555 conjugate (5 µg/ml in PBS; Molecular Probes Inc., Oregon, USA) and DAPI (1 µg/ml) for 20 minutes at room temperature. The whole-mounts were then rinsed three times in PBS and transferred to the microscope slides to make the slides. Images were taken with the Zeiss LSM 510 Meta scanning confocal microscope.

2.3.3.4 Detection of apoptotic cells

2.3.3.4.1 Annexin-V-affinity assay

In the early stages of apoptosis, changes occur at the cell surface (Creutz, 1992; Fadok *et al.*, 1992b). One of these plasma membrane alterations is the translocation of phosphatidylserine from the inner part of the plasma membrane to the outer layer, by which phosphatidylserine becomes exposed at the external surface of the cell (Vermes *et al.*, 1995). The analysis of phosphatidylserine on the outer leaflet of apoptotic lens epithelial membranes was performed using Annexin-V-Fluorescein (Roche Applied Science, Germany). Propidium iodide (PI) was used simultaneously to differentiate the apoptotic cells from necrotic cells.

The bovine lenses were dissected quickly after they were taken out of the eyes. Once the fibre mass was removed, 200 µl of Annexin-V-Fluorescein labelling solution (including 4 µl Annexin-V-Fluorescein labelling reagent, 4 µl PI solution, and 0.2 µl DAPI in 192 µl of incubation buffer) was put on the lens epithelium whole-mount and covered the cells for 12 minutes at room temperature. After the labelling solution was removed, the cells were gently washed in PBS twice and fixed in 4% (w/v) PFA for 20 minutes in order to avoid further cell necrosis or cell loss during the following slide preparation. All the whole-mounts were then rinsed three times with PBS and transferred to the microscope glass to make the slides, which were observed and taken images with the same confocal microscope.

2.3.3.4.2 TUNEL assay

The TdT-mediated dUTP nick end labelling (TUNEL) reaction preferentially labels 3'-OH termini of broken DNA strands during apoptosis. To detect the DNA strand breaks in apoptotic lens epithelial cells, the lens epithelium whole-mounts of bovine, mouse, rat, and human were first fixed in 4% PFA (w/v) for 20 minutes at room temperature immediately after removing the lens fibre mass. After three rinses in PBS, the lens epithelial cells were permeabilised with 0.1% (v/v) Triton X-100 in PBS for 2 minutes on ice, followed by two washes in PBS. Prior to the labelling procedures, the lens epithelial cells used as a positive control for DNA breaks were incubated with benzonase nuclease (100 U/ml in PBS; Novagen, Germany) for 10 minutes at room temperature to introduce DNA strands breaks. TUNEL staining was carried out by using an *in situ* cell-death detection kit, TMR red (Roche Diagnostics GmbH, Germany). The reaction mixture was prepared immediately before use and kept on ice. 100 ∫l of label solution containing TMR red labelled nucleotides was removed from the original Eppendorf and set aside for a negative control. 50 ∫l of enzyme solution containing terminal deoxynucleotidyl transferase, which catalyses TMR red labelled nucleotides to free 3'-OH DNA strand breaks in apoptosis, was added to the remaining 450 ∫l label solution to obtain a 500 ∫l TUNEL reaction mixture. The samples and the positive control were incubated with TUNEL reaction mixture while the negative control was just incubated with the label solution in a humidified container for 60 minutes at 37ºC. All the samples were rinsed in PBS three times and then incubated with DAPI for 10 minutes at room temperature. After three rinses in PBS, they were transferred to the microscope slides. The slides were observed and images were taken with the same confocal microscope.

2.3.4 Data analysis

2.3.4.1 Calculation of lens epithelial cell density

All the lens epithelium whole-mounts used for cell density calculation were stained with DAPI. Since one lens epithelial cell only contains one nucleus, the nucleus number was counted and used as the epithelial cell number.

After the slide for immunofluorescence microscopy was ready, the lens epithelium whole-mount was left flat between the microscope slide and the glass coverslip so that

the capsule covered with epithelial cells showed a circle shape. A ruler was used to measure the radius (r) of the capsule covered with epithelial cells (Figure 2.1). This radius is the sum of the radius of the anterior lens capsule and the length of the TZ at the equator. In this way, the area of the lens capsule covered with epithelial cells could be calculated without considering the curvature influence. When images were taken with the confocal microscope, the same magnification was chosen so the size of each image was the same. Each image was a square and a was used to represent its width. In order to calculate the cell density in different areas and the total cell number in each whole-mount, a series of images from the anterior pole to the end of the TZ were taken. The image number, n, was decided by r and a (n=r/a). For each species, at least three different series of images were taken and each came from a different lens sample. The area of each image (S_1) was calculated from its width a ($S_1=a\times a$). The cell number (N_1) of each image was counted using ImageJ or a special software package called delineator, which was written by Dr. Christopher Saunter in the Physics department of the University of Durham. The cell density (D) of each image was calculated according to the cell number in this image and the image area ($D=N_1/S_1$). The mean and standard deviation (SD) of the cell density at each area of the anterior lens capsule were obtained by counting at least three series of images.

For the study of the lens epithelial cell density change with age, the human lenses were collected and divided into four groups: 20-30, 40-50, 60-70 and 80-90 years old, according to the donors' age. In order to compare the lens epithelial cell density change in different human age groups, the length of each series of images should be the same. Since the lens dimension increased with age, the radius of the capsule covered with epithelial cells in the younger group was smaller than that in the older group. The cell density near the centre of CZ was similar in each sample. Therefore, the radius of the youngest group was used as the length of the series of images. The images were taken from the end of the TZ to the CZ. One or two series of images were taken from each sample. The mean and standard deviation of the cell density in each group were calculated and made into line charts. Student's t-Test was used to analyse the cell density difference in the four groups. A *p* value below 0.05 was considered to have statistically significant difference.

For the study of lens epithelial cell density in males and females, one or two series of images from the end of the TZ to the CZ were taken in the epithelium whole-mounts of the 26 lenses. The epithelial cell density was calculated and Student's t-

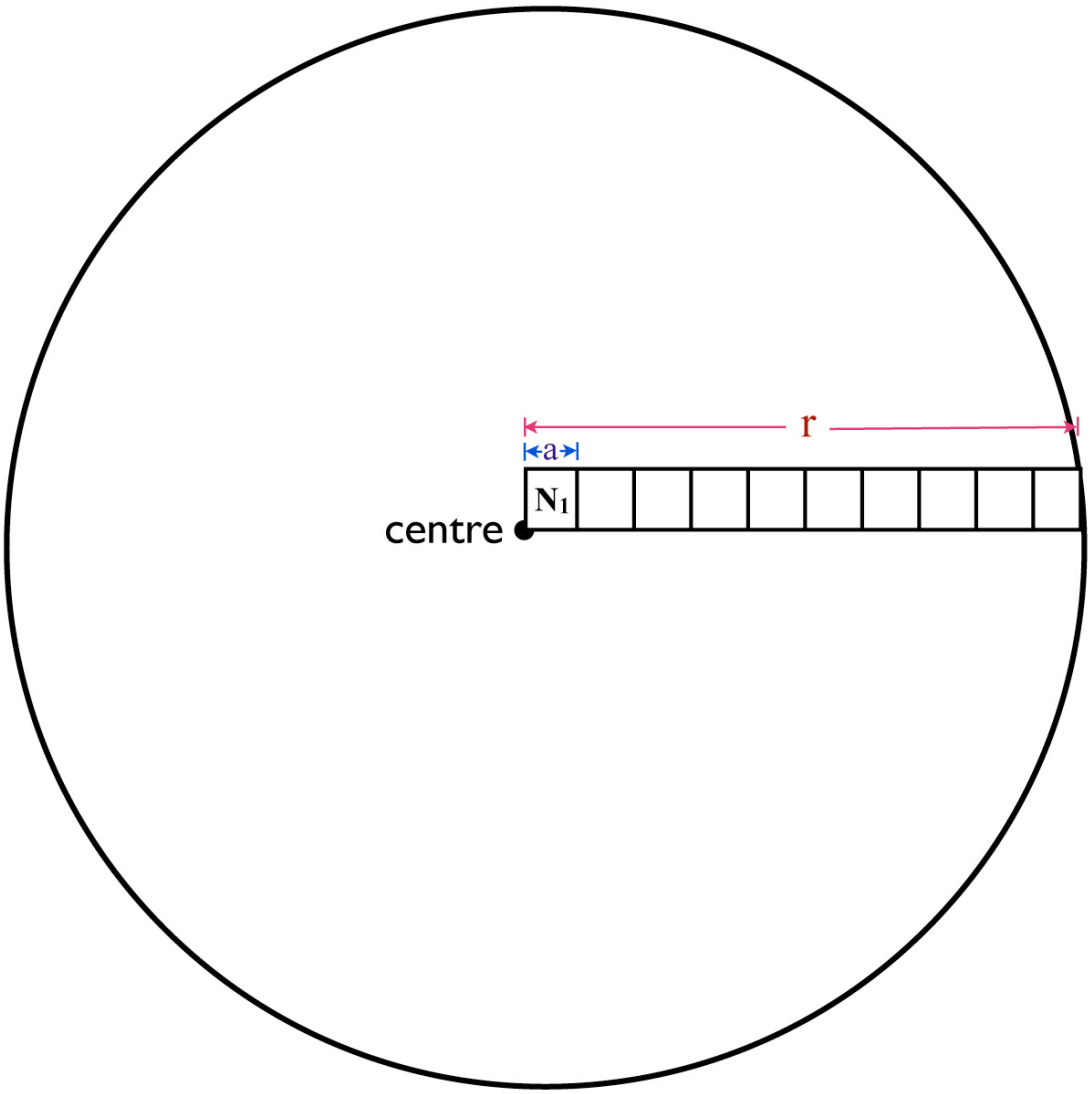

$$S_1 = a \times a$$

$$D = N_1 / S_1$$

Figure 2.1. Calculation of the lens epithelial cell density.

r: radius of the lens capsule covered with the epithelial cells.
a: width of each square image.
$\mathbf{S_1}$: area of the image
$\mathbf{N_1}$: cell number of the image
$\mathbf{D_1}$: cell density of the image

Test was used to analyse the difference between males and females. Again a p value below 0.05 was considered to have statistically significant difference.

2.3.4.2 Calculation of the total lens epithelial cell number

At least three series of images were taken from the anterior pole to the end of the TZ. The anterior lens capsule covered with epithelial cells was a circular shape. However, the series of images taken in each lens epithelium whole-mount was mounted and shown as a rectangular shape. This rectangle consisted of two equal triangles (Figure 2.2). Then the area of the triangle whose smallest angle (**α**) faced the periphery was assumed to be equal to the area of the circle with the same central angle. As **α** was very small, this assumption would not introduce any big errors. Then the tangent value of **α** could be calculated by the height of image and the radius of the circle ($\tan\alpha=a/r$). The exact value of **α** was obtained by calculating its arc tangent. After the **α** value was known, the percentage of it in the 360 degrees of the central angle could be achieved by $\alpha/360$. If the cell number (N_a) in this triangle was known, the total lens epithelial cell number (N_t) could be calculated by using this percentage ($N_t=N_a\times360/\alpha$). N_a was the total of the cell number of each single image in the triangle (N_m). N_m could be obtained by using the area of the image in the triangle (S_m) to multiply the cell density of this image ($N_m=S_m\times D$). S_m could be calculated by using the two bases (a_m and a_{m+1}), which was from $\tan\alpha$ multiplying the length to the centre, and the height (a) of the right-angled trapezium [$S_m=(a_m+a_{m+1})\times a/2$].

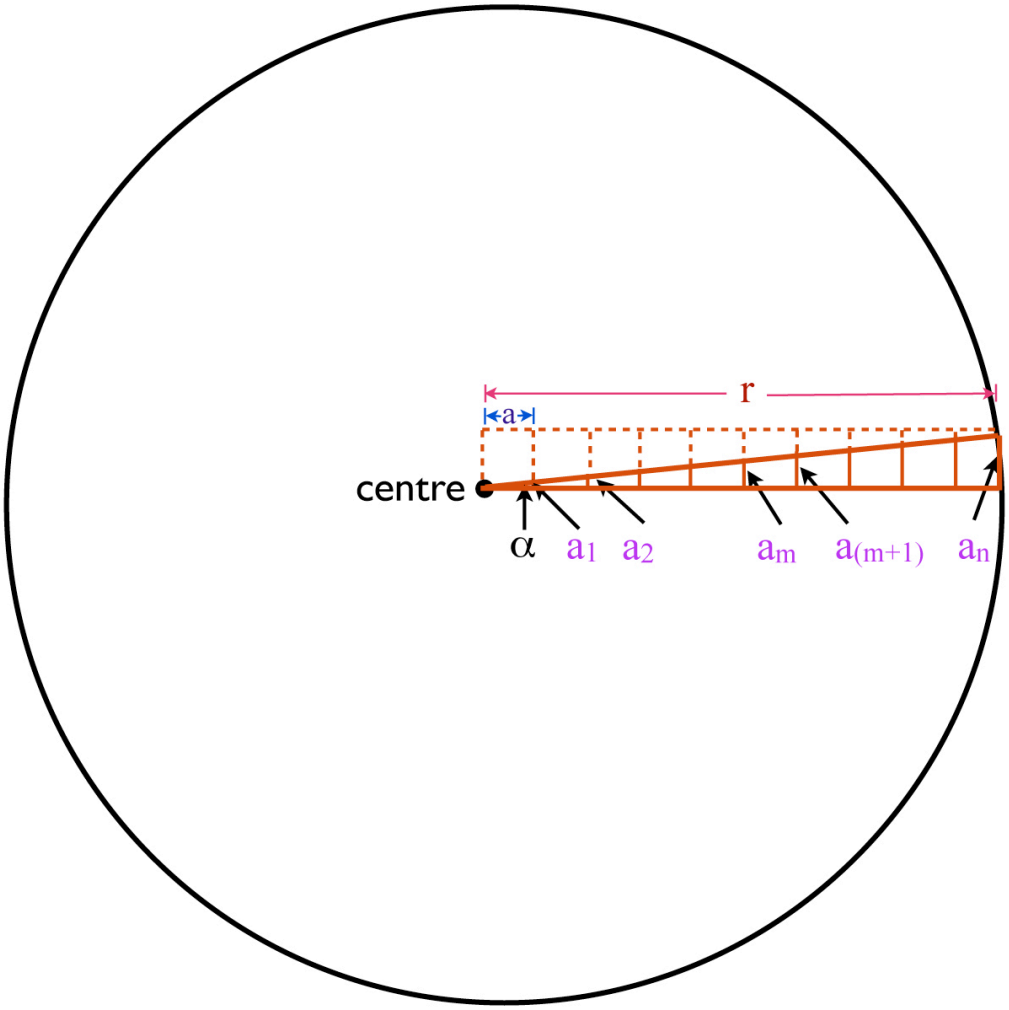

$\tan\alpha = a/r \longrightarrow \alpha = \arctan a/r$

$a_m = \tan\alpha \times (a \times m)$ $\qquad$ $a_{(m+1)} = \tan\alpha \times [a \times (m+1)]$

$S_m = (a_m + a_{m+1}) \times a/2$

$N_m = S_m \times D$

$N_a = N_1 + N_2 + \cdots + N_m + \cdots + N_n$

$N_t = N_a \times 360/\alpha$

Figure 2.2. Calculation of the total lens epithelial cell number.

The series of pictures from the anterior pole to the end of the TZ comprises a square. A line separates it into two equal triangles. The cell number in the triangle at the bottom with unbroken lines is calculated and used to calculate the total lens epithelial cell number.

α: the angle of the triangle facing the periphery.
a: height of each square image.
r: radius of the lens capsule covered with epithelial cells.
m: image number
$\mathbf{a_m}$: height of the triangle in the image **m**.
$\mathbf{a_{(m+1)}}$: height of the triangle in the image **m+1**.
$\mathbf{S_m}$: area of the trapezium.
D: cell density in the image **m**.
$\mathbf{N_m}$: cell number in the trapezium of image **m**.
$\mathbf{N_a}$: the total cell number in the triangle.
$\mathbf{N_t}$: the total lens epithelial cell number.

2.3.4.3 Calculation of the total proliferating epithelial cell number

After the lens epithelial cell whole-mounts were stained with Ki-67 and DAPI, at least three series of images from different whole-mounts were taken from the end of the TZ to the region of the GZ (Figure 2.3). The GZ length ($\mathbf{l_G}$) was the length from the first Ki-67-positive cell near the CZ side to the last one near the TZ side. The TZ length ($\mathbf{l_T}$) meant the length between the last Ki-67-positive cell and the end of the meridional lines. The total number of the Ki-67-positive cells in the GZ (the series of images) was counted and the average ($\mathbf{N_p}$) per square millimeter was calculated. The Ki-67-positive cell density ($\mathbf{D_G}$) could be obtained by dividing the average Ki-67-positive cell number $\mathbf{N_p}$ by the area of the GZ ($\mathbf{S_{G1}}$), which was calculated by multiplying $\mathbf{l_G}$ by the width **a** of each image ($\mathbf{S_{G1}=a\times l_G}$). The total proliferating cell number in the lens epithelium was the product of $\mathbf{D_G}$ multiplied by the total GZ area ($\mathbf{S_{tG}}$) ($\mathbf{N_{tG}=D_G\times S_{tG}}$). According to the method used to calculate total lens epithelial cell number, the GZ area ($\mathbf{S_G}$) in the small triangle could be calculated by the angle value **α**. $\mathbf{S_{tG}}$ was the product of $\mathbf{S_G}$ and **360/α** ($\mathbf{S_{tG}=S_G\times 360/\alpha}$). The proliferation index (**PI**) could be obtained by the total proliferating cell number ($\mathbf{N_{tG}}$) divided the total lens epithelial cell number ($\mathbf{N_t}$) ($PI=\mathbf{N_{tG}/N_t}$).

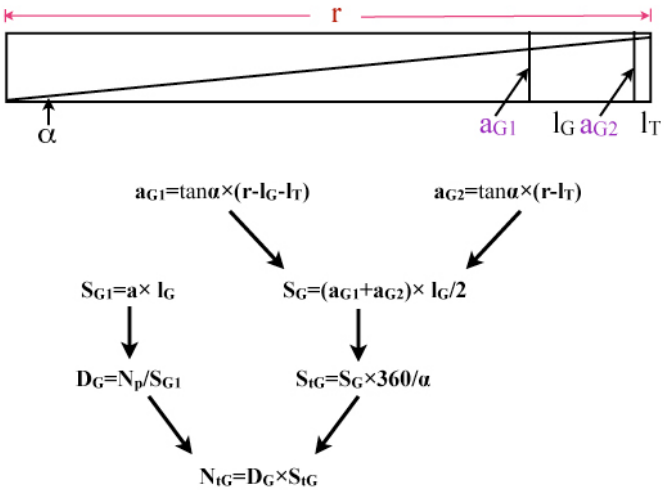

Figure 2.3. Calculation of the total proliferating cell number in the lens epithelium.

r: radius of the lens capsule covered with epithelial cells.
α: the angle of the triangle facing the periphery.
$\mathbf{a_{G1}}$, $\mathbf{a_{G2}}$: heights of the trapezium of the GZ in the triangle.
$\mathbf{I_G}$: length of the GZ.
$\mathbf{I_T}$: length of the TZ. Here it means the length of the cell columns in the TZ.
a: height of each square image.
$\mathbf{S_{G1}}$: area of the GZ.
$\mathbf{S_G}$: GZ area in the triangle.
$\mathbf{D_G}$: Ki-67-positive cell density in the GZ.
$\mathbf{N_p}$: the average number of the Ki-67-positive cells per square millimeter in the GZ.
$\mathbf{S_{tG}}$: the total GZ area in the lens epithelium
$\mathbf{N_{tG}}$: the total proliferating cell number in the lens epithelium.

2.3.4.4 Calculation of the number of the meridional lines in the TZ

A image including the meridional lines stained with DAPI in the TZ was taken (Figure 2.4A). The meridional line number **n** was counted and the width of the counted meridional line ($\mathbf{l_n}$) was measured by the software in the Zeiss LSM 510 Meta confocal microscope. The single meridional line width (**l**) was calculated by $\mathbf{l_n}$ divided by **n**. At least three images from three different samples were used to calculate **l** and the average meridional line width was obtained. The radius of the equator ($\mathbf{r_1}$) was measured after the lens was dissected from the eye (Figure 2.4B). The circle length of the equator ($\mathbf{l_e}$) was calculated by the following formula: $\mathbf{l_e=2\pi r_1}$. $\mathbf{l_e}$ divided by **l** was the meridional line number $\mathbf{N_c}$ in the TZ.

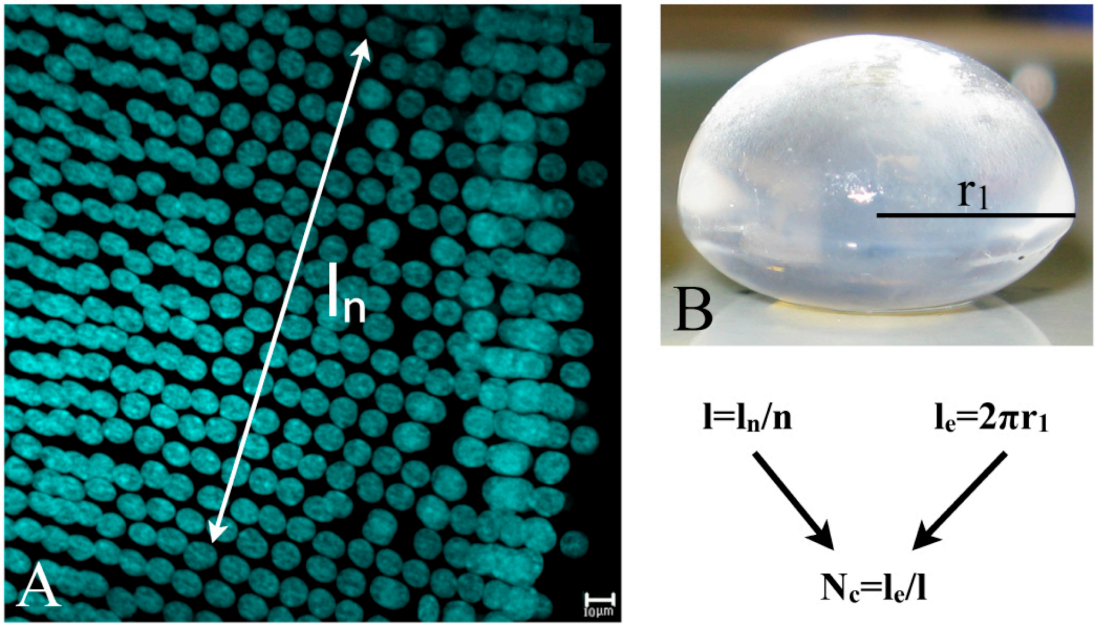

Figure 2.1. Calculation of the meridional line number in the TZ of the lens epithelium.

n: meridional line number.
$\mathbf{l_n}$: width of the meridional line.
l: average meridional line width.
$\mathbf{r_1}$: radius of the lens.
$\mathbf{l_e}$: circle length of the lens in the equator.
$\mathbf{N_c}$: total meridional line number in the TZ of the lens.

2.3.4.5 Analysing the influence of delivery time on the human lens epithelial cell apoptosis

Since human eyes were delivered within 2 to 4 days postmortem and their corneas had already been removed for cornea transplantation, it was difficult to tell whether the TUNEL-positive staining cells were normally present in the lens epithelium or were caused by being left in 0.9% (w/v) NaCl during the postmortem time. In order to clarify this problem, four pairs of eyes from four donors were equally divided into the PFA group and the control group. Each group included one eye from each donor. The eyes in the PFA group were fixed in 4% (w/v) PFA immediately after cornea removal. The other four eyes were left in 0.9% (w/v) NaCl as the control. All the eyes were dissected and the lens epithelial cells were processed for TUNEL labelling at the same time. The number of the TUNEL-positive cells in each lens epithelium whole-mount was counted. Then all the numbers in two groups were analysed using the paired Student's t-Test. A p value below 0.05 was considered to have statistically significant difference.

2.3.4.6 Human lens epithelial cell apoptosis change with age

In order to study the influence of age on lens epithelial cell apoptosis, the lens from younger humans (45-46 years old) and older humans (79-81 years old) were collected and a TUNEL assay was carried out on them. In the younger group, six eyes from three donors were included. The donors' average age was 45.3 ± 0.58 (mean ± SD) years old. The old group consisted of four eyes from two donors and the donors' average age was 80 ± 1.4 (mean ± SD) years old. The TUNEL-positive cell number in each lens of the two groups was counted and the difference between the two groups was analysed by Student's t-Test (two sample unequal variance). A p value below 0.05 was considered to have statistically significant difference.

2.3.4.7 Measurements of the lens epithelial cell height, cross-sectional area and volume

The bovine lens epithelium whole-mounts were stained with N-cadherin, which is a member of cadherin family and is located at the adherens junctions to mediate cell-cell adhesion through its extracellular amino terminus (Pontoriero *et al.*, 2009).

As adherens junctions are present in the lens epithelial cell lateral membranes, N-cadherin staining can show the cell outline from the top to the bottom. A series of images in a Z-stack were taken from the anterior pole to the end of TZ. The cross section and longitudinal section of the cells in each image were saved for measurements. The cell height and cross-sectional area in each image were measured using ImageJ. The cell volume was calculated by multiplying the cell height by the cell cross-sectional area. At least 30 cells per image were randomly chosen for counting. The final results were shown as means ± SD.

In order to study the cell size change with age, the lens epithelium whole-mounts of a 29-year-old woman, a 48-year-old man and a 64-year-old man were fixed and stained with WGA. A series of images in a Z-stack were taken from the end of TZ to the CZ in each epithelium whole-mount. The cell height and cross-sectional area were measured using ImageJ. The cell volume was calculated according to the cell height and cross-sectional area. All the results were shown as means ± SD.

2.3.4.8 Measurement of the lens epithelial cell nuclear volume

One human lens epithelium whole-mount of an 88-year-old man and one bovine's were fixed in ice-cold methanol/acetone (1:1) at -20ºC for 20 minutes. After three rinses in PBS, they were incubated with DAPI for 20 minutes. The DAPI staining of the nuclei with methanol/acetone fixation was clearer than that with PFA fixation. A series of images in a Z-stack were taken from the anterior pole to the end of TZ. Since in the bovine lens epithelial cells, the nuclei were oval and their position was different, measuring the height and cross-sectional area of a large number of nuclei could not be done using ImageJ. Therefore, only the volume of the lens epithelial cells in each image was measured by ImageJ. The results were shown as means ± SD and made into charts comparing the cell volume with the cell density change.

2.4 Results

2.4.1 Lens epithelial cell turnover

2.4.1.1 Lens epithelial cell proliferation

2.4.1.1.1 Lens epithelial cell proliferation in the GZ

The proliferation marker Ki-67 is present in the nuclei of cells in the G_1, S, G_2, and M phases of the cell cycle. Quiescent or resting cells in the G_0 phase do not express the Ki-67 protein (Endl and Gerdes, 2000). Therefore, the immunofluorescence labelling of the bovine, human, rabbit, and rat lens epithelium whole-mounts with Ki-67 was used to detect the lens epithelial cell proliferation. Furthermore, in order to confirm the accuracy of Ki-67 staining in the dividing cells, the human and rat lens epithelial cells were co-stained with another cell cycle marker, proliferating cell nuclear antigen (PCNA). PCNA, a 36 kD nuclear polypeptide, acts as a homotrimer and helps aid the processing of leading strand synthesis during DNA replication. It is expressed in the nuclei of cells in late G1 phase and throughout the S phase but is detectable throughout the proliferating cell cycle due to its long half-life (20 hours) (Roels *et al.*, 1999). Results showed that the human and rat lens epithelial cells in the cell cycle were stained by both Ki-67 and PCNA (Figure 2.9 and 2.10). This indicated that Ki-67 was a stable cell marker in studying lens epithelial cell proliferation.

The Ki-67 staining showed that most lens epithelial cell proliferation occurred in a narrow zone located in the periphery of the lens epithelium whole-mounts of the bovine (Figure 2.5A), rabbit (Figure 2.7A), rat (Figure 2.9A-I) and human (Figure 2.10). This narrow zone was the GZ (McAvoy *et al.*, 1999). The proliferating cells here were in different phases of the cell cycle (Figure 2.5B-K, 2.7B-K, 2.9A-I and 2.11). The lens size was quite variable in different species of mammalian lenses included in the present study, so the length of the GZ was different. However, it was interesting to find that the GZ proportions [the ratio of the GZ length and the radius of the anterior capsule covered by epithelial cells, GZ proportion = (GZ length/anterior capsule radius) × 100%] were similar in the lens epithelium of bovine, rabbit and human (Table 2.5). The GZ length of the rat lens was not calculated because some cells in the GZ were lost during lens dissection. The proliferation index was variable

in different species of mammalian lenses. Compared with the human and 30-month-old bovine (about teenage in human years), the six-month old rabbit (about 16 years in human years) had a higher proliferation index, which was 1%. This suggests that the proliferation index was influenced by species. In the human, the proliferation index in the 80-90-year-old people was only half that in the human below 50 years old. This means it decreases with age in human.

Table 2.5. Characteristics of the lens epithelium whole-mounts in different species (mean ± SD)

Species	Sample number	Radius (mm)	GZ length (mm)	GZ / radius	Total cell number	Proliferating cell number	Proliferation index
Bovine	5	8.76±0.037	1.34±0.11	15.3%	1395792±18249	5439±1067	0.39%±0.08%
Rabbit	3	6.39±0.42	0.86±0.14	13.5%	819425±23774	8594±1482	1%±0.18%
Human (30-50ys)	13	4.89±0.23	0.82±0.17	16.8%	513240±22564	2130±629	0.42%±0.12%
Human (80-90ys)	12	5.24±0.35	0.76±0.11	14.5%	540270±28530	1197±567	0.22%±0.1%

Four human lens capsular bags with implanted IOLs were included in the present study. The central parts of the anterior capsules had already been removed during cataract surgery. The DAPI staining showed that many cells migrated to the posterior capsule. The Ki-67 staining showed that cell proliferation occurred in both the anterior and posterior lens capsule. Interestingly most proliferating cells were detected in the periphery of the anterior capsule where there the GZ was (Figure 2.12). This result indicates that the cells in the GZ still retain their proliferation ability when the normal lens epithelial cell environment is changed after cataract surgery. Some Ki-67-positive cells were also observed near the rhexis margin. Fibrosis situation was quite variable between each donor capsular bags and cell proliferation was also different. As the central part of the anterior capsule was absent and the total lens epithelial cell number could not be calculated, the proliferation index in the capsular bags was not calculated.

2.4.1.1.2 Lens epithelial cell proliferation in the CZ

Beside the GZ, epithelial cell proliferation was also observed in the CZ of some lenses. The proliferating cell number in the CZ was quite variable in different species of mammalian lenses. No more than ten proliferating cells were found in the CZ of each bovine lens epithelium whole-mount (Figure 2.6) (Table 2.6). This means that a very low number of cells divide in the CZ of the 30-month-old bovine (13-19 years old in human year). As the chromatin of these Ki-67-positive cells did not obviously condense, they were not in the M phase but in the phase between G1 and G2. By contrast, more cells were dividing in the CZ of the 6-month-old rabbits (equivalent to 16 years in human year) (Figure 2.8) and 4-month-old rats (equivalent to 16 years in human year) (Figure 2.9J-K). These cells were in different phases of the cell cycle including the M phase. This is different from the proliferating cells in the CZ of the bovine lenses. Since some cells in the CZ of the rabbit and rat lenses were lost during the sample preparation, the exact proliferating cell number in this zone could not be calculated. In all the human lens epithelium whole-mounts stained with Ki-67 and PCNA, no proliferating cell was observed in the CZ. These results indicate that cell proliferation occurs often in the CZ of the rabbits and rats who just reach sexual maturity or social maturity, but not in the CZ of the matured or old human lenses.

Table 2.6. Cell proliferation in the CZ of the different mammalian lens epithelia

Species	**Age**	**Age in human years**	**Cell proliferation in the CZ**
Bovine	30 months	13-19	0-10
Rabbit	6 months	16	>100
Rat	4 months	16	>100
Human	30-90 years	30-90	0

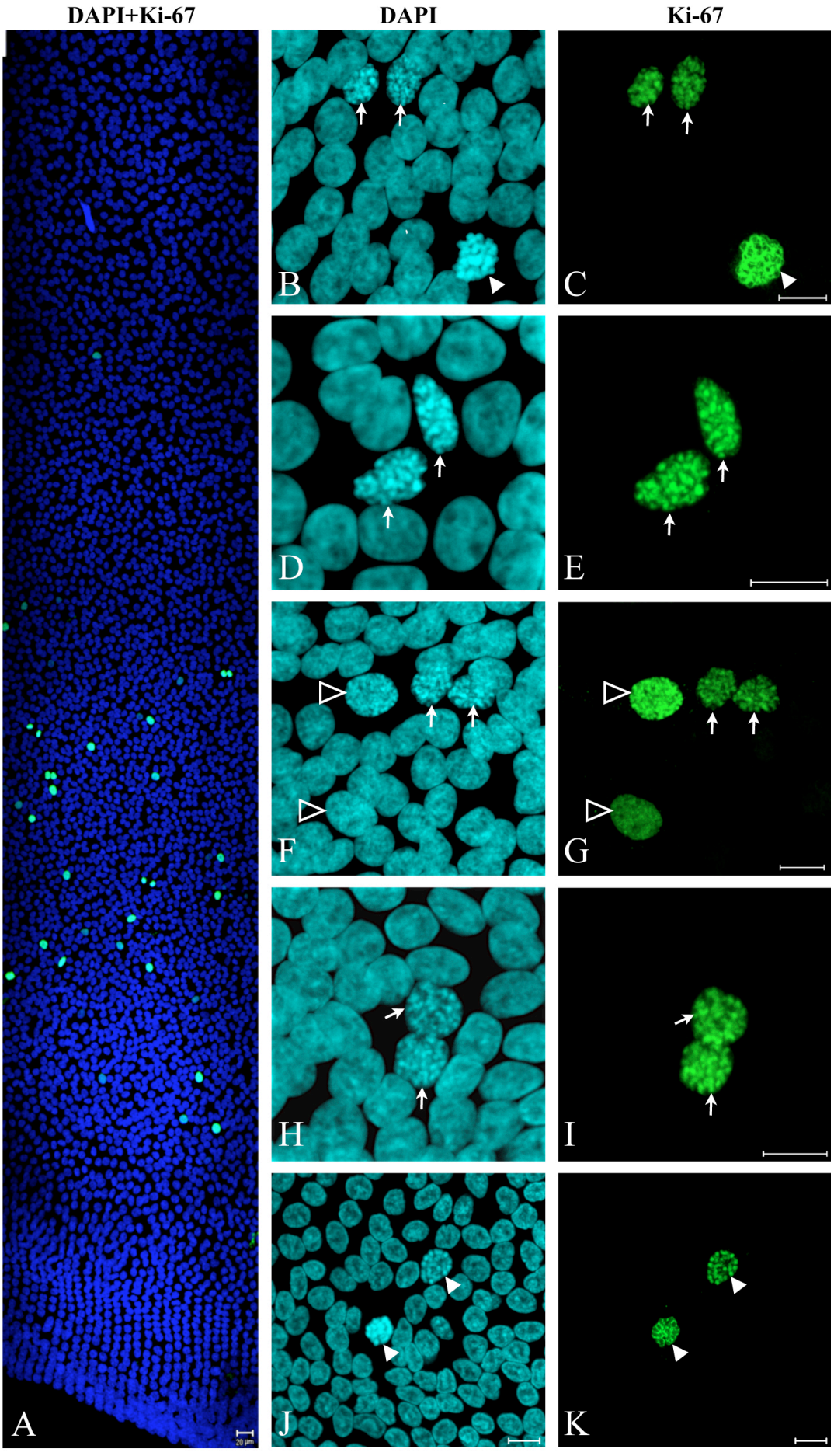
DAPI+Ki-67
DAPI
Ki-67
A
B
C
D
E
F
G
H
I
J
K

Figure 2.5. Cell proliferation in the GZ of the bovine lens epithelium.

Bovine lens epithelial cells were stained with the proliferation marker Ki-67 (green) and the DNA indicator DAPI (blue). A series of images in the periphery of the lens epithelium whole-mount were taken.

A. Ki-67-positive cells are mainly located in a narrow zone near the periphery called the GZ. Scale bar=20 ⌠m.

B-K: The proliferating cells in the GZ labelled by Ki-67 are in different phases of the cell cycle. At higher magnification, the DAPI staining (B, D, F, H and J, white arrows and arrow heads) of the Ki-67-positive nuclei is much brighter than those Ki-67 negative cells. Some of the proliferating cells are in pairs (C, E, G and I, white arrows) or have condensed chromosomes (C and K, white arrow heads). This indicates they are in the M phase. Some single Ki-67-positive cells have slightly bigger nuclei (G, hollow arrow heads) than those Ki-67 negative cells. These cells are in the phase between G1 and G2. Scale bars=10 ⌠m.

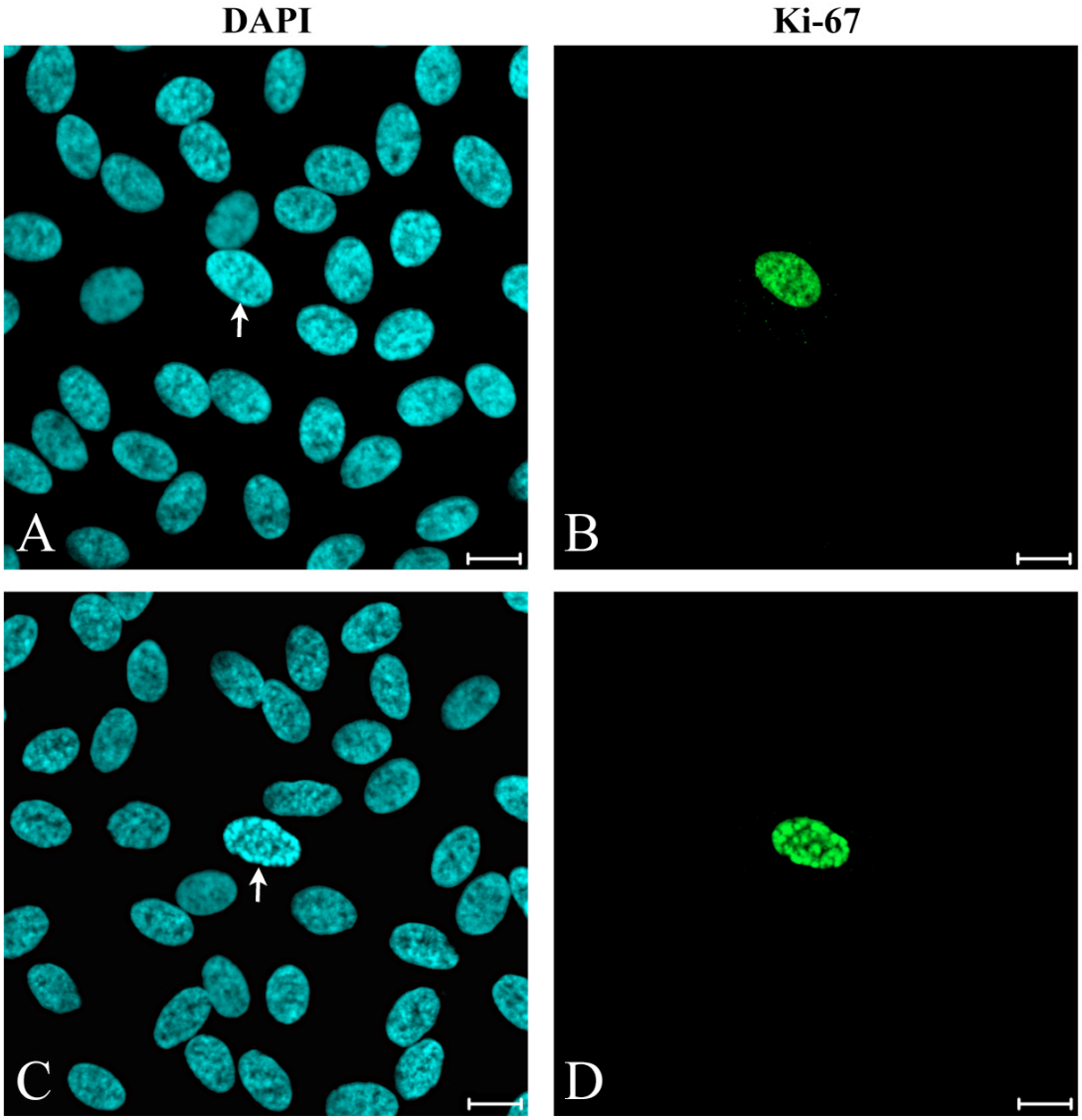

Figure 2.6. Cell proliferation in the CZ of the bovine lens epithelium.

Bovine lens epithelial cells were stained with the proliferation marker Ki-67 (green) and the DNA indicator DAPI (blue). A very low number of Ki-67-positive cells were detected in the CZ. Scale bars=10 μm.

A, C: The DAPI staining of these Ki-67-positive cell nuclei (white arrows) is similar to or slightly brighter than other quiescent cells around.

B, D: The Ki-67 staining shows that these proliferating cells usually appear as single.

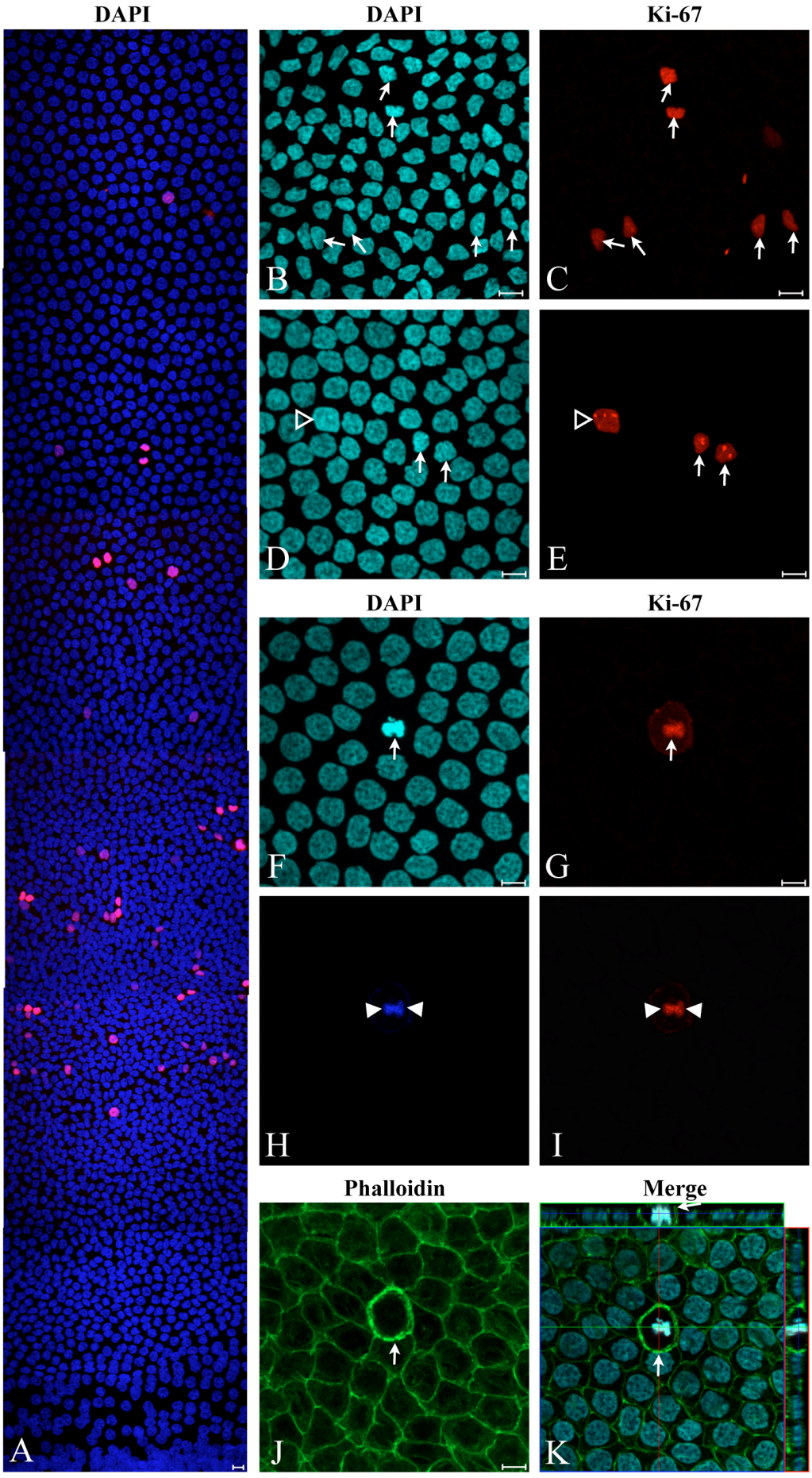
DAPI
DAPI
Ki-67
A
B
C
D
E
DAPI
Ki-67
F
G
H
I
Phalloidin
Merge
J
K

Figure 2.7. Cells proliferation in the GZ of the rabbit lens epithelium.

The rabbit lens epithelial cells were stained with DNA indicator DAPI (blue), proliferation marker Ki-67 (red) and F-actin binder phalloidin (green). Higher and lower magnification of images in the periphery of the lens epithelium were taken. Scale bars=10 ⌠m.

A. At lower magnification, the Ki-67 staining shows that cell proliferation is mainly restricted to the GZ of the lens epithelium.

B-E: At higher magnification, the Ki-67 staining shows that the proliferating cells are in the M phase (C, E, arrows, pairs of cells) or in between G1 and G2 phase (E, hollow arrow head, single cell), while the DAPI staining of their chromosomes is similar to or slightly higher than that in those quiescent cells around (B, D, arrows).

F-K: A cell in the anaphase of M phase is stained with DAPI, Ki-67 and phalloidin. The condensed chromosomes are stained brightly by DAPI (F) and Ki-67 (G). In one section of the Z-stack, the sister chromatids are seen clearly to separate from each other (H, I: head arrows). The phalloidin staining shows that layers of F-actin surround this cell (J). Its cell area is similar to other resting cells in cross section (J). However, the longitudinal section shows this cell is taller than the other cells around (K).

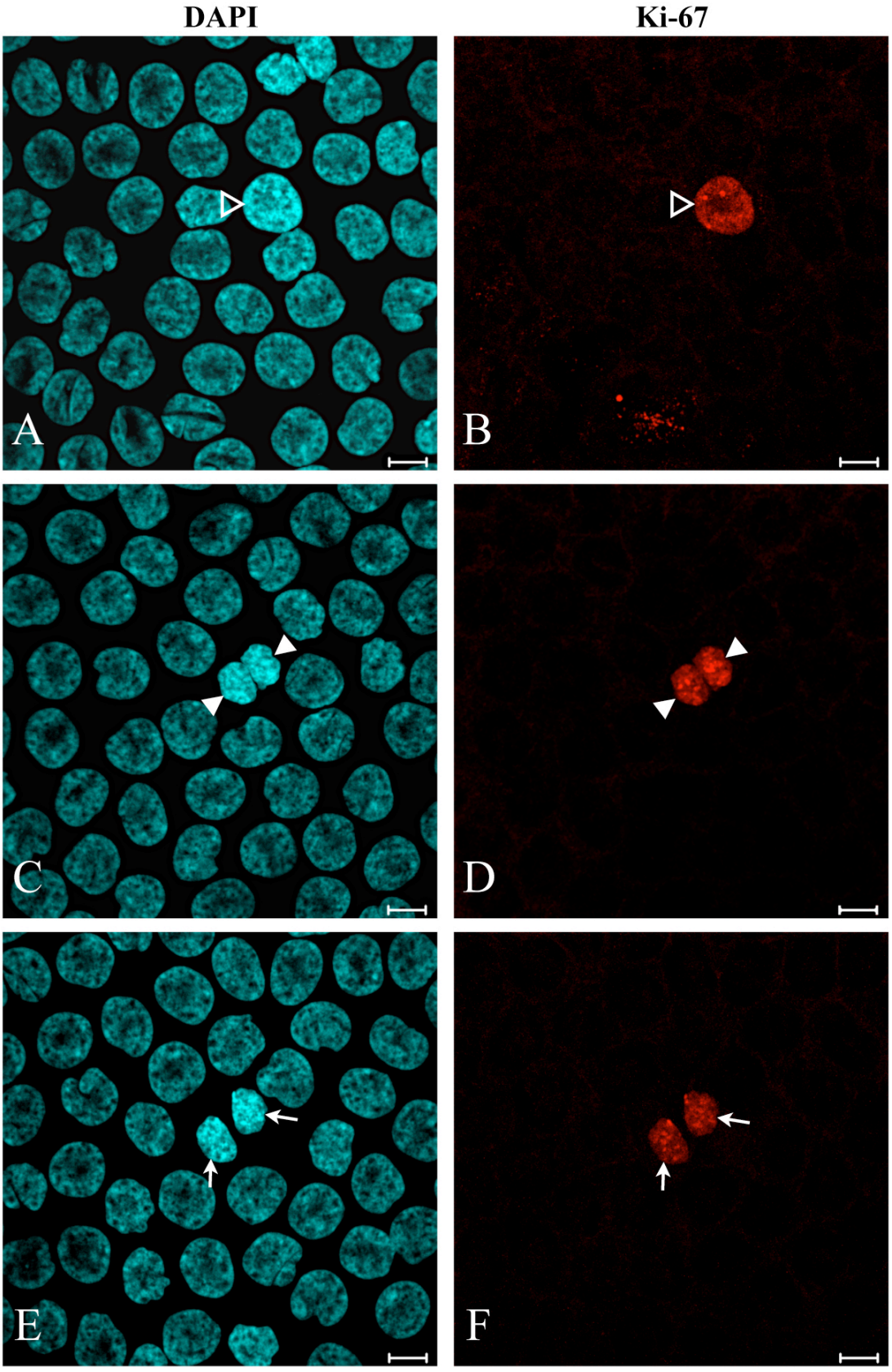
DAPI
Ki-67
A
B
C
D
E
F

Figure 2.8. Cell proliferation in the CZ of the rabbit lens epithelium.

The rabbit lens epithelial cells were stained with DNA indicator DAPI (blue) and proliferation marker Ki-67 (red). Images of the proliferating cells in the CZ were taken and the cells in different phases of the cell cycle are shown. Scale bars=10 ⌈m.

A, B: The cell in the phase between G1 and G2 has a slightly bigger nucleus (hollow arrow heads), which is stained brightly by DAPI and Ki-67.

C, D: The DAPI and Ki-67 staining shows that the sister chromatids are separating from each other in the early M phase (arrow heads).

E, F: In late M phase, the sister chromatids move further away from each other and are still stained brightly by DAPI and Ki-67 (arrows).

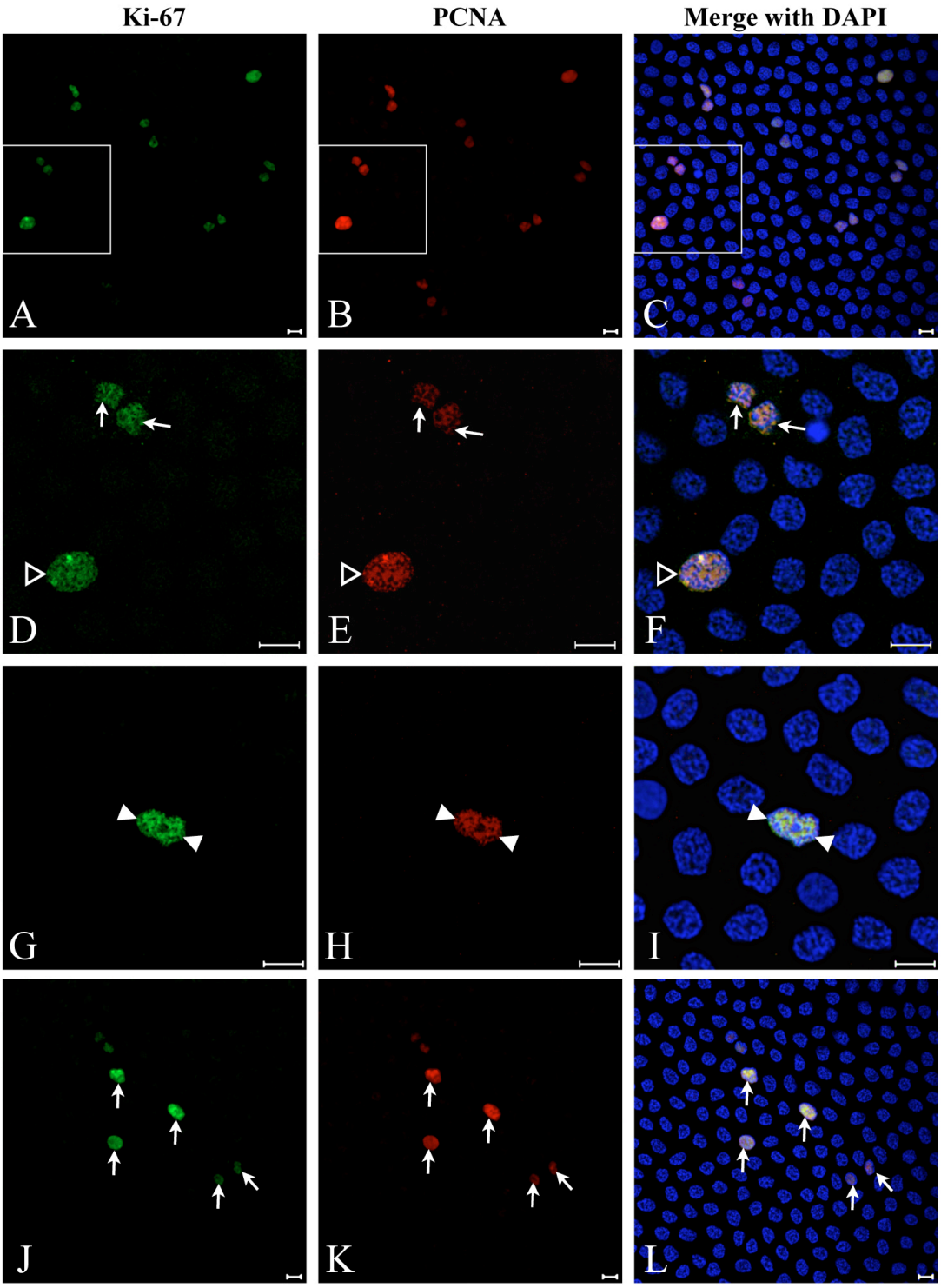
Ki-67
PCNA
Merge with DAPI
A
B
C
D
E
F
G
H
I
J
K
L

Figure 2.9. Cell proliferation in the GZ and the CZ of the rat lens epithelium.

The rat lens epithelial cells were stained with DNA indicator DAPI (blue) and proliferation markers Ki-67 (green) and PCNA (red). The co-stained proliferating cells were found in both the GZ and the CZ. The white squares in image A-C show the areas where the higher magnification of images D-F were taken. Scale bars=10 ⌈m.

A-I: At lower magnification, the Ki-67 and PCNA staining shows many proliferating cells scatter in the GZ and many of them are in pairs (A-C). At higher magnification, the sister chromatids in the M phase are separating from each other (D-F, arrows), and the cell in between the G1 and G2 phase shows a slightly bigger nucleus than other quiescent cells around (D-F, hollow arrow head). In the early M phase, the sister chromatids are just going to separate (G-I, arrow heads).

J-K: Some Ki-67 and PCNA co-stained cells are also detected in the CZ (arrows). They show the same staining as those in the GZ.

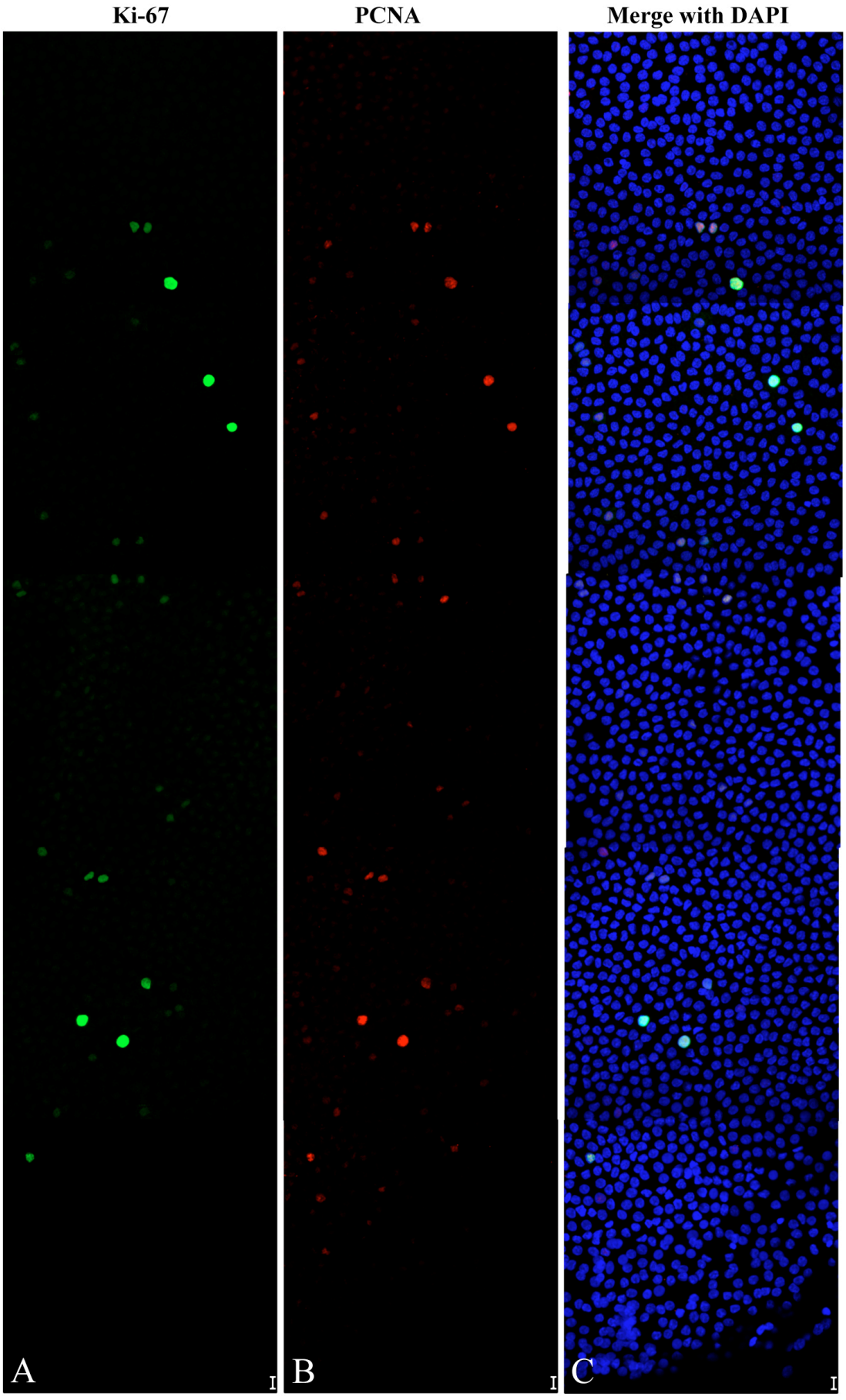
Ki-67
PCNA
Merge with DAPI
A
B
C

Figure 2.10. Cell proliferation in the GZ of the human lens epithelium.

The human lens epithelial cells were stained with proliferation markers Ki-67 (green) and PCNA (red) and DNA indicator DAPI (blue). A series of images in the periphery of the lens epithelium whole-mount were taken. Scale bars=10 ⌠m.

A-C: All the Ki-67 and PCNA positive cells are located in the GZ of the human lens epithelium. They are stained with both Ki-67 and PCNA.

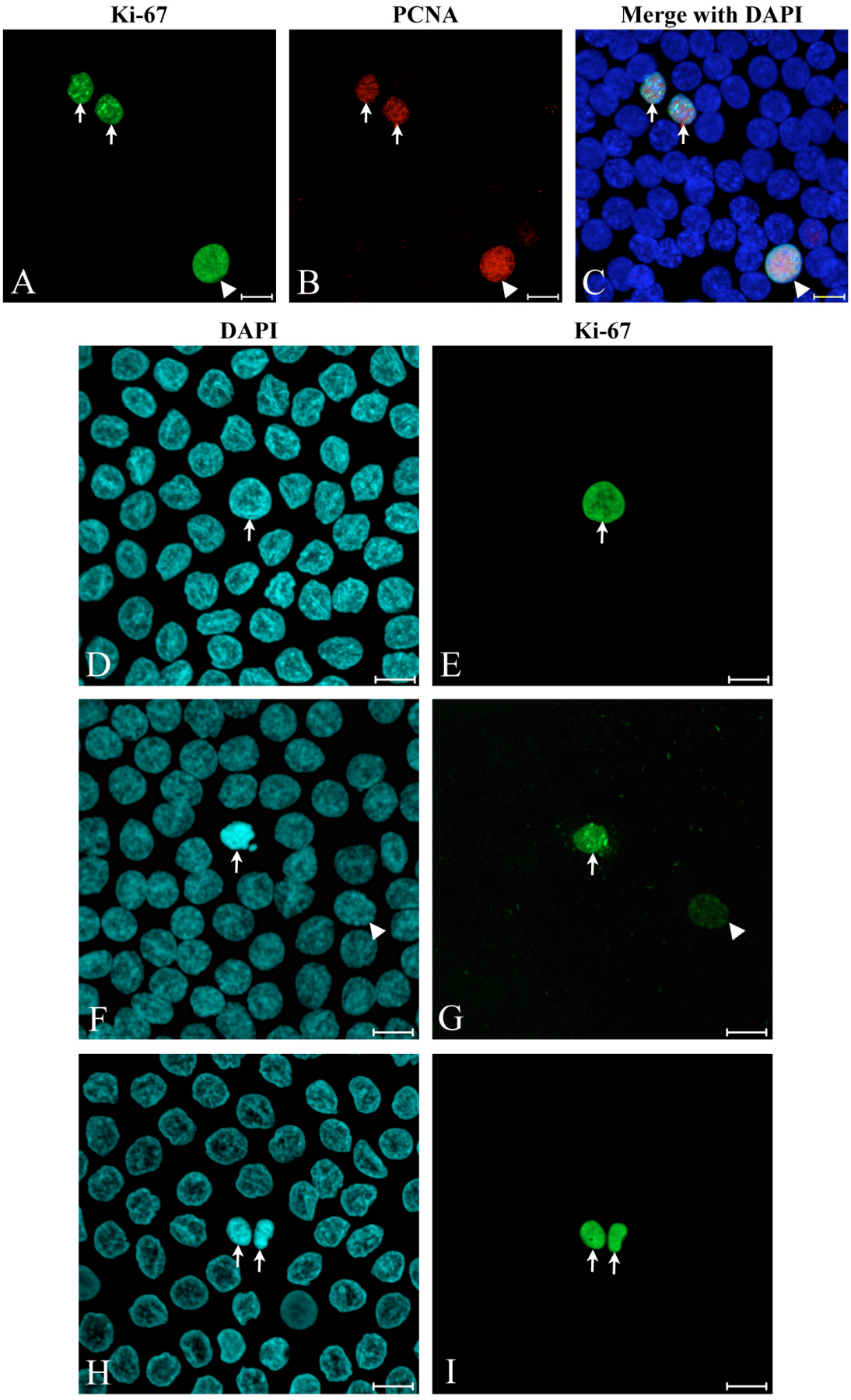
Ki-67
PCNA
Merge with DAPI
A
B
C
DAPI
Ki-67
D
E
F
G
H
I

Figure 2.11. The proliferating cells in the GZ of the human lens epithelium are in different phases of the cell cycle.

The human lens epithelial cells were stained with proliferation markers Ki-67 (green) and PCNA (red) and DNA indicator DAPI (blue). Images of the proliferating cells in the GZ were taken. Scale bars=10 ⌠m.

A-C: The co-staining of Ki-67 and PCNA in the proliferating cells is clearly shown at higher magnification. These cells are in pairs (arrows) or in single (arrow head), which means they are in the M phase or in the phase between G1 and G2.

D, E: The nucleus of the Ki-67-positive cell in the phase between G1 and G2 (arrow) is slightly bigger than those cells in G0 phase, but its DAPI staining is similar to other cells.

F, G: In the early M phase, the chromosomes condense and are stained brightly by DAPI and Ki-67 (arrows). The cell in the very early stage of the cell cycle has weak DAPI and Ki-67 staining (arrow heads).

H, I: In the late M phase, the two sister chromatids separate from each other and are still stained brightly by DAPI and Ki-67.

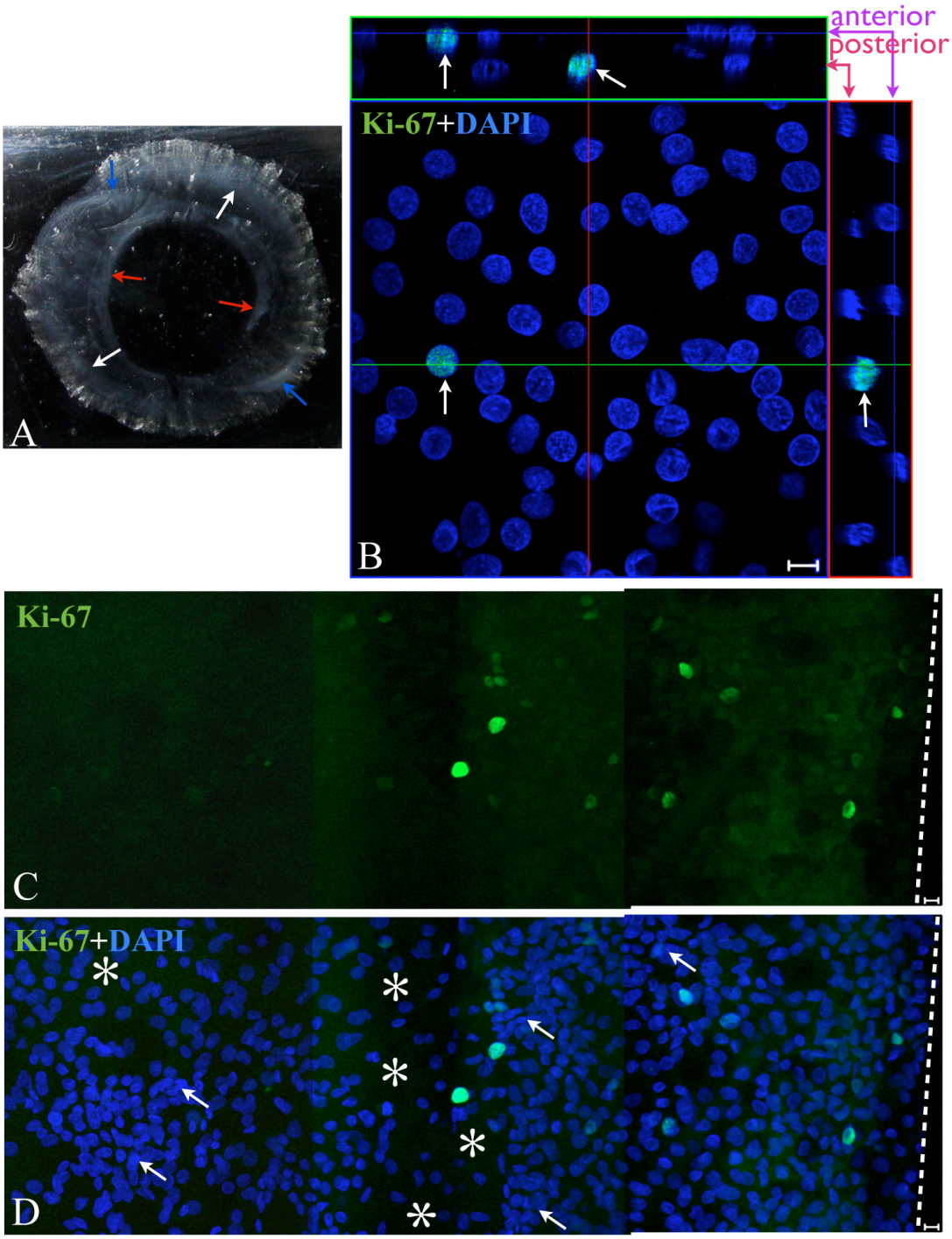
anterior
posterior
Ki-67+DAPI
A
B
Ki-67
C
Ki-67+DAPI
D

Figure 2.12. Cell proliferation in the human lens capsular bag implanted with an IOL.

A 79-year-old woman lens capsular bag implanted with an IOL was stained with DNA indicator DAPI (blue) and cell proliferation marker Ki-67 (green). Images in the periphery of the capsular bag were taken. Scale bars=10 μm.

A. The general appearance of the capsular bag without the IOL. The central part of the anterior capsule was removed during cataract surgery. Some white fibrosis is present along the rhexis margin (red arrows), the IOL haptics (blue arrows) or in the equatorial region (white arrows).

B. The Z-stack of an image taken in the periphery of the lens capsule shows that cell proliferation (arrows) happens on both the anterior and the posterior capsule.

C, D: Three images about the cells on the anterior capsule were taken from the periphery and tiled to produce a montage. The Ki-67 staining shows that many cells still proliferate in the periphery where the GZ is (dotted lines indicate the edge of the capsule). The DAPI staining shows that some epithelial cells were lost during cataract surgery (*) and some grow into multilayer (arrows).

2.4.1.2 Lens epithelial cell apoptosis

2.4.1.2.1 Lens epithelial cell apoptosis analysed by Annexin-V-Fluorescein

After the living bovine lens epithelial cells were incubated with the Annexin-V-Fluoscein labelling solution for 12 minutes, the plasma membranes of many cells were stained with Annexin-V-Fluorescein (Figure 2.13A, D and G). This indicated that the phosphatidylserine had translocated from the inner part of the plasma membrane to the outer layer and was exposed to the external surface of the cell. The nuclei of these cells were also stained with PI (Figure 2.13B, E and H), which is membrane-impermeable and generally excluded from viable cells. The PI staining implies that these cells were undergoing necrosis. One important difference between necrosis and apoptosis is that the cell membrane is intact in the apoptotic cell but breaks down in the necrotic cell. Furthermore, the DAPI staining was stronger in the Annexin-V-Fluorescein- and PI-positive cells than in the Annexin-V-Fluorescein- and PI-negative cells. DAPI can pass through an intact cell membrane and is used to stain both live and fixed cells, while it usually passes through the membrane less efficiently in live cells than in necrotic cells. Therefore, the stronger staining in the Annexin-V-Fluorescein- and PI-positive cell nuclei means that these cell membranes are not intact any more or have already broken down.

The Annexin-V-Fluorescein and PI staining results showed that many lens epithelial cells started to die after a 12-minute incubation in staining solution at room temperature. In this situation, it was very difficult to pick out the truly apoptotic cells, which is why the TUNEL assay was preferred.

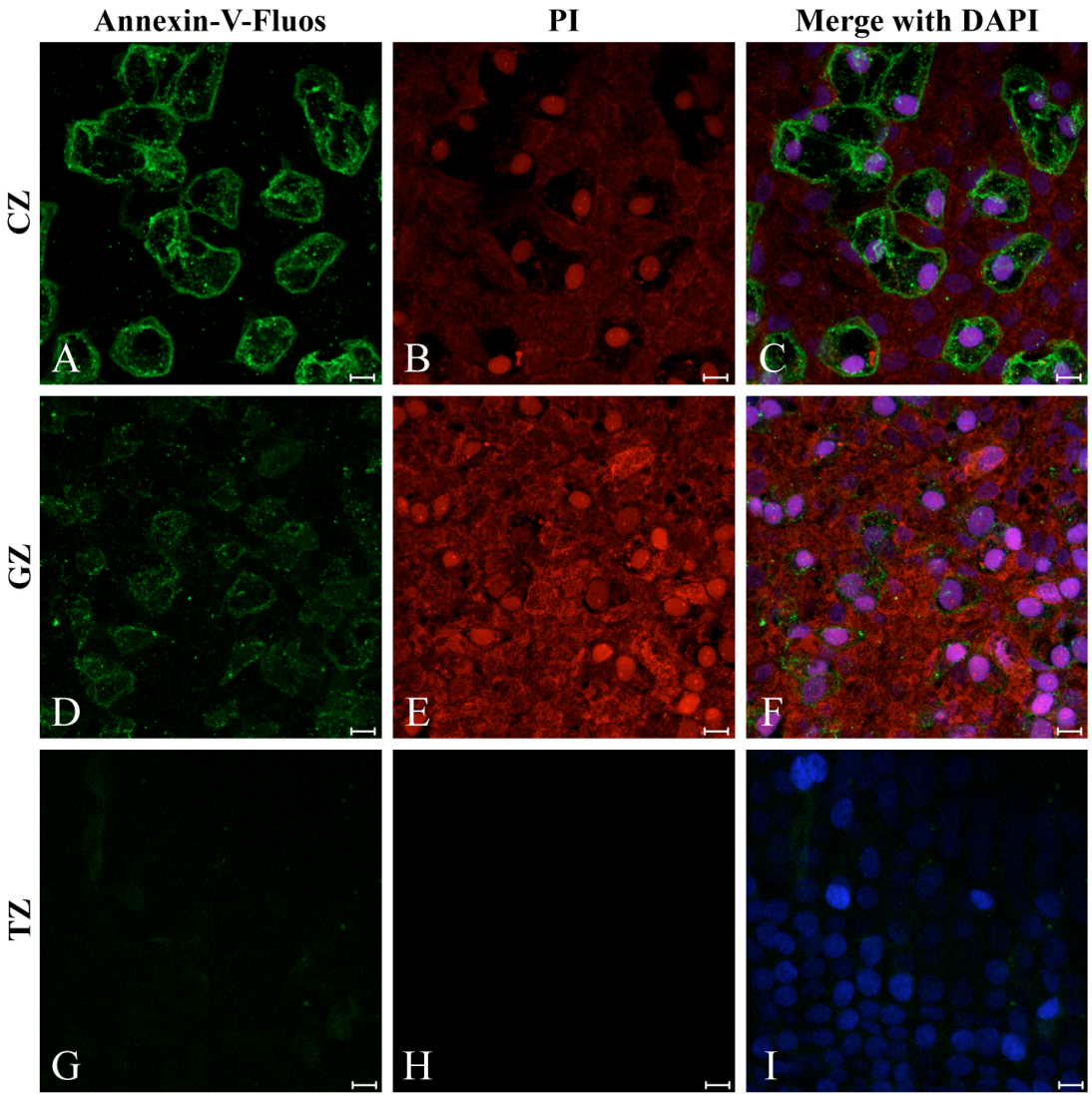

Figure 2.13. The Annexin-V-Fluorescein staining of the bovine lens epithelial cells.

The living bovine lens epithelial cells were incubated with Annexin-V-Fluorescein labelling solution [including Annexin-V-Fluorescein labelling reagent (green), PI solution (red), and DAPI (blue)] for 12 minutes at room temperature and then fixed in 4% (w/v) PFA. Images in the CZ, GZ and TZ were taken. Scale bars=10 μm.

A-C: In the CZ, the plasma membranes of many cells are stained with Annexin-V-Fluorescein (A), and their nuclei are labelled by PI (B). All the cell nuclei are stained with DAPI (C).

D-F: In the GZ, some cell membranes and nuclei are also respectively stained with Annexin-V-Fluorescein (D) and PI (E).

G-I: In the TZ, no Annexin-V-Fluorescein or PI positive cells are found. The nuclei stained with DAPI align into regular columns.

2.4.1.2.2 Lens epithelial cell apoptosis analysed by TUNEL assay

2.4.1.2.2.1 Cell apoptosis in the bovine, mouse and rat lens epithelia

TUNEL assay was performed on the epithelium whole-mounts of six bovine (30 months old) lenses, three mouse (6 weeks old) lenses, and three rat (4 months old) lenses. In all the bovine lens epithelium whole-mounts, only one TUNEL-positive nucleus was observed (Figure 2.14G-I). No TUNEL-positive nuclei were detected in mice (Figure 2.15G-I). One or two TUNEL-positive nuclei were found in each rat lens epithelium whole-mount (Figure 2.16C). All the stained nuclei displayed classic apoptotic morphology, i.e., the nucleus became smaller with condensed chromatin and therefore was stained strongly with DAPI.

In all the negative controls, no TUNEL-positive nuclei were found (Figure 2.14A-C, 2.15A-C, and 2.16). For the positive control, cells were pretreated with benzonase nuclease prior to the TUNEL assay, and then numerous TUNEL-positive nuclei were detected in the whole lens epithelium (Figure 2.14D-F, 2.15D-F, and 2.16B). Some fibre nuclei on the top of the TZ were also stained. Compared with the apoptotic nuclei, the TUNEL-positive nuclei in the positive control did not show obvious chromatin condensation or smaller shape in the DAPI staining.

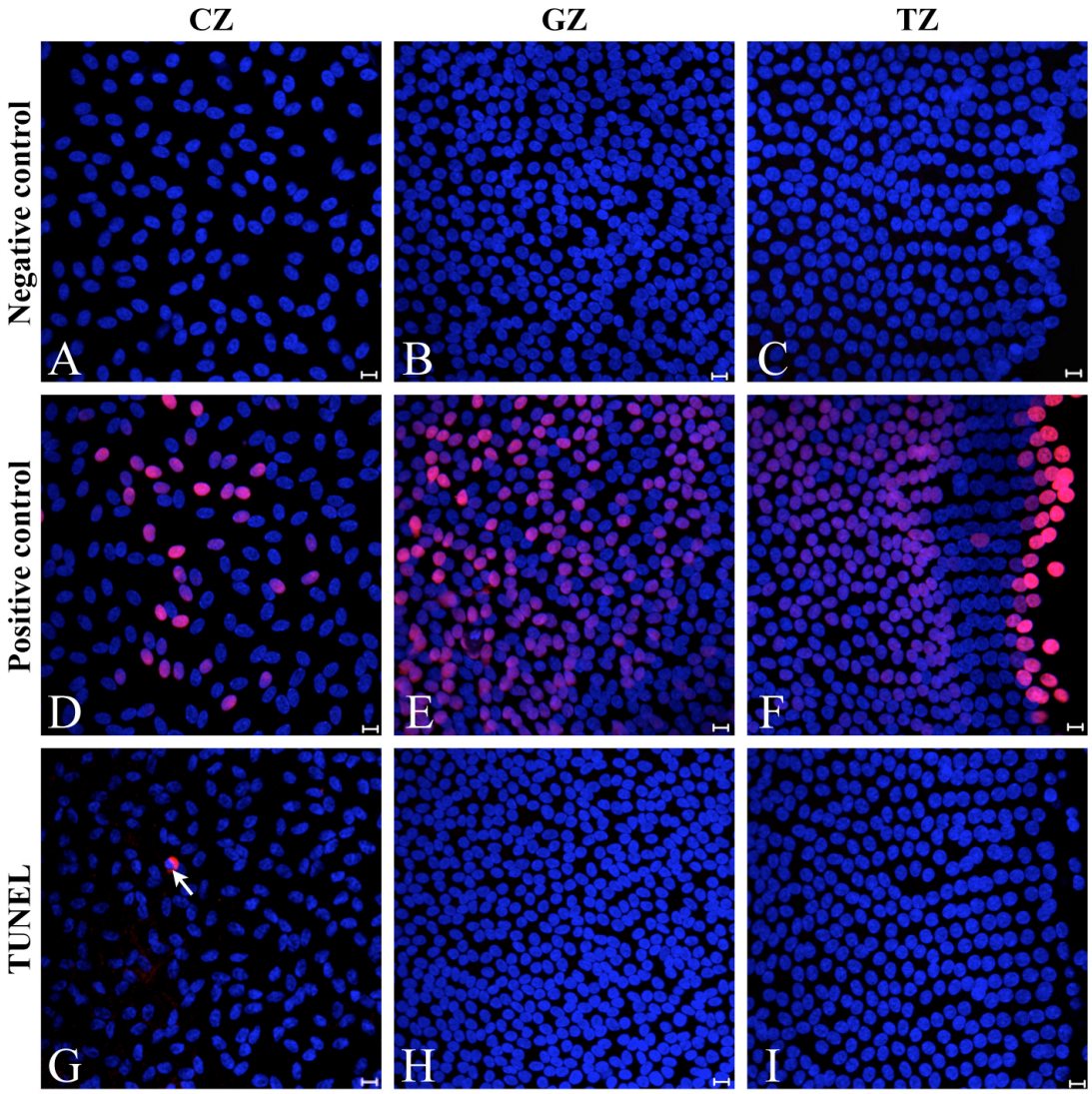

Figure 2.14. Cell apoptosis in the bovine lens epithelium.

The epithelium whole-mounts of 30-month-old bovine lenses underwent the TUNEL assay (red) and DAPI staining (blue). The epithelial cells as the negative control were just incubated with the label solution containing TMR red labelled nucleotides. The epithelial cells as the positive control were digested with benzonase nuclease (100 U/ml) to break DNA strands before the TUNEL assay. The images in different zones were taken. Scale bars=10 μm.

A-C: In the negative control, no TUNEL-positive nucleus is detected in the CZ, GZ and TZ.

D-F: In the positive control, numerous TUNEL-positive nuclei are apparent in the three zones. Some fibre nuclei on the top of the TZ are also labelled (F). The stained nuclear shape does not change much and the chromatin does not obviously condense. The staining intensity is not uniform. Slightly weakened and very strong positive staining was observed sometimes.

G-I: Very occasionally the TUNEL-positive nuclei are observed in the bovine lens epithelium (arrow). The chromatin in the TUNEL-positive nucleus condenses and is strongly stained by DAPI.

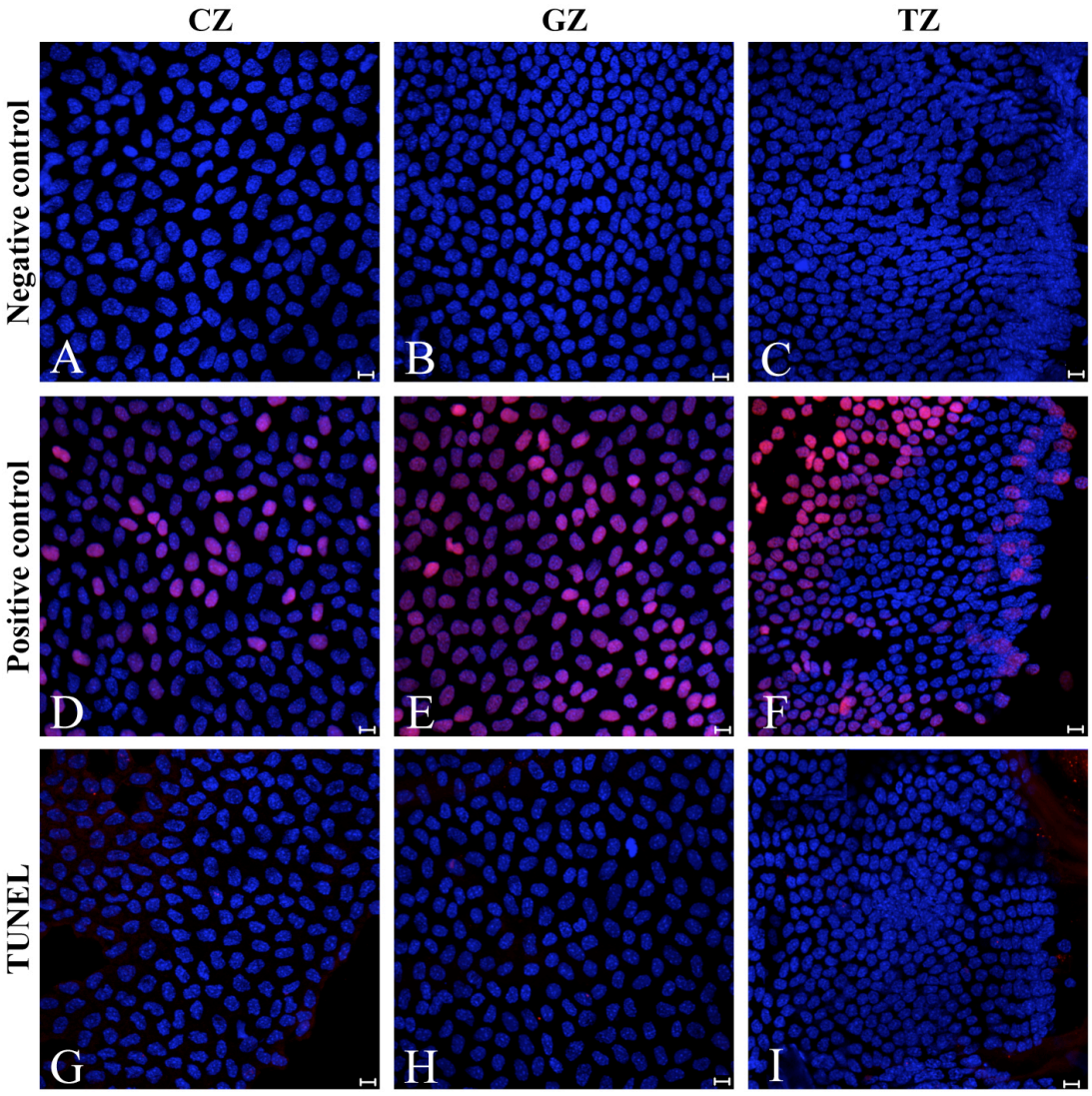

Figure 2.15. Cell apoptosis in the mouse lens epithelium.

The TUNEL assay (red) and DAPI staining (blue) were performed on the epithelial cells of 6-week-old mouse lenses. The cells as the negative control were just incubated with the label solution containing TMR red labelled nucleotides. The cells as the positive control were pre-treated with benzonase nuclease (100 U/ml) to break DNA strands before the TUNEL assay. The images in the CZ, GZ and transitional TZ were taken. Scale bars=10 μm.

A-C: No TUNEL-positive nuclei are detected in the negative control.

B-F: In the positive control, many TUNEL-positive cells are present in the three zones.

G-I: No TUNEL-positive nuclei are detected in the three zones of the mouse lens epithelium.

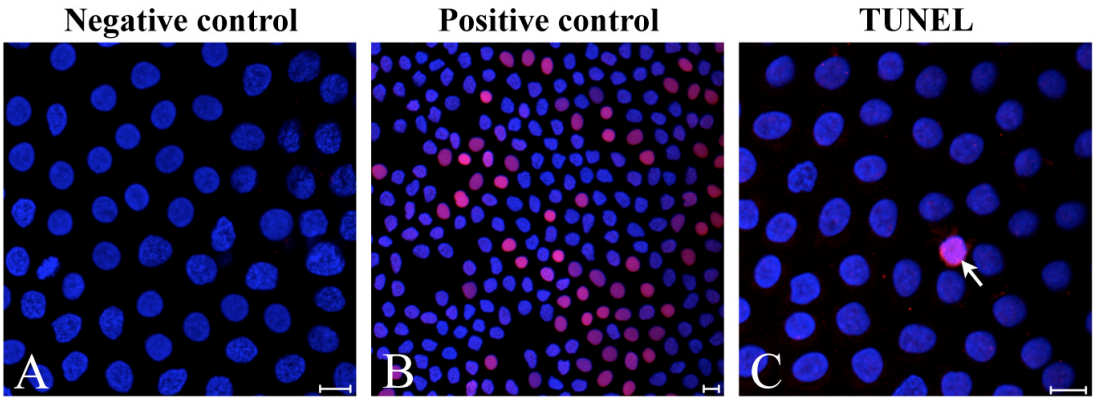

Figure 2.16. Cell apoptosis in the rat lens epithelium.

The lens epithelium whole-mounts of 8-month-old rats underwent the TUNEL assay (red) and DAPI staining (blue). The epithelial cells that were just incubated with label solution were used for the negative control. The epithelial cells that were digested by benzonase nuclease (100 U/ml) in order to break DNA strands before the TUNEL assay were used for the positive control. Images in each sample were randomly taken. Scale bars=10 μm.

A: No TUNEL positive cells are found in the negative control.

B: Numerous TUNEL-positive nuclei are observed in the positive control.

C: A very low number of TUNEL-positive nuclei are detected in the rat lens epithelium (arrow). The chromatin of this nucleus condenses and is strongly stained with DAPI.

2.4.1.2.2.2 Cell apoptosis in the human lens epithelium

TUNEL assay was carried out on 14 lenses from seven people aged from 45 to 81. In order to find out whether leaving the eyes in saline solution for up to three days would increase lens epithelial cell apoptosis, the eyes were divided into the fixed-immediately group and fixed-later group. The results were shown in Table 2.7. The lenses fixed 3 days after postmortem did not have more apoptotic cells compared with those fixed immediately after removing their corneas. In the forth donor, there were even more apoptotic epithelial cells in the fixed-immediately lens than in the fixed-later lens. These results indicate that storage in 0.9% (w/v) of NaCl for up to three days does not increase cell apoptosis.

Table 2.7. TUNEL-positive cell numbers in the fixed-immediately group and fixed-later group

Donor	Age	Sex	Fix-immediately	Fix-later
1	46	F	0	2
2	79	M	10	9
3	59	F	5	5
4	59	F	17	2

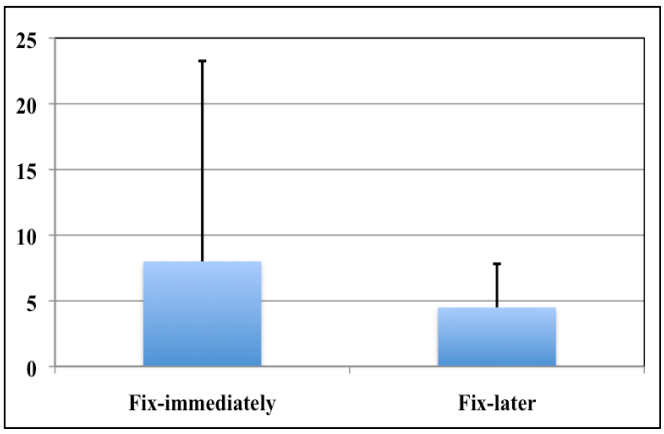

In each human lens, the number of TUNEL-positive cells was variable from zero to 23 (Table 2.8) and the apoptosis rates were very low, ranging from 0% to 0.004%. These TUNEL-positive cells were in different stages of apoptosis (Figure 2.17). Furthermore, the lenses from middle-aged people (45-46 years old) had similar TUNEL-positive cells to those from old people (59-81 years old). The result of

Student's t-Test did not show statistically significant difference. This means that cell apoptosis does not change with age, mean +/- SD?

Table 2.8. The TUNEL-positive epithelial cell number in each human lens

Donor	Age	Sex	Eye 1	Eye 2
1	46	F	0	2
2	45	M	14	22
3	45	F	8	7
4	59	F	5	5
5	59	F	17	2
6	79	M	10	9
7	81	F	23	14

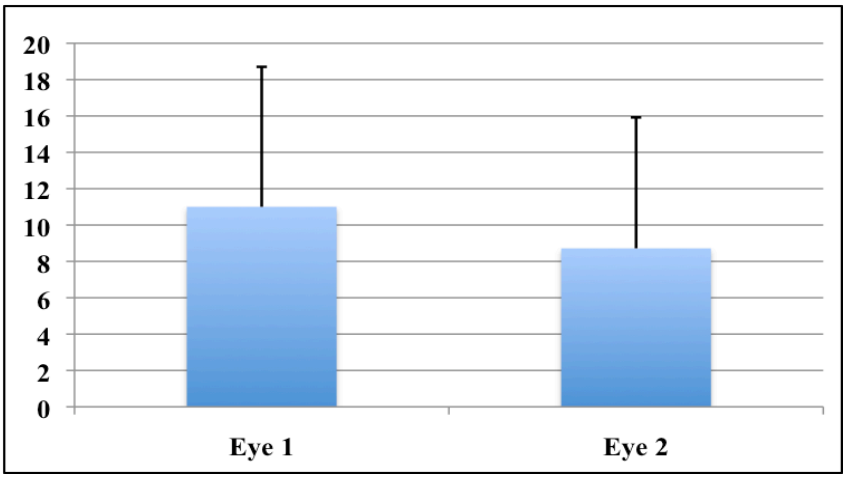

In order to observe lens cell apoptosis after cataract surgery, TUNEL assay was carried out on four human capsular bags with IOLs. Approx. 20-30 TUNEL-positive cells were detected in each capsular bag. They were located on both the anterior and posterior capsules (Figure 2.19). This indicated that cell apoptosis happens not only in the epithelial cells on the anterior capsule but also in the cells experiencing EMT on the posterior capsule. As the sample number was too low, it was difficult to draw any conclusion about the apoptotic cell number comparison between the capsular bags and the normal lenses.

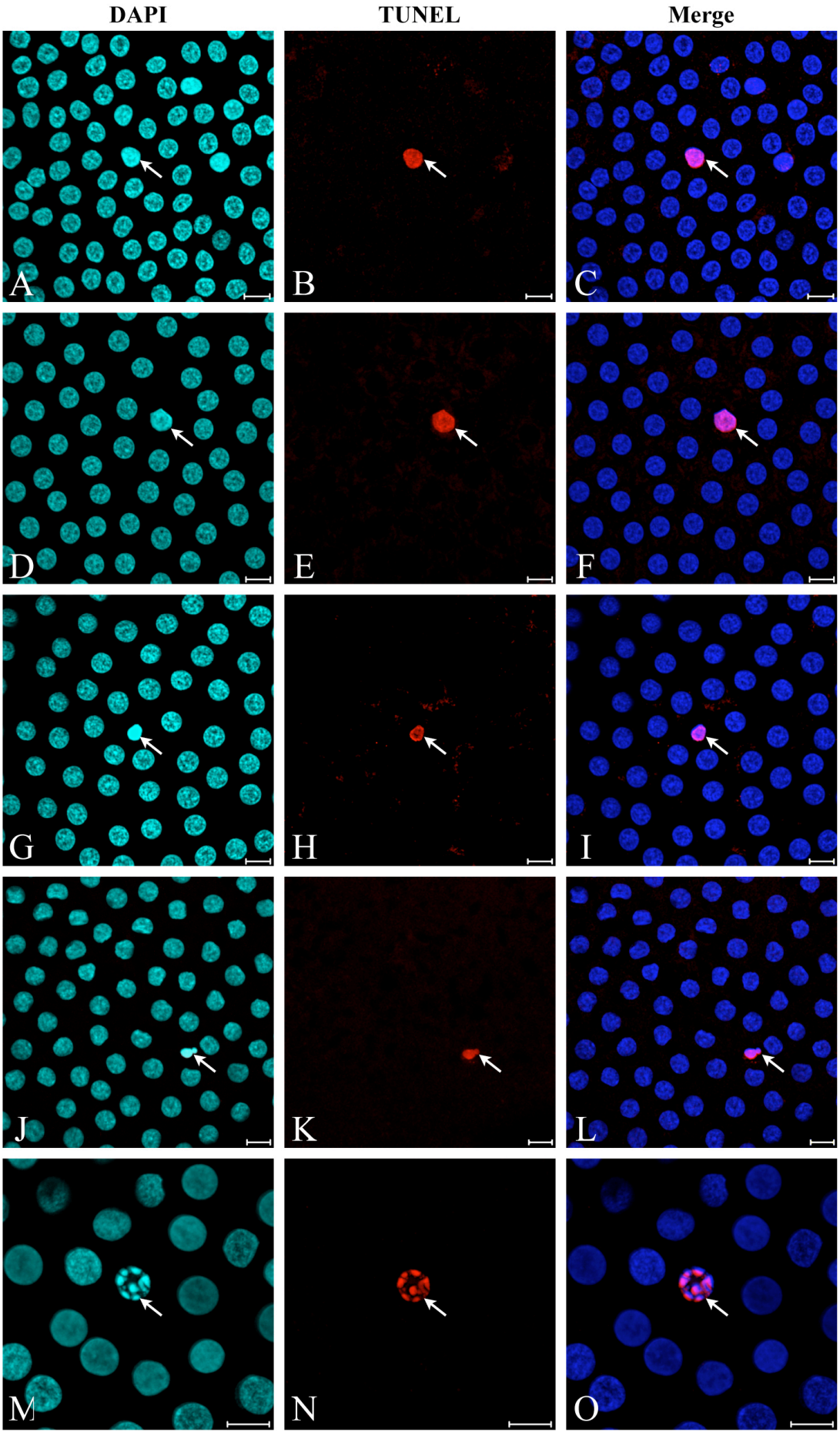
DAPI
TUNEL
Merge
A
B
C
D
E
F
G
H
I
J
K
L
M
N
O

Figure 2.17. Morphological changes of the apoptotic nuclei in the human lens epithelium.

The human lens epithelial cells underwent the TUNEL assay (red) and DAPI staining (blue). Some TUNEL-positive cells were observed. According to the difference of their nuclear morphology, they are divided into four groups. Each group is in one stage of the apoptosis process.

A-C: Stage 1. The nucleus of the TUNEL-positive cell doesn't show very obvious morphologic alternation except that its chromatin starts to condense and shows strong DAPI staining (arrows).

D-F: Stage 2. The nucleus of the TUNEL-positive cell becomes marginated because of the compacted chromatin, and is stained brightly with DAPI (arrows).

G-I: Stage 3. With the continuous condensation of chromatin, the nucleus of the TUNEL-positive cell becomes much smaller and denser than the other normal cells, and can be easily recognized in DAPI staining (arrows).

J-O: Stage 4. Finally, The nucleus of the TUNEL-positive cells breaks up into fragments (arrows). Scale bars=10 ⌈m.

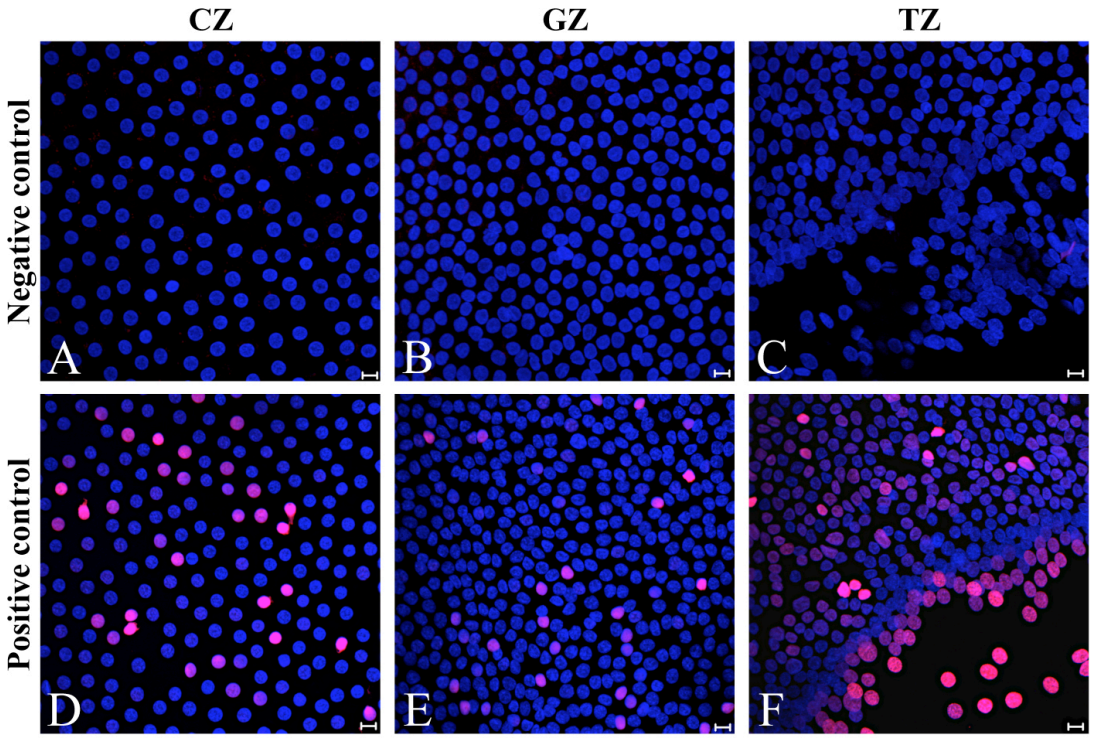

Figure 2.18. The negative and positive controls of the TUNEL assay performed on the human lens epithelial cells.

For the negative control, the human lens epithelial cells were just incubated with label solution containing TMR red labelled nucleotides (red) and DAPI (blue). For the positive control, the lens epithelial cells were digested by benzonase nuclease (100 U/ml) to break DNA strands before the TUNEL assay (red) and DAPI staining (blue). Images in the CZ, GZ and TZ were taken. Scale bars=10 μm.

A-C: No TUNEL-positive nuclei are observed in the three zones.

D-F: Numerous TUNEL-positive nuclei are found in each zone. Their morphology is the same as those TUNEL-negative nuclei in the DAPI staining.

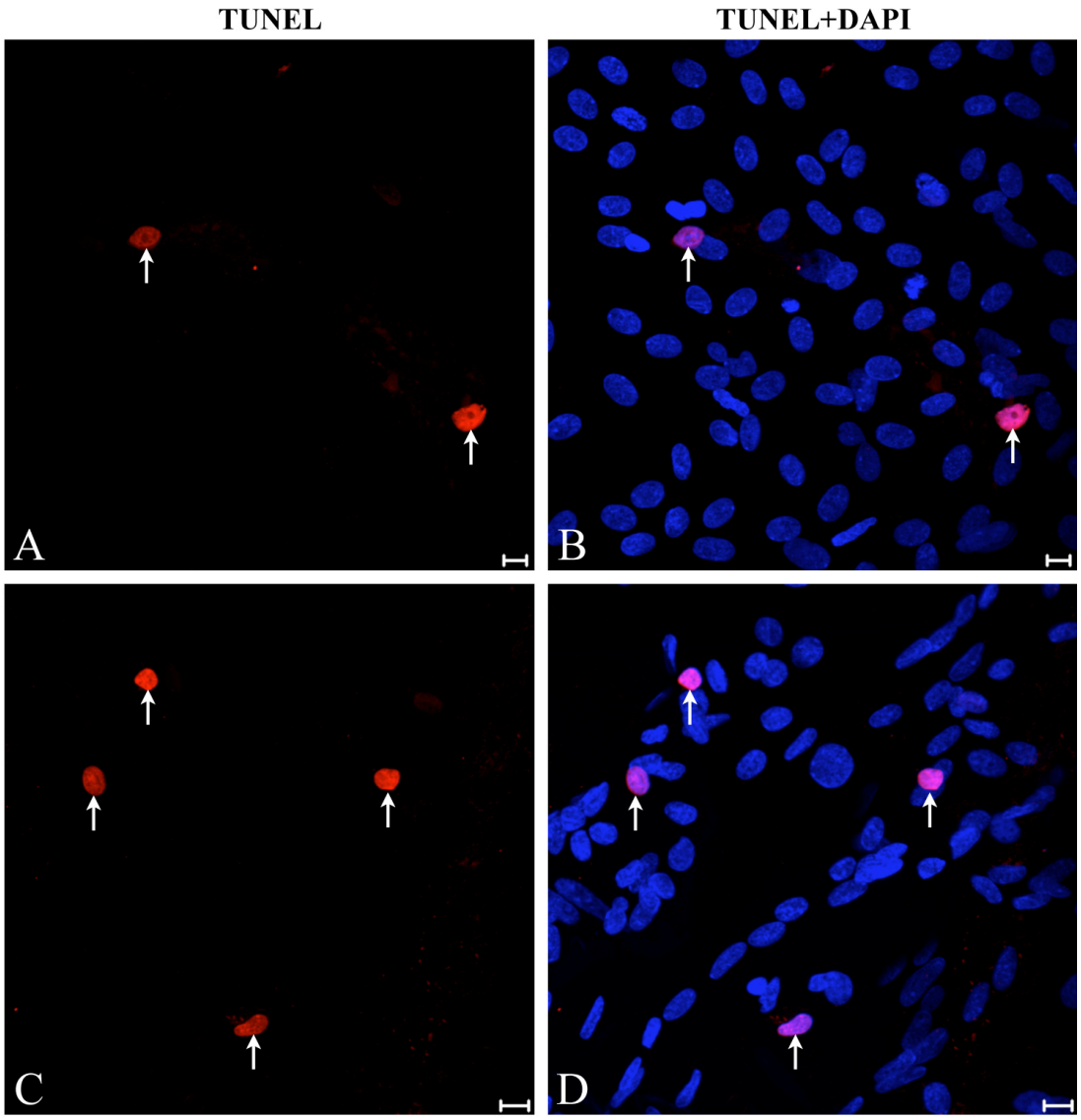

Figure 2.19. Cell apoptosis in a human lens capsular bag implanted with an IOL.

A lens capsular bag from a 79-year-old male donor was dissected out of the eye. After the IOL was gently removed, four cuts were made from the rhexis. The anterior capsule was then peeled off from the posterior capsule along the cuts and pinned down on the Sylgard. The flat whole-mount was processed with the TUNEL essay (red) and DAPI (blue) staining. The images with TUNEL-positive cells were taken from the anterior and posterior lens capsule. Scale bars=10 μm.

A, B: In the anterior capsule, some TUNEL-positive cells are detected (arrows). Their chromatin condenses and the nuclei are slightly smaller than those TUNEL-negative cells in DAPI staining.

C, D: In the posterior capsule, TUNEL-positive cells are also found and their nuclear shape is similar with those in the anterior capsule. DAPI staining also shows many elongated nuclei, which belong to the fibre-like cells.

2.4.1.3 Lens epithelium homeostasis

In the lens epithelium, new cells are continuously produced in the GZ, some cells die by apoptosis, and the epithelial cells at the end of the TZ consistently differentiate into fibre cells. Does a cell number balance exist between cell production (cell proliferation in the GZ) and cell loss (cell apoptosis and fibre cell differentiation) in the lens epithelium to maintain its homeostasis? In order to answer this question, the proliferating cells number, the apoptotic cell number and the meridional line number in the TZ of bovine, rabbit and human lens epithelium were calculated. Here it was assumed that all the cells at the end of the meridional lines would differentiate into fibre cells at the same time. Therefore, the meridional line number was equal to the newly differentiated fibre cell number.

In the bovine, rabbit and human lens epithelium, results showed that this cell balance did not exist (Table 2.9). More cells were produced but less cells were lost in the bovine and rabbit lens epithelium. Although the apoptotic cell number in the rabbit lens epithelium was not studied, it should be very low according to the studies on the bovine, mouse and rat lens, which were in similar human years with the rabbit lenses. In the 30-50-year-old human lens epithelium, the produced cell number was similar to the lost cell number, while the lost cell number was much bigger than the produced cell number in the 80-90-year-old human lens epithelium.

Table 2.9. Numbers of the proliferating cells, apoptotic cells and meridional lines (mean ± SD)

Species	Sample number	Number of proliferating cells	Number of apoptotic cells	Number of meridional lines
Bovine	8	5439±1067	1	4264±180
Rabbit	6	8594±1482	Not available	3210±240
Human (30-50)	13	2130±629	0-22	2258±106
Human (80-90)	12	1197±567	9-23	2420±162

2.4.2 Lens epithelial cell density

2.4.2.1 Lens epithelial cell density in different mammals

The results showed that the epithelial cell density gradient in the bovine, mouse, rat and rabbit lenses was very similar (Figure 2.20A-D). In each species the cell density was unchanged in the CZ, started to increase at the end of the CZ, increased quickly and dramatically in the GZ, and started to decline in the TZ (Figure 2.20 and 21). The Ki-67 staining proved that the region with increased cell density was the GZ. The lens epithelial cell density in each zone was slightly variable in different species (Table 2.10). In the CZ, it was higher in the mouse and lower in the rabbit. All of them had a striking cell density peak in the GZ, which varied between 13200 cells/mm^2 and 15900 cells/mm^2. When the lens epithelial cells in the GZ withdrew from the cell cycle and migrated to the TZ to arrange into regular columns, the cell density decreased, especially in bovine and rabbits (Figure 2.22). The human lens epithelial cell density was different from the other animals', and it continued to increase from the periphery of the CZ to the TZ (Figure 2.20E). Furthermore, the cell density in each zone was much lower than that in the other studied mammals.

Table 2.10. Cell density and proliferation index with respect to age (mean ± SD)

Species	Age	Sample number	Proliferation index	Density in the CZ	Highest density in the GZ	Density in the TZ
Bovine	30 months	8	0.0039±0.0008	3736±133	13160±307	7419±423
Rabbit	6 months	6	0.01±0.0018	3491±228	14667±617	7579±1187
Rat	4 months	3	Not available	4497±662	15856±2566	12496±2219
Mouse	6 weeks	3	Not available	5384±61	13395±399	12356±780
Human	33-46 years	13	0.0042±0.0012	4639±347	10864±950	9404±1234
Human	80-98 years	13	0.0022±0.001	4387±444	8649±527	8916±1117

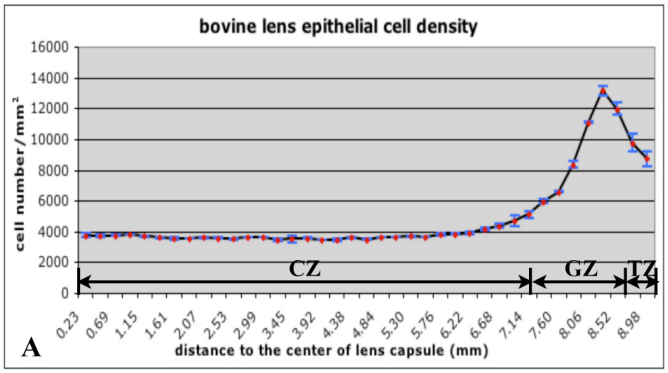
bovine lens epithelial cell density
cell number/mm²
16000
14000
12000
10000
8000
6000
4000
2000
0
CZ
GZ
TZ
0.23 0.69 1.15 1.61 2.07 2.53 2.99 3.45 3.92 4.38 4.84 5.30 5.76 6.22 6.68 7.14 7.60 8.06 8.52 8.98
distance to the center of lens capsule (mm)
A

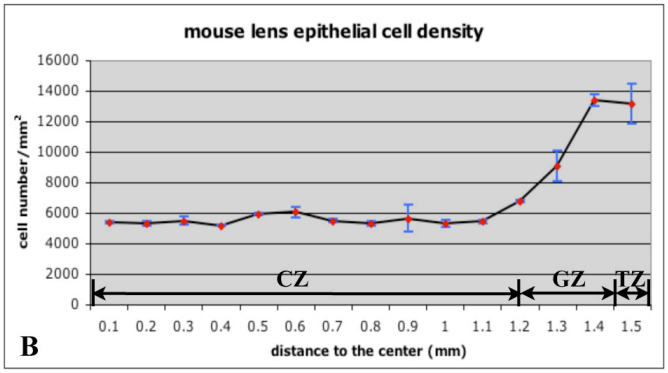
mouse lens epithelial cell density
cell number/mm²
16000
14000
12000
10000
8000
6000
4000
2000
0
CZ
GZ
TZ
0.1 0.2 0.3 0.4 0.5 0.6 0.7 0.8 0.9 1 1.1 1.2 1.3 1.4 1.5
distance to the center (mm)
B

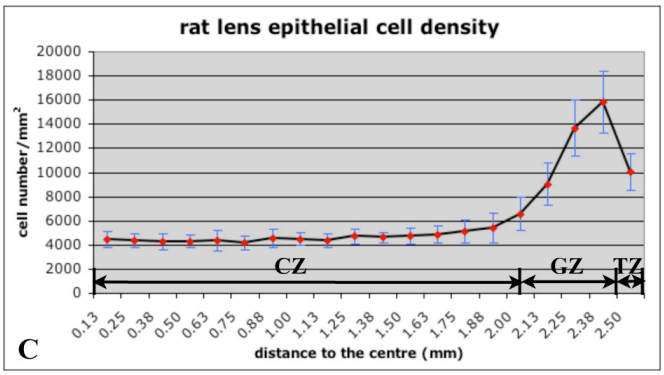
rat lens epithelial cell density
cell number/mm²
20000
18000
16000
14000
12000
10000
8000
6000
4000
2000
0
CZ
GZ
TZ
0.13 0.25 0.38 0.50 0.63 0.75 0.88 1.00 1.13 1.25 1.38 1.50 1.63 1.75 1.88 2.00 2.13 2.25 2.38 2.50
distance to the centre (mm)
C

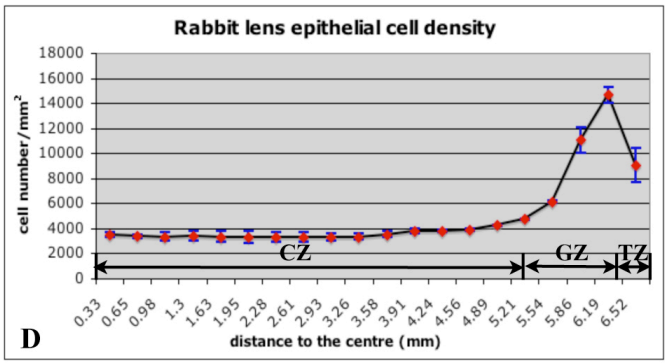
Rabbit lens epithelial cell density
cell number/mm²
18000
16000
14000
12000
10000
8000
6000
4000
2000
0
CZ
GZ
TZ
0.33 0.65 0.98 1.3 1.63 1.95 2.28 2.61 2.93 3.26 3.58 3.91 4.24 4.56 4.89 5.21 5.54 5.86 6.19 6.52
distance to the centre (mm)
D

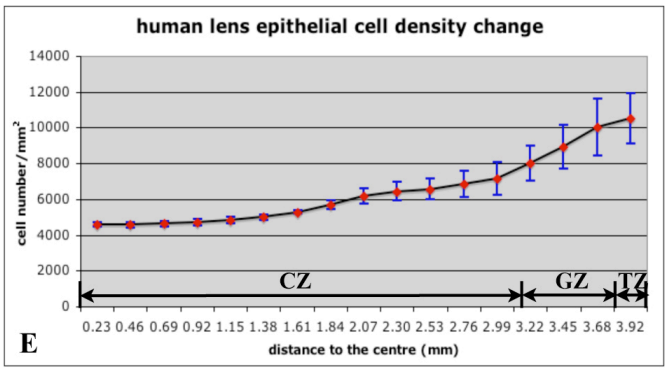
human lens epithelial cell density change
cell number/mm²
14000
12000
10000
8000
6000
4000
2000
0
CZ
GZ
TZ
0.23 0.46 0.69 0.92 1.15 1.38 1.61 1.84 2.07 2.30 2.53 2.76 2.99 3.22 3.45 3.68 3.92
distance to the centre (mm)
E

Figure 2.20. Epithelial cell density in different mammalian lenses.

The epithelial cell density of bovine, mouse, rat, rabbit and human lenses from the anterior pole to the end of the TZ was calculated and charted. The data are shown as mean ± SD ($n \geq 3$)

A-D: The cell density change across the lens epithelium is consistent in the bovine, mouse, rat and rabbit lenses. The cell density does not change in the CZ but increases dramatically in the GZ and starts to decline in the TZ. In each zone, the cell density is slightly variable in different species of the lenses.

E: The human lens epithelial cell density is different from the animals above. It continues to ascend from the periphery of the CZ to the end of the TZ. The highest density in the GZ is much lower than that in the animals' above.

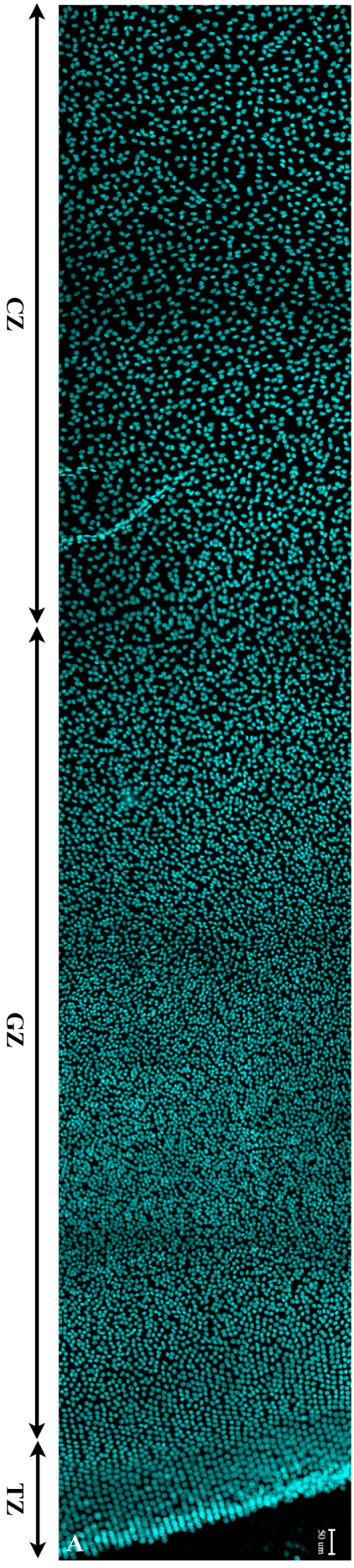

Figure 2.21. The cell density change in the periphery of the bovine lens epithelium.

The bovine lens epithelial cell nuclei were stained with DNA indicator DAPI (blue). In the periphery, a series of images were taken from the end of the TZ to the periphery of the CZ. These images were tiled together to produce a montage.

The stained nuclei show that cell density is slightly low in the CZ and continues to increase when closing to the GZ. In the middle of the GZ, cell density enhances strikingly and some nuclei even attach to each other. In the periphery of the TZ, the cells line into regular columns and the cell density decreases. Scale bar=50 μm.

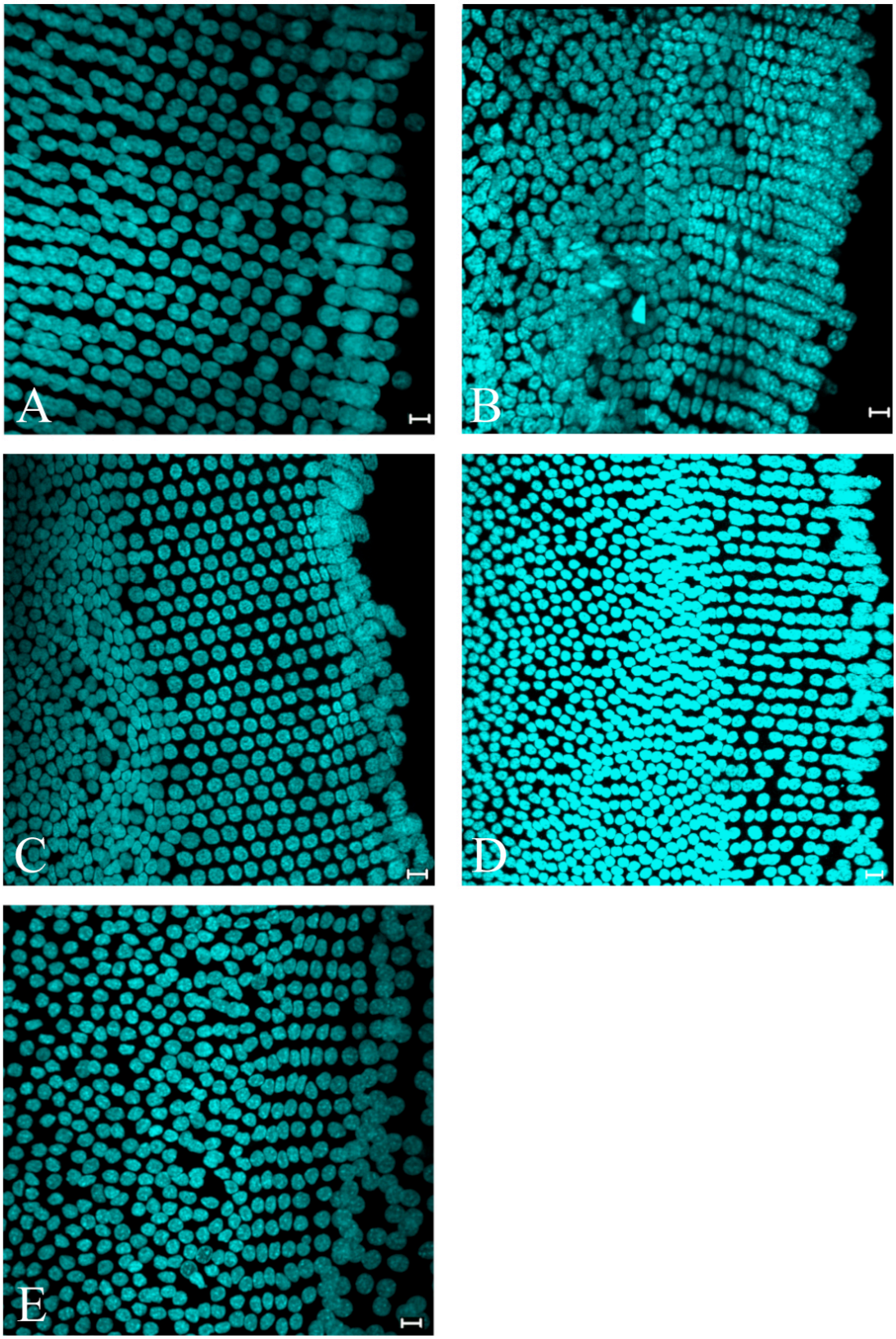
A
B
C
D
E

Figure 2.22. Nucleus arrangement in the TZ of the lens epithelium of different mammals.

The epithelial cell nuclei of the bovine (A), mouse (B), rat (C), rabbit (D) and human lenses (E) were stained with DNA indicator DAPI. The images in the periphery of the TZ were taken. Scale bars=10 ⌠m.

In all of the lenses, the epithelial cell nuclei line into regular columns in the periphery of the TZ, which are called the meridional lines. The lengths of these columns are quite variable in different mammalian lenses. The nuclei in the columns are much rounder and bigger than the others located inside of the meridional lines.

2.4.2.2 Human lens epithelial cell density changes with age

Human lens epithelial cell density in the four age groups was similar in the CZ but decreased with age in the GZ and TZ (Figure 2.23). In the inner side of the CZ, the cell density in each group was about 4600 cells/mm^2 and the increase in the slope was similar. In the outside of the CZ, from 1.38 mm to 0.92 mm away from the end of the TZ, the cell density in the 20-30 age group increased faster than the other three groups, and Student's t-Test results showed that its increase was statistically significant (Table 2.11). Furthermore, the cell density in the 40-50 age group was also statistically higher than that in the 80-90 age group in this region. When coming to the GZ, the cell density in the younger groups still increased faster than the older groups. All the other comparisons had statistically significant difference except the comparison between the 60-70 age group and the 80-90 age group. These results suggest that the epithelial cell density in the GZ of the human lenses decreases with the increase of age.

Table 2.11. The *p* values of Student's t-Test in the comparison of cell density in the lens periphery of the four human age groups

Distance to the end of TZ (mm) / Age group	**1.38**	**1.15**	**0.92**	**0.69**	**0.46**	**0.23**
20-30 VS 40-50	**0.002**	**<0.001**	**0.003**	**0.025**	**0.021**	0.071
40-50 VS 60-70	0.348	0.237	0.128	**0.038**	**0.014**	**0.011**
60-70 VS 80-90	0.680	0.819	0.577	0.198	0.291	0.265
20-30 VS 60-70	**0.002**	**0.001**	**<0.001**	**0.002**	**<0.001**	**0.001**
20-30 VS 80-90	**<0.001**	**<0.001**	**<0.001**	**<0.001**	**<0.001**	**<0.001**
40-50 VS 80-90	**0.011**	**0.002**	**0.0014**	**<0.001**	**<0.001**	**<0.001**

$p<0.05$: statistically significant difference

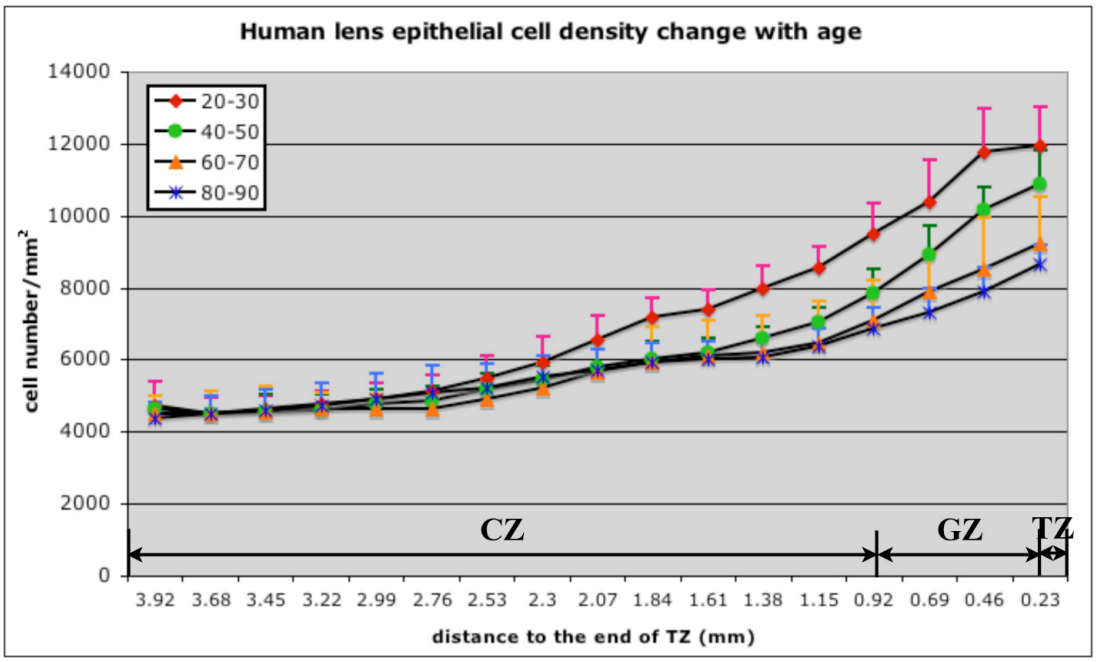

Figure 2.23. The changes of the human lens epithelial cell density with age.

The human lenses were divided into 20-30-, 40-50-, 60-70- and 80-90-year-old groups. The lens epithelial cell densities in the four groups were calculated and made into a line chart.

In each group, the cell density is low in the CZ, but continuously increases from the periphery of the CZ to the TZ. The cell densities in the four groups are similar in the inner side of the CZ. From the outer side of the CZ to the TZ, cell density decreases with the increase of age.

2.4.2.3 Difference of lens epithelial cell density in males and females

The age of 13 women and 13 men was matched and their lens epithelial cell density was calculated. Results showed that the lens epithelial cell density in males and females was similar in each zone (Figure 2.24). The statistical difference was not significant in their comparison. This means that no lens epithelial cell density difference is present in males and females.

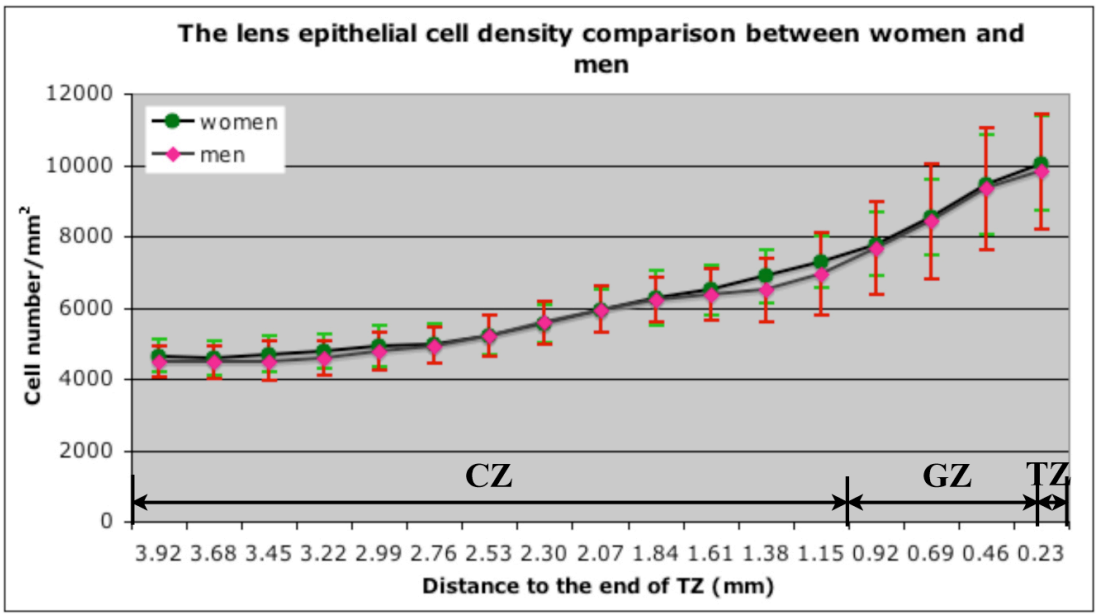

Figure 2.24. Difference of the lens epithelial cell density in women and men.

Twenty-six lenses from thirteen female and thirteen male donors were collected. The age of the female and male donors was matched. The lens epithelial cell densities in women and men were calculated and made into a line chart.

Results show that the cell density is similar across the lens epithelium of women and men.

2.4.3 Lens epithelial cell morphology and size

2.4.3.1 Changes of lens epithelial cell morphology and size in different mammals

The epithelial cells in the CZ, the GZ and the proximal region of the TZ of the bovine, mouse, rat, rabbit and human lenses were polygonal (Figure 2.25, 2.26, 2.27, 2.28). In the periphery of the TZ, the cells arrayed as meridional lines and became regular hexagons.

The changes in cell cross-sectional area across the lens epithelium were similar in the bovine, mouse, rat, rabbit and human lenses (Figure 2.25A and C, 2.26, 2.27 and 2.28). The cross-sectional areas of the bovine and human lens epithelial cells were measured. In the bovine lenses, it started to slowly decrease from the peripheral CZ, and the decrease became quicker in the GZ. The cell cross-sectional area came to the smallest at the position with the highest cell density, and then it slowly increased in the TZ (Figure 2.30). In different ages of the human lenses, it continually and slowly decreased from the anterior pole to the end of the TZ (Figure 2.32B).

The lens epithelial cells were flat in the CZ and became taller in the GZ and the TZ (Figure 2.25B, D, E; Figure 2.26B-E; Figure 2.29). The measured results of bovine and human lens epithelial cells showed that the cell height slowly increased across the CZ but this increase became quick from the GZ to the TZ, especially in the periphery of the TZ (Figure 2.30 and 2.32A).

When the cell cross-sectional area and height changed across the lens epithelium, the cell volume also changed. In the bovine lens epithelium, the cell volume decreased suddenly and dramatically at the position with the highest cell density in the GZ, where it was only half of that in the other area (Figure 2.31). In the other regions, the cell volume was similar. In the human lens epithelium, the cell volume continually but slowly decreased from the CZ to the TZ (Figure 2.32C).

Furthermore, it was found that the cell cross-sectional area and volume were quite variable in the same region of the bovine or human lens epithelium. This was why big error bars were present in the measurement results (Figure 2.30, 2.31, 2.32B and C).

CZ
A
Z-stack
B
TZ
GZ
C
Z-stack
D
Z-stack
E

Figure 2.25. The changes of the cell cross-sectional area and height across the bovine lens epithelium.

The bovine lens epithelial cells were stained with tight junction marker ZO-1 (red), F-actin binder phalloidin (green) and DNA indicator DAPI (blue). Images of the flat section (A, C) and Z-section (B, D, E) in the CZ, the GZ and the TZ are shown. Scale bars=10 ⌈m.

A: In the CZ, the ZO-1 staining shows that the bovine lens epithelial cells are polygonal and their cross-sectional areas are quite variable.

B: In the Z-section of the CZ, the phalloidin staining shows that the bovine lens epithelial cells are flat. Their nuclei are contacted with the apical and basal membranes.

C: In the GZ and TZ, the bovine lens epithelial cells are much smaller than those in the CZ. Their cross-sectional areas are also variable. In the periphery of the TZ, the cells align into columns and become regular hexagons (white rectangle). In the other areas, they are polygonal.

D: In the Z-section of the periphery of the TZ, the bovine lens epithelial cells elongate quickly and are much higher than those in the CZ.

E: In the GZ, the bovine lens epithelial cells become columnar. They are taller than those in the CZ, but are shorter than those in the TZ.

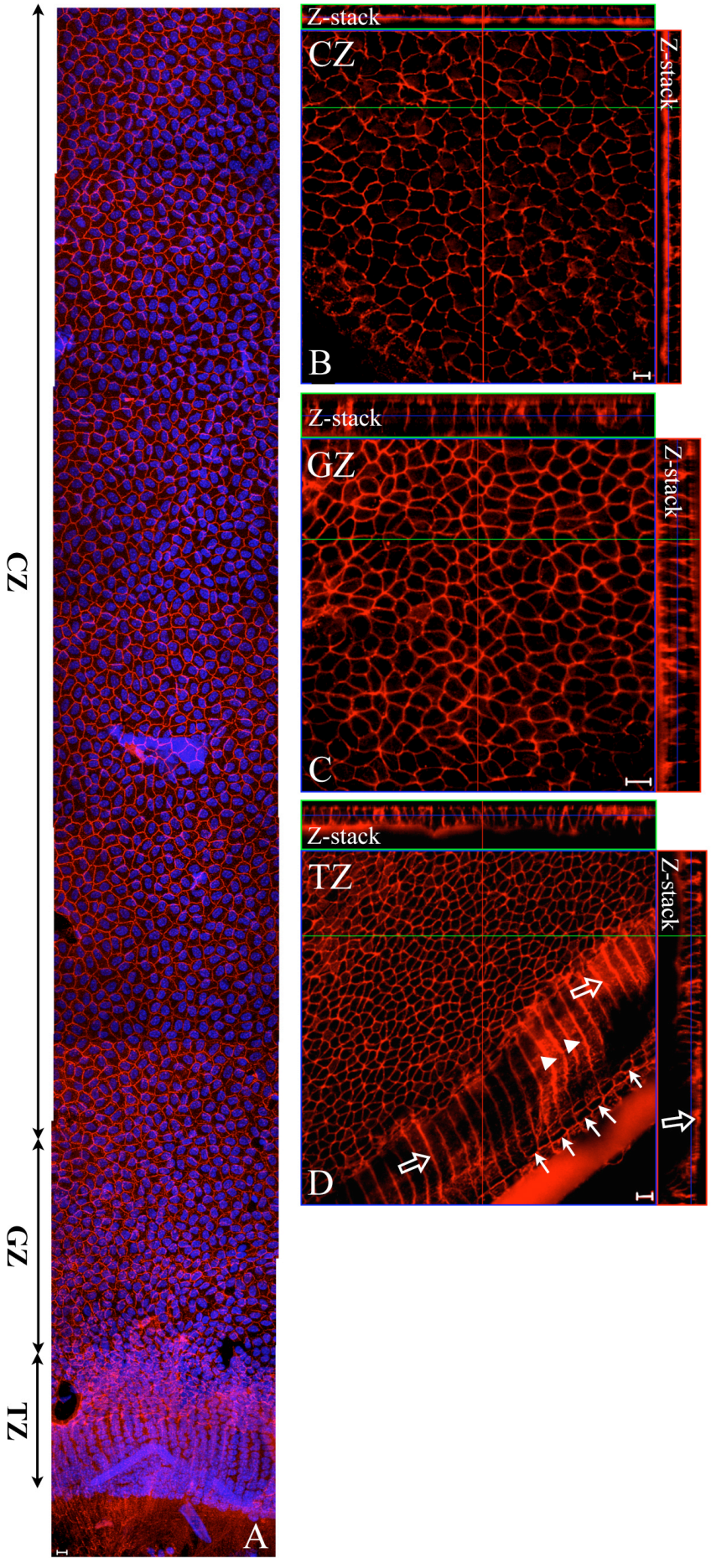
CZ
GZ
TZ
A
Z-stack
CZ
Z-stack
B
Z-stack
GZ
Z-stack
C
Z-stack
TZ
Z-stack
D

Figure 2.26. The changes of the cell cross-sectional area and height across the mouse and rat lens epithelia.

The mouse lens epithelial cells were stained with tight junction marker ZO-1 (red) and DNA indicator DAPI (blue). A series of images from the anterior pole to the end of the TZ were taken and tiled together to produce a montage. The rat lens epithelial cell membranes were stained with wheat germ agglutinin (WGA) (red). Images of the flat section and Z-section in the CZ, the GZ and the TZ are shown. Scale bars=10 ⌈m.

A: The ZO-1 staining shows that the mouse lens epithelial cells are polygonal. The nuclei scatter in the epithelial cells. The cell cross-sectional areas are bigger in the CZ but become smaller in the GZ and TZ.

B. In the CZ of the rat lens epithelium, WGA staining shows that the polygonal cells are big and flat.

C. In the GZ of the rat lens epithelium, the cells become smaller in cross-sectional area but taller in height.

D. In the TZ of the rat lens epithelium, the cells become much taller than those in the GZ. In the periphery of the TZ, the cells array into columns (arrow heads) and become regular hexagons (arrows). Here a layer of fibre cells attach to the top of the epithelial cells (hollow arrows).

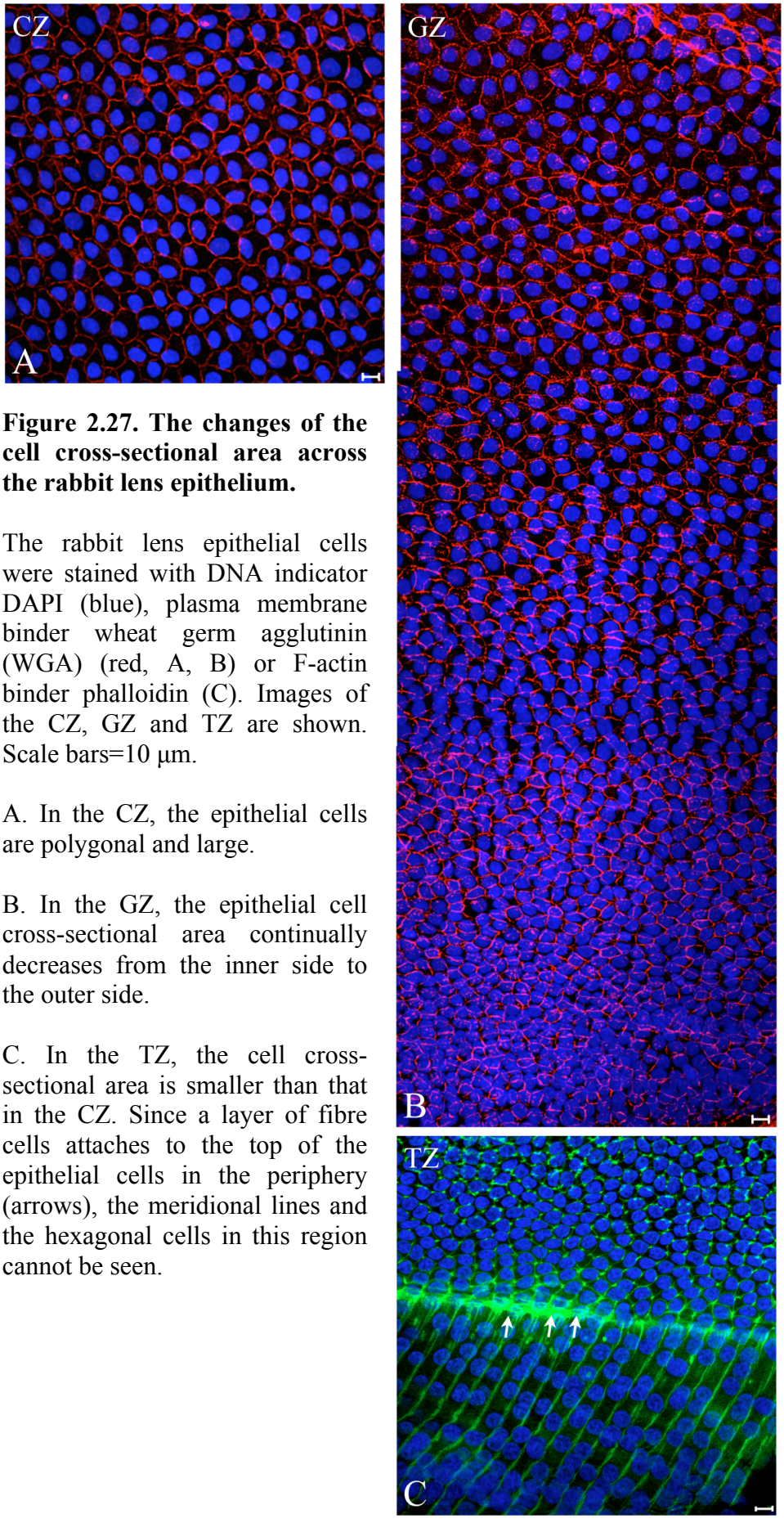

Figure 2.27. The changes of the cell cross-sectional area across the rabbit lens epithelium.

The rabbit lens epithelial cells were stained with DNA indicator DAPI (blue), plasma membrane binder wheat germ agglutinin (WGA) (red, A, B) or F-actin binder phalloidin (C). Images of the CZ, GZ and TZ are shown. Scale bars=10 μm.

A. In the CZ, the epithelial cells are polygonal and large.

B. In the GZ, the epithelial cell cross-sectional area continually decreases from the inner side to the outer side.

C. In the TZ, the cell cross-sectional area is smaller than that in the CZ. Since a layer of fibre cells attaches to the top of the epithelial cells in the periphery (arrows), the meridional lines and the hexagonal cells in this region cannot be seen.

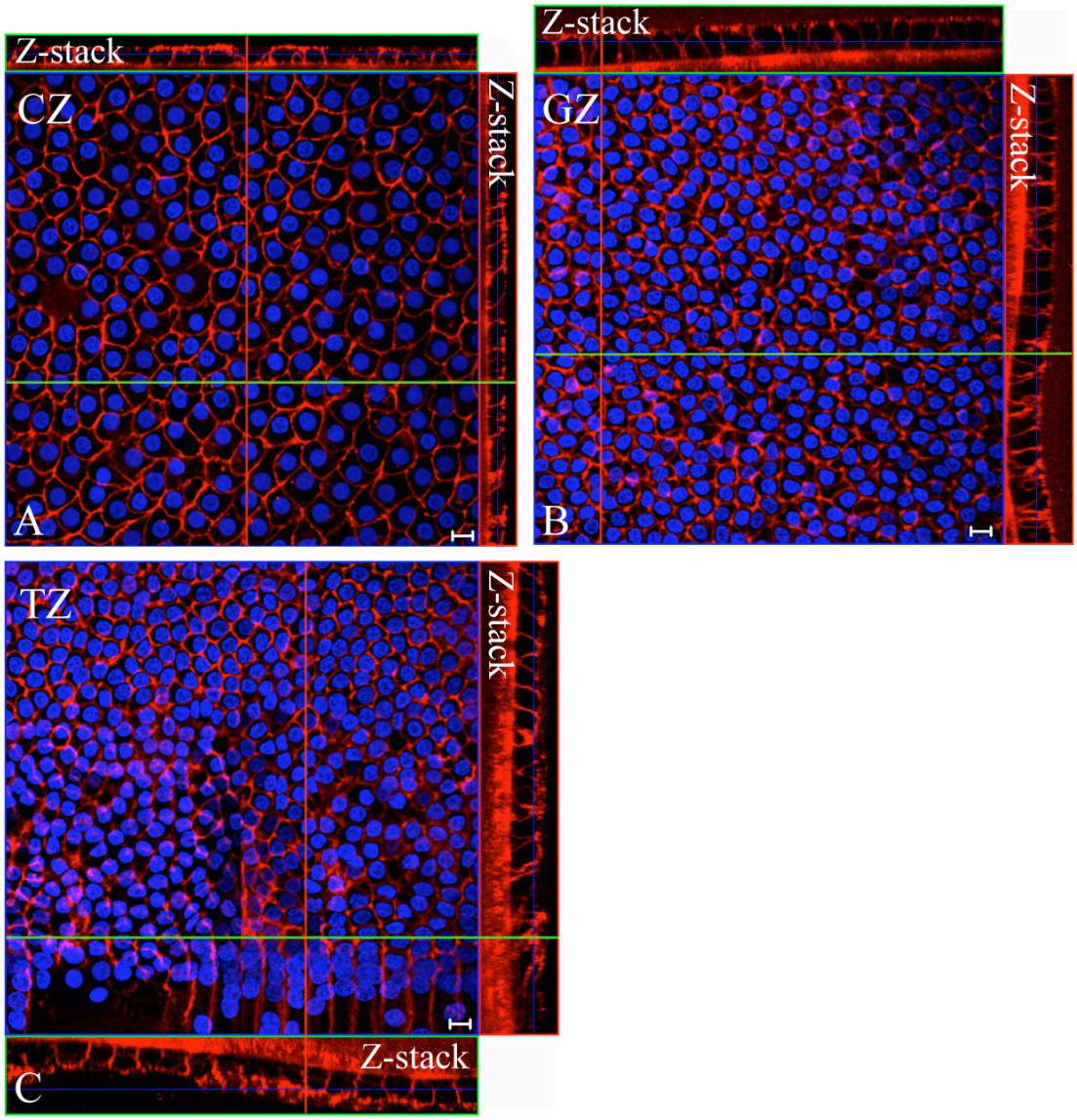

Figure 2.28. The changes of cell cross-sectional area and cell height in the human lens epithelium.

The human lens epithelial cells were stained with DNA indicator DAPI (blue) and plasma membrane binder wheat germ agglutinin (WGA) (red). Images of the flat section and Z-section in the CZ, the GZ and the TZ are shown. Scale bars=10 μm.

A. In the CZ, the polygonal epithelial cells are large in cross-sectional area and appear lower in height. The round nuclei scatter in the cells.

B. In the GZ, the cell cross-sectional area is much smaller than that in the CZ. The cells become columnar.

C. In the TZ, the cell cross-sectional area is still small. The cells in the periphery align into columns and become taller.

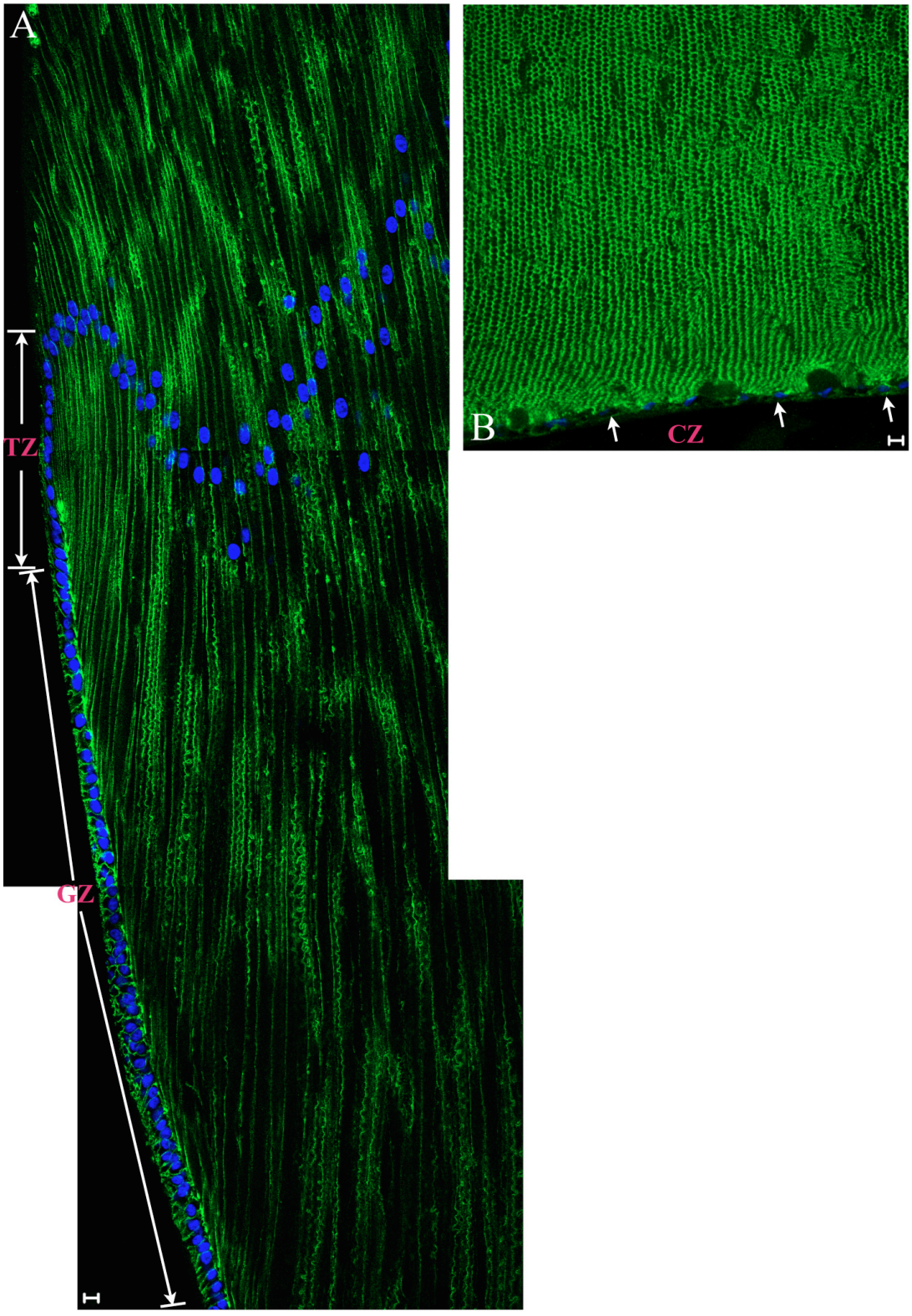
A
TZ
GZ
I
B
CZ
I

Figure 2.29. The changes of cell height in the bovine lens epithelium.

The bovine lenses were sectioned into 12-14-μm-thick sections, which were stained with adhesion junction molecule N-cadherin (green) and DNA indicator DAPI (blue). Images in the CZ, the GZ and the TZ were taken. The images in the GZ and the TZ were tiled together to produce a montage. Scale bars=10 ⌠m.

A. In the GZ and the TZ, the N-cadherin and DAPI staining show that the bovine epithelial cells are located in the outside of the fibre mass. They are much taller in the TZ than in the GZ.

B. In the CZ, the single layer of epithelial cells (arrows) is much flatter than those in the GZ and TZ.

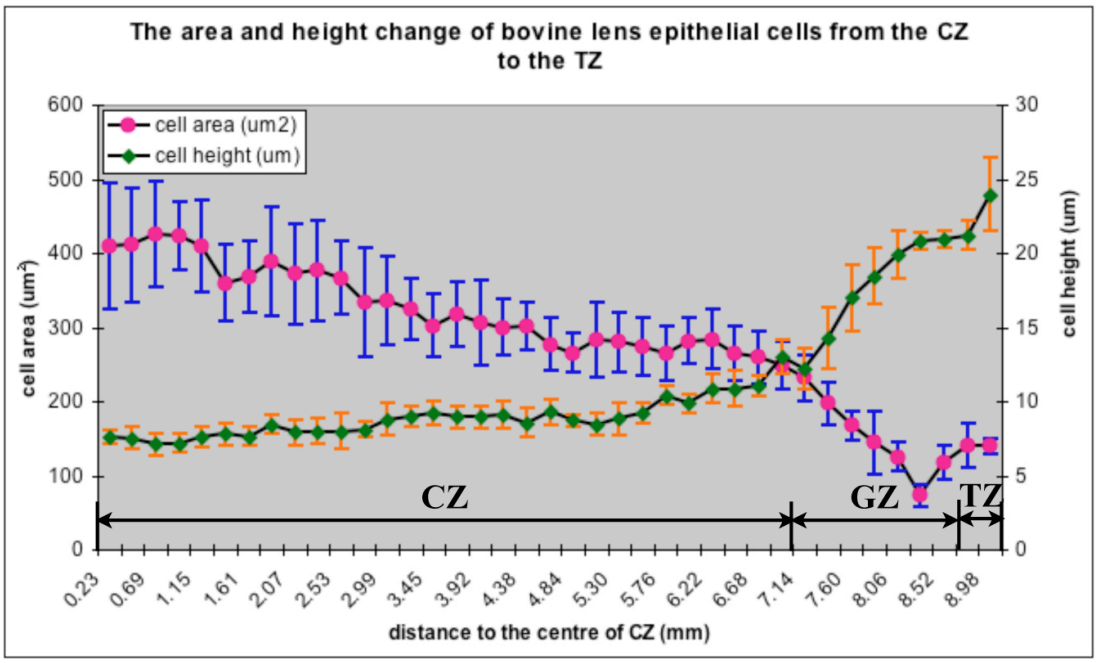

Figure 2.30. The changes of the cell height and cross-sectional area across the bovine lens epithelium.

In the CZ, the bovine lens epithelial cell height does not change in the inner side, but starts to slowly increase in the outer side. In the GZ and TZ, this increase becomes much faster. On the contrary, the cell cross-sectional area decreases slowly in the outer side of the CZ, but fast in the GZ. From the outer side of the GZ to the TZ, the cell cross-sectional area starts to increase.

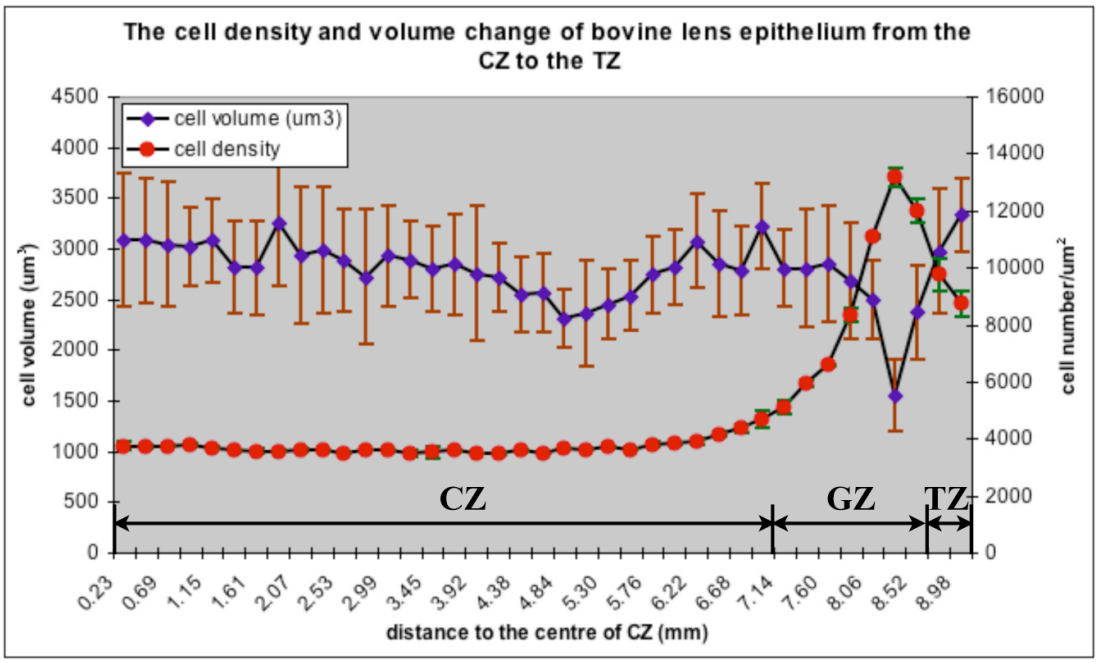

Figure 2.31. The changes of cell volume and density across the bovine lens epithelium.

The bovine lens epithelial cell density is stable in the most area of the CZ and starts to increase in at the end of the CZ. This increase becomes dramatic in the GZ, and then the cell density decreases in the TZ. The cell volume of the bovine lens epithelium is similar in the CZ and part of the GZ. In the region of the GZ with the highest cell density, the cell volume decreases dramatically. It then starts to increase in the TZ.

2.4.3.2 Changes of human lens epithelial cell size with age

The lens epithelial cell height, cross-sectional area and volume of a 29-year-old woman, a 48-year-old man and a 64-year-old man were measured (Figure 2.32). The results showed that the cell height was similar in the three lenses. It was approx. 8-10 μm in the CZ. It started to increase in the GZ and TZ and was approx. 15 μm at the end of the GZ and 17 μm in the middle of the TZ. Unlike the cell height, the cell cross-sectional area and volume continued to decrease from the CZ to the TZ in the three lenses; they were much larger in the oldest lens than in the youngest one.

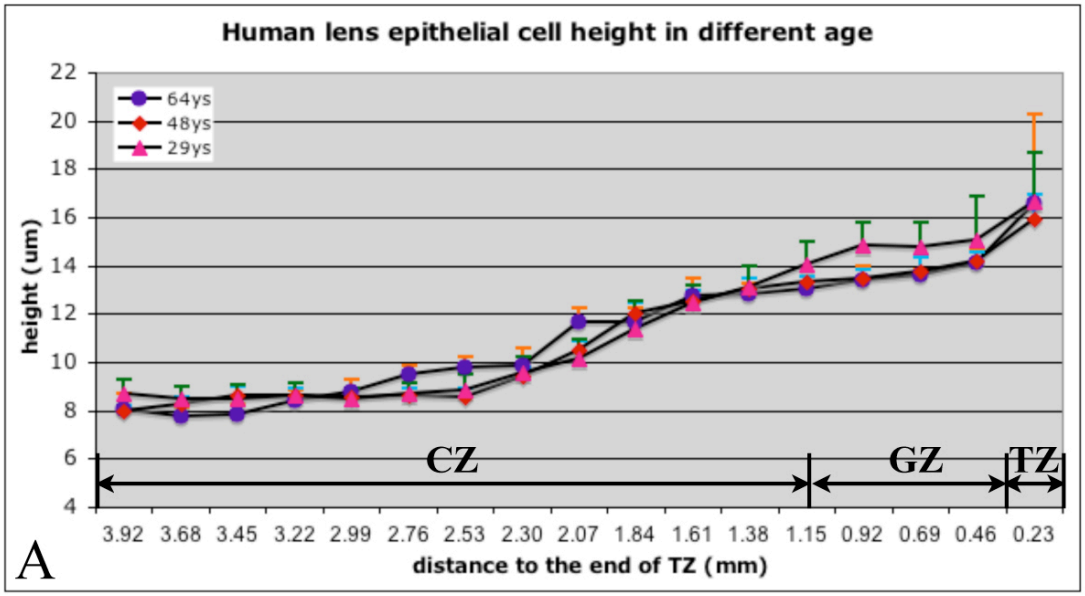
Human lens epithelial cell height in different age
64ys
48ys
29ys
height (um)
22
20
18
16
14
12
10
8
6
4
CZ
GZ
TZ
3.92 3.68 3.45 3.22 2.99 2.76 2.53 2.30 2.07 1.84 1.61 1.38 1.15 0.92 0.69 0.46 0.23
distance to the end of TZ (mm)
A

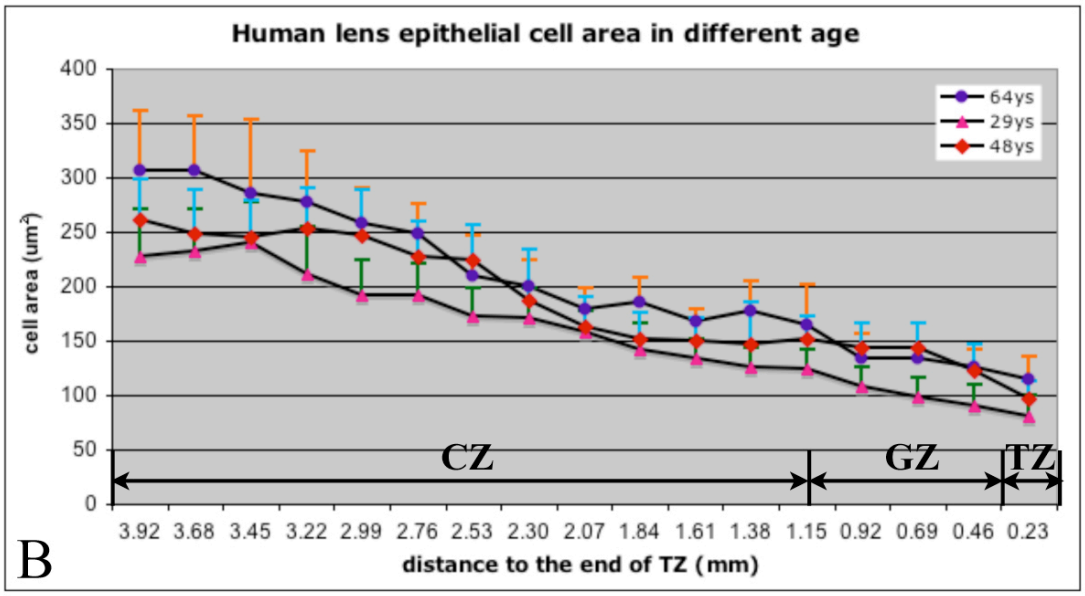
Human lens epithelial cell area in different age
64ys
29ys
48ys
cell area (um²)
400
350
300
250
200
150
100
50
0
CZ
GZ
TZ
3.92 3.68 3.45 3.22 2.99 2.76 2.53 2.30 2.07 1.84 1.61 1.38 1.15 0.92 0.69 0.46 0.23
distance to the end of TZ (mm)
B

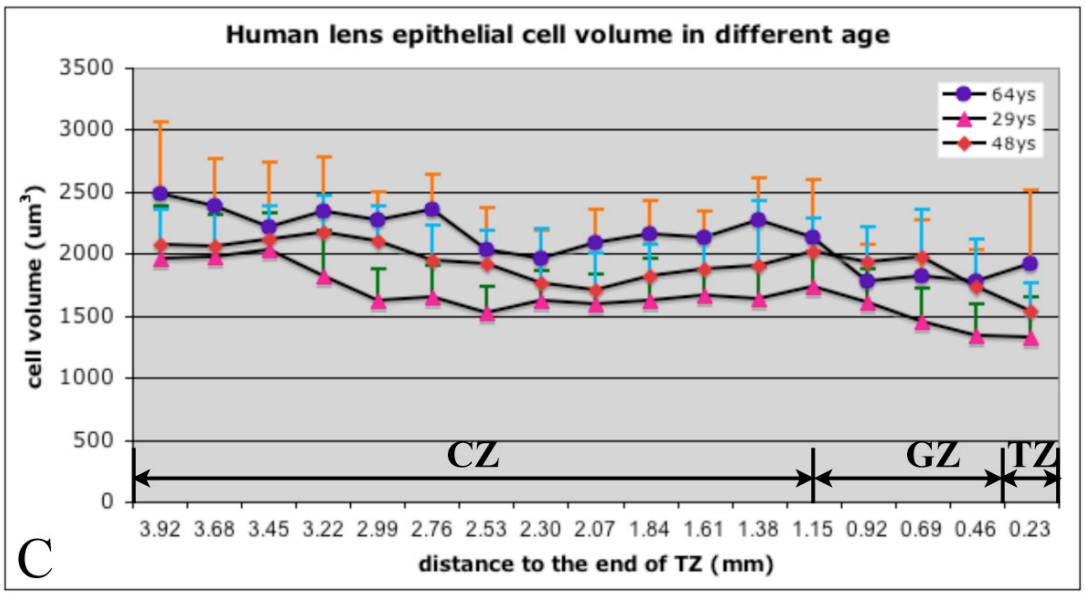
Human lens epithelial cell volume in different age
64ys
29ys
48ys
cell volume (um³)
3500
3000
2500
2000
1500
1000
500
0
CZ
GZ
TZ
3.92 3.68 3.45 3.22 2.99 2.76 2.53 2.30 2.07 1.84 1.61 1.38 1.15 0.92 0.69 0.46 0.23
distance to the end of TZ (mm)
C

Figure 2.32. The changes of cell height, cross-sectional area and volume across the lens epithelia of different ages of people.

The epithelial cell height, cross-sectional area of a 29-year-old lens, a 48-year-old lens and a 64-year-old lens were measured from the CZ to the TZ. The cell volume was calculated by cell height multiplying cell cross-sectional area.

A: The human lens epithelial cell height starts to increase from the outer side of the CZ until the end of the TZ. This increase is consistent in different ages of lenses.

B: In each lens, the epithelial cell cross-sectional area continuously decreases from the CZ to the TZ. It is much bigger in the 64-year-old lens than in the 29-year-old lens.

C: The cell volume is slightly smaller in the GZ and the TZ of each lens epithelium. However, the change process is not smooth across the lens epithelium. The cell volume is bigger in the 64-year-old lens than in the 29-year-old lens.

2.4.3.3 Changes of human lens cell morphology in the capsular bags with IOLs

In the human donor capsular bags with IOLs, the rhexis margin contacting with IOL thickened and became fibrotic to varying degrees because of cell multilayering (Figure 2.33). White fibrosis was present in the equatorial region of the bag and scattered light (Figure 2.33A and B). The amount of fibre-like materials varied from a thin layer of white fibrosis covering the lens capsule (Figure 2.34D, 2.35A) to the Soemmerring's ring formation (Figure 2.33A and B) in the space between the outer margin of IOL and the bag edge. In most specimens, the central region of the posterior lens capsule still remained clear. Occasionally in some capsule bags, the regenerated fibre cells were observed to form a confluent sheet and migrate toward the centre of the posterior capsule. Since there were no records about how long the IOLs had been implanted, it was impossible to evaluate the development of PCO.

With the exception of variable amounts of regenerated fibres in the equatorial region, cell distribution on the anterior and posterior lens capsules was similar in most capsular bags. On the anterior capsule, multilayer of elongated cells with elongated nuclei were located around the rhexis where contacted the IOL optics (Figure 2.33 and 2.34). These cells twisted and interwove into a network. On the outside of the rhexis, DAPI staining showed that some cells were absent (Figure 2.34A). They were probably lost during cataract surgery. In the periphery of the anterior capsule, most epithelial cells were still shown as a single layer and a cobblestone appearance in many capsular bags (Figure 2.34A-C). The majority of the cells retained the polygonal outline and had round or oval nuclei. Fibrotic proliferation was sometimes observed near the equator and along the IOL haptics (Figure 2.35C and D).

On the posterior capsule, the cells that had migrated here from the equator formed a multilayered or monolayer sheet (Figure 2.35B). They lost the regular polygonal structure. Some cells started to elongate but many of them still showed an intermediate morphology (Figure 2.35E-H). In most of the capsular bags studied, the cell migration did not extend to the centre of the posterior capsule. They stopped at the edge of the IOLs and scattered as cell colonies (Figure 2.35I-L). In one or two specimens, the cells covered the central region of the posterior capsule.

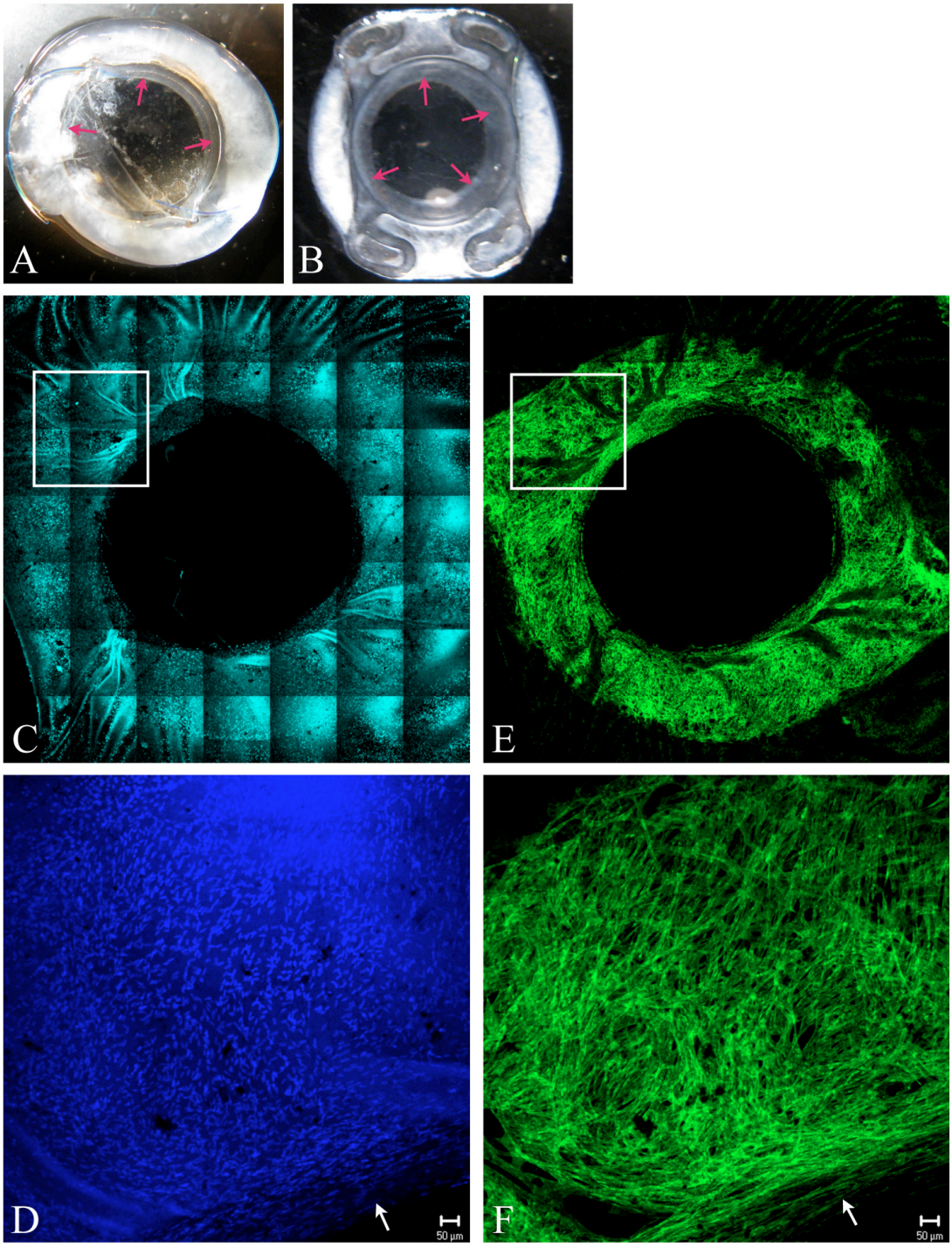
A
B
C
E
D
50 µm
F
50 µm

Figure 2.33. The multilayer of elongated cells along the rhexis of the human donor capsular bag.

A, B: The general appearance of the capsular bags with different types of IOLs. The IOLs are centred in the capsular bags. The white fibrosis fills in the space between the outer edge of the IOL and the capsular bag edge. The rhexis margin contacting with IOL optics (pink arrows) becomes slightly white and obstructs light into the eye.

C: The DAPI staining shows that multilayer of nuclei surround the rhexis.

D: These nuclei are oval or elongated at higher magnification. In the inner side, they are parallel to the rhexis (arrow).

E: The staining of F-actin binder phalloidin shows that these cells elongate and interwove into a network.

F: The F-actin structure is much clearer at higher magnification. Some elongated cells near the edge of the rhexis align parallel to the rhexis (arrow).
D, F: scale bars=50 μm.

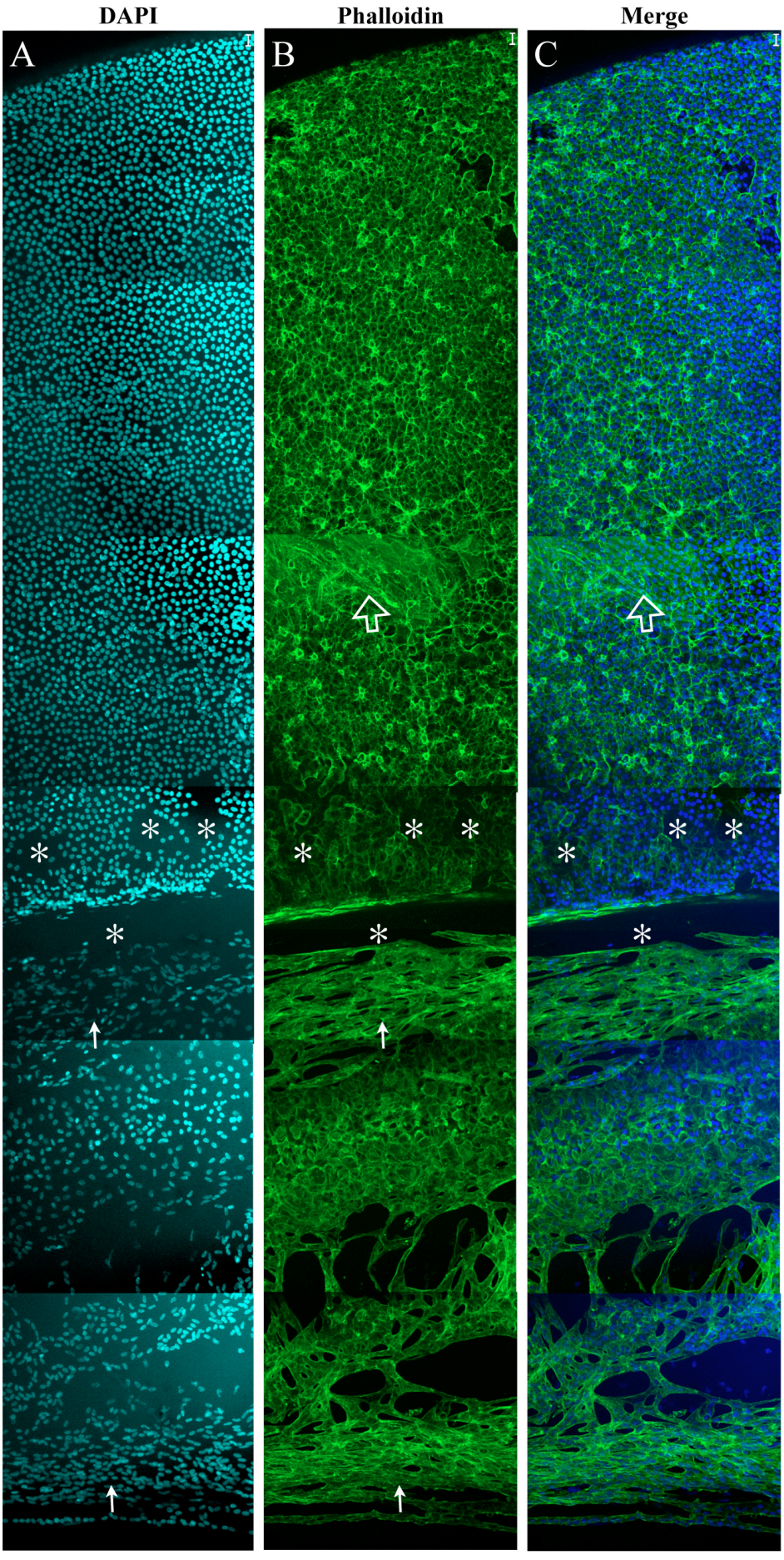
DAPI
Phalloidin
Merge
A
B
C

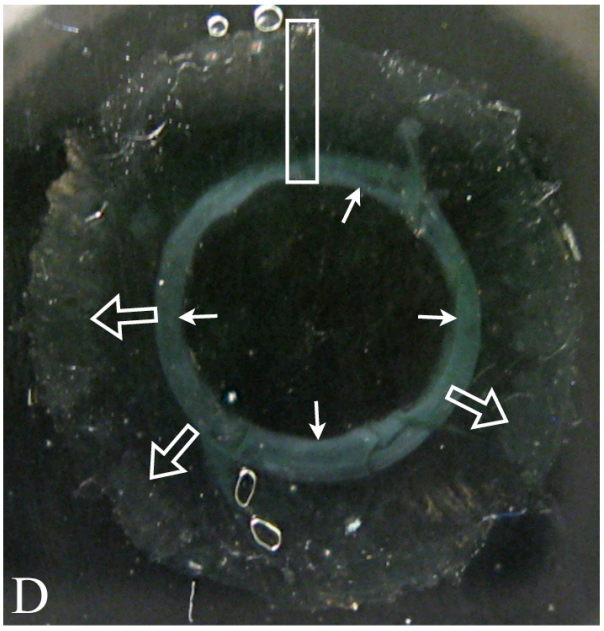

Figure 2.34. The cells on the anterior capsular bag.

After the IOL was gently removed, the capsular bag from a 56-year-old woman was stained with F-actin binder phalloidin (green) and DNA indicator DAPI (blue). A series of images were taken from the rhexis to the capsular bag edge in the anterior capsule and tiled together to produce a montage. Scale bars=20 μm.

A. In the area surrounding the rhexis, DAPI shows than many cell nuclei are elongated (arrows). Outside the rhexis, some nuclei are lost (stars). In most region of the peripheral anterior capsule, the epithelial cells are still retained as a single layer and show a cobblestone appearance.

B. The phalloidin staining shows that the fibre-like cells surrounding the rhexis elongate and interwove into a network. Most cells in the peripheral capsular bag are still polygonal as normal epithelial cells in the lens without cataract surgery. Some fibrosis is detected on the surface of the epithelial cells (hollow arrow).

C. The merged image shows that the DAPI stained nuclei are located in the cells outlined by phalloidin staining.

D. The general appearance of the lens capsular bag. The picture was taken after the capsular bag was stained and ready for observing under microscope. The central part of the anterior capsule is already removed during cataract surgery. Thick fibrosis is present along the rhexis and shows weak green staining (arrows, green phalloidin staining). Some patches of fibrosis are faintly seen in the periphery of the capsular bag (hollow arrows). The rectangle shows the position where the montage picture in image A-C is.

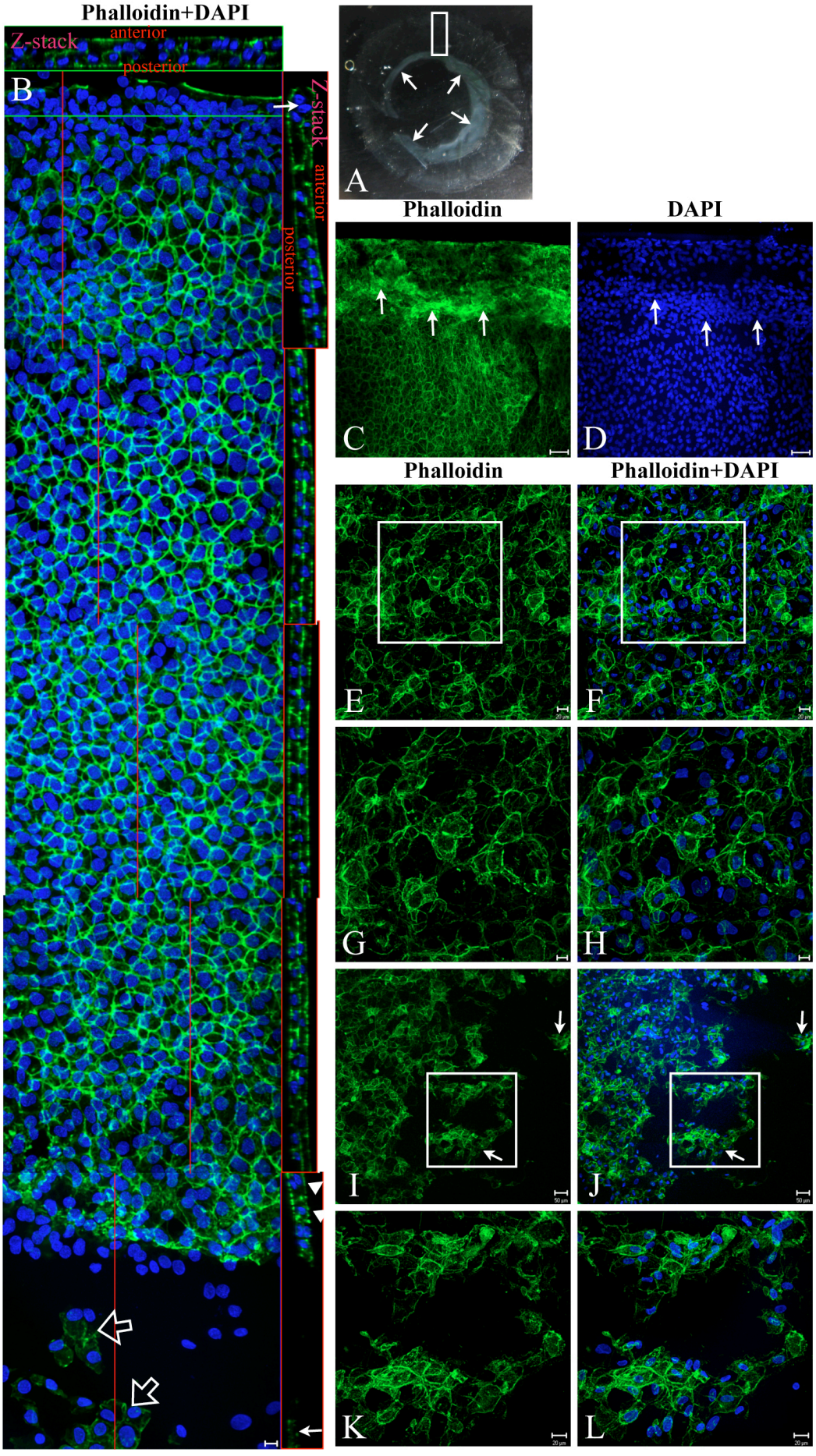
Phalloidin+DAPI
Z-stack
anterior
posterior
B
Z-stack
anterior
posterior
A
Phalloidin
DAPI
C
D
Phalloidin
Phalloidin+DAPI
E
F
G
H
I
J
K
L

Figure 2.35. The cells at the equator and on the posterior lens capsular bag.

The capsular bag from a 56-year-old woman (the same donor as the one in Figure 2.34) was labelled with F-actin binder phalloidin (green) and DNA indicator DAPI (blue).

A. The general appearance of the capsular bag. The central part of the anterior capsule is absent and a ring of fibrosis surrounds the rhexis (arrows). Most peripheral area of the capsular bag looks transparent. The rectangle shows where the series of images in Figure B are taken.

B. A series of images about the cells on both the anterior and posterior capsules were taken from the outside of the rhexis to the capsular bag edge. Many cells on both capsules are still polygonal as the epithelial cells in normal lenses. Z-stack shows that the cells on each capsule are in a single layer. At the edge of the capsular bag, the cells on the anterior capsule migrate to the posterior capsule (arrow). Some cell colonies are formed near the central region of the posterior capsule (hollow arrows). On the anterior capsule, many cells are lost just in the outside region of the rhexis (arrow heads).

C, D: In some region of the peripheral capsular bag, multilayer of fibre-like cells are present (arrows).

E-H: The cells on the posterior lens capsule lose the epithelial cell characteristics and become fibre-like cells with variable shape of nuclei (E and F). At higher magnification, some cells are polygonal but many do not have a clear cell outline. The actin filaments are not so prominent in these cells as it in normal lens epithelial cells (G and H).

I-L: On the posterior lens capsule beneath the rhexis, patches of cells are observed and some are isolated from the confluent sheet of cells (I and J, arrows). The images at higher magnification show that these cells lose the normal polygonal shape and have elongated nuclei (K and L).
B, C, D, G and H: scale bars=10 μm. E, F, K and L: scale bars=20 μm. I and J: scale bars=50 μm.

2.4.3.4 Changes of nuclear morphology and volume in the bovine and human lens epithelial cells

The bovine lens epithelial cell nuclei were oval in the CZ but became round in the GZ and TZ (Figure 2.36A-C). As well as the cell volume change, the nuclear volume also changed across the bovine lens epithelia. It decreased in the GZ and then started to increase in the TZ (Figure 2.36D). All of the human lens epithelial cell nuclei were round in the three zones (Figure 2.37A-C). Their volume was slightly bigger in the inner side of the CZ but decreased and remained stable in the other area (Figure 2.37D). As with the cell volume, the nuclear volume was also quite variable in the same region of the bovine and human lens epithelia. In both of the lenses, the karyoplasmic ratio (the ratio of the nuclear volume to cell volume) remained constant across the lens epithelium, respectively 0.067±0.009 and 0.023±0.003. This suggests that the nucleus proportion in the cell is consistent in different regions of the epithelium. Moreover, it indicates that the nucleus has a higher proportion in the bovine lens epithelial cells than in human.

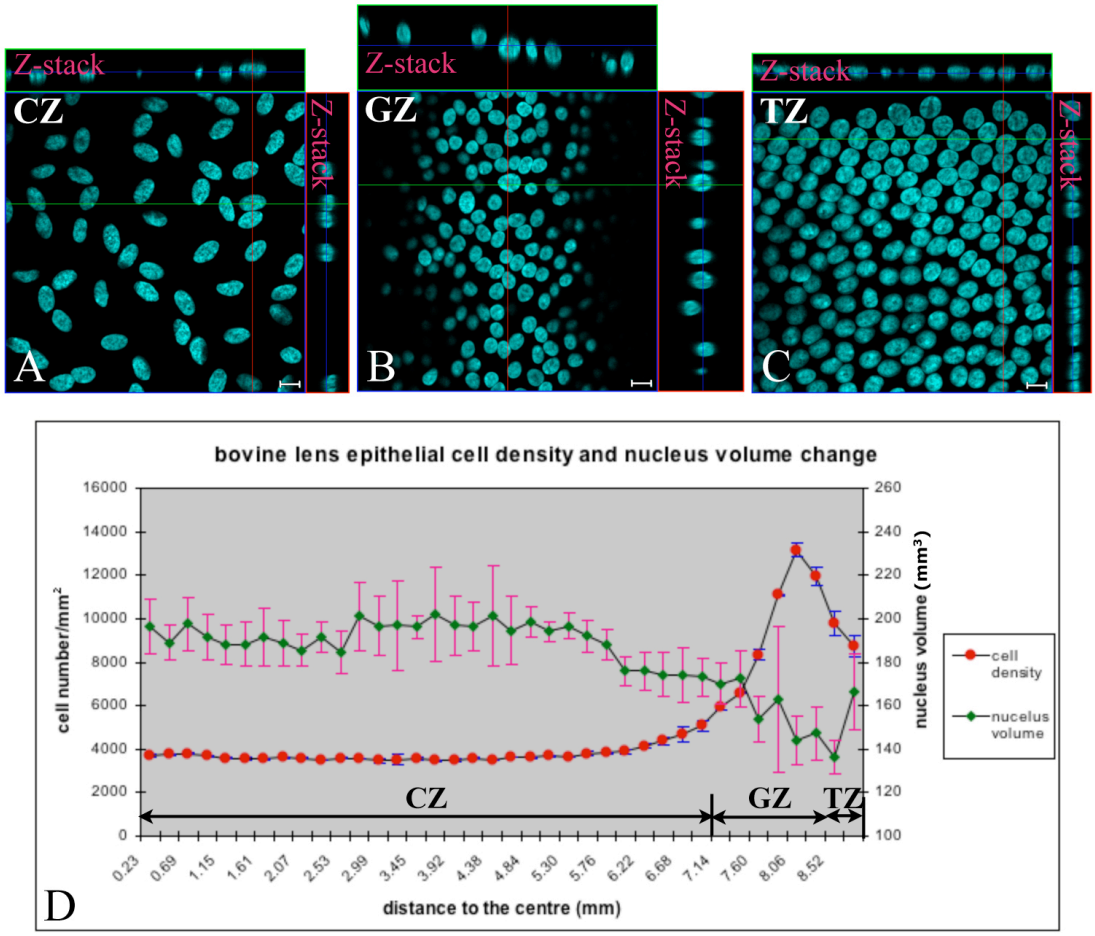

Figure 2.36. The changes of nuclear volume across the bovine lens epithelium.

The bovine lens epithelial cells were stained with DNA indicator DAPI. A series of images were taken from the anterior pole to the end of the TZ. The nuclear volume and cell density in each image were measured.

A-C: DAPI staining shows that the bovine lens epithelial cell nuclei are oval in the CZ, and become round in the GZ and TZ. Scale bars=10 μm.

D. The bovine lens epithelial cell density starts to increase from the end of the CZ, has a dramatic peak in the GZ and starts to decrease in the TZ. The nuclear volume is similar in the CZ, but decrease in the GZ and start to increase in the TZ. The big error bars in each region suggest the nuclear volume is quite variable even at the same place.

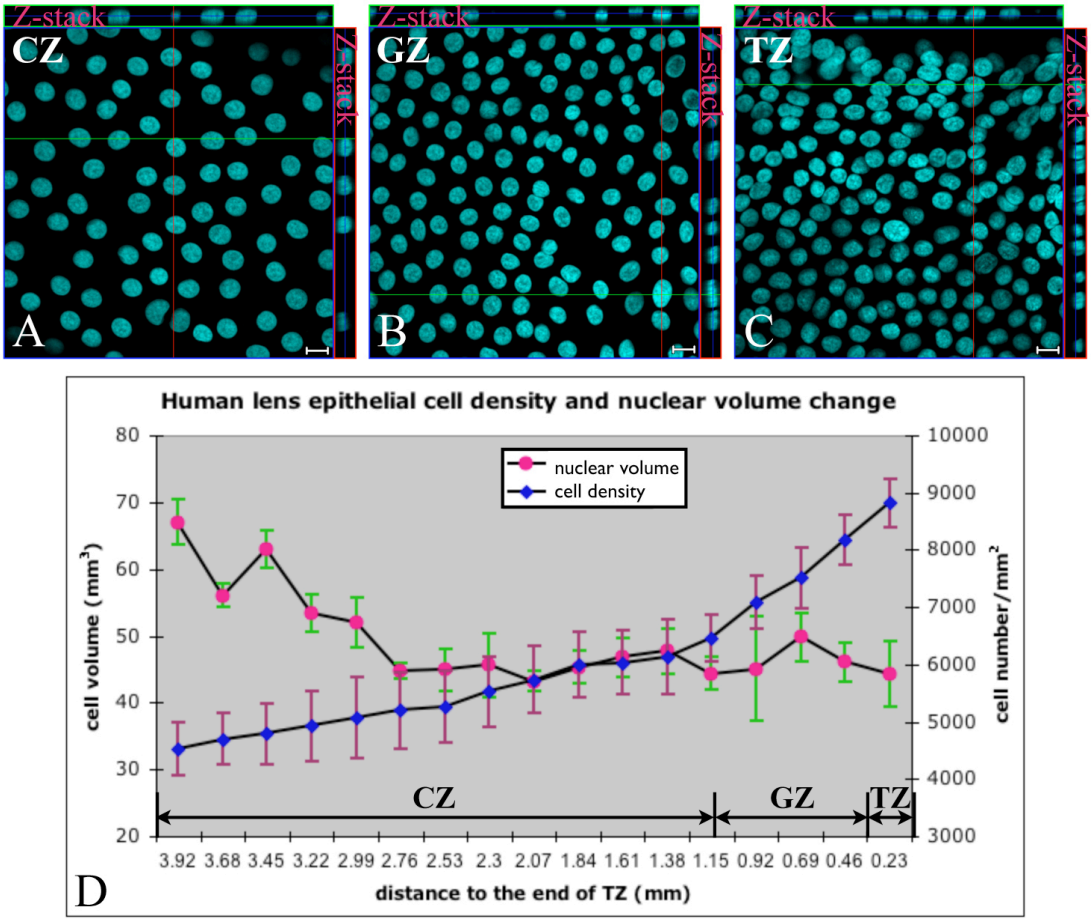

Figure 2.37. The changes of nuclear volume across the human lens epithelium.

The human lens epithelial cell nuclei were stained with DAPI. A series of pictures were taken from the anterior pole to the end of the TZ. The nuclear volume and cell density in each image were measured.

A-C: The human lens epithelial cell nuclei are all round in the CZ, the GZ and the TZ. They are slightly bigger at the centre of the CZ than in the GZ and TZ. Scale bars=10 μm.

D. The nuclear volume continually decreases in the inner side of the CZ, and remains consistent from the middle of the CZ to the TZ.

2.4.4 Lens epithelial cell centrosome

2.4.4.1 Loss of γ-tubulin and pericentin and the cytoskeleton change of the epithelial cells in the further half of the meridional lines

The γ-tubulin and pericentrin staining showed that each epithelial cell included only one centrosome in the bovine and human lenses (Figure 2.38-2.42). The centrosome was located at the cell apical side, at similar level with ZO-1 (Figure 2.38E-G and I, 2.39A and B, 2.41A and C-E). The staining of γ-tubulin usually showed one single focus at lower magnification (Figure 2.38) and two small foci at higher magnification (Figure 2.40) in the bovine lens epithelial cells. In the human lens epithelial cells, the γ-tubulin staining showed two small foci in some cells but one focus in the others in the images at lower magnification (Figure 2.41). It consisted of two small foci in the cells in the images at higher magnification (Figure 2.42). Unlike the γ-tubulin staining, the pericentrin staining appeared like a cloud of rather than as individual spots in the human lens epithelial cells (Figure 2.44).

In the further half of the meridional lines of the TZ, as the epithelial cells already elongated and prepared for subsequent fibre cell differentiation, the immunofluorescent signals for both γ-tubulin and pericentrin disappeared (Figure 2.38A, 2.39B, 2.40, 2.41B, 2.42, 2.43, and 2.44). Furthermore, the apical protein marker ZO-1 was also not detectable in the bovine lens epithelial cells (Figure 2.38A and D, 2.39D). In the bovine lens epithelium, this observation was restricted to the eight or so of most posterior epithelial cells of the meridional lines (Figure 2.38 and 2.39). Since the meridional lines of the human lens epithelium was very short, this only occurred in the most posterior three or four cells (Figure 2.41, 2.42 and 2.44). At higher magnification, no γ-tubulin and pericentrin staining was detected in these cells (Figure 2.40, 2.42C-D and 2.44 G). In the cryosections of the bovine lens that were co-immunolabelled with antibodies against γ-tubulin and CP49, or filensin and ZO-1, the fibre cell markers CP49 and filensin were not detected in those cells lacking in γ-tubulin and ZO-1 staining (Figure 2.39). This indicates that these cells have not fully differentiated into fibre cells and still belong to the epithelial cells.

Interestingly, many γ-tubulin and pericentrin foci were observed in the middle of the meridional lines, just before they were absent. Their numbers were more than the nucleus number in that area, and their morphology was the same as those in the

other area (Figure 2.38D, 2.39B, 2.40, 2.41B, 2.42, 2.43C and D, and 2.44). In the lens epithelial cells stained with ZO-1 and γ-tubulin, Z-stack showed that most γ-tubulin foci were located at similar level to ZO-1 while some were above the ZO-1 level and belonged to the newly-formed fibre cells whose apical sides faced the apical sides of the epithelial cells in the TZ (Figure 2.38D). These newly-formed fibre cells usually attach tightly to the epithelial cells in the TZ. This was why their γ-tubulin and pericentrin staining was only observed in this region. Carefully observation in Z-stack suggested the number of the γ-tubulin foci from the newly-formed fibre cells was very low.

This apparent loss of γ-tubulin and ZO-1 in the further half of the meridional lines coincided with an obvious structure change of F-actin and α-tubulin. α-tubulin formed a basket of microtubules in the lens epithelial cells of the CZ, GZ and the part of the TZ. With the loss of γ-tubulin in the epithelial cells of the further half of the meridional lines of the TZ, α-tubulin lost its basket structure and changed to a broom shape and sprayed its microtubules to the end of the TZ. The last γ-tubulin focus located at the anterior end of the broom-shaped α-tubulin microtubule filaments (Figure 2.43). The F-actin detected by phalloidin was associated with the plasma membrane and drew the polygonal outline of the human epithelial cells in the CZ, the GZ and part of the TZ. As with α-tubulin in the further half of the TZ, F-actin also became a wave distribution in the epithelial cells and sprayed from the middle to the end of the TZ (Figure 2.44). No characteristically polygonal outline of the epithelial cells could be detected in these cells.

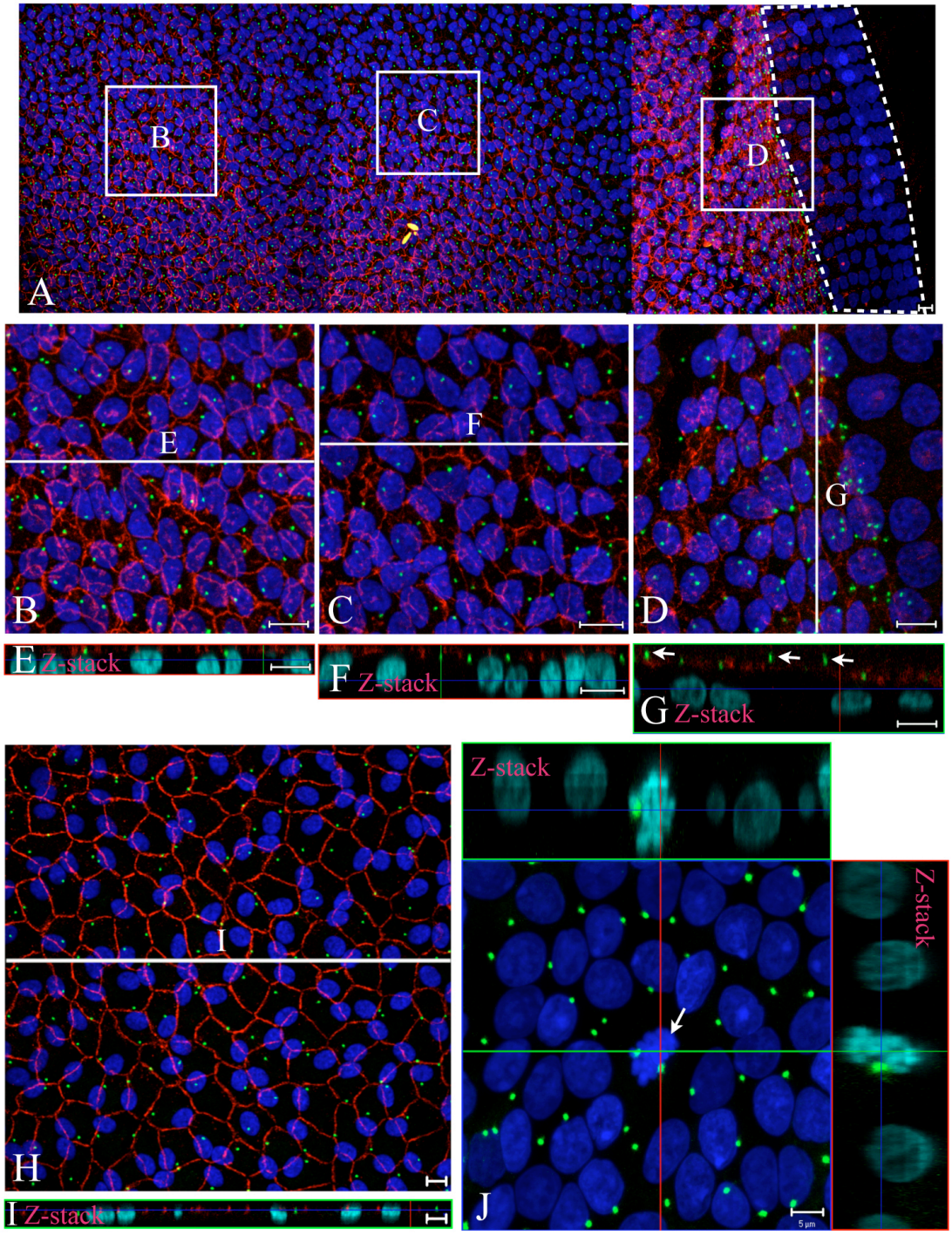
A
B
C
D
E
F
G
B
C
D
E Z-stack
F Z-stack
G Z-stack
H
I
I Z-stack
J
Z-stack
Z-stack

Figure 2.38. The location of γ-tubulin in the bovine lens epithelial cells.

The bovine lens epithelial cells were stained with centrosome marker γ-tubulin (green), tight junction marker ZO-1 (red) and DNA indicator DAPI (blue). Images in the CZ, the GZ and the TZ were taken.

A. Three images including the periphery of the GZ and the TZ are tiled together to produce a montage. ZO-1 and γ-tubulin are present in all of the cells in the GZ and part of the TZ. In the further half of the meridional lines (the area outlined by broken line), they are absent. The rectangles show where the images B-D at higher magnification were taken.

B-D: At higher magnification, ZO-1 shows the polygonal cell morphology. γ-tubulin is located at each cell except some cells in image D. In the middle of meridional lines (D), ZO-1 staining disappears while many γ-tubulin staining foci are observed. These γ-tubulin foci have the same morphology as those in the GZ. The white line in each image shows where the Z-stack images in Figure E-G were taken.

E-G: In the Z-stack, ZO-1 locates at the apical sides of the epithelial cells. γ-tubulin is at similar level to ZO-1. From the GZ to the TZ, cells start to elongate and the nuclei leave the apical sides to stay in the middle, while the γ-tubulin still locates at the apical sides. In the middle of the meridional lines where many γ-tubulin foci are found, some γ-tubulin foci are above the ZO-1 staining (G, arrows). They are from the newly-formed fibre cells that attach to the epithelial cells in this region.

H, I: In the CZ, ZO-1 shows that the epithelial cells are polygonal. γ-tubulin is present in each cell. In the Z-stack (I), both ZO-1 and γ-tubulin are at the apical sides of the epithelial cells.

J: In the epithelial cell at the early stage of M phase (arrow), γ-tubulin foci locate at the lateral sides of the cell instead of the apical side.
A-H: scale bars=10 μm. J: scale bars=5 μm.

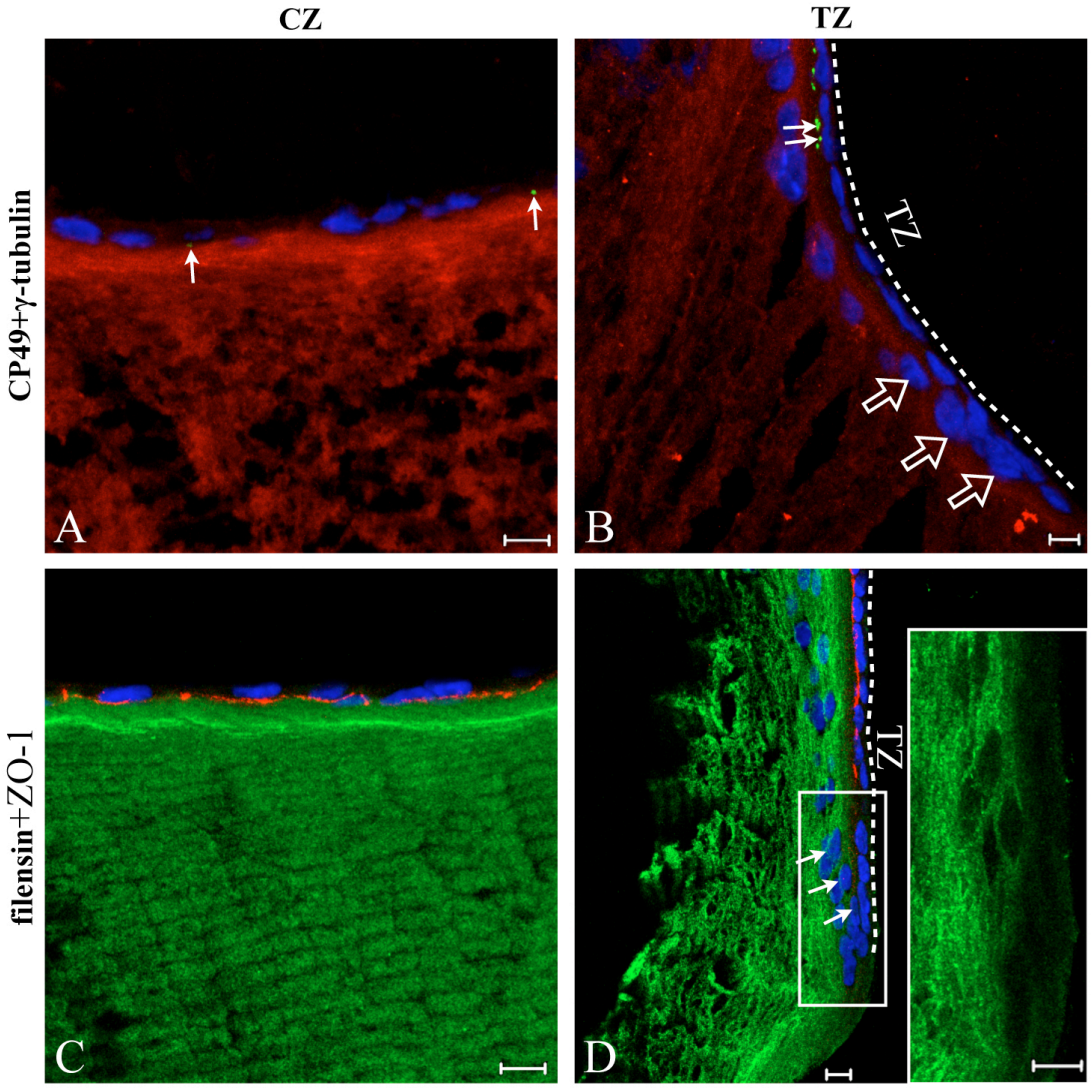

Figure 2.39. The location of γ-tubulin and ZO-1 in the bovine lens epithelial cells.

The bovine lens cryosections were labelled for either fibre cell marker CP49 (red) and centrosome marker γ-tubulin (green), or fibre cell marker filensin (green) and tight junction marker ZO-1 (red) and DNA indicator DAPI (blue). Images including the CZ and the periphery of the TZ of the epithelium were taken. Scale bars=10 μm.

A: In the CZ, γ-tubulin (arrows) is located at the apical side. CP49 is only expressed in the fibre cells, which are below the epithelial cells.

B: At the equator, the γ-tubulin staining is seen at the apical sides of some cells, but is absent in the distal part of the TZ. Before the γ-tubulin staining disappears, a cluster of γ-tubulin foci is detected (arrows). CP49 is not expressed in the cells of the TZ but starts to appear in the early-differentiated fibre cells (hollow arrows) below the TZ.

C: In the CZ, the ZO-1 staining is located at the apical sides of the epithelial cells and is absent from the fibre cells, which are below the epithelial cells and express filensin.

D: At the equator, ZO-1 is absent in the epithelial cells in the distal part of the TZ. Filensin is not detected in the TZ but starts to express in the early-differentiated fibre cells (arrows).

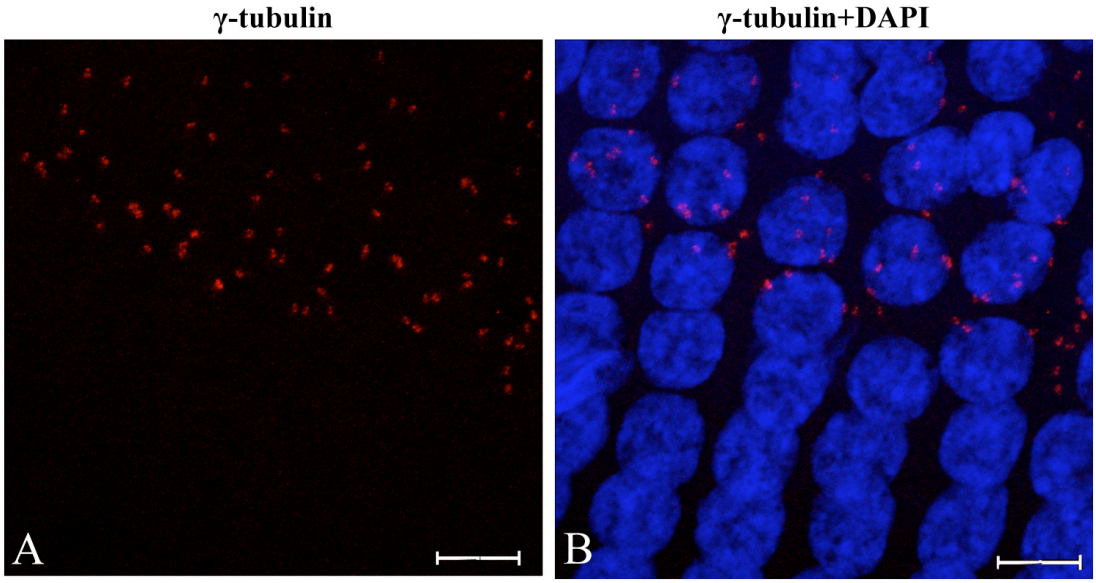

Figure 2.40. The γ-tubulin staining in the middle of the meridional lines of the bovine lens epithelium.

The bovine lens epithelial cells were stained with centrosome marker γ-tubulin (red) and DNA indicator DAPI (blue). Images in the middle of the meridional lines in the TZ were taken. Scale bars=10 μm.

A, B: At higher magnification, DAPI stained nuclei shows the meridional lines in the periphery of the TZ. The γ-tubulin staining is made of two small foci. It is absent in the further half of the meridional lines. Just before it disappears, many γ-tubulin foci are present in the middle of the meridional lines. The γ-tubulin focus number in this region is more than the nucleus number.

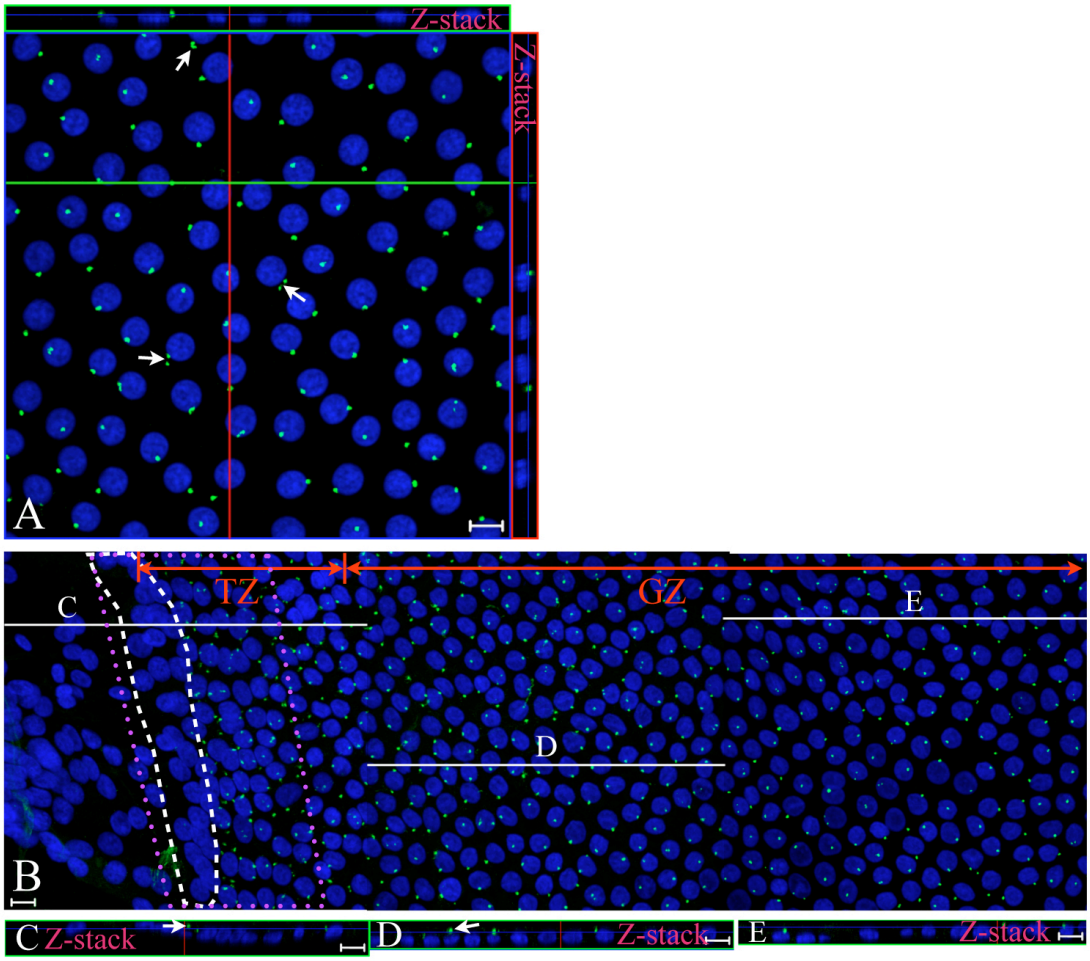

Figure 2.41. The location of γ-tubulin in the human lens epithelial cells.

Human lens epithelial cells were stained with centrosome marker γ-tubulin (green) and DNA indicator DAPI (green). Images in the CZ, the end of the GZ and the TZ were taken. Scale bars=10 μm.

A: In the CZ, the γ-tubulin staining is present in all of the cells. It shows one focus or two small foci (arrows). Z-stack shows that γ-tubulin staining is located at the apical sides of the epithelial cells.

B: γ-tubulin is present in the cells at the end of the GZ and the first part of the TZ, but is absent in the distal part of the meridional lines (area with white broken line). DAPI stained nuclei shows the meridional lines in the periphery of the TZ (area outlined with purple dotted line). The white lines shows where the Z-stacks in Figure C-E are.

C-E: Z-stacks show that all the γ-tubulin foci are located at the apical sides of the epithelial cells.

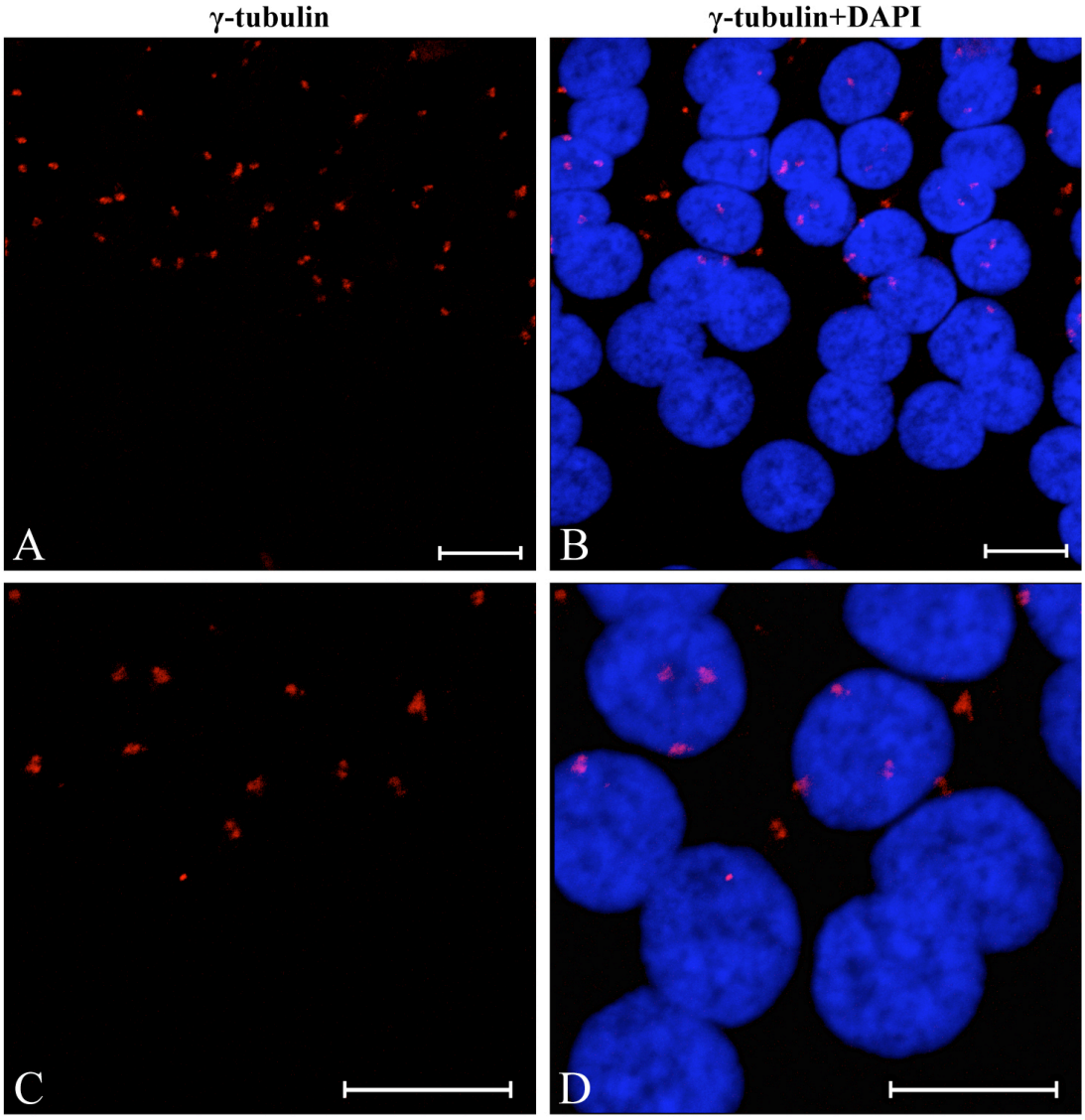

Figure 2.42. The γ-tubulin staining in the meridional lines of the human lens epithelium.

The human lens epithelial cells were stained with centrosome marker γ-tubulin (red) and DNA indicator DAPI (blue). Images of the meridional lines in the peripheral TZ were taken. Scale bars=10 μm.

A, B: At lower magnification, DAPI stained nuclei shows the ordered cells in the meridional lines. The γ-tubulin staining is present in the first part of the meridional lines but disappears in the distal part. Before it disappears, many γ-tubulin signals are present at the middle. They show as one focus or two small foci.

C, D: At higher magnification, each γ-tubulin signal mainly consists of two small foci.

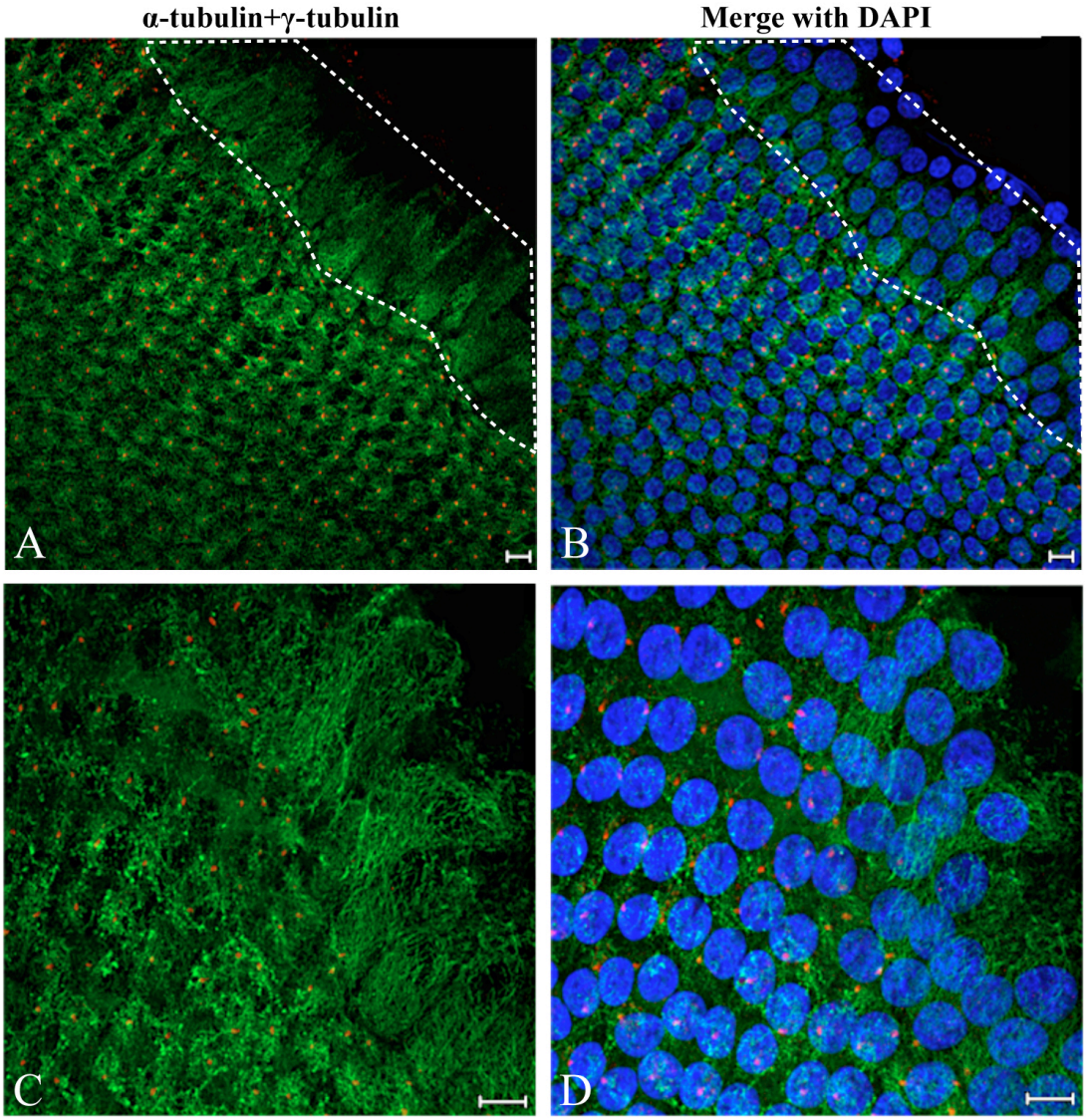

Figure 2.43. The α-tubulin structure changes with the loss of γ-tubulin in the further half of the meridional lines in the bovine lens epithelium.

The bovine lens epithelial cells were stained with α-tubulin (green), centrosome marker γ-tubulin (red) and DNA indicator DAPI (blue). Images in the TZ were taken. Scale bars=10 μm.

A, B: α-tubulin forms a basket of microtubules in the cells in the proximal side of the TZ. γ-tubulin staining is present in each cell of this region. With the absence of γ-tubulin in the further half of the meridional lines, α-tubulin cytoskeleton becomes broom-like structure (areas with broken lines).

C, D: At higher magnification, the broom-like α-tubulin structure is much clear in the cells without γ-tubulin staining. Many γ-tubulin foci are observed in the middle of the meridional lines before they disappear.

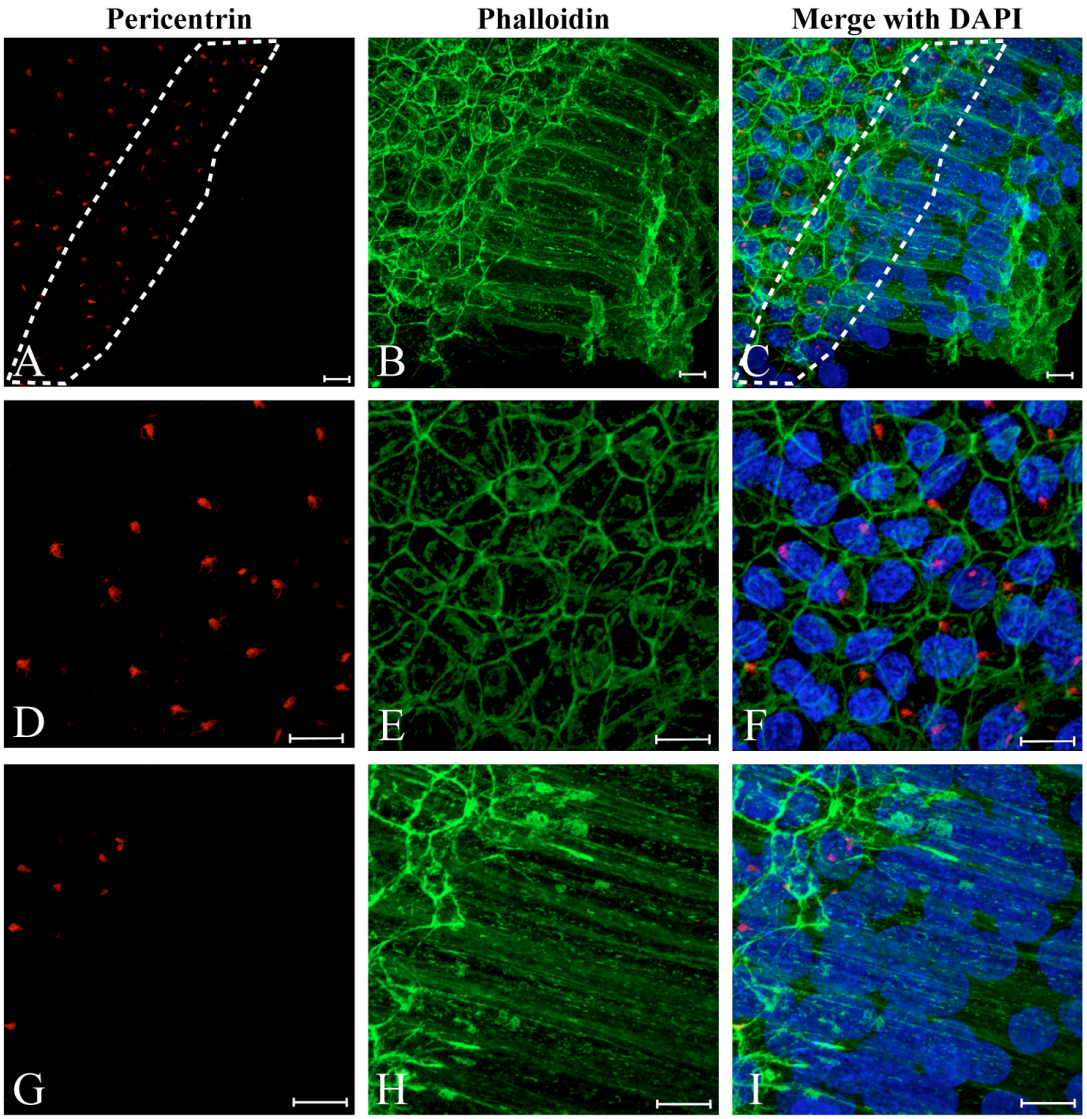

Figure 2.44. The F-actin structure changes with the loss of pericentrin in the further half of the meridional lines in the human lens epithelium.

Human lens epithelial cells were labelled with centrosome marker pericentrin (red), F-actin binder phalloidin (green) and DNA indicator DAPI (blue). The images in the TZ were taken. Scale bars=10 μm.

A-C: At lower magnification, the DAPI staining shows that the cells align into regular meridional lines. Pericentrin signals are present in the cells in the first half of the meridional lines, but are absent in the distal half. Before its signal disappears, many pericentrin signals are present at the middle (the area outlined with broken line). The F-actin shows a strong association with the plasma membrane in the epithelial cells with pericentrin staining, and becomes broom-like structure in the cells of the further half of the meridional lines without pericentrin staining.

D-F: At higher magnification, pericentrin staining appears like a cloud in the first half of the meridional lines. F-actin shows the polygonal outline of the epithelial cells.

G-I: In the distal half of the meridional lines, pericentrin staining is lost and F-actin structure becomes broom-like at higher magnification.

2.4.4.2 Cell centrosome in the human donor capsular bags with IOLs

In the human donor capsular bags after cataract surgery, γ-tubulin staining was detected in all the cells on the anterior lens capsule (Figure 2.45B). It was shown as a bigger or two smaller foci around the nucleus, which was similar to γ-tubulin staining in the normal human lens epithelial cells. In order to observe the γ-tubulin staining in the cells at the capsular bag edge where the TZ used to be, the anterior capsule was cut into six pieces and pinned down on the Sylgard to make the anterior-posterior boundary at the capsular bag edge (Figure 2.45A). In the flat anterior-posterior boundary, the normal meridional lines in the TZ were lost and cells migrated from the anterior capsule to the posterior capsule (Figure 2.45C). γ-tubulin was present in all of the cells. On the posterior capsule, γ-tubulin was located near the elongated nuclei or slightly far away from the nuclei (Figure 2.45D).

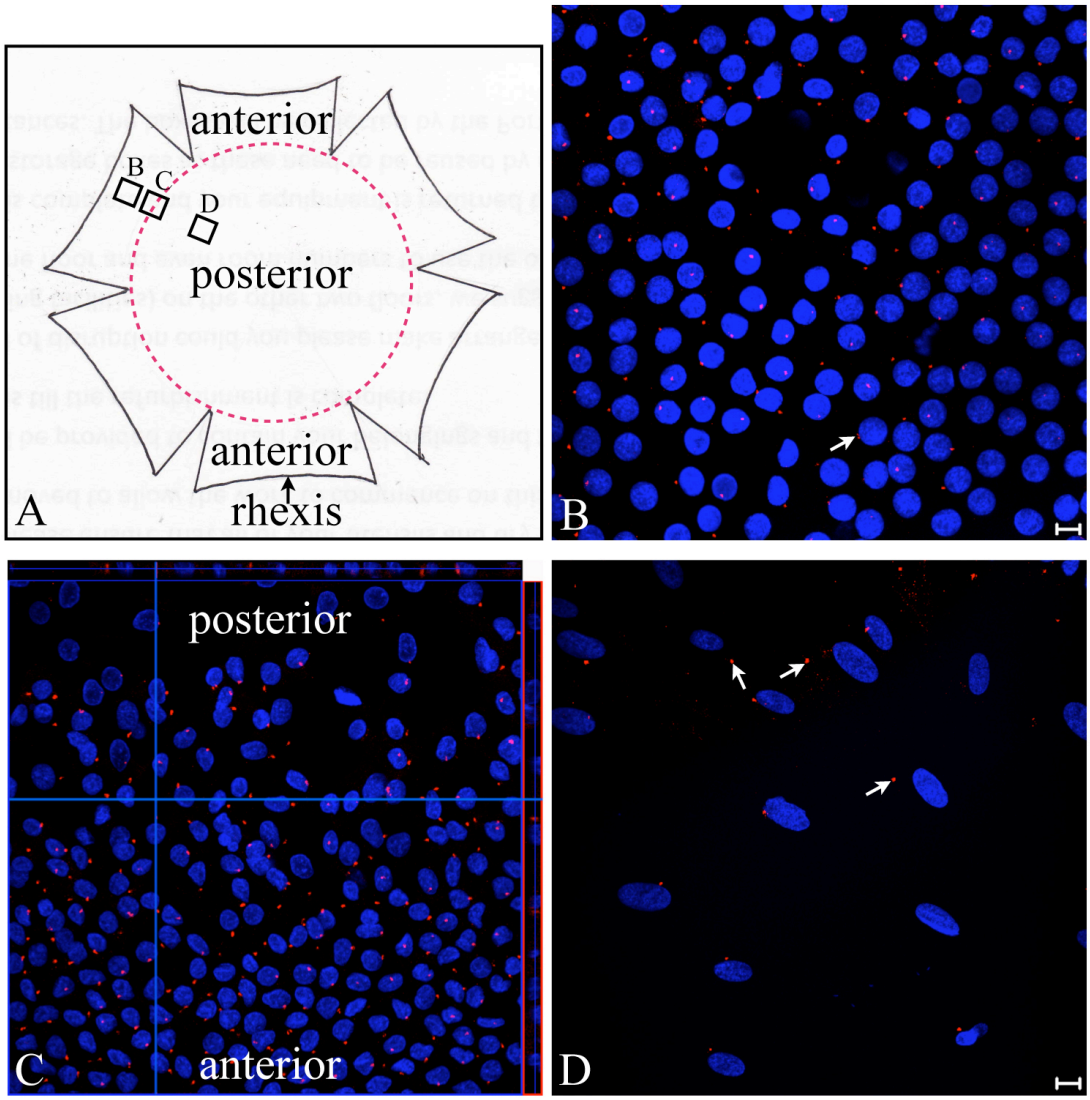

Figure 2.45. The γ-tubulin staining in the human donor lens capsular bag.

A lens capsular bag from a 70-year-old male donor was dissected out of the eye and the IOL was gently removed. Six cuts were made from the rhexis, and then the anterior capsule was peeled off from the posterior capsule along the cuts and pinned down on the Sylgard. The whole-mount was stained with centrosome marker γ-tubulin (red) and DNA indicator DAPI (blue). Images in different regions of the capsule were taken. Scale bars=10 μm.

A. A diagram shows the dissected capsular bag. Rectangles B, C and D mean the position where the images were taken.

B. On the anterior capsule, most of the cell nuclei are round as those in the normal human lens epithelial cells, and the γ-tubulin staining is present in each cell and appears as one bigger focus or two smaller foci (arrow).

C. At the anterior-posterior boundary (the capsular bag edge), the cell number decreases from the anterior side to the posterior side. The meridional lines in the TZ disappear. The γ-tubulin staining is present in all of the cells in this region.

D. On the posterior capsule, γ-tubulin staining stays close to or a little further away (arrows) from the elongated nuclei.

2.5 Discussion

2.5.1 Lens epithelial cell proliferation

2.5.1.1 The lens epithelial cell proliferation in the GZ

In the present study, most lens epithelial cell proliferation occurred in the GZ. A low number of proliferating cells were observed in the CZ of bovine, rabbit and rat lenses. No cell proliferation was detected in the CZ of the human lenses aged from 30 to 90 years old. The GZ length was variable in different mammalian lenses but its proportion in the lens epithelium was consistent. The proliferation index in the lens epithelial cells of six-month-old rabbit (equivalent to 16 years in human year) was much higher than in the 30-month-old bovine (about teenage in human year) and in the 30-90-year-old human. In addition, both the proliferating cell number and the proliferation index decreased with age in the human lens epithelium.

Most studies on the proliferation index of the lens epithelium are performed on mice and rats. Yamamoto and colleagues used flow cytometry to measure cell percentage in different cell cycle stages and found that the lens epithelial cells in S and G2/M in the 2-week-old mice (equivalent to six months in human year) were about 8% and this value decreased to 1% in the 4-week-old mice (about 10-12 years old in human year) (Yamamoto *et al.*, 2008a). This method calculated the percent of dividing cells in the total lens epithelial cells and the values could correctly reflect the proliferation index. Shui and Beebe reported the proliferation index in the 8-month-old rats (equivalent to 24 years old in human year) was about 0.7% ± 0.1% (Shui and Beebe, 2008). Although they used the flat epithelial whole-mounts, they just counted the BrdU-positive cells and the cells in the GZ instead of all of the epithelial cells on the anterior and equatorial lens capsule, and used these two values to calculate the proliferation index. Therefore, the index value that they obtained is much higher than the really one. Tseng and colleagues reported the proliferation index in the adult mouse lenses was 1.0% by counting the dividing cells in the lens sections (Tseng *et al.*, 1999). It is difficult to calculate the total cell number and the number of dividing cells by several lens sections, so the accuracy of their result is still controversial. In the present study, the flat lens epithelial whole-mounts were used. The total proliferating cell number and the total cell number in the lens epithelium were

calculated to obtain the proliferation index. This method is much better than lens sections and the values are relatively correct. As most cell divisions occur in the GZ of the lens in this study, the values can represent the proliferation index in the whole lens epithelium. This method is better for the studies using big lenses like the bovine and human lenses, but has some limitations when the small lenses like mouse and rat lenses are used. The cells are easily lost during sample preparation in these small sized lenses. This is why the proliferation indexes of rat and mouse lens epithelia were not obtained in the present study. However, the proliferation indexes in the bovine, rabbit and human lens epithelia reflect the lens growth in these mammalian lenses. Both the rabbit and bovine lenses are at similar age in human year, but the proliferation index of rabbit lens epithelium is much higher than that of the bovine lens epithelium. If their cells have similar cell cycle time, the rabbit lens probably has a higher lens growth speed than the bovine lens.

It was interesting to find that the GZ length proportion in the lens epithelium was similar in the bovine, rabbit, 30-50-year-old and above 80-year-old human. This result suggests that the GZ length proportion in the lens epithelium is probably consistent in different species of the mammalian lenses. This conclusion is different from previous studies on rat and mouse (McAvoy, 1978b; Yamamoto *et al.*, 2008b) (1.2.1.2, Table 1). McAvoy and colleagues found the GZ proportion was respectively 28.6% and 25.5% in the 1-day-old and 6-7-week-old rat lenses (McAvoy, 1978b). Yamamoto and colleagues reported the GZ proportion was respectively 13.2% and 5.3% in the 2-week-old and 4-week-old mouse lenses (Yamamoto *et al.*, 2008b). The difference is possibly caused by the methods used. In the present study, the flat lens epithelium whole-mounts were used and the GZ was easily observed under microscope by the Ki-67 and PCNA staining. However, In McAvoy and Yamamoto's studies, the mouse and rat lenses were sectioned. It is difficult to correctly measure the length of GZ in the sectioned slides because not all the proliferating cells can be sectioned. Furthermore, the results in the present study showed that some cells still proliferated in the CZ of the 4-month-old rat lens epithelium. This indicates that more proliferating cells must appear in the CZ of the 1-day-old and 6-7-week-old rat lens epithelia, and probably some are included in the GZ in McAvoy's study. These results also suggest that not all the cells in the CZ are quiescent in the young lenses. With the fast lens growth in the young rats, the CZ area also increases. The cell proliferation in the CZ helps to fit in with the increased area. Since some cells may proliferate near

the boundary of the CZ and GZ in the young lens, how to distinguish the GZ and CZ becomes an important problem. In the present study, epithelial cell density was found to increase dramatically in the GZ in all the young mammalian lenses. The change of cell density can be used to distinguish the CZ and GZ.

The different proliferation indexes in the middle-aged and old human lenses showed that cell proliferation decreased with age. Similar results are also found in the mouse and rat studies (Mikulicich and Young, 1963; Wiley *et al.*, 2010; Yamamoto *et al.*, 2008a). It is reported that the epithelial cells in S and G2/M in the 2-week-old mouse lenses are about 8% and this value decreases to 1% in the 4-week-old mice (Yamamoto *et al.*, 2008a). Other studies about the epithelial cell proliferation index in the human lenses are mainly taken on capsulotomy specimens obtained from patients during cataract surgery (Karim *et al.*, 1987; Liu *et al.*, 2000). The proliferation indexes in those specimens (from 0.0001% to 0.008%) are much lower than the values in the present study. This is because the proliferating cells in the GZ of the capsular bag are not included in the capsulotomy specimens and cell proliferation does not happen often in the CZ of the epithelium of old lenses.

2.5.1.2 Are there stem cells in the lens epithelium?

Since lens epithelial cell proliferation is detected in both the CZ and the GZ in the bovine, rabbit and rat lenses, are any of these proliferating cells stem cells? Stem cells are similar in morphology to normal cells. They can be recognised by their unlimited proliferative capacity or special stem cell markers. In this study, the Ki-67 and PCNA staining just showed the proliferation situation when the lens epithelial cells were fixed. The cells' proliferative capacity was not studied as in some reports to inject the animals with ^{3}H-thymidine or BrdU and detect the label-retaining cells (LRCs) (Lavker and Sun, 2003; Tsujimura *et al.*, 2002; Zhou *et al.*, 2006). The neural stem cell marker nestin was tried on the bovine lens epithelial cells in the present study, but none of the cells was labelled. So the result is not shown in this thesis. Therefore, it is impossible to locate the stem cells in the lens epithelium in the present study. Oka and colleagues reported that stem cells were in the GZ by using different kinds of stem cell markers to stain the lens epithelial cells (Oka *et al.*, 2010). In the present study, the Ki-67 and PCNA staining shows that proliferating cells in the GZ are in different phases of the cell cycle. They are probably just mature transit

amplifying cells with very limited proliferative ability, and their progeny migrate to the TZ to differentiate into fibre cells after cell proliferation.

Zhou and colleagues reported that stem cells might be in the CZ by repeatedly injecting pregnant mice and utero-labelled neonatal mice with ^{3}H-thymidine and detecting the LRCs in the lens (Zhou *et al.*, 2006). In the present study, some proliferating cells are detected in the CZ of the rabbit and rat lens epithelia. They are also in different phases of the cell cycle and look like those proliferating cells in the GZ. Since the stem cell number is usually very low, these proliferating cells in the CZ are probably not stem cells. Those lenses are from young rabbits and rats. The lenses grow much faster in the young mammals than in the old (Augusteyn, 2008). The area of the anterior capsule increases with lens growth. The purpose of cell proliferation in the CZ may be to fit in with the increased capsule area. Interestingly, a very low number of proliferating cells (no more than ten cells in each lens) are found in the CZ of the bovine lens epithelium. The Ki-67 staining shows that they are in the G1-G2 phases but not in the M phase. They are possibly normal mature transit amplifying cells like those in the GZ, or probably different from them because none of them is found in the M phase. Whether they are stem cells needs to be confirmed by other methods in the future.

2.5.2 Lens epithelial cell apoptosis

In the present study, results of the Annexin-V-Fluorescein staining showed that necrosis started to occur in the bovine lens epithelial cells as early as 12 minutes after lens dissection. Therefore, all the lens epithelial whole-mounts were fixed immediately after dissection and performed with the TUNEL assay. The TUNEL assay results showed that apoptosis incidence was very low in the lens epithelium of normal young bovine, rat and mouse lenses. In the middle-aged and old human lenses, the apoptotic cells were more often detected, but their number was still quite low. In addition, a low number of TUNEL-positive cells were also detected on the anterior and posterior of the human donor capsular bags after cataract surgery.

The plasma membrane of many kinds of cells maintains an asymmetric distribution of different phospholipids in the inner and outer leaflets (Bretscher, 1972). For example, the choline-containing phospholipids, phosphatidylcholine and sphingomyelin are located in the outer leaflet, while the aminophospholipids

phosphatidylethanolamine and phosphatidylserine are found in the cytoplasmic face. It is reported that plasma membrane loses its asymmetry at the early stage of apoptosis, and phosphatidylserine moves from the inner leaflet to the outer leaflet (Fadok *et al.*, 1993; Fadok *et al.*, 1992a). The exposed phosphatidylserine in the cell surface acts as a tag for specific recognition by macrophages and for phagocytosis of the dying cell. Since Annexin-V specifically binds to phosphatidylserine in the presence of calcium (Andree *et al.*, 1990; Tait *et al.*, 1989), fluorescein labelled Annexin-V can be used to detect the occurrence of cell apoptosis (van Engeland *et al.*, 1998). Annexin-V cannot bind to normal living cells because the molecule is not able to penetrate the phospholipid bilayer. However, it is able to bind to the available inner leaflet of the necrotic cells because these cells already lose the integrity of the plasma membrane. In order to discriminate the necrotic and apoptotic cells, a membrane-impermeable DNA stain such as PI can be added to the staining solution at the same time (van Engeland *et al.*, 1998). If the cells are labelled by both Annexin-V and PI, they are undergoing necrosis. If they are only labelled by Annexin-V, they are in apoptosis. In the present study, the live bovine lens epithelial cells were first incubated with Annexin-V-Fluorescein and PI for 12 minutes and then fixed with PFA. Fixing would stop the cells undergoing necrosis when they were observed under the microscope. Results showed that many cells across the whole lens epithelium were both stained with Annexin-V-Fluorescein and PI. The stained cells did not show obvious nucleus-shrinkage or chromatin-condensation, which are the typical characteristics of apoptotic cells. Therefore, they were not in apoptosis but undergo necrotic cell death. These results suggest that the lens epithelial cells start the process of necrosis soon after lens dissection. They also show that the high apoptosis rates in the capsulotomy specimens reported by Li and colleagues (Li *et al.*, 1995) are most likely necrosis rates. What they did was to collect the samples on microscope slides, returned them to the laboratory, dissected them in saline and then fixed them. In this case, the delay between surgery and fixation would allow the occurrence of cell necrosis. In the present study, in order to obtain the correct apoptotic rates, all the lens epithelial cells were fixed immediately after dissection and labelled with the TUNEL assay.

During cell apoptosis, nucleases are activated and degrade the nuclear DNA intro fragments of approximately 200 base pairs in length. The DNA breaks expose a large number of 3'-hydroxyl ends, which can be identified by terminal

deoxynucleotidyl transferase. This enzyme then catalyses the addition of dUTPs that are secondarily labelled with a fluorescein. In the present study, all the TUNEL-positive nuclei displayed the morphologic characteristics of the different stages of apoptosis, including chromatin condensation and nuclear fragmentation. These characteristics make the apoptotic nuclei quite different from the TUNEL-positive nuclei in the positive controls predigested with benzonase nuclease. The low TUNEL-positive cell rates in the bovine, mouse and rat lens epithelia indicate that apoptosis does not occur often in these young lenses (equivalent to 16 human years). By contrast, apoptotic epithelial cells were observed more often in some of the middle-aged and old human lenses. In order to test whether cell apoptosis happened when the eyes were stored in the eye bank and delivered to the lab, four eyes were fixed immediately after removing the corneas and their opposite fellow eyes were kept in 0.9% (w/v) of NaCl. Results showed that the apoptotic cell numbers in these two groups of eyes were similar. This means that no more cells undergo apoptosis during eye storing and delivering. It also ensures the accuracy of the results about human lens epithelial cell apoptosis. There are three possible reasons to explain why the human lens epithelial cells remain alive for about three days postmortem. Firstly, the lens capsules are still intact and separate the epithelial cells from their surrounding environment. Secondly, the lenses are still located at the original place after removing the corneas, facing vitreous humour in the posterior side and iris in the anterior side. Thirdly, the osmolarity of 0.9% (w/v) of NaCl (290 milli-osmoles per kilogram) is similar to normal human reference range of osmolarity in plasma (275-299 milli-osmoles per kilogram). As the aqueous humour is secreted by the ciliary body into the posterior chamber to nutrify the lens cells (Dahm *et al.*, 2011), its osmolarity may be similar to blood plasma osmolarity. If so, storing in 0.9% (w/v) of NaCl will not lead to lens oedema.

Although the apoptotic cell number in some of the middle-aged and old human lenses was slightly higher than those in the young bovine, mouse and rat lenses, no more than 23 cells were in apoptosis in each lens. This result is consistent with previous reports. Harocopos and colleagues only found two TUNEL-positive cells in the 28 capsulotomy specimens of the cataractous and non-cataractous lenses from the eye bank eyes (Harocopos *et al.*, 1998), which is much lower than the result of the present study. One reason is possibly because they just studied the CZ of the lens

epithelium. Li and colleagues also found the cell apoptosis rate in normal lenses from the eye bank eyes was lower than 0.01% (Li *et al.*, 1995).

2.5.3 Homeostasis of the lens epithelium

In the present study, the number of the proliferating cells in the GZ (N_p), the number of apoptotic cells in the lens epithelium (N_a), and the number of the epithelial cells at the end of the meridonal lines that will differentiate into fibre cells (N_f) were calculated in the bovine, rabbit and human lens epithelia. Results showed that there were more proliferating cells than the apoptotic cells and the epithelial cells at the end of the meridional lines ($N_p>N_a+N_f$) in the bovine and rabbit lens epithelia. In the lens epithelium of the human aged 30-50 years and 80-90 years, the proliferating cell number was smaller than the sum of the apoptotic cell number and the epithelial cell number at the end of the meridional lines ($N_p<N_a+N_f$). These results indicate that a cell number balance does not exist in these lens epithelia.

Tissues such as skin epidermis, cornea and intestinal epithelium maintain their homeostasis by providing new cells to replace the lost cells during tissue turnover or following injury (Barker *et al.*, 2008; Blanpain and Fuchs, 2009; Ladage *et al.*, 2002). The lens is different from these tissues. Due to the enclosure of the lens capsule, the lens cells are not lost throughout life except those which die of cell apoptosis. The epithelial cells still continually proliferate and differentiate into fibre cells at the lens equator to maintain the lens growth. The size of a tissue cell population is determined by the cell birth rate (K_b) and the cell loss rate (K_l) (Budtz, 1994). If $K_b>K_l$, the tissue is growing. If $K_b<K_l$, the tissue is regressing. If $K_b=K_l$, then the tissue is in kinetic equilibrium. That is assuming that cells do not change size. In the lens, the equatorial diameter and anterior and posterior sagittal thickness consistently increase throughout life (Augusteyn, 2008; Augusteyn, 2010). This means that the area of the anterior capsule and part of the equator covered with epithelial cells is enlarging. Therefore, K_b should be bigger than K_l all the time in the lens epithelium. This situation exists in the 30-month-old bovine lenses and 6-month-old rabbit lenses (both are about 16 years old in human years), but not in 30-50-year-old and 80-90-year-old human lenses. Does $K_b<K_l$ in this study means the human lens epithelium is regressing with age? In fact, the surface area covered with epithelial cells in the 80-90-year-old human lenses is bigger than that in the 30-50-year-old's. So the numbers of produced

cells and lost cells are not enough to reflect lens epithelial homeostasis. In other words, other factors must participate in the regulation of this process.

One important factor is the time that the epithelial cells spend during proliferation, apoptosis and differentiation. The cell cycle time in the GZ is quite variable in different animals and also changes with age. It is about two days in the neonatal mice, three days in the 10-day-old mice and 16 days in the 2- to 3-month-old mice (Gloor *et al.*, 1985). It is about three days in the 6-30-day-old rats (Mikulicich and Young, 1963) and 23 days in the 3-4-month-old rats (Riley and Devi, 1967). No cell cycle time has been reported in the bovine and rabbit lens epithelia. For cell apoptosis, the morphologically identifiable stages last only approximately three hours (Bursch *et al.*, 1990; Messam and Pittman, 1998). It is not clear how long it will take the epithelial cells at the end of the meridional lines to differentiate into fibre cells. Rafferty and colleagues used ^{3}H-thymidine injection method to find that 43 days are required for the epithelial cells to transit the meridional lines and differentiate into anucleate lens fibres in the 2-month-old mice (Rafferty and Rafferty, 1981b). The big difference between the proliferating cell number and the epithelial cell number at the end of the meridional lines (shown as TZ column number) probably depends on the regulation of cell cycle time and fibre cell differentiation time. A very important limitation of the present study is not detecting the epithelial cell cycle time, apoptosis time and the time for the epithelial cells at the end of the meridional lines to differentiate into fibre cells. These need to be studied on live animals; however, it is impossible to inject ^{3}H-thymidine to cows or humans.

Another factor that helps to understand lens epithelium homeostasis is cell size. In the present study, it is found that the cell cross-sectional areas are variable in each zone. In the bovine and rabbit lens epithelia, the cell cross-sectional area at the end of the TZ is slightly bigger than that in the GZ. In order to maintain the epithelium homeostasis, more cells should be produced in the GZ. In addition, the human lens epithelial cell cross-sectional areas in each zone are found to increase with age. Similar results are also reported in the primate lens epithelium (Kuszak, 1997). This cross-sectional area increase makes up the difference between the increase of anterior surface area and the decrease of cell proliferation index with age. Furthermore, the changes in epithelial cell cross-sectional area also lead to the cell density change with age in the human lenses. So to investigate how cell size parameters are influenced by

the position within the epithelium and age of the epithelium is very important in studying lens epithelium homeostasis.

In conclusion, the lens epithelial proliferating cell number and lost cell number are not enough to show the lens epithelium homeostasis. Other factors such as the cell cycle time, the apoptotic time, the time for the epithelial cells at the end of the meridional lines to differentiate into fibre cells and epithelial cell size also influence this process.

2.5.4 Cell density change across the lens epithelium

In the present study, the cell density gradient of the lens epithelium was similar in bovines, mice, rats and rabbits. It remained stable in the CZ, increased dramatically in the GZ and then declined in the TZ. The epithelial cell density in each zone was slightly variable in these mammalian lenses. The human lens epithelial cell density was different. It increased from the periphery of the CZ to the TZ, and the highest cell density was much lower than that of the other mammals in this study. Moreover, the cell density in the peripheral lens epithelium decreased with age. No cell density difference was found between the female and male lens epithelia.

In some studies about the normal human lenses, the epithelium was divided into the central region and the peripheral region (Guggenmoos-Holzmann *et al.*, 1989; Harocopos *et al.*, 1998) (Table 2.1). However, the exact position in the peripheral region is not described. Furthermore, most studies were performed on the capsulotomy specimens, which are obtained from the cataractous lenses and just include the CZ of the lens epithelium (Argento and Zarate, 1990; Fagerholm and Philipson, 1981; Hara, 1988; Harocopos *et al.*, 1998; Hass *et al.*, 1995; Konofsky *et al.*, 1987; Kumamoto *et al.*, 2007; Saitoh *et al.*, 1990; Struck *et al.*, 1997; Tkachov *et al.*, 2006; Tseng *et al.*, 1994). Therefore, no consistent conclusion has been drawn from those studies about cell density in each zone and its change with age and cataract development. The present study used the flat human lens epithelium whole-mounts and calculated the cell density from the anterior pole to the end of the TZ. The results are more correct than those previous studies.

It is interesting to find that lens epithelial cell density is stable in the CZ but increases dramatically in the GZ of the young animal lenses. What is the significance of this kind of cell density gradient in the lens epithelium? The studies of neutral crest

cells show that migratory behavior is influenced by cell number and cell-cell contact, and high cell density promotes cell migration (Rovasio *et al.*, 1983; Simpsona *et al.*, 2010; Thomas and Yamada, 1992; Young *et al.*, 2004). As the lens epithelial cells in the GZ need to migrate towards the TZ to prepare for differentiation, the high cell density in the GZ probably causes high population pressure, which pushes cells to migrate to the periphery. If the high cell density improves cell migration, why do the cells not move towards the CZ? It is reported that isolated embryonic chicken pigmented retinal epithelial cells or neutral crest cells spread and migrate poorly, while their migration is promoted when they make contact with other cells (Middleton, 1977; Thomas and Yamada, 1992). This indicates that cell-cell contact improves migration. The results in the present study showed that the epithelial cells in the GZ were much taller than those in the CZ. Furthermore, the density of the lens epithelial cells in the peripheral region of the GZ is much higher than in the inner side of the GZ that is next to the CZ. Therefore, the average cell-cell contact area is much bigger in the peripheral side of the GZ than in the inner side. This may cause the cells to migrate towards the periphery, not the inner side. Another possible reason is that the cells in the inner side of the GZ produce a higher force, which prevents the cells moving inside to the CZ.

The human lens epithelial cell density gradient is slightly different from other mammals in the periphery. One important reason is probably age. The mammalian lenses in this study were respectively from 30-month-old cows, six-month-old rabbits and mice and four-month-old rats. These animals were quite young, about 16 years old in human year. However, all the human lenses came from 20 to 90 years old people and most were from 40 to 80 years old. In the present study, the proliferation index was found to decrease with age. This is possibly why cell density is low in the GZ of the human lens epithelium and why cell density continuously decreased with age. The decrease of cell density with age has also been found in the rat and mouse lens epithelia cells (Uga *et al.*, 1983; Uga *et al.*, 1996). Furthermore, the TZ of the human lens epithelium is much shorter than that of other mammalian lenses. The length of human meridional lines is only about half of that in the bovine. Therefore, the cell density decrease in such a short region is not obvious. This is why the e cell density does not decrease in the TZ of the human lens epithelium but starts to decrease in other mammalian lens epithelia.

By comparing the epithelial cell density in the same position of the female and male human lenses, it is found that there is no gender difference. This is consistent with the results of Nejsum and Tseng's studies (Nejsum and Nelson, 2009; Tseng *et al.*, 1994). The other studies that show lens epithelial cell density is higher in women than in men (Konofsky *et al.*, 1987; Saitoh *et al.*, 1990; Vasavada *et al.*, 1991) probably do not consider the age and position influence on cell density. Most lenses studied in these reports have different kinds of cataract. Cataract development also influences lens epithelial cell density.

2.5.5 Changes of cell morphology and size across the lens epithelium

2.5.5.1 The consistency of the epithelial cell morphology and size change in different mammalian lenses

In the present study, the epithelial cells of bovine, rat, mouse, rabbit and human lenses were polygonal in the CZ, the GZ and the proximal region of the TZ. In the meridional lines of the TZ, the cells became regularly hexagonal and lined up into columns. The cell cross-sectional area was bigger in the CZ and became smaller in the GZ and TZ. The cell height increased slowly in the periphery of the CZ and fast in the GZ and TZ. The cell volume of the bovine lens epithelium was similar in the CZ and TZ but decreased in the GZ where the highest cell density was. The cell volume of human lens epithelium slowly and continuously decreased from the CZ to the TZ. In addition, the human lens epithelial cell cross-sectional area and volume increased with age. These results show that the lens epithelial cell size and morphology are different in the three zones and also change with age.

Why do the epithelial cell size and morphology need to change in the GZ and TZ? One important function of the lens epithelium is continuously providing new cells for lens growth throughout life. This is achieved by epithelial cell proliferation in the GZ and fibre cell differentiation at the end of the TZ (McAvoy, 1978a; Ong *et al.*, 2003). The cell morphology and size are quite different between the epithelial cells and newly-formed fibre cells. The epithelial cells are flat or columnar polygons while the fibre cells are long and thin hexagons (Bassnett, 2005; Kuszak, 1997). The epithelial cell morphology and size changes in the GZ and TZ are the preparation for the following fibre cell differentiation.

Why do the human lens epithelial cell cross-sectional area and volume change with age? Is this important for retaining lens epithelium homeostasis? One characteristic of lens growth is the increase of lens size (Bron *et al.*, 2000). With the increase of anterior and equatorial lens capsular area, cell cross-sectional area and/or the epithelial cell number should increase. In the present study, no proliferating cells were detected in the CZ of 30-90-year-old human lens epithelium. This means that the cells can only increase their cross-sectional area in order to fill in the increased capsular area in this region. Furthermore, the proliferation index decreased with age in the human lens epithelium in the present study. This suggests that less cells will be produced in the GZ in the older lenses. Probably less cells will be remained in the GZ and TZ to filled in the increased capsular area in these two regions, compared with the younger lenses. This is also why cell density decreases with age in the GZ and TZ of the human lens epithelium. The calculation of the total lens epithelial cell number in 30-50-year-old and 80-90-year-old people did show that the older lenses have more lens epithelial cells. However, the increase of cells number may be still lower than the increase of anterior and equatorial capsular area. In conclusion, the epithelial cell size change helps to retain the epithelium homeostasis when the proliferation index and capsular area change with age.

2.5.5.2 Lens epithelial cell nuclear volume change

In the present study, although the nuclear volume of bovine and human lens epithelial cells was different in the CZ and GZ, the karyoplasmic ratio (the ratio of the nuclear volume to cell volume) remained steady across each lens epithelium, about 0.067 and 0.023 respectively. Eukaryotes have the ability to maintain cell size and organelle volume that are appropriate for different growth styles and differentiation states. It has been reported that cells, from single-celled eukaryotes to mammalian cells, maintain a roughly constant karyoplasmic ratio (Cavalier-Smith, 2005; Huber and Gerace, 2007). Jorgensen observes that nuclear volume occupies 8% of the cellular volume in the mutants of budding yeast (Jorgensen *et al.*, 2007), which is higher than the karyoplasmic ratio of bovine and human lens epithelial cells. It is still unclear what controls nuclear size. The drugs that affect actin and microtubules have no effect on karyoplasmic ratio of fission yeast, which indicates that these filaments probably do not influence nuclear size (Neumann and Nurse, 2007). Lamina has been

found to strongly influence nuclear size as well as shape in higher eukaryotes (Gruenbaum *et al.*, 2005; Newport *et al.*, 1990; Worman and Courvalin, 2005; Yang *et al.*, 1997). It may control nuclear size change.

2.5.6 Lens epithelial cell centrosome

In the present study, both γ-tubulin and pericentrin were located at the apical sides of the bovine and human lens epithelial cells and stayed at similar level with ZO-1. Their staining was absent from the cells in the further half of the meridional lines in the TZ. In the middle of the meridional lines, many γ-tubulin and pericentrin staining foci were detected. Furthermore, ZO-1 was also not observed in the further half of the meridional lines. α-tubulin and F-actin filaments displayed a basket appearance in the epithelial cells with γ-tubulin or pericentrin staining, but changed to a broom-like morphology in those cells without γ-tubulin or pericentrin staining.

γ-tubulin and pericentrin are two key components of the pericentriolar material and play an essential role in microtubule organisation (Doxsey *et al.*, 1994; Moritz *et al.*, 1995; Oakley, 1995; Zheng *et al.*, 1995). Therefore, they cannot be absent from the lens epithelial cells. At first, it was presumed that the γ-tubulin and pericentrin proteins changed from one single microtubule focus to multiple microtubule nucleating sites in these cells. It means that they were divided into pieces and scattered in the cells. However, the images at higher magnification neither show any morphology change before the γ-tubulin and pericentrin signals disappear nor display any traces of their staining in these cells. This indicates that the assumption is not right. Another possibility is that the γ-tubulin and pericentrin in the further half of the meridional lines are located in a special area. Many of their staining foci were detected in the middle of the meridional lines and the number is more than the nuclear number in that region. This suggest that these extra staining foci may belong to the cells in the further half of the meridional lines. When the TZ cells differentiate and are forced to migrate to the posterior capsule (Beebe D. C., 1980), their apical end became tapered and associated with each other to form a distinct structure called modiolus (Zampighi *et al.*, 2000). The bovine lens sections labelled with N-cadherin showed that the modiolus was just located in the middle of the meridional lines (based on the nuclear number in the meridional lines) (Figure 2.46). As γ-tubulin and

pericentrin locate in the apical side, all of the γ-tubulin and pericentrin staining should be present in the modiolus. This can also explain the disappearance of ZO-1 from the most distal cells in the TZ cells. Conditional depletion of aPKCλ, a central effector of the partitioning defective polarity complex, results in the failure of modiolus formation in mouse lens epithelium (Sugiyama *et al.*, 2009). γ-tubulin staining is observed in all of the cells in the periphery of the TZ. This indicates that γ-tubulin in the further half of the TZ is localised at the modiolus and is not absent from those cells.

The lens epithelial cells are polarised cells and the centrosome markers γ-tubulin and pericentrin are located at the apical sides. Is this centrosome location important for maintaining cell polarisation in the immobile cells in the CZ and the migrated cells in the GZ and TZ? Does it play a role in maintaining the normal epithelial cell morphology? It is reported that removal of centrosome using near-infrared laser irradiation in migrating polarised U2OS and PtK2 cells leads to the loss of cell polarisation and the changes of cell shape (Wakida *et al.*, 2010). Changes in cell shape are caused by the modifications in microtubule and actin organisation. This suggests that the centrosome is necessary for the maintenance of cell polarisation and cell morphology. Along with intermediate filament vimentin, actin and tubulin consist of the cytoskeleton structure of the lens epithelial cells and play an important role in maintaining the cell morphology and in the cell migration in the GZ and TZ (Leonard *et al.*, 2011; Quinlan *et al.*, 1999). In the present study, the F-actin and α-tubulin organisation in the further half of the meridional lines is quite different from that in the proximal half. The centrosome, which is located at the tapered apical end and accumulates at the modiolus, may play a role in their organisation change during cell migration.

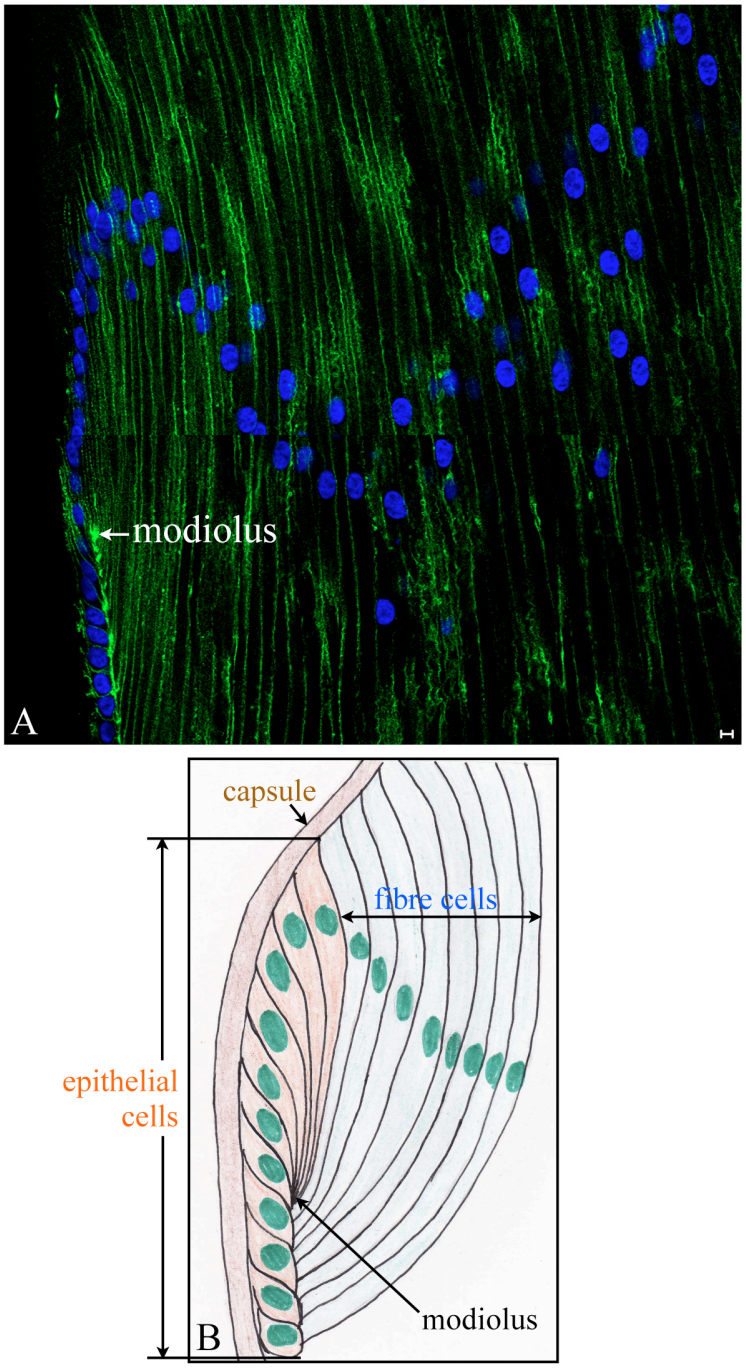

Figure 2.46. Morphological characteristics of the modiolus.

The 12-14-μm-thick bovine lens sections were labelled with adhesion junction molecule N-Cadherin (green) and DNA indicator DAPI (blue). The image in the periphery of the TZ, where the meridional lines were, was taken. Scale bar=10 μm.

A. In the periphery of the TZ, the epithelial cells elongate fast, and their apical sides become tapered. In the last 11 epithelial cells, the tapered apical ends associate with each other and form a distinct structure called modiolus (arrow).

B. The diagram shows the formation of the modiolus.

2.5.7 The cells in the periphery of the human capsular bags with IOLs retain many characteristics of the epithelial cell organisation

In the present study, cell proliferation in the human lens capsular bags with IOLs was still mainly restricted to the periphery of the anterior capsule where the GZ was in the normal lens. The apoptotic cell number was very low here. The majority of the cells were still in a single layer and retained their polygonal morphology. γ-tubulin was located at the apical sides of these cells. These results suggest that the cells in the periphery of the anterior capsule still retain some characteristics of cell organisation in the normal lens epithelium. Because some cells in the periphery of the anterior capsule were lost in some capsular bags during cataract surgery, the cell density was not studied. Furthermore, PCO occurred all of the capsular bags with IOLs in the present study. Therefore, the normal meridional lines in the TZ also lost in these capsular bags, and some fibrosis usually attached to this single layer of cells and filled in the space between the IOL edge and the capsular edge. These changes made it impossible to measure the cell height, cross-sectional area and volume.

The removal of the central anterior lens capsule and fibre mass during cataract surgery breaks the enclosed environment of the lens and the normal fibre cell differentiation process (Asbell *et al.*, 2005). The implants of IOLs to the residual capsular bags induce the cell elongation and differentiation in the region along the rhexis (Marcantonio *et al.*, 2000). How can the cells in the periphery of the anterior capsule still retain their original morphology and proliferation ability? Autocrine and the growth factors from the aqueous humour probably play an important role here. Human lens epithelial cells in the capsular bags can maintain their proliferation ability in a protein-free medium for more than one year, and FGF-2, FGFR-1 and HGF are detected in the capsular bags (Wormstone *et al.*, 2001; Wormstone *et al.*, 2000). This suggests that the epithelial cells can synthesize and secret growth factors. Moreover, the growth factors in the aqueous humour will still pass through the lens capsule and the space between the IOL and the capsular rhexis to act on the residual cells on the anterior capsule after cataract surgery.

2.6 Summary

The purpose of this chapter was to study the lens epithelial cell organisation and detect its consistency in the bovine, rabbit, rat, mouse and human lenses. Results show that the main location of cell proliferation, the number of apoptotic cells, the cell density gradient and the changes in their cell height and cross-sectional volume were all consistent in those lens epithelia. Moreover, in the human lens epithelium, the proliferation index and cell density in the periphery decreased with age, while the cell cross-sectional area and cell volume increased with age. In the human capsular bags with IOLs and variable degrees of PCO, cell proliferation was still mainly restricted to the periphery where there used to be the GZ, and cell apoptosis occurred in both the anterior and posterior capsule. The majority of the residual cells still retained the original morphology and were shown as a single layer on the peripheral anterior capsule, while the cells on the posterior capsule elongated and became multilayered. The epithelial cell centrosomes of the bovine and human lenses were located at the apical side. In the periphery of the TZ, the cells elongated and their apical side tapered to form a special structure called the modiolus. The centrosomes of these cells then accumulated at the modiolus.

FGF-2 plays a critical role in regulating cell proliferation and differentiation in the GZ and TZ. It is stored in the lens capsule before it binds to its receptor on the epithelial cell membrane. In chapter 3, the FGF-2 distribution on the inner surface of the bovine lens capsule is studied in order to detect whether a higher level of FGF-2 is present in the equatorial capsule where the GZ and TZ are located.

3 FGF-2 and perlecan distribution in the inner surface of the bovine lens capsule and the capsule structure

3.1 Introduction

The lens capsule is an uninterrupted basement membrane that completely encloses the lens and separates it from the other ocular tissues. It is composed of multiple laminae that are synthesised by the epithelial cells and fibre cells in its inner surface (Haddad and Bennett, 1988; Young and Ocumpaugh, 1966). Each lamina is made of interacting networks of laminin, collagen IV, nidogen, heparan sulphate proteoglycans (HSPGs) and fibronectin (Danysh and Duncan, 2009), which bind to their receptors in the lens cells and regulate epithelial cell proliferation, migration and fibre cell differentiation (Oharazawa *et al.*, 1999). Smaller molecules required for cell metabolism such as glucose, salts, water, O_2, CO_2 and the resulting metabolic waste can freely pass through these networks (Fisher, 1977), while the intermediate sized molecules present in the aqueous and vitreous humours or produced by the lens cells can only selectively pass through the lens capsule based on their molecular size and charge (Lee *et al.*, 2006).

The lens capsule plays an important role in lens epithelial cell proliferation and fibre cell differentiation. Besides supplying vital epitopes for the lens cell surface receptors, the lens capsule also provides an important reservoir for sequestered growth factors. The HSPGs in the lens capsule can bind FGF-1, FGF-2, HGF, and PDGF by their sulphated glycosaminoglycan (GAG) and protect these factors from proteases (Chu *et al.*, 2005; Kreuger *et al.*, 2005; Taipale and Keski-Oja, 1997). There are two major HSPGs in the lens capsule, perlecan and collagen XVIII. Perlecan is a large multidomain HSPG found in all of the basement membranes. It is incorporated into the main scaffolding of the lens capsule by a core protein and three to four GAG side chains. Perlecan has been found to co-localise with FGF-1 and FGF-2 in the lens capsule (Lovicu and McAvoy, 1993). Its deficiency in mice causes a smaller size of the lenses and decreased lens epithelial cell proliferation (Rossi *et al.*, 2003). FGFs and other growth factors are released from perlecan by matrix metalloproteinases (MMPs) (Tholozan *et al.*, 2007).

FGF-2 is found to stimulate lens epithelial cell proliferation and fibre cell

differentiation in a progressive dose-dependent manner (Chamberlain and McAvoy, 1989). The lower concentration of FGF-2 induces cell proliferation while the higher concentration initiates cell differentiation. FGF-2 needs to pass through the lens capsule before it reaches lens cells. The lens epithelial cells proliferate in the GZ and migrate to the TZ to prepare for fibre cell differentiation. Both the GZ and the TZ are located at the equator of the lens capsule. Based on these studies, a hypothesis is proposed that FGF-2 probably has a gradient distribution in the lens capsule, higher at the equator and lower in the anterior and posterior. In the present study, the distribution of FGF-2 and its HSPG binding partner perlecan on the inner surface of the lens capsule was studied by immunogold labelling.

3.2 Aims

Based on the location of lens epithelial cell proliferation and the function of FGF-2 in regulating cell proliferation, the aim of this chapter was to study the hypothesis that the FGF-2 level was higher at the equator than in the anterior and posterior lens capsule. In addition, the lens capsule structure was studied using scanning electron microscopy (SEM).

3.3 Materials and methods

3.3.1 The lens capsules

The bovine lens capsule was used to study the distributions of FGF-2, perlecan and collagen IV on the inner surface. Four capsules were included for every independent repeat. Three were labelled with their primary antibodies and one was used as the negative control, which was just incubated with the secondary antibody but without the primary antibody. For the studies of the bovine lens capsule structure on the inner and outer surface and the cross-sectional side, three capsules were included for every independent repeat. Two were used for the study of the inner and outer surface structure. The last one was cut into two halves from the centre of the anterior lens capsule and used for the study of the cross-sectional side. In order to compare the bovine lens capsule structure to other species', the human lens capsule was included in this study. As with the bovine lens capsules, two human lens capsules

were used each time. All of the bovine and human lenses were randomly chosen from the eyes got each time. They were taken from about 30-month-old cows or 60- to 80-year-old humans. Each experiment was repeated three times.

3.3.2 Lens capsule cleaning

The bovine and human lenses were dissected and the capsules with epithelial cells were pinned down on the Sylgard as before (2.3.2). In order to label the inner surface of the capsule, the epithelial cells needed to be removed first. Three methods were tried to remove the cells while protect the capsule structure. (1) Sodium dodecyl sulphate (SDS). SDS is a highly effective anionic surfactant, so 2% (v/v) SDS was chosen here to lyse and remove the epithelial cells. (2) Tween 20-Tris-buffered saline (TTBS). As Tween 20 is also a detergent, TTBS including 0.1% (v/v) Tween 20 is used here to remove the cells. (3) Deionised water. Deionised water has no ions. If the cells are bathed in it, water molecules will continue to diffuse into the cell by osmosis. Finally the cells swell and rupture. In this way, the epithelial cells on the capsule could also be removed. Three lens capsules with epithelial cells were respectively washed with 2% (v/v) SDS, TTBS and deionised water for 1 hour and then fixed in 2% (v/v) glutaraldehyde (Agar Scientific Ltd, England) in 200 mM sodium cacodylate (pH 7.4) (Agar Scientific Ltd, England) for 20 minutes. One capsule was fixed in glutaraldehyde immediately after dissection as the control. The four capsules were processed for SEM. Results showed that the epithelial cells were still attached to the capsule in the control sample without any kinds of washing (Figure 3.1). SDS and TTBS altered the surface meshwork of the capsule and caused many big or small holes. The architecture was still compacted and all the cells were removed in the capsule washed with deionised water. These results indicate that deionised water is good to remove the epithelial cells and also protect the capsule structure. Therefore, all the capsules in the following study were washed with deionised water for one hour.

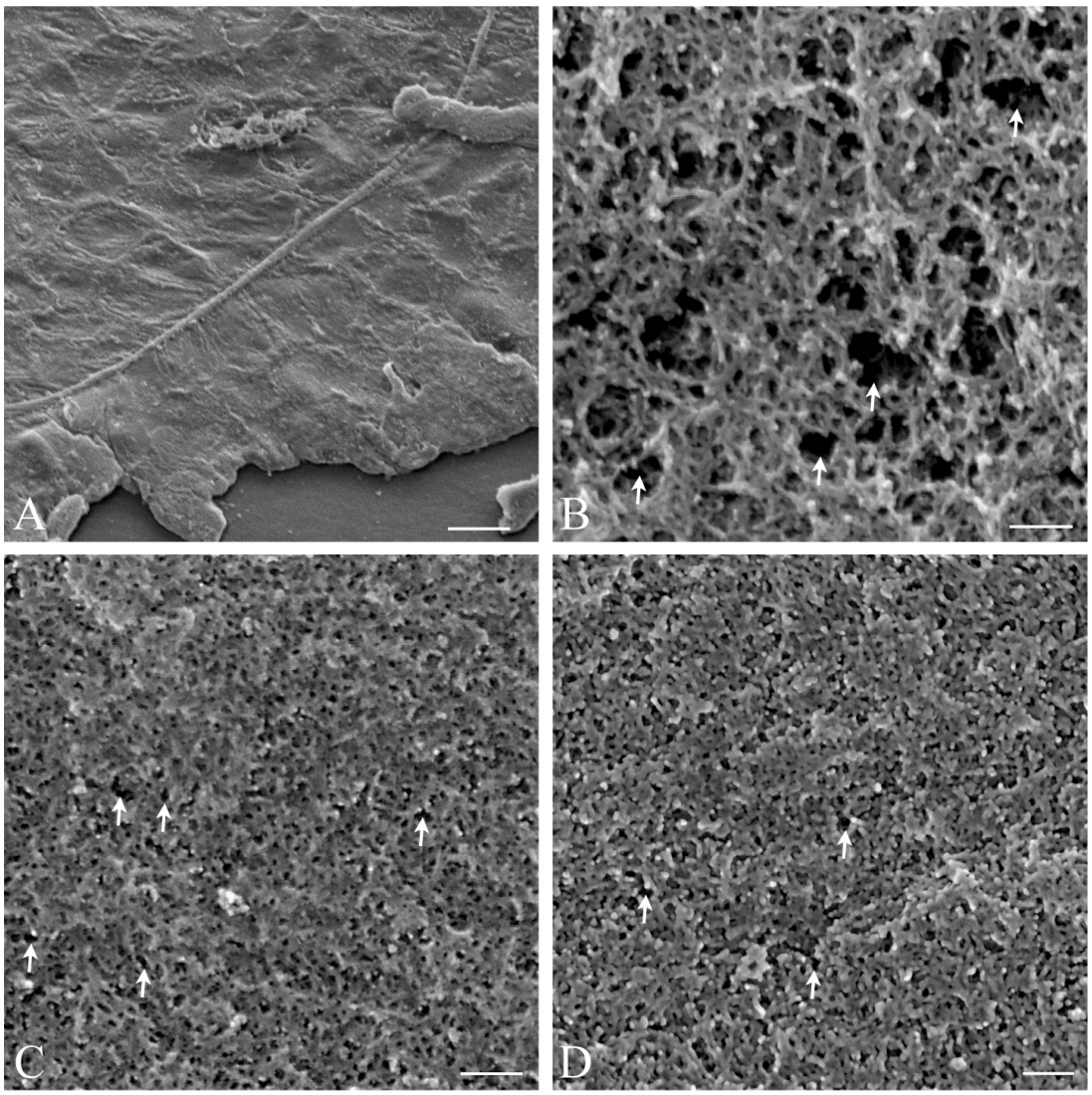

Figure 3.1. The structural changes in the inner surface of the bovine lens capsule with different kinds of cleaning.

A. The capsule without any kinds of cleaning. The single layer of epithelial cells attach to the lens capsule in some region, especially in the area near the equator, after removing the fibre mass.

B. The lens capsule washed in 2% (v/v) SDS for one hour. All the epithelial cells are removed, but many holes in different sizes (arrows) are present in the meshwork structure of the capsule.

C. The capsule washed in TTBS for one hour. Although the epithelial cells are all cleaned, many small holes (arrows) are still observed in the surface of the capsule meshwork.

D. The capsule washed in deionised water for one hour. All the epithelial cells were removed. The lens capsule meshwork is compact and only some small holes (arrows) scatter in the surface.
A: scale bar=10 μm; B-D: scale bars=100 nm.

3.3.3 Lens capsule fixing

Glutaraldehyde is a standard fixative for SEM. It is a cross-linker of amine groups and is gently reactive with the structure. Furthermore, it provides the needed cross-links to fix the samples but it does not cross-link excessively, so that the structure still retains its natural shape. Also its interaction with proteins is faster than PFA. However, one disadvantage of glutaraldehyde fixation is that glutaraldehyde can easily cause non-specific binding of proteinaceous reagents. In the present study, the primary antibodies were used to bind the epitopes of FGF-2, perlecan and collagen IV in the capsule. If glutaraldehyde had been used to fix the capsules, it would probably result in some non-specific binding with the antibodies and affect the results.

PFA is a common fixative used in immunofluorescence and histochemistry. It is the insoluble polymer of formaldehyde and becomes formaldehyde monomer when dissolved in buffer. Formaldehyde is a quite strong cross-linking fixative and can cause obvious distortion of cellular or tissue structures at high levels of magnification used in SEM.

In the present study, in order to decrease the non-specific binding and protect the natural capsule structure, the lens capsules were fixed in 4% (w/v) PFA for 20 minutes and then processed with immunogold labelling. Finally they were post-fixed in 2% (v/v) glutaraldehyde in 200 mM sodium cacodylate (pH 7.4) for 20 minutes. A control capsule was fixed in 2% (v/v) glutaraldehyde in 200 mM sodium cacodylate (pH 7.4) for 20 minutes. The capsules in the two kinds of fixing were observed by a scanning electron microscope. Results showed that the surface architecture of the lens capsules was similar (Figure 3.2). Therefore, all the lens capsules used for immunogold labelling were first fixed in PFA and later post-fixed in glutaraldehyde. The other bovine or human capsules used for the capsule structure study were fixed in glutaraldehyde directly in order to obtain the best structure under SEM.

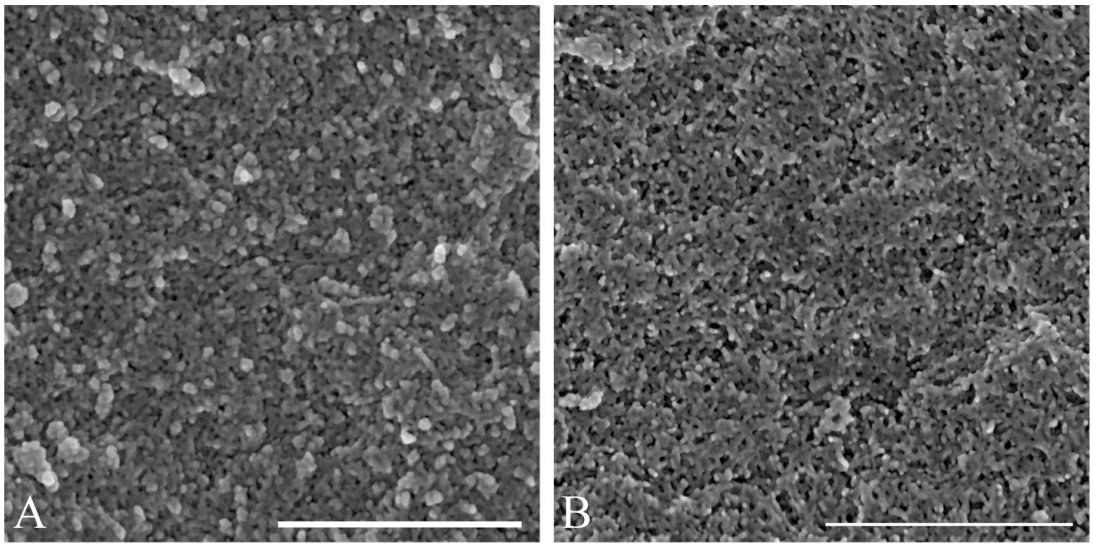

Figure 3.2. The SEM images of the inner surface of the bovine lens capsule fixed with glutaraldehyde and PFA.

A. The inner surface structure at the centre of the anterior lens capsule with glutaraldehyde fixing. The bovine lens capsule was fixed in 2% (v/v) glutaraldehyde for 20 minutes after cleaning the epithelial cells. It then underwent the procedure of immunogold labelling and was prepared for SEM. The constituents of the lens capsule interact into a compact and uniform meshwork in the inner surface. No obvious holes are observed.

B. The inner surface structure at the centre of the anterior lens capsule with PFA fixing. The bovine lens capsule was fixed with 4% (v/v) PFA for 20 minutes once the epithelial cells were removed. After the immunogold labelling process, it was post-fixed in 2% (v/v) glutaraldehyde and prepared for SEM. The uniform meshwork is still present but becomes slightly loose.
A, B: scale bars=500 nm.

3.3.4 Immunogold labelling

After PFA fixing, the lens capsules were washed three times with PBS for 15 minutes and blocked in 10% (v/v) normal goat serum for 20 minutes. Then they were incubated with the primary anti-FGF-2 (Calbiochem, USA; diluted 1:3 in PBS), perlecan (Chemicon International, Inc., USA; diluted 1:4 in PBS) and collagen IV (Abcam, UK; diluted 1:30 in PBS) for two hours at room temperature. For the negative control, the samples were just incubated with PBS instead of the primary antibodies. After three rinses in PBS, all the samples were then incubated with the secondary goat anti-rabbit IgG conjugated to 10 nm gold or goat anti-mouse IgG conjugated to 10 nm gold (both from BBInternational, Cardiff, UK; diluted 1:10 in PBS). The samples were washed three times in PBS and post-fixed in 2% (v/v) glutaraldehyde in 200 mM sodium cacodylate (pH 7.4) for 20 minutes before the following specimen preparation.

3.3.5 SEM

3.3.5.1 Specimen preparation for SEM

3.3.5.1.1 Specimen post-fixation and dehydration

The capsules were rinsed in 200 mM sodium cacodylate (pH7.4) for 5 minutes after removing glutaraldehyde. They were then post-fixed in 1% (v/v) osmium tetroxide (Agar Scientific Ltd, England) in 200 mM sodium cacodylate (pH7.4) for 20 minutes, followed by three washings in deionised water for 15 minutes. Finally, the samples were dehydrated through an ethanol series (50%, 75%, 95% and 100%, 5 minutes for each) and put into a holder for critical point drying.

3.3.5.1.2 Specimen drying

Critical point drying is a technique used to prepare naturally hydrated specimens for examination under high vacuum conditions in SEM. Such specimens can suffer damage because of the surface tension of the evaporating water during normal drying. Critical point drying avoids this problem by placing the specimen in an environment where the fluid within the specimen can pass from the liquid phase to gas phase with

zero surface tension (Bozzola *et al.*, 1999).

After the samples were transferred into a holder, some 100% ethanol was added into the chamber. Then the holder with specimens was soaked in ethanol in the Critical Point Dryer**.** The chamber was pre-cooled to 10°C and filled with CO_2. The ethanol was continuously vented with the help of CO_2. After all the ethanol was vented, the chamber was heated to 40°C, which was just above the CO_2 critical temperature of 31°C. The subsequent critical pressure was achieved and CO_2 was vented slowly through a needle valve to avoid specimen distortion. After the drying process, the specimens were gently taken out and attached to silicon chips (Si-Mat silicon materials, Germany) by a double-sided adhesive tape (Agar Scientific Ltd, England).

3.3.5.1.3 Specimen coating for conductivity

For conventional imaging in the SEM, the surface of the specimen must be electrically conductive and also grounded to prevent the accumulation of electrostatic charge at the specimen surface. This is done by coating with an ultrathin coating of electrically-conducting material such as platinum or chromium. All the specimens were put in a Cressington 308 coater and pumped for at least 2 hours. Then they were coated with 7 nm of chromium. After the coating process, the samples were kept in vacuum first or observed by a scanning electron microscope immediately.

3.3.5.1.4 Specimen imaging

Specimens were viewed in a Hitachi SU-70 FEG SEM (Hitachi High-Technologies Europe GmbH, Germany) or an FEI Helios Nanolab 600 SEM (FEI company, USA). The images of the lens capsule structure were taken in a secondary electron imaging mode, in which secondary electrons were efficiently collected through the capsules to provide images with an extremely high spatial resolution. For the immunogold-labelled specimens, a backscattered electron-imaging mode was chosen to take the images with gold particles. An E×B filter was used to block high-energy secondary electron signals from the lens capsule structure in order to just show the gold particles. Equal sized images were taken at the centre of the anterior, equator and posterior of the lens capsule (Figure 3.3). Three images were randomly captured

in each region. The gold particle number in each image was counted using ImageJ. The particle concentration (gold number/μm^2) was calculated. Student's t-Test was used to analyse the difference of gold particle concentration in different regions of the capsule. A *p* value below 0.05 was considered to have statistically significant difference.

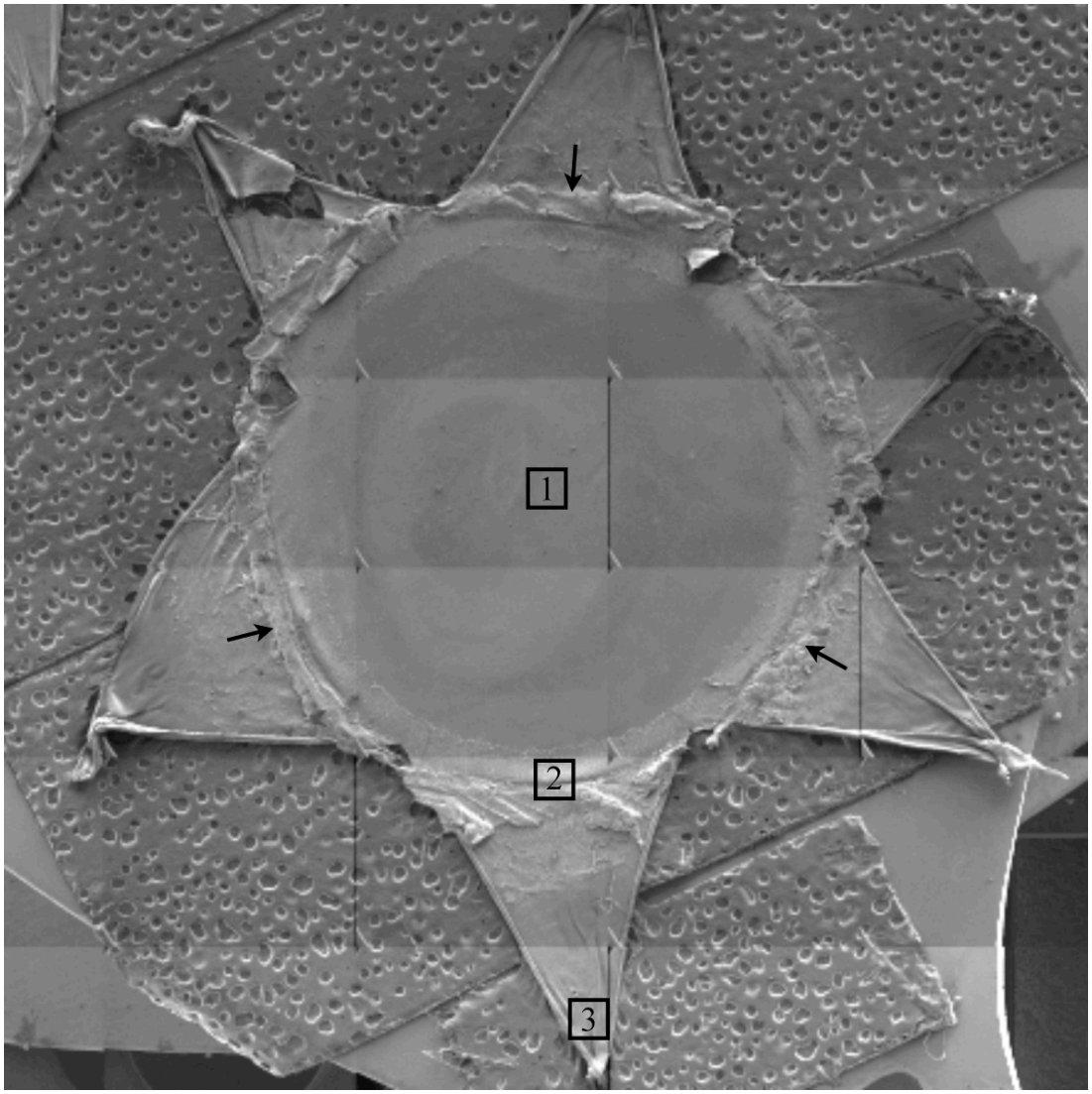

Figure 3.3. A montage of the lens capsule prepared for SEM.

The posterior lens capsule was cut into six pieces and pinned down. The capsule was then prepared for the study with SEM. Images were taken at the centre of the anterior (square 1), at the equator (square 2) and at the centre of the posterior (square 3) for the following studies from the lens capsule. As this sample is used to study the zonule fibres in the outer surface of the capsule, the zonule fibres can be seen to attach to the equatorial region of the capsule (arrows).

3.4 Results

3.4.1 FGF-2 and perlecan had a gradient distribution on the inner surface of the bovine lens capsule

Collagen IV is a very important scaffolding protein of the lens capsule. Due to its abundance in the capsule, it was used as a positive control here to confirm the success of FGF-2 and perlecan immunogold labelling. Results showed that many gold particles were detected across the inner surfaces of the bovine lens capsules (Figure 3.4A-C). They accumulated into small groups or scattered individually. More gold particles were observed in the anterior and at the equator than in the posterior. The quantification results showed that the gold particle concentration was 287±29/μm^2 at the centre of anterior, 263±52/μm^2 at the equator and 140±30/μm^2 at the centre of the posterior. Student's t-Test showed the comparison in the anterior-posterior and equator-posterior had statistical significance (p=0.003 and p=0.02) (Figure 3.4G). This indicates that the collagen IV epitopes are significantly more abundant on the anterior and equatorial surface than on the posterior surface. The collagen IV labelling showed that the immunogold labelling was successful and could be used to study the distribution FGF-2 and perlecan on the inner surface of the capsule.

The capsules with the secondary antibodies but not the primary antibodies were used as the negative controls. Results showed that the gold particle number was very low in these capsules (Figure 3.4D-F, Figure 3.5G-I), compared with the capsules with the primary antibodies. These particles were probably trapped in the meshwork of the capsule and not washed way, or they were non-specific binding. This result means that the gold particles in the FGF-2 and perlecan labelling really bind to their epitopes.

The gold particles of FGF-2 and perlecan labelling scattered on the inner surface of the bovine lens capsule. Compared with collagen IV, both of their gold particle concentrations were much lower (Figure 3.5A-F). It was 4±2/μm^2 at the centre of the anterior, 8±3/μm^2 at the equator and 4±2 /μm^2 at the centre of the posterior. Statistical difference was present in the comparison of anterior-equator (p=0.01) and posterior-equator (p=0.01). Although the gold particle numbers were low in the FGF-2 and perlecan labelling, the statistical results still indicate that more FGF-2 and perlecan are present on the surface of the equatorial capsule.

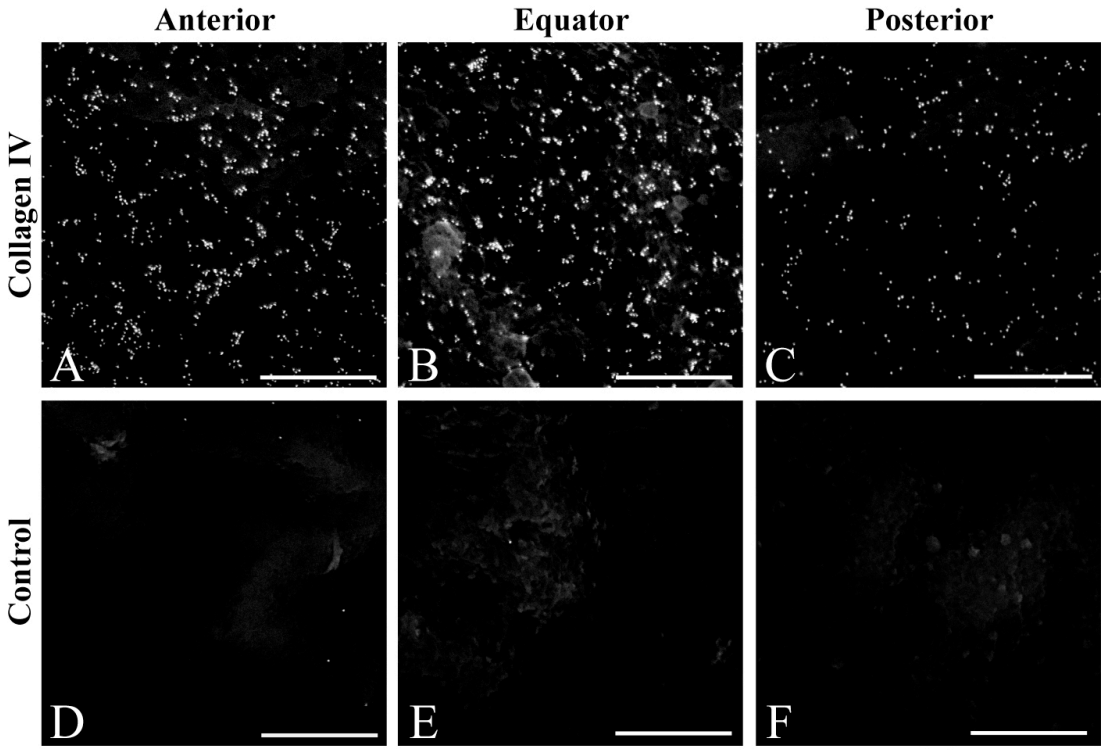
Anterior
Equator
Posterior
Collagen IV
Control
A
B
C
D
E
F

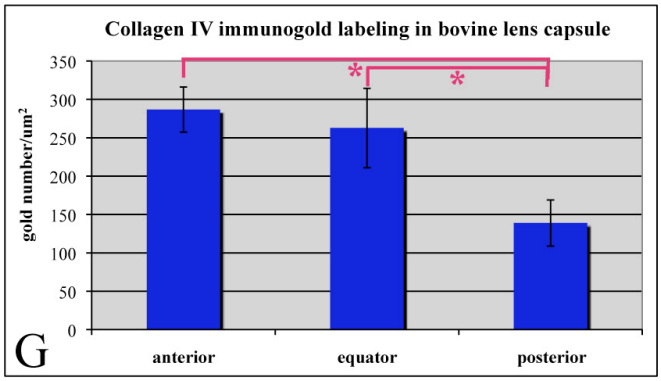
Collagen IV immunogold labeling in bovine lens capsule
gold number/um²
350
300
250
200
150
100
50
0
*
*
anterior
equator
posterior
G

Figure 3.4. The collagen IV distribution in the inner surface of the bovine lens capsule.

The inner surface of the bovine lens capsules were labelled with collagen IV and then probed with secondary antibody conjugated to 10 nm gold, after the epithelial cells were removed. The control capsules were just incubated with the secondary antibody. Equal sized images were taken at the centre of the anterior, at the equator, and at the centre of the posterior. At each position three images were taken. The gold particle number in each image was counted and the gold particle concentration was calculated. The experiments were repeated three times and each time two capsules were included.

A-C: The SEM images of the immunogold labelling of collagen IV. The gold particles scatter on the inner surface of the capsule. More gold particles are present at the anterior centre and the equator and less are at the posterior centre.

D-F: The SEM images of the control. A very low number of gold particles, no more than ten, are detected in the three positions.

G: The gold particle concentration of collagen IV in different positions of the capsule. The quantification results show that the collagen IV epitopes are more abundant in the anterior and equator than in the posterior area. Statistically significant differences (*) of Student's t-Test are present in the comparison of anterior-posterior (between the centre of the anterior and posterior) and equator-posterior (between the equator and the centre of the posterior).
A-F: scale bars=500 nm.

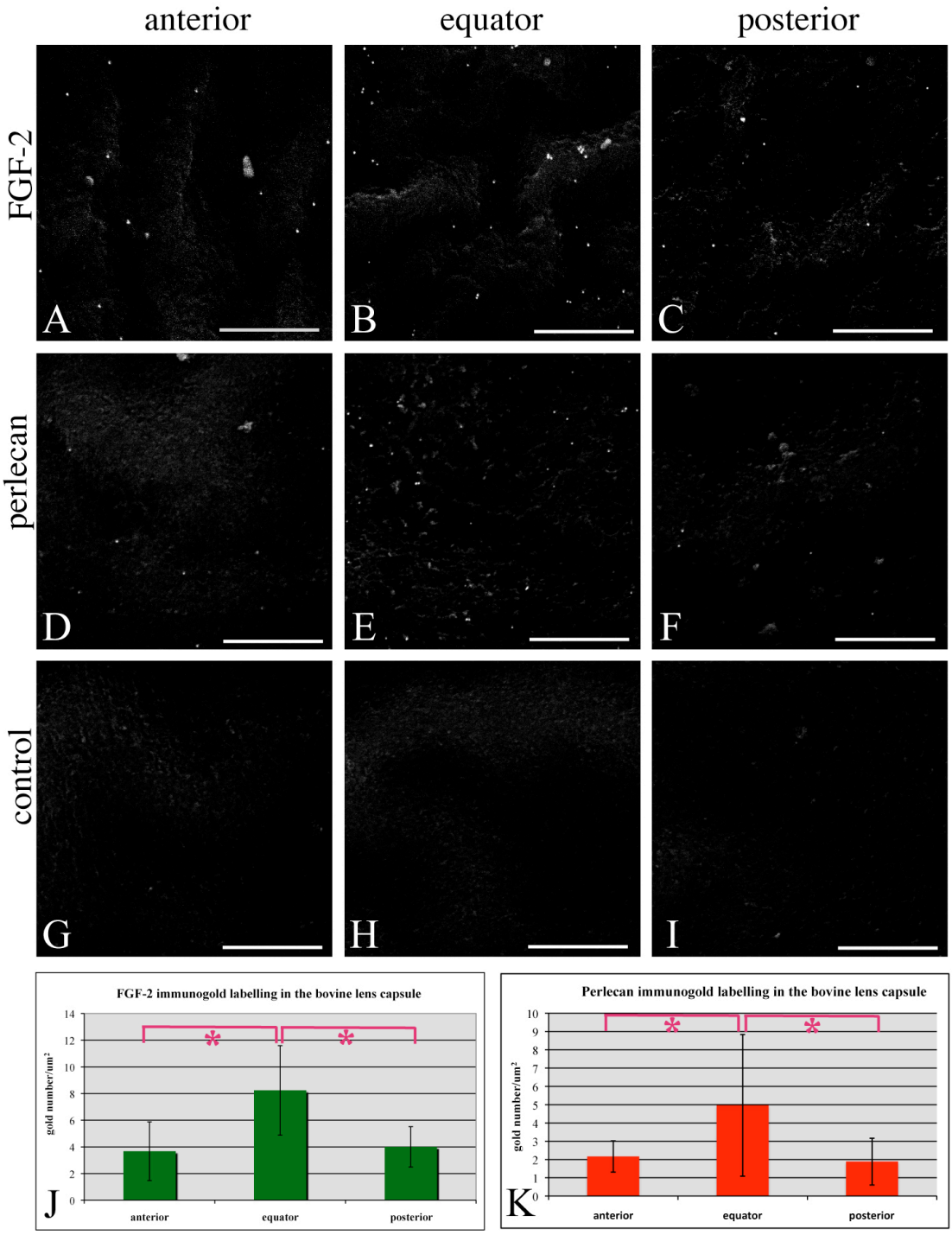
anterior
equator
posterior
FGF-2
perlecan
control
A
B
C
D
E
F
G
H
I
FGF-2 immunogold labelling in the bovine lens capsule
gold number/um²
anterior
equator
posterior
J
Perlecan immunogold labelling in the bovine lens capsule
gold number/um²
anterior
equator
posterior
K

Figure 3.5. The distribution of matrix-bounded FGF-2 and perlecan in the inner surface of the bovine lens capsule.

The epithelial cells were removed from the inner surfaces of the bovine lens capsules. The capsules were incubated with primary anti-FGF-2 and anti-perlecan antibodies and secondary conjugated to 10 nm gold. The controls were incubated with just the secondary antibody. In each position (centre of the anterior, equator and posterior) at least three SEM images were taken and the experiment was repeated three times. The gold particle numbers were counted and the particle concentration in each position was calculated.

A-C: The SEM images of the immunogold labelling of FGF-2. Few gold particles are found in the inner surface of the bovine lens capsule labelled with FGF-2. There are more gold particles at the equator than at the centre of the anterior and posterior lens capsule.

D-F: The SEM images of the immunogold labelling of perlecan. The perlecan labelling is similar to the FGF-2 labelling. The overall gold particle numbers are low at the centre of the anterior, equator and posterior capsule. More particles are present at the equator.

G-I: The SEM images of the control lens capsule. Only one or two particles are seen in each image of the control.

J-K: The gold particle concentrations of FGF-2 and perlecan labelling in the inner surface of the bovine lens capsule. The quantification results show that both FGF-2 (J) and perlecan (K) epitopes are significantly more abundant at the equatorial region than either in the anterior or in the posterior regions of the lens capsule. The statistical differences (*) of Student's t-Test are present in the comparison of equator-anterior and equator-posterior in FGF-2 and perlecan.
A-I: Scale bars=500 nm.

3.4.2 The morphology was different on the two surfaces of the lens capsule

The anterior bovine lens capsule was cut into halves to observe the morphology of the cross-sectional sides. The SEM images show that the dry central anterior capsule was about 20 μm thick and consisted of many layers of basement membrane (Figure 3.6). These layers of basement membrane compacted together and formed a dense capsule architecture.

The inner and outer surface morphology of the bovine lens capsule were different (Figure 3.7). This difference was also detected in the two sides of the human lens capsule (Figure 3.8). The inner surface morphology in the bovine and human capsules was similar in SEM. The scaffolding compacted into a dense network, and this morphology was relatively homogenous throughout the capsule. The network on the outer surface of the capsule was a bit loose. The pore size of the scaffolding is greater in this surface than in the inner surface. The composition of the capsule could be seen more clearly on the outer surface. The morphology of the outer surface in the bovine and human capsules was similar.

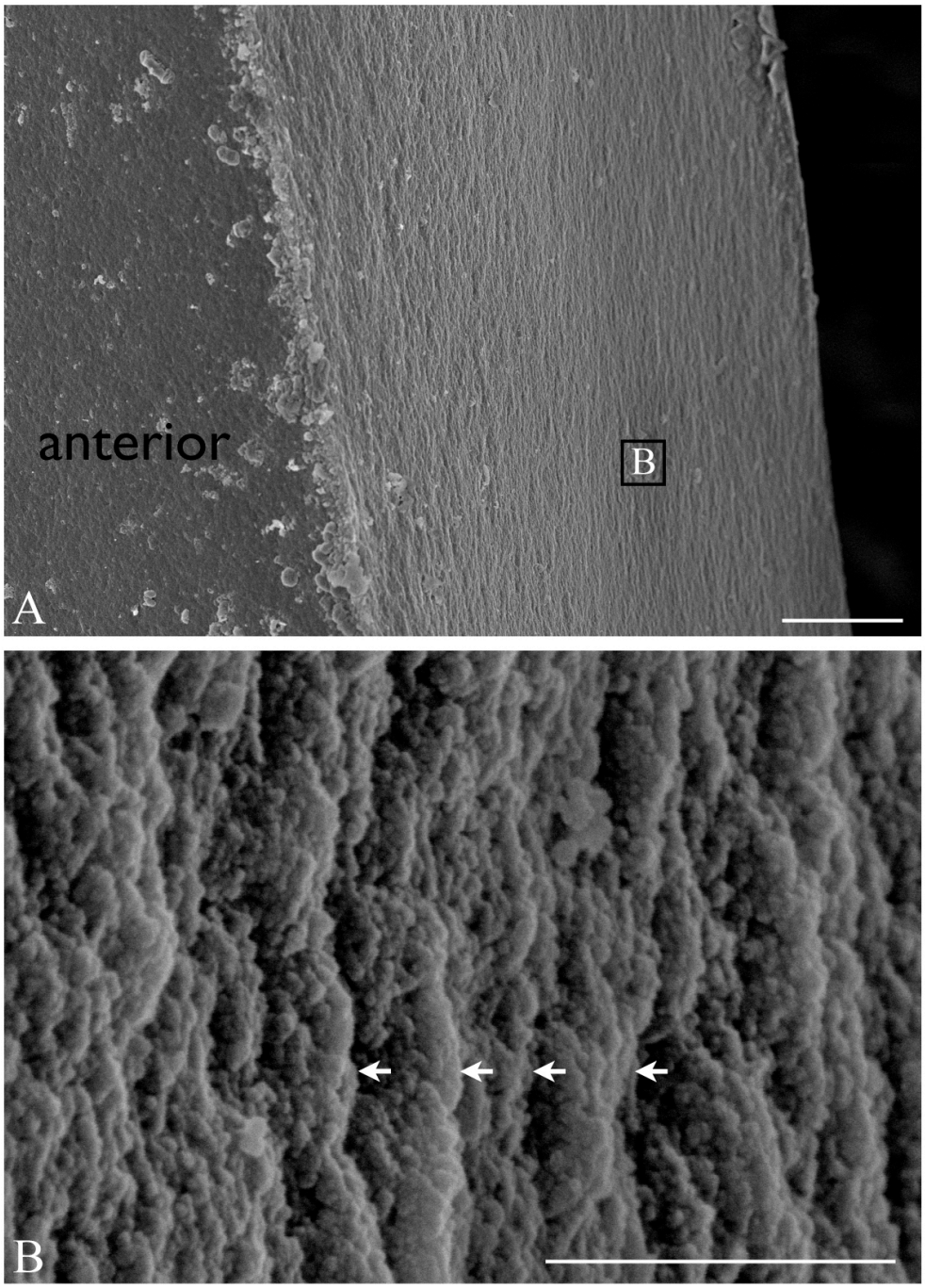

Figure 3.6. The bovine lens capsule morphology in the cross-sectional side.

The bovine lens capsule was cut into equal halves from the centre of the anterior side and the cross-section was observed by SEM.

A: The centre of the anterior lens capsule is about 20 μm thick and where the layer structure of the capsule can be seen.

B. At higher magnification, the composition of the layers (arrows) can be discerned clearly. The basement membrane is tightly compacted.
A: scale bar=4 μm. B: scale bar=400 nm.

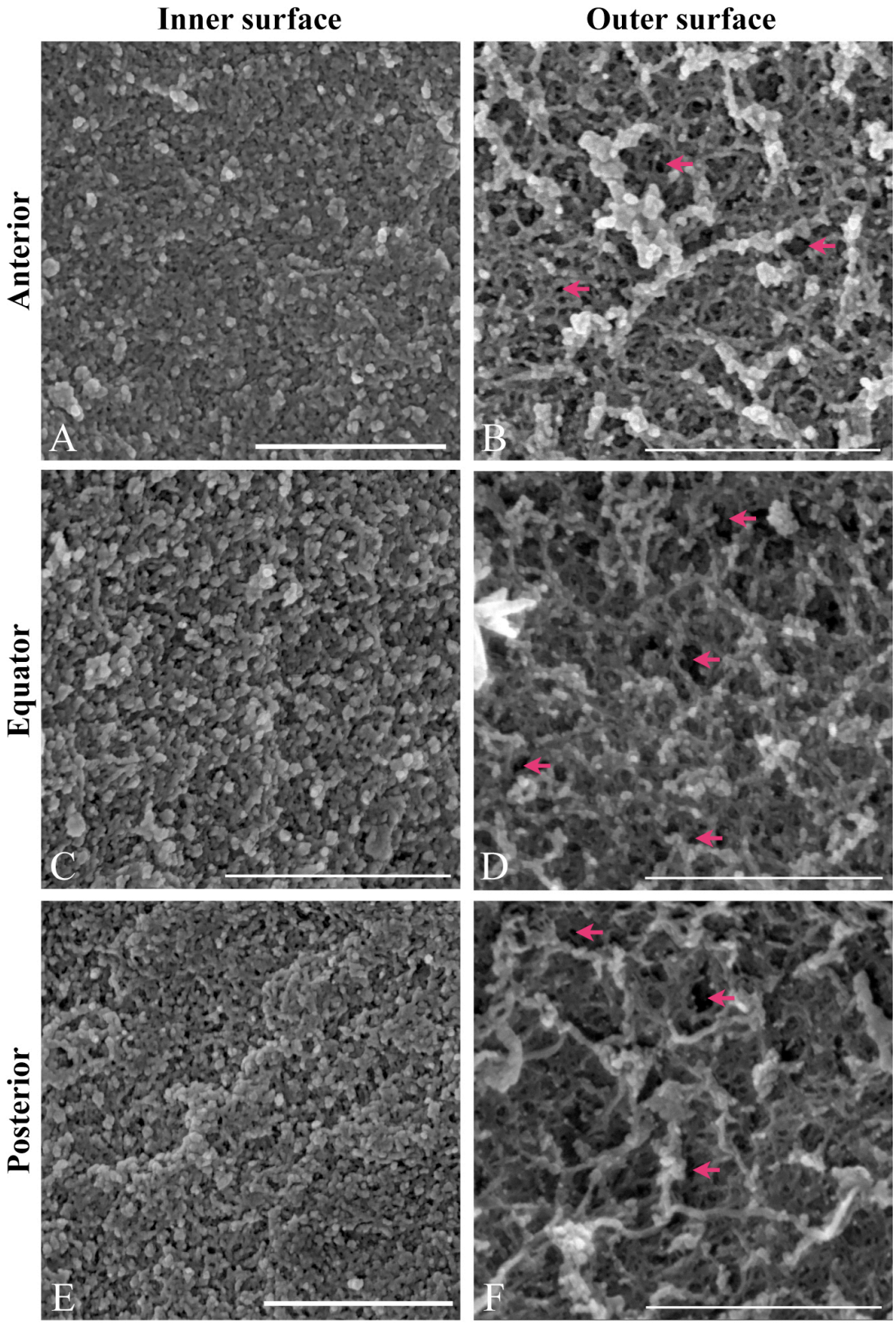
Inner surface
Outer surface
Anterior
Equator
Posterior
A
B
C
D
E
F

Figure 3.7. The SEM images of the inner and outer surfaces of the bovine lens capsule.

The epithelial cells were removed from the inner surface of the capsules. The capsules were fixed in glutaradehyde and then processed for SEM.

A, C, and E: the surface architecture is similar at the centre of the anterior (A), equator (C) and posterior (E) of the inner surface. The scaffolding is compacted.

B, D, and F: Different constituents of the lens capsule interwove into a meshwork in the outer surface, which is much looser than that in the inner surface. Many different sizes of holes can be seen (arrows).
A-F: scale bars=500 nm.

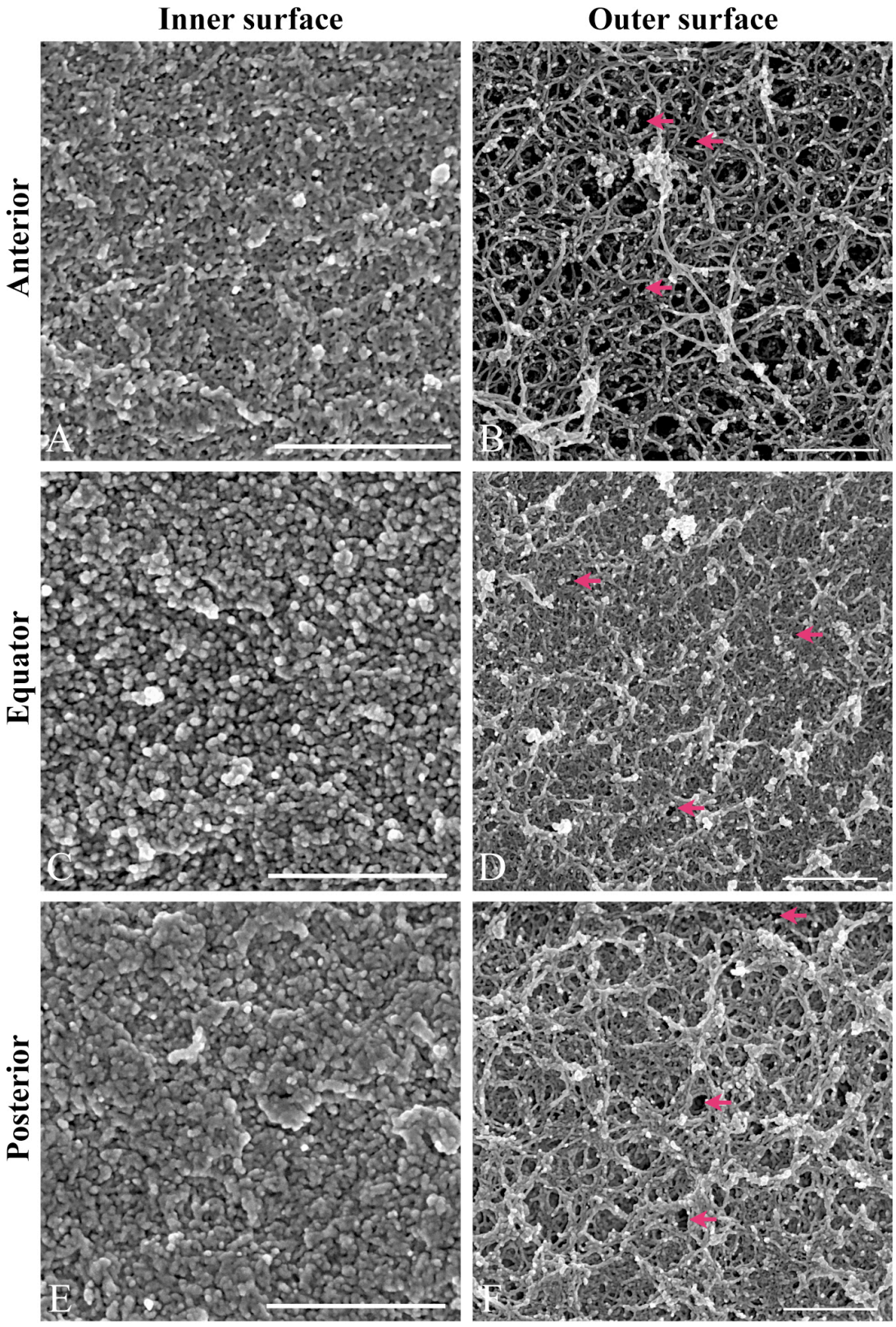
Inner surface
Outer surface
Anterior
Equator
Posterior
A
B
C
D
E
F

Figure 3.8. The SEM images of the inner and outer surfaces of the human lens capsule.

The epithelial cells were removed from the inner surface of the capsules. The capsules were fixed in glutaraldehyde and processed for SEM.

A, C, E: the surface architecture is similar at the centre of the anterior (A), equator (C) and posterior (E) of the inner surface. The scaffolding is compacted and uniform in all of the regions.

B, D, F: The pore size of the scaffolding in the outer surface is greater than in the inner surface. The structure is relatively homogenous throughout the outer surface as for the inner surface, apart from the fact that the scaffolding sub-structure can be seen more clearly in the anterior part.
A, C, E: scale bars=500 nm. B, D, F: scale bars=1 μm.

3.5 Discussion

FGF-2 is synthesised in the ciliary body and retina and is released into the aqueous and vitreous humours (Chamberlain and McAvoy, 1997). It then diffuses into the lens capsule and binds to perlecan. It is released by MMPs and regulates lens epithelial cell proliferation and differentiation. Previous studies have shown that the vitreous humour and high concentration of FGF-2 induce cell differentiation, while the aqueous humour and low concentration of FGF-2 lead to cell proliferation (Iyengar *et al.*, 2006; Lovicu *et al.*, 1995). These results indicate that a FGF-2 gradient may be present in the eye. The result of this study showed that a higher concentration of FGF-2 was located at the equator region of the lens capsule, where lens epithelial cell proliferation and the preparation for differentiation were observed in chapter 2. A lower level of FGF-2 was still present at the centre of the anterior and posterior capsule in order to maintain cell survival. These results indicate that the hypothesis about the FGF-2 gradient in the lens capsule is right. Interestingly, perlecan, which is an important component of the lens capsule and binds to FGF-2, also displays a similar distribution to FGF-2 in the inner surface of the lens capsule. Therefore, does the FGF-2 gradient on the inner surface of the capsule determined by this perlecan gradient or by FGF-production by the ciliary body that is very close to the equator? It is difficult to answer this question now. The perlecan distribution indicates that it probably has a regionally different distribution in the lens capsule. A similar phenomenon was also observed in collagen IV labelling. The concentration of gold particles for collagen IV was higher in the anterior and equatorial lens capsule than in the posterior capsule. In addition, the concentrations of gold particles for FGF-2, perlecan and collagen IV were quite low. This is probably because not all of their epitopes are expose to the inner surface of the capsule and bound by the antibodies. Furthermore, some FGF-2 at the inner surface binds to its receptors in the lens epithelial cells. When the cells are removed from the capsule, some FGF-2 is also lost. However, the absence of gold particles in the control capsules proves that the gold particles in FGF-2, perlecan and collgen IV labelling really bind to their target epitopes. Collagen IV is much richer than perlecan in the lens capsule (Danysh and Duncan, 2009). That is why the concentration of gold particles for collagen IV is greater than that for perlecan. This result is consistent with previous collagen IV immunogold labelling study (Schulz *et al.*, 1997).

The lens capsule is an interacting network mainly made of laminin, collagen IV, perlecan and entactin/nidogen. The results in this study showed that the meshwork in the inner and outer surfaces was different. It was compact on the inner surface but loose on the outer surface. This occurred in both the bovine and human lens capsules. The difference is possibly set to suit the function of the lens capsule in the two sides. Both sides act as a molecular sieve modulating the transport of solutes into or out of the capsule (Danysh *et al.*, 2010), but the inner surface also provides the anchor points for the epithelial cells in the anterior and fibre cells in the posterior. These lens cells are able to bind laminin, collagen IV and perlecan within the lens capsule by their membrane-bound integrins (Walker and Menko, 2009). These cell-capsule interactions are necessary for lens cell proliferation, migration and differentiation (Menko *et al.*, 1998; Oharazawa *et al.*, 1999). The outer surface of the lens capsule is just bathed in the liquid aqueous humour in the anterior side and in the jelly-like vitreous humour in the posterior side. The loose meshwork in the outer side makes it easy for the zonule fibres to insert themselves into the capsule. In addition, the outer and inner surfaces are formed at different time by different cells. During lens development, the lens capsule is first observed as cytoplasmic processes associated with network forming fibrils between the head ectoderm and the optic vesicle (Hunt, 1961; McAvoy, 1981). This network becomes thicker later because of matrix molecular secretion by the pit cells after the lens pit is formed (Csato, 1989). The lens vesicle is then formed when this pinches off from the surface ectoderm. The two edges of the network also fuse into an enclosed basement membrane to complete the lens vesicle (Lovicu and McAvoy, 2005; Parmigiani and McAvoy, 1989). The cells on the posterior side of the lens vesicle elongate into the primary fibre cells, while the cells on the anterior side develop into the epithelial cells. The epithelial cells then proliferate and differentiate into secondary fibre cells. Both lens epithelial cells and fibre cells then continuously synthesize and secrete basement membrane molecules to support the growth of lens capsule throughout the life (Haddad and Bennett, 1988; Parmigiani and McAvoy, 1984; Young and Ocumpaugh, 1966). The newly-formed layer of extracellular matrix deposits on the old one. This is why layers of lamellae were observed in the cross-sectional side of the capsule in the present study. Therefore, the outer surface of the lens capsule is formed by this cytoplasmic process in the early stage of lens development while the inner surface is synthesised by the lens cells.

3.6 Summary

The results in this chapter showed that FGF-2 and perlecan distributions had a gradient on the inner surface of the bovine lens capsule, higher at the equator and lower in the anterior and posterior. The lens capsule structure was compact in the inner side but loose in the outer side. The FGF-2 gradient in the inner side of the lens capsule is consistent with its function in lens epithelial cell proliferation and preparation fibre cell differentiation, which is studied in chapter 2. FGF-2 on the inner surface of the lens capsule binds to their receptors on the epithelial cell membranes and activates downstream MAPK and PI3-K signalling pathways. In chapter 4, the activation of MAPK and PI3-K signalling proteins in different zones of the bovine lens epithelium was studied. The primary bovine lens epithelial cells were treated with a low proliferating concentration of FGF-2 in order to detect its ability in inducing epithelial cell proliferation.

4 Regulation of lens epithelial cell proliferation by MAPK signalling pathways

4.1 Introduction

The lens has a distinct architecture, with a single layer of epithelial cells covering the anterior side and the elongated fibre cells making up the bulk of the lens. The lens epithelial cells proliferate in the GZ and prepare for fibre cell differentiation in the TZ. Both the GZ and the TZ are located at the lens equator (Figure 1.2). The lens capsule separates the lens cells from the surrounding ocular media, the aqueous humour and the vitreous humour, which contain many growth factors such as FGFs, IGF, PDGF, EGF and TGFβ synthesised and secreted by the ciliary body and retina (Lovicu and McAvoy, 2005). These growth factors pass through the lens capsule and bind to the extracellular domain of their transmembrane receptors to phosphorylate the intracellular RTK. Activation of RTK in turn phosphorylates GTPases such as Ras, which interact with several downstream effect proteins and turn on signalling pathways (Xie *et al.*, 2006).

The lens epithelial cell proliferation and fibre cell differentiation induced by aqueous and vitreous humours are mainly dependent on MAPK/ERK1/2 and PI3-K/AKT signalling pathways (Iyengar *et al.*, 2006; Wang *et al.*, 2010). Typical MAPK cascades are made of three tiers of effectors, involving MAPKKKs, MAPKKs and MAPKs. Once GTPases are activated, they activate MAPKKKs. MAPKKKs subsequently phosphorylate MAPKKs, which in turn phosphorylate MAPKs. ERK1/2 has been found to be the most important MAPK involved in lens epithelial cell proliferation and differentiation, and it can be activated by aqueous humour, vitreous humour and FGF-2 (Iyengar *et al.*, 2006; Iyengar *et al.*, 2007; Lovicu and McAvoy, 2001; Wang *et al.*, 2010; Zatechka and Lou, 2002). It regulates lens epithelial cell proliferation and fibre cell differentiation by the duration of its activation. In the rat lens epithelial explants, aqueous humour or a low proliferating dose of FGF-2 activates ERK1/2 for a short period (about six hours) and can only induce cell proliferation, while vitreous humour or a high fibre-differentiating dose of FGF-2 causes a sustained phosphorylation of ERK1/2 (up to 18 hours) and results in cell differentiation (Iyengar *et al.*, 2007). Unactivated ERK1/2 is usually localised in the

cytoplasm of resting cells. After activation, most of the phosphorylated ERK1/2 translocate to the nucleus either by a passive diffusion or with the help of a nuclear translocating signal, which binds to importin7 to escort ERK1/2 into the nucleus via nuclear pore complexes (Chuderland *et al.*, 2008; Zehorai *et al.*, 2010). In the nucleus, activated ERK1/2 phosphorylates several important transcriptional regulators such as Elk-1, cAMP-responsive element binding protein (CREB), and histone 3 (Sharrocks, 2001). This results in rapid transcriptional activation of immediate early genes, including transcription factors like *c-Fos* that control the cell cycle and/or cell differentiation (Murphy and Blenis, 2006). In addition, in the transgenic mice that constitutively express MEK1, the direct upstream kinase of ERK1/2, a high level of ERK1/2 is detected in the lens epithelial cells and the mice develop macrophthalmia (Gong *et al.*, 2001). The occurrence of macrophthalmia might be caused by consistent ERK1/2-induced cell proliferation and differentiation. It is also found that homozygous deletion of Nf1, the Ras GTPase gene underlying human neurofibromatosis type 1 syndrome, causes the significant decrease of ERK phosphorylation during the lens vesicle stage and failure of lens formation at the end in mice (Carbe and Zhang, 2011). These studies indicate that ERK1/2 plays an important role in lens development.

As well as ERK1/2, MAPKs also have other important members, JNK and p38. JNK and p38 are not in as significant proportions as ERK in the cells. They are strongly activated by cytokines, UV irradiation and growth factor deprivation and less activated by serum and growth factors (Krishna and Narang, 2008). Like ERK1/2, the phosphorylated JNK and p38 relocalise from the cytoplasm to the nucleus to activate their downstream targets such as Pax6, p53 and c-Jun (Ben-Levy *et al.*, 1998; Mizukami *et al.*, 1997). JNK and p38 mainly regulate cell apoptosis, cell survival, cell inflammation and differentiation (Krishna and Narang, 2008).

PI3-K/AKT signalling pathway is another important signalling pathway in regulating cell proliferation and differentiation. With activation by growth factors such as IGF-1 and FGF-2, PI3-K promotes the conversion of membrane lipid phosphatidylinositol 4, 5-biphosphate (PIP2) into the secondary messenger phosphatidylinositol 3, 4, 5-triphosphate (PIP3). Increasing levels of PIP3 translocate AKT to the cell membrane and phosphorylate its two conserved residues, Thr308 and Ser473 (Brunet *et al.*, 2001). Activated AKT consequently phosphorylates its downstream substrates such as GSK3. GSK3 is a serine/threonine protein kinase and

consists of two isoforms, GSK3α and GSK3β. Phosphorylation of GSK3 causes cytoplasmic signalling molecule β-catenin to translocate to the nucleus. Once in the nucleus, β-catenin interacts with a number of transcription factors such as cyclin D1 and $p27^{kip}$ and induces gene expression (Osaki *et al.*, 2004). Previous studies have found that PI3-K/AKT signalling pathway plays a crucial role in regulating lens epithelial cell proliferation and differentiation (Iyengar *et al.*, 2006; Wang *et al.*, 2009b; Weber and Menko, 2006; Zatechka and Lou, 2002). In the rat lens epithelial explants, the PI3-K/AKT signalling pathway in the epithelial cells can be activated by the growth factors in the aqueous and vitreous humours. Blocking of this signalling pathway by its inhibitor results in the inhibition of rat lens cell proliferation and differentiation. Moreover, the activation of PI3-K signalling pathway by PDGF is found to enhance cell migration in the human lens epithelial explants (Xiong *et al.*, 2010). This is very important for the lens epithelial cells as the cells in the GZ migrate to the TZ to prepare for differentiation.

A cross-communication is also found between the MAPK/ERK1/2 and PI3-K/AKT signalling pathways. Inhibition of PI3-K/AKT signalling pathway induces the decrease of ERK1/2 phosphorylation, while inhibition of ERK1/2 does not change the phosphorylation of AKT (Iyengar *et al.*, 2006). It is proposed that AKT may act upstream of ERK1/2 signalling (Sato *et al.*, 2004). Raf is an upstream kinase required for the subsequent activation of ERK1/2. As the activation of Raf is severely decreased when PI3-K signalling pathway is blocked (Zatechka and Lou, 2002), it is probably the target of AKT in the upstream of ERK1/2 signalling pathway.

4.2 Aims

Based on the results in chapter 3 that a higher level of FGF-2 was present at the equator of the lens capsule, a hypothesis was made that this might induce more protein phosphorylation in the MAPK and PI3-K signalling pathways in the peripheral lens epithelium. This hypothesis was test in the central and peripheral parts of the bovine lens epithelium. Furthermore, the questions that how FGF-2 regulated lens epithelial cell proliferation by ERK1/2 and where phosphorylated ERK1/2 was located were also investigated.

4.3 Materials and methods

4.3.1 Protein extraction

In order to study the expression of MAPK and PI3-K signalling proteins in the CZ, the GZ and the TZ, the epithelial cells in these three zones were obtained from the bovine lenses. In chapter 2, the lengths of GZ and the TZ of the bovine lens epithelium were measured and respectively 1.3 mm and 0.2 mm. Because the TZ was very short and difficult to separate from the GZ, the GZ and TZ were put together in this study and the total length was 1.5 mm. The GZ is located at the anterior of the lens bow and the TZ lies at the posterior of the lens bow. Therefore, two cuts were made on each bovine lens (Figure 4.1). One was on the anterior lens capsule and 1.3 mm away from the lens bow. The other was on the posterior lens capsule and 0.2 mm away from the lens bow. In this way, the bovine lens epithelium was divided into two regions, the CZ and the GZ+TZ.

The lens capsules with the epithelial cells in each region were gently peeled off from the fibre mass and put into lysis buffer [10 mM Tris-HCl (pH 7.5), 0.15 M NaCl, 1% (w/v) Nonidet P-40 (NP-40), 1 mM ethylene diamine tetra acetate (EDTA), 1 mM Na_3VO_4 (Sigma, USA), 100 mM NaF (Sigma, USA), 1 mM $Na_4P_2O_7 \cdot 10H_2O$ (Sigma, USA) and Complete^{TM} proteinase inhibitor cocktail (Roche Diagnostics GmbH, Germany)] for 60 minutes on ice. The capsules were then removed. The protein extracts were homogenised by passing through a 25-gauge needle and centrifuged at 12,000 rpm at 4ºC for 10 minutes. The supernatant was transferred to another Eppendorf and boiled at 95ºC for 5 minutes. Protein concentration was determined by using bicinchoninic acid (BCA) protein assay kit (PerBio Science, UK). The proteins were diluted in 2 × loading buffer [10 mM Tris-HCl (pH 6.8), 40% (v/v) glycerol, 0.2 mM EDTA, 2% (w/v) SDS, 0.01 (w/v) bromophenol blue] in 1:1 ratio and stored at -20ºC.

In order to study the phosphorylation of MAPK and PI3-K signalling proteins stimulated by FGF-2 in the CZ and the GZ+TZ, the bovine lens epithelium whole-mounts were exposed to 20 ng/ml of FGF-2 (BioVision, USA) for 5 minutes or 20 minutes immediately after lens dissection. FGF-2 was added into Dulbecco's modified Eagle's medium (DMEM, Sigma, UK), supplemented with 2 mM L-glutamine, 100 U/ml penicillin and 100 μg/ml streptomycin (all from Sigma, UK), in advance. This concentration of FGF-2 was reported to induce lens epithelial cell

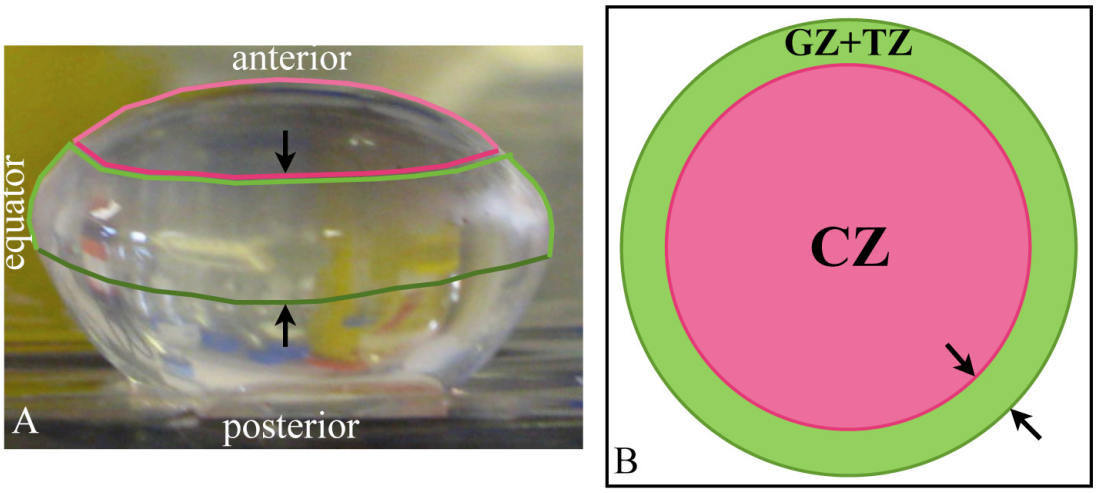

Figure 4.1. The pictures showing the cutting line between the CZ and the GZ+TZ zones of the bovine lens epithelium.

A: A bovine lens is put on the bench with the anterior side facing upwards. The epithelium is separated by cutting along the boundary of the CZ and the GZ, shown as the dark pink line (arrow). The GZ and TZ zones, which are located at the lens equator, are cut along the dark green line (arrow).

B: This diagram shows the cutting lines (arrows) and the two parts of the lens epithelium.

proliferation (Awasthi and Wagner, 2006). The levels of phosphorylated ERK1/2 and AKT were reported to increase at 5 minutes after the lens epithelial cells were exposed to FGF-2 (Iyengar *et al.*, 2006; Wang *et al.*, 2009b). Since many epithelial cells were observed to detach from the lens capsule 20 minutes later, the FGF-2 exposure was stopped at that time. The control whole-mounts were just cultured in DMEM without FGF-2 for 5 minutes. Then the CZ and the GZ+TZ were cut and proteins were extracted as described above.

As cells detached from the lens capsule when the bovine lens epithelium whole-mounts were cultured in DMEM, the epithelial cells were detached from the capsule by accutase (Sigma, UK) and cultured in flasks. The bovine lens epithelium whole-mounts were first pinned down on the Sylgard in a 6-well plate and incubated with 2 ml of accutase at 37ºC for 40 minutes. The detached cells with accutase were then collected and centrifuged at 1000 rpm for 5 minutes. The lens epithelial cells in the pellet (passage 0) were cultured in 75-cm^2 flasks in DMEM supplemented with 10% foetal calf serum (FCS). The cells used in this study were between passage 2 and passage 6. Confluent cells cultured on 10-cm Petri dish plates were exposed to 20 ng/ml of FGF-2, with or without the presence of U0126, for 5 minutes, 20 minutes, 1 hour, 6 hours, 12 hours and 24 hours respectively. At the end of each time point, the cells were rinsed twice in cold PBS and lysed in lysis buffer to extract proteins as above. U0126 [1,4-diamino-2,3-dicyano-1,4-bis (2-aminophenylthio) butadiene; cell signalling, UK] is a highly selective inhibitor of both MEK1/2 and ERK1/2 (Favata *et al.*, 1998). According to the manufacturer's instruction, it was added into the medium two hours before addition of FGF-2 and the final concentration was 10 μM. The experiment was repeated three times.

To study whether FGF-2 could activate MAPK signalling pathway in other species of epithelial cells, a human lens epithelial cell line, FHL124, was chosen to detect this. This cell line was a kind gift from Dr. Michael Wormstone (University of East Anglia, UK). The cells were exposed to the same concentration of FGF-2 for 5 minutes, 20 minutes and 1 hour, respectively, with or without the presence of U0126 (10 μM). The FHL124 cell collection and protein extraction were the same as primary bovine lens epithelial cells described above.

4.3.2 SDS- polyacrylamide gel electrophoresis (SDS-PAGE) and immunoblotting

The phosphorylation status (activation) of MAPK and PI3-K signalling proteins was assayed using SDS-PAGE and immunoblotting. First, 12% SDS-PAGE gels were made using the solutions provided in Table 4.1. Then appropriate volumes of protein, which were extracted from bovine lens epithelial cells or FHL124 cells, were loaded onto the gels. For the detection of ERK1/2, phosphorylated ERK1/2 and β-actin, 10 μg of proteins were loaded in each lane. For the detection of the total level of p38, JNK, AKT and GSK3α/β and their phosphorylation, 100 μg of proteins were loaded in each lane. The higher volume of protein loading was because their signals were very weak when 10 μg was loaded. The gels were run at 200 V for 45 minutes in the presence of running buffer [25 mM Tris base, 192 mM glycine, 0.1% (w/v) SDS)]. Later the proteins were transferred from gels to nitrocellulose membranes (0.45 μm, Merck-BDH, UK) by a semi-dry electrotransfer (Bio-Rad Laboratories, UK) at 0.8 mA/cm^2 for 2 hours. The membranes were stained with 0.2% (w/v) Ponceau S (Fluka analytical, Sigma-Aldrich, USA) in 3% (v/v) glacial acetic acid for 5 minutes to check the protein transfer efficiency. After they were destained with TTBS (20mM Tris-HCl (pH 7.4), 150 mM NaCl, 0.2% (v/v) Tween 20), they were blocked with 5% (w/v) non-fat dried milk in TTBS for 1 hour at room temperature. Thereafter, the membranes were incubated with primary antibodies (Table 4.2) diluted in 5% (w/v) BSA in TTBS overnight at 4ºC, followed by three rinses in TTBS. They were then incubated with horseradish peroxidase (HRP)-conjugated anti-mouse IgG (1:3000; GE Healthcare UK Limited, UK) or anti-rabbit IgG (1:3000; Sigma, USA) for 1 hour at room temperature. After three rinses in TTBS, the signals were detected using the enhanced chemiluminescence reagents (ECL plus, Amersham Biosciences, UK) in a Luminescent image analyser (LAS-1000 plus, Fuji film, Japan) with Image Gauge Software (Version 4.0, Fuji Film, Japan). Quantification of the immunoblotting bands was performed by the same software.

The experiments were repeated on at least three separate occasions and the representive blots were presented and analyzed. As it was impossible to have completely equal loading every time, the quantified values of the immunoreactive species were stadardised, with β-actin as a loading control. In order to make the comparison of the CZ and the GZ+TZ clear, a relative ratio was calculated. The

quantified value in the CZ was assumed as 1. The relative value in the GZ+TZ was calculated by using the quantified value in the GZ+TZ to divide the quantified value in the CZ. An independent Student's t-Test was used to detect the difference between the CZ and the GZ+TZ. A *p* value below 0.05 was considered to indicate a statistically significant difference.

Table 4.1. List of the solutions used in making SDS-PAGE gels

Solution components	4% stacking gel	12% separating gel
H_2O	3 ml	3.35.ml
30% (w/v) acrylamide	0.67 ml	4 ml
10% (w/v) SDS	50 μl	100 μl
10% (w/v) APS	75 μl	50 μl
Tris-HCl	1.25 ml (0.5 M, pH6.8)	2.5 ml (1.5M, pH8.8
TEMED	5 μl	5 μl
Total volum	5 ml*	10 ml*

*: The volume is for two gels

Table 4.2. Primary antibodies used for immunoblotting and immunofluorescence

Antigen	Source	Epitope	Dilution (IB)	Dilution (IF)	Supplier
ERK1/2	mMouse[1]		1:1000	1:100	Cell signalling, #4696
ERK1/2	pRabbit[2]		1:1000	1:50	Cell signalling, #9301
p-ERK1/2	mRabbit[3]	Thr202/Tyr204	1:1000	1:100	Cell signalling, #4370
Akt (pan)	mRabbit		1:1000		Cell signalling, #4691
p-Akt	mRabbit	Ser473	1:500		Cell signalling, #4060
GSK3α	mRabbit		1:500		Cell signalling, #4818
GSK3βb	mRabbit		1:500		Cell signalling, #9315
p-GSK3α/β	pRabbit	Ser21/9	1:500		Cell signalling, #9331
p38	pRabbit		1:500		Cell signalling, #9212
p-p38		Thr180/Tyr182	1:500		Cell signalling, #9211
JNK	mRabbit		1:500		Cell signalling, #9258
p-JNK	pRabbit	Thr183/Tyr185	1:500		Cell signalling, #9251
actin	mMouse		1:1000		MP Biolmedicals, LLC., USA, #69100
Ki-67	mMouse			1:100	Dako, USA
α-tubulin	mMouse			1:100	Sigma
γ-tubulin	mMouse	GTU-88		1:1000	Sigma

[1]: monoclonal antibody is produced from mice

[2]: polyclonal antibody is produced from rabbits

[3]: monoclonal antibody is produced from rabbits

4.3.3 Immunofluorescence

4.3.3.1 FGF-2 treatment

Primary bovine lens epithelial cells (between passage 2 and passage 6) were cultured in 10% FCS-supplemented DMEM in a 75-cm^2 flask. When the cells were in 90% - 95% confluence, they were seeded on 13-mm glass coverslips in two 12-well plates and cultured in DMEM without FCS for 1-2 days. During the 1-2 days, the cells that were in the cell cycle when they were seeded on coverslips could finish their

proliferation. Furthermore, the DMEM without FCS could avoid new cell proliferation induced by the growth factors in the FCS. One day later, most of the cells were attached to the coverslips and the cell confluence was about 70%. Two days later, some cells died and detached from the coverslip, and the cell confluence was only about 50%. The medium with dead cells was removed. The cells were washed in PBS once and then incubated in fresh DMEM without FCS. They were divided into seven groups and each group included two or three coverslips: (1) the control group without FGF-2 or U0126 treatment; (2) the group treated with 20 ng/ml of FGF-2 for one hour; (3) the group pre-treated with 10 μM of U0126 for two hours and then 20 ng/ml of FGF-2 for 1 hour with the presence of U0126; (4) the group treated with 20 ng/ml of FGF-2 for 1 hour and 10 μM of U0126 for 26 hours; (5) the group treated with 20 ng/ml of FGF-2 for 24 hours; (6) the group pre-treated with 10 μM of U0126 for two hours and then 20 ng/ml of FGF-2 for 24 hours; (7) the group pre-treated with 10 μM of U0126 for 2 hours and 20 ng/ml of FGF-2 for 24 hours with the presence of U0126. FGF-2 or U0126 was added into the medium of different of groups at the same time. At the end of each timepoint, the medium was removed and the cells were washed in PBS once, then new medium was added. All the cells were fixed together 26 hours after the start of treatment and stained with Ki-67 in order to detect cell proliferation. This experiment was independently repeated three times. Two durations of FGF-2 exposure were chosen here in order to detect the difference of short-period and long-period activation to cell proliferation. Two durations of U0126 exposure were used to detect which could inhibit the cell proliferation.

In order to observe the translocation of phosphorylated ERK1/2 after its activation, the primary bovine lens epithelial cells cultured in DMEM without FCS were exposed to 20 ng/ml of FGF-2 for 24 hours. These cells were fixed in 4% (w/v) PFA and co-labelled with phosphorylated ERK1/2 and γ-tubulin, or phosphorylated ERK1/2 and α-tubulin.

4.3.3.2 Immunofluorescence

The cells used for immunofluorescence included the bovine lens epithelial cells on the capsule and the primary bovine lens epithelial cells on coverslips. They were fixed in 4% (w/v) PFA for 20 minutes and rinsed three times in PBS, followed by

permeabilised with 1% (v/v) Igepal CA-630 (Sigma-Aldrich, USA) for 15 minutes at room temperature, and blocked with 10% (w/v) goat serum in PBS/BSA/Na-Azide for 20 minutes at room temperature. After one wash in PBS/BSA/Na-Azide, the cells were incubated with the primary antibodies (diluted in PBS/BSA/Na-Azide) (Table 4.2) at 4ºC overnight, followed by three washes in PBS/BSA/Na-Azide. For secondary antibodies, the cells were incubated with DAPI and goat anti-mouse IgG FITC-conjugated and goat anti-rabbit IgG TRITC-conjugated secondary antibodies for 1 hour at room temperature. The lens epithelium whole-mounts and coverslips were rinsed with PBS/BSA/Na-Azide three times and mounted onto microscope slides using fluorescent protecting agent Citifluor. The slides were examined by a Zeiss LSM 510 Meta confocal laser scanning microscope.

For the primary bovine lens epithelial cells treated with FGF-2 and/or U0126 and stained with Ki-67 and DAPI, ten images were randomly taken in each coverslip. The total cell number and the Ki-67-positive cell number in each image were obtained using ImageJ, and the proliferation index was then calculated. Finally, the mean of the proliferation index and the standard error of the mean (SEM) in each group were calculated from the three repeats. χ^2 test was used to compare the proliferation indexes in the groups. A p value below 0.05 was considered to indicate a statistically significant difference.

4.4 Results

4.4.1 The levels of phosphorylated MAPK and PI3-K signalling proteins were higher in the GZ+TZ than in the CZ of the bovine lens epithelium

The immunoblotting results showed that the total levels of ERK1/2, p38, JNK, AKT, GSK3α and GSK3β were similar in the CZ and the GZ+TZ of the bovine lens epithelium (Figure 4.2). However, their phosphorylation levels were found to be higher, about 30%-65%, in the GZ+TZ than in the CZ. Student's t-Test showed that statistically significant differences were present in phosphorylated p38, AKT and GSK3α/β in the comparison of the CZ and the GZ+TZ. The p value was 0.051, very close to 0.05, in the comparison of phospho-ERK between the CZ and the GZ+TZ.

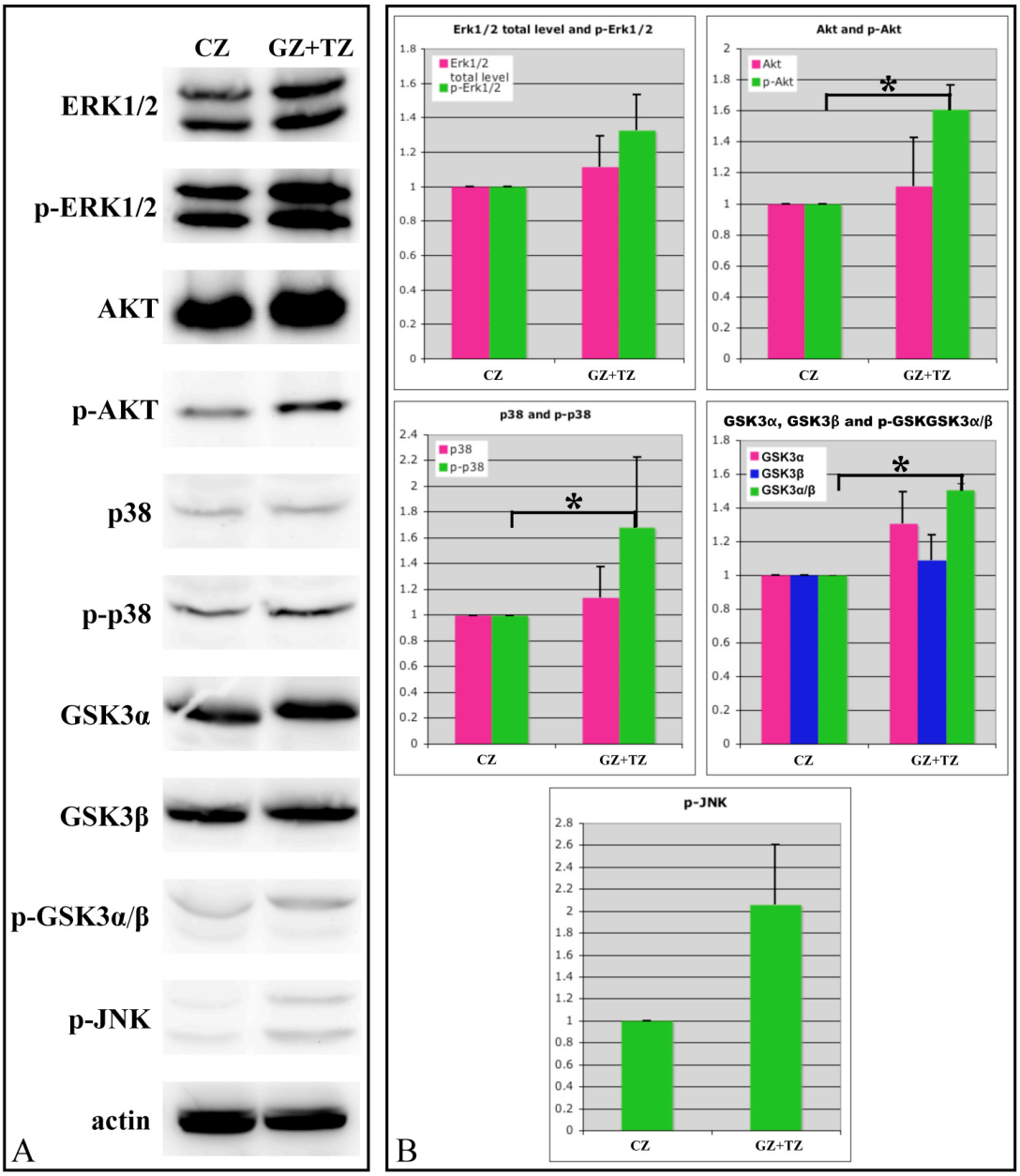

Figure 4.2. The expression of MAPK and PI3K/Akt signalling proteins in the central and peripheral regions of the bovine lens epithelium.

A: Representative immunoblotting results of the bovine lens epithelial cells in the CZ and the GZ+TZ. Equal levels of proteins from the CZ and GZ+TZ were loaded. Actin was used as the loading control. ERK1/2, AKT and phosphorylated ERK1/2 are richly expressed in the bovine lens epithelial cells. The total levels of ERK1/2, AKT, p38, GSK3α and GSK3β in the CZ are similar to the GZ+TZ, while their phosphorylated levels and the phosphorylated JNK level are slightly higher in the GZ+TZ than in the CZ.

B: Each immunoblotting band in the three repeated experiments was quantified. In order to make the comparison of the CZ and the GZ+TZ clear, a relative ratio was calculated. The quantified value in the CZ was assumed as 1. The relative value in the GZ+TZ was obtained by using the quantified value in the GZ+TZ dividing the quantified value in the CZ. The levels of phosphorylated ERK1/2, AKT, p38, GSK3α/β and JNK are higher in the GZ+TZ than in the CZ. Student's t-Test shows that only the increase in phosphorylated p38, AKT and GSK3α/β are significantly different.

As ERK1/2 was the richest protein in all of the proteins in the present study, it was investigated by immunofluorescence. No staining of the total level of ERK1/2 was detected in the bovine lens epithelial cells. The phosphorylated ERK1/2 staining was only observed in some nuclei of the proliferating cells in the GZ, but was not detected in the cytoplasm of any cells (Figure 4.3A-D). The staining was punctate and localised in the nucleus. The condensed chromosomes shown by DAPI and Ki-67 suggested that these cells were in the M phase of the cell cycle. Other dividing cells, which were in the G1-G2 phases according to DAPI and Ki-67 staining, did not display any phosphorylated ERK1/2 staining in the nuclei (Figure 4.3E-H). This punctate staining of phosphorylated ERK1/2 of the proliferating cells in the M phase was confirmed in the primary bovine lens epithelial cells cultured on glass coverslips (Figure 4.3I-L). In the same way as for the epithelial cells on the lens capsule, no staining was detected in the proliferating cell in G1-G2 phase (Figure 4.3M-P).

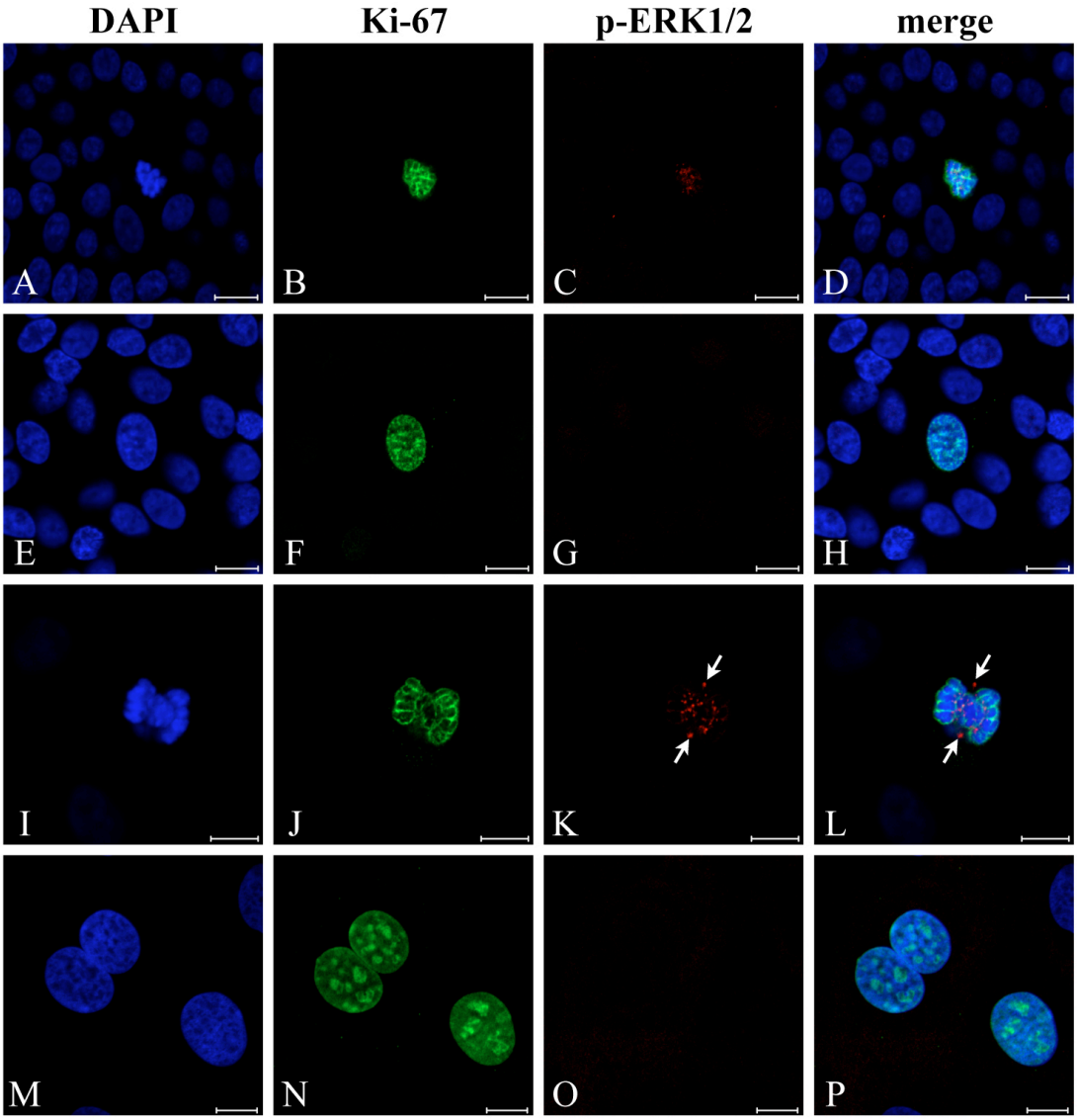

Figure 4.3. The phosphorylated ERK1/2 staining is only present in the proliferating bovine lens epithelial cells in the M phase.

The bovine lens epithelial cells on the capsule (A-H) or cultured on coverslips (I-P) were stained with DNA indicator DAPI (blue), proliferation marker Ki-67 (green) and MAPK signalling protein phosphorylated ERK1/2 (red). Scale bars=10 μm.

A-D: The punctate phosphorylated ERK1/2 staining is only detected in the nucleus of one proliferating cell in the GZ. The DAPI and Ki-67 staining shows the condensed chromosomes and suggests that this cell is in the M phase.

E-H: No phosphorylated ERK1/2 staining is observed in the proliferating cell between the G1 and G2 phase indicated by the DAPI and Ki-67 staining.

I-L: The punctate phosphorylated ERK1/2 staining is observed in the nucleus of a proliferating cell grown on a coverslip. Two strong staining points were located at the opposite sides of the condensed chromosomes. The DAPI and Ki-67 staining shows that this cell is in the M phase.

M-P: No phosphorylated ERK1/2 staining is detected in the proliferating cells, which are grown on a coverslip and are between the G1 and G2 phase according to their DAPI and Ki-67 staining.

4.4.2 FGF-2 increased the phosphorylated ERK1/2 level and cell proliferation index

In order to study whether FGF-2 could increase the levels of MAPK and PI3-K signalling proteins in the GZ+TZ, the bovine lens epithelium whole-mounts were exposed to 20 ng/ml of FGF-2 in DMEM immediately after lens dissection. Unfortunately some cells were observed to detach from the lens capsule 5 minutes later, and more cells detached 20 minutes later. Therefore, FGF-2 exposure was stopped and the remaining cells in the CZ and the GZ+TZ were collected separately for immunoblotting. Compared with the control without FGF-2 treatment, the phosphorylated ERK1/2 increased only in the CZ treated with FGF-2 for 5 minutes (Figure 4.4). In the samples of the GZ+TZ exposed to FGF-2 for 5 and 20 minutes, the phosphorylated ERK1/2 levels were even lower than that in the control. These results were opposite to those in 4.4.1, and they did not show that FGF-2 exposure would increase the phosphorylated ERK1/2 level as reported before (Iyengar *et al.*, 2007). This might be because the bovine lens epithelial cells started to detach from the capsule when the original epithelial cell environment was broken and the cells were cultured in DMEM. Therefore, the following studies about FGF-2 exposure were used the primary bovine lens epithelial cells that were detached from the lens capsule and cultured in flasks.

The primary bovine lens epithelial cells were treated with FGF-2 and/or U0126 for different lengths of time. The immunoblotting results showed that ERK1/2 had been activated after 5 minutes' exposure to FGF-2 (Figure 4.5). The phosphorylation level came to the highest at 1 hour and then continuously decreased. Compared with the control, the phosphorylated ERK1/2 level was still higher 24 hours later. This indicates that 20 ng/ml of FGF-2 can induce a sustained ERK1/2 phosphorylation, which is critical for cell proliferation. The FGF-2 induced ERK1/2 phosphorylation could be effectively blocked by U0126. Moreover, It also occurred in FHL124 cells (Figure 4.6). In the same way as for the bovine lens epithelial cells, the phosphorylated ERK1/2 level continuously increased from 5 minutes to one hour. U0126 effectively blocked FGF-2-induced ERK1/2 phosphorylation.

The FGF-2-induced cell proliferation was confirmed in the primary bovine lens epithelial cells by immunofluorescence. Compared with the control cells without FGF-2 treatment, Ki-67 staining showed that more cell proliferation occurred in the

cells exposed to FGF-2 for 1 hour and 24 hours (Figure 4.7), and statistically significant differences were present in their proliferation index comparisons (Table 4.3). However, there was no statistically significant difference between the comparison of proliferation indexes in 1 hour and 24 hours of FGF-2 treatments. For the cell proliferation inhibition study, the lens epithelial cells were exposed to U0126 for 2-3 hours or for 26 hours. The results showed that cell proliferation was not inhibited by 2-3 hours' exposure but inhibited by 26-hour's exposure.

Table 4.3. The *p* values of χ^2 test in the comparisons of proliferation indexes of the primary bovine lens epithelial cells treated with FGF-2 and/or U0126

	Control	**FGF-2 1 h**	**FGF-2 1h/U0126 3h**	**FGF-2 1h/U0126 26h**	**FGF-2 24h**	**FGF-2 24h/U0126 2h**	**FGF-2 24h/U0126 26h**
Control		**<0.01**	**0.024**	0.81	**0.01**	**0.01**	0.41
FGF-2 1 h	**<0.01**		0.50	**<0.01**	0.51		
FGF-2 1h/U0126 3h	**0.024**	0.50		**0.035**			
FGF-2 1h/U0126 26h	0.81	**<0.01**	**0.035**				
FGF-2 24h	**<0.01**	0.51				0.11	**<0.01**
FGF-2 24h/U0126 2h	**<0.01**				0.11		**<0.01**
FGF-2 24h/U0126 26h	0.41				**<0.01**	**<0.01**	

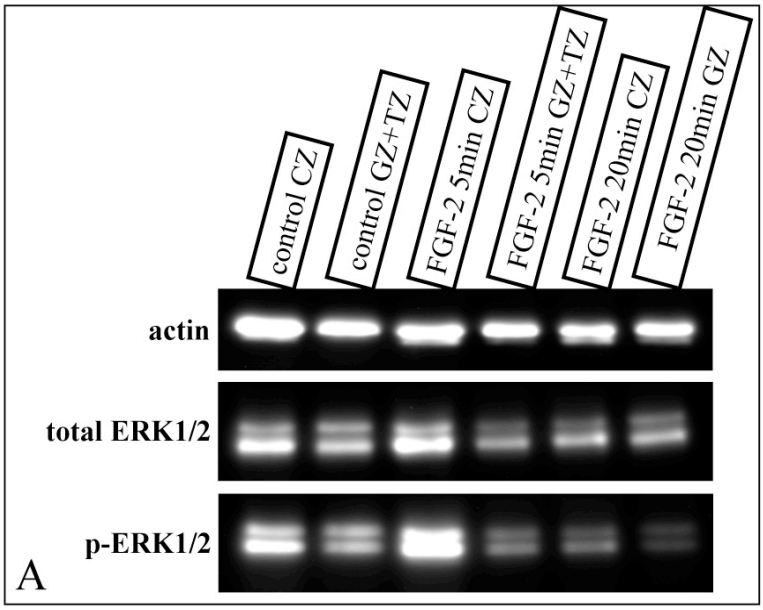

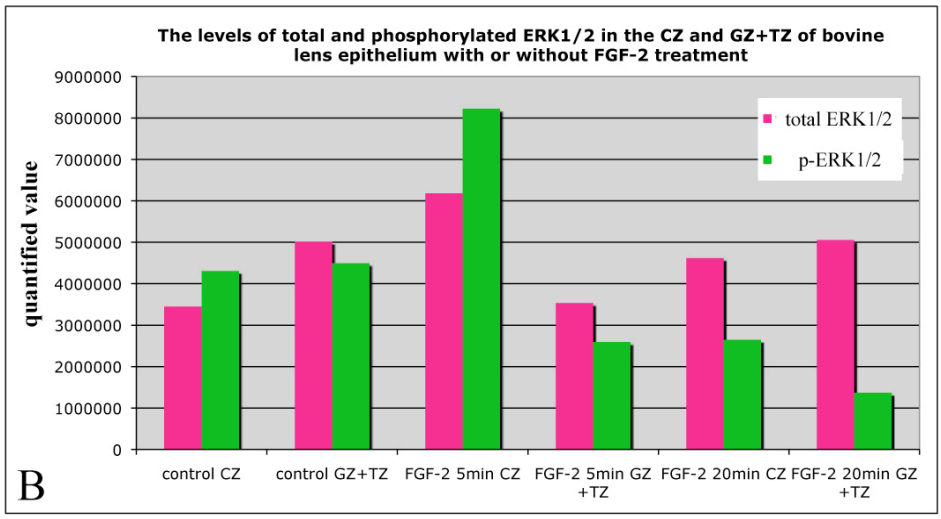

Figure 4.4. The changes of the total and phosphorylated ERK1/2 levels in the bovine lens epithelial cells with or without FGF-2 treatment.

The bovine lens epithelium whole-mounts were cultured in Dulbecco's modified eagle's medium (DMEM) with 20 ng/ml of FGF-2 for five and 20 minutes. The cells in the CZ and the GZ+TZ were separately collected for immunoblotting. The controls were just cultured in DMEM without FGF-2 for five minutes.

A: Representative immunoblotting results of total and phosphorylated ERK1/2. Actin was used as the loading control. The variable signal intensity of actin in the lanes indicates that the loaded protein amount is not equal. The levels of total and phosphorylated ERK1/2 only increase in the cells of the CZ with five minutes of FGF-2 treatment.

B. The quantification of the bands in picture A. In the control, the levels of phosphorylated ERK1/2 in the CZ and the GZ+TZ were similar. In the FGF-2-treated cells, the phosphorylated ERK1/2 level is only higher in the CZ at five minutes than the control, but is lower in all the other three samples.

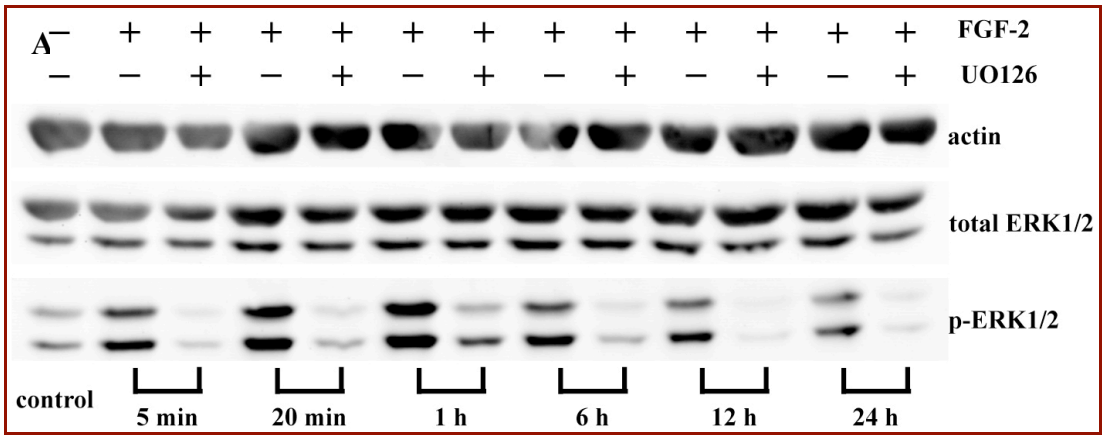

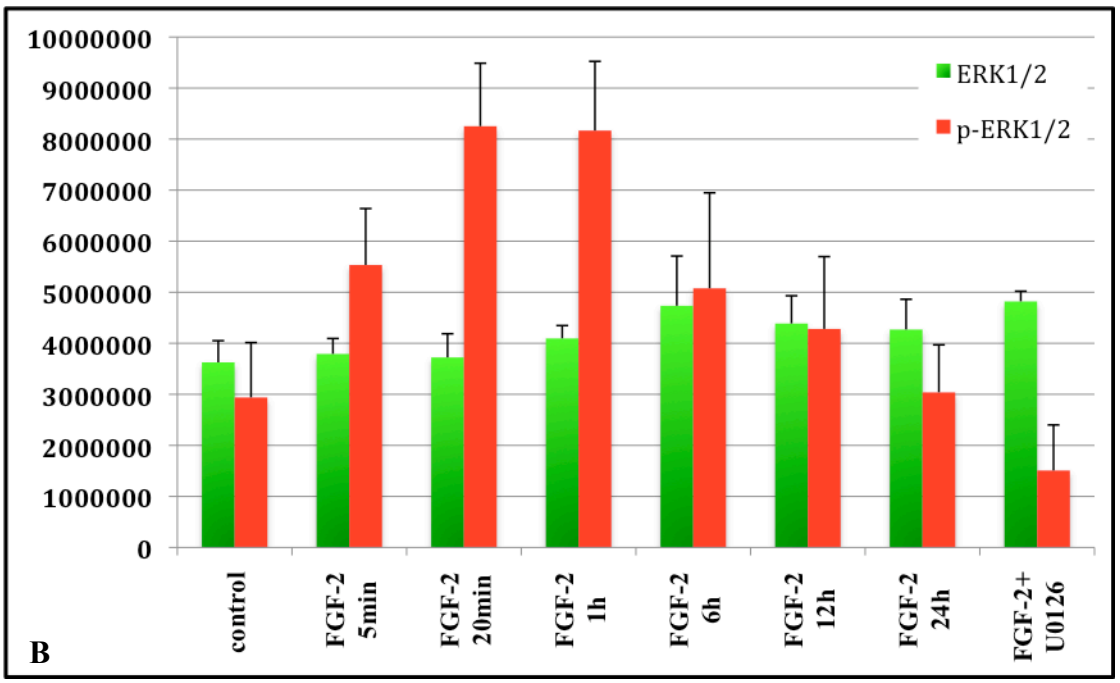

Figure 4.5. Immunoblotting results of ERK1/2 and phosho-ERK1/2 of the primary bovine lens epithelial cells exposed to FGF-2 and/or U0126.

Primary bovine lens epithelial cells (passages 2-6) were exposed to 20 ng/ml FGF-2 for different lengths of time in the absence or presence of U0126. The cells as the control were not treated with FGF-2. Actin is used as a loading control.

A. Representive immunoblotting results of actin, ERK1/2 and phospho-ERK1/2.

B. The levels of total ERK1/2 are similar in the cells with or without FGF-2 and/or U0126 treatment. Compared to the control, the level of phospho-ERK1/2 increases after 5 minutes of FGF-2 exposure and comes to the highest at 20 minutes and 1 hour. Then the level continuously decreases to the basic level at 24 hour. U0126 blocks the majority of ERK1/2 phosphorylation, and very low levels of phospho-ERK1/2 are detected in these samples. Data are expressed at mean ± SD (n=3).

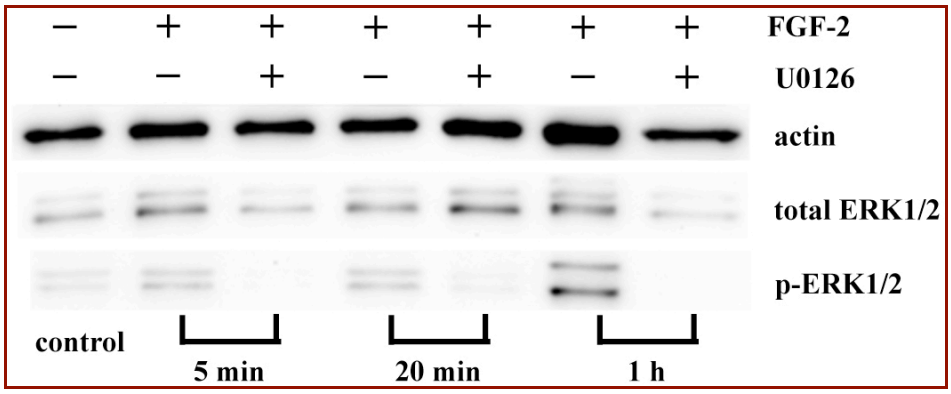

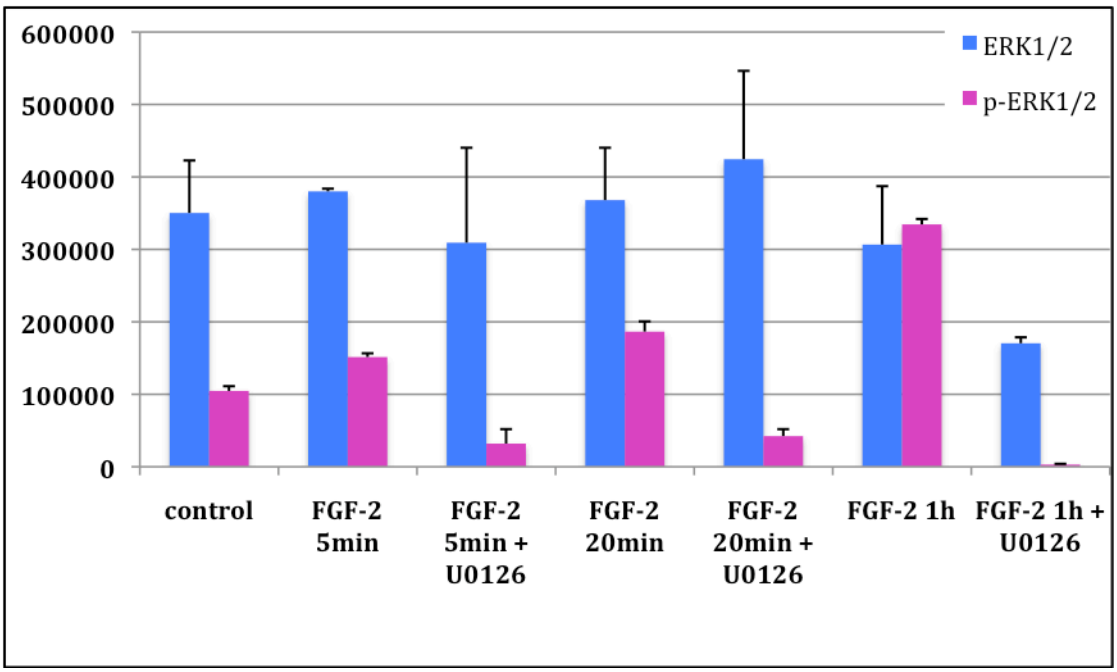

Figure 4.6. Representative immunoblotting results of FHL124 cells exposed to FGF-2 and/or U0126.

FHL124 cells were exposed to 20 ng/ml of FGF-2 for 5 minutes, 20 minutes and 1 hour, with or without the absence of U0126. The cells as the control were not treated with FGF-2. Actin is used as the loading control.

A. Representive immunoblotting results of actin, ERK1/2 and phospho-ERK1/2.

B. The total levels of ERK1/2 are slightly variable in all the samples. When the cells were exposed to FGF-2, the level of phospho-ERK1/2 increases at 5 minutes and becomes higher at one hour. U0126 effectively blocks the phosphorylation of ERK1/2. Data are expressed at mean ± SEM (n=3).

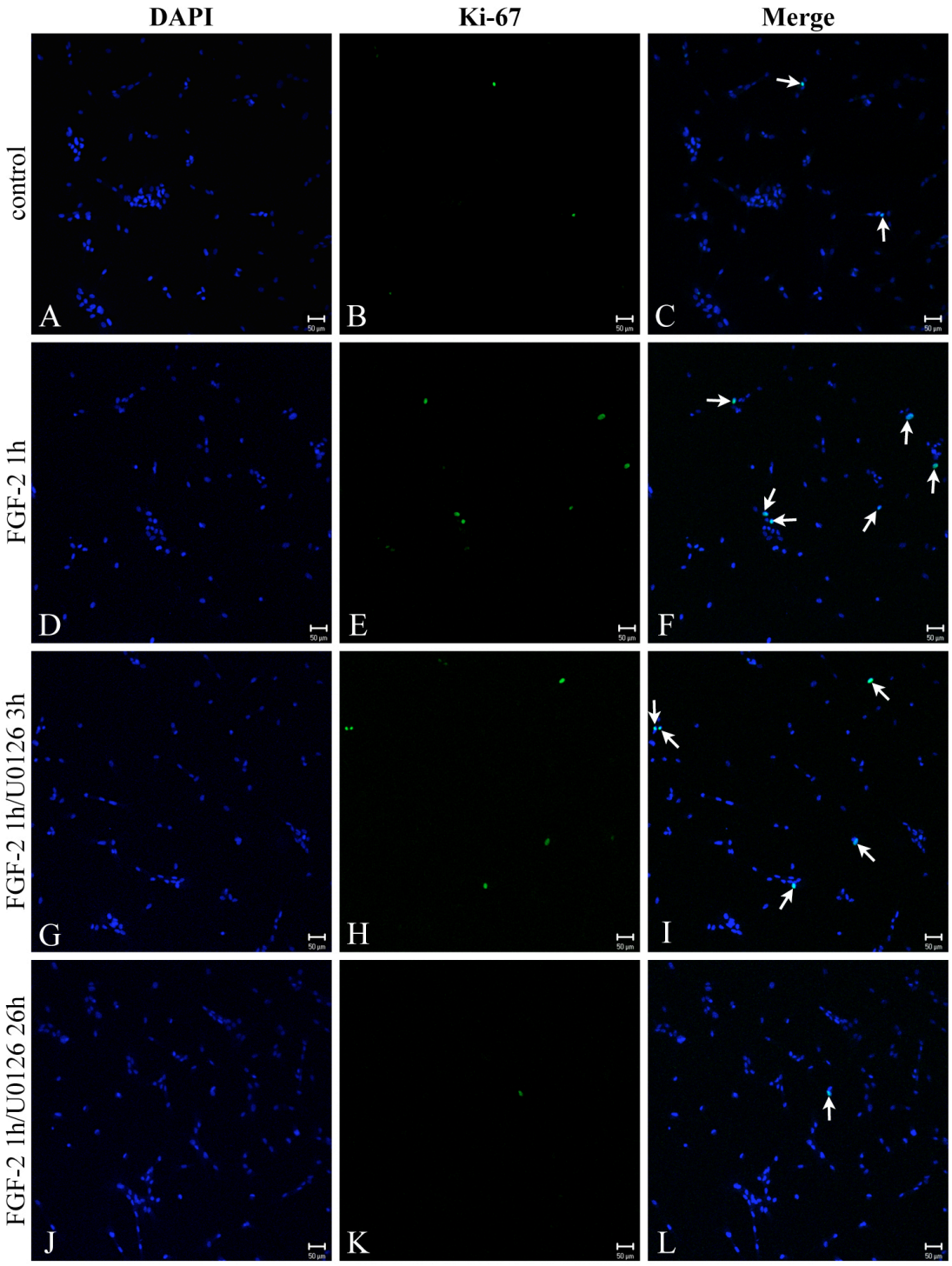
DAPI
Ki-67
Merge
control
FGF-2 1h
FGF-2 1h/U0126 3h
FGF-2 1h/U0126 26h
A
B
C
D
E
F
G
H
I
J
K
L

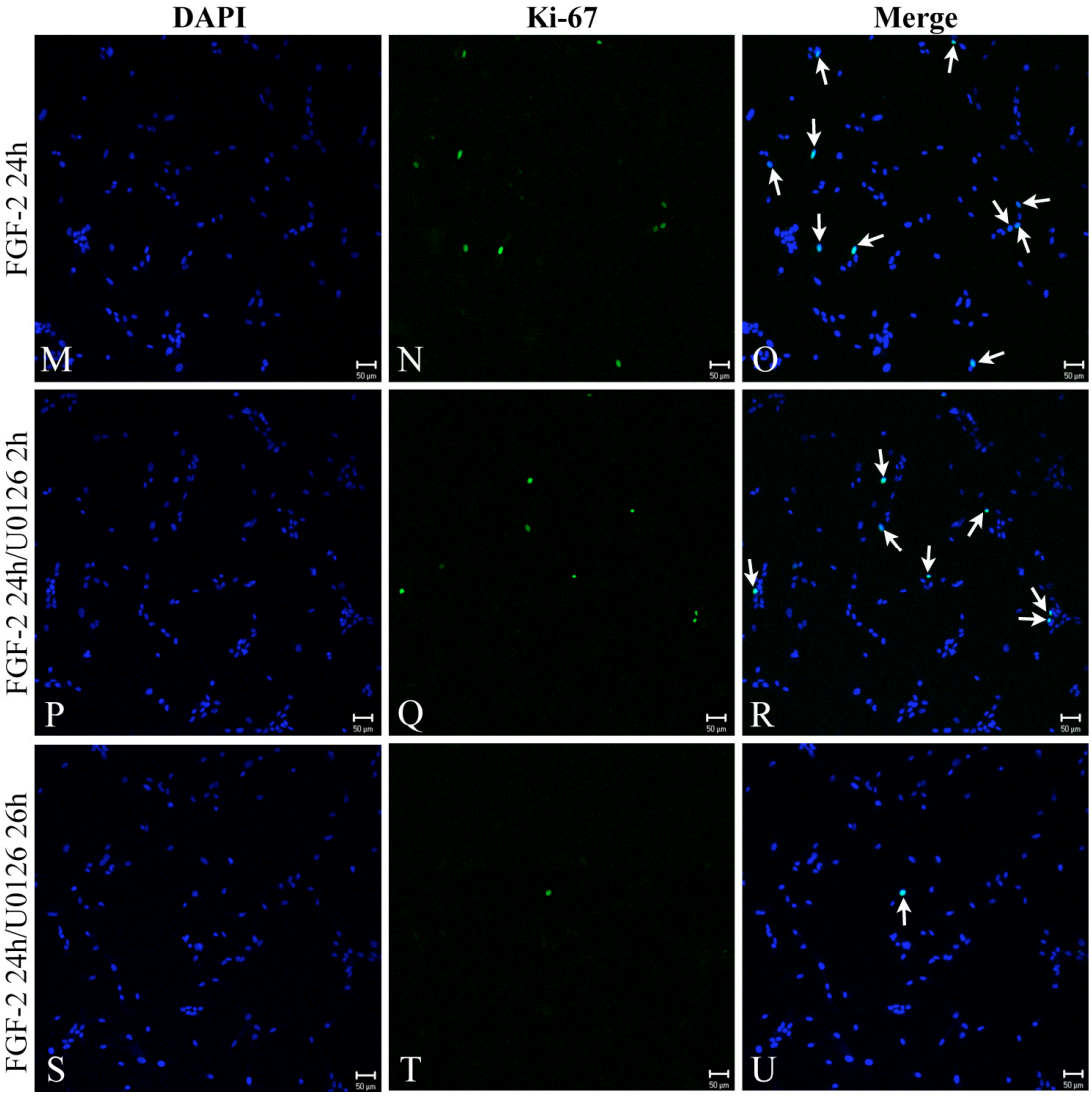
DAPI
Ki-67
Merge
FGF-2 24h
FGF-2 24h/U0126 2h
FGF-2 24h/U0126 26h
M
N
O
P
Q
R
S
T
U

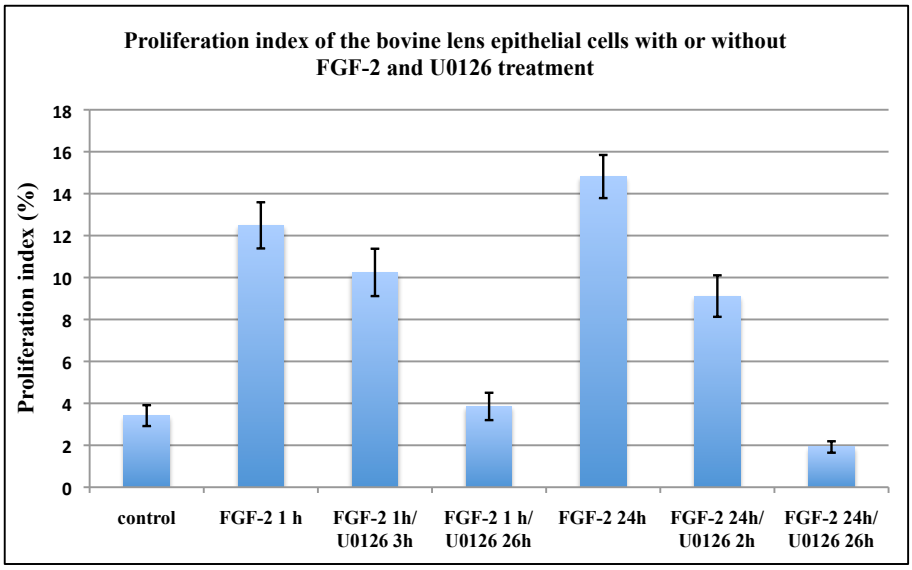
Proliferation index of the bovine lens epithelial cells with or without FGF-2 and U0126 treatment
Proliferation index (%)
18
16
14
12
10
8
6
4
2
0
control
FGF-2 1 h
FGF-2 1h/ U0126 3h
FGF-2 1 h/ U0126 26h
FGF-2 24h
FGF-2 24h/ U0126 2h
FGF-2 24h/ U0126 26h

Figure 4.7. Cell proliferation in the bovine lens epithelium with or without the presence of FGF-2 and U0126.

The primary bovine lens epithelial cells were cultured in Dulbecco's modified Eagle's medium (DMEM) without foetal calf serum (FCS) for one or two days. Then they were exposed to 20 ng/ml of FGF-2 for 1 hour or 24 hours. For ERK1/2 inhibition study, the cells were just pre-treated with MEK1/2 inhibitor U0126 for two hours, or U0126 was still present when the cells were exposed to FGF-2. All the cells were fixed at the end of FGF-2 exposure and stained with DNA indicator DAPI (blue) and cell proliferation marker Ki-67 (green). The experiment was repeated three times. The proliferation index of each group was calculated and made into a bar chart [mean ± SEM (standard error of the mean)].

A-C: In the control cells without FGF-2 treatment, a very low number of cells undergo cell proliferation (arrow).

D-F: When the cells were exposed to FGF-2 for one hour, the proliferating cell number increases (arrows).

G-I: When the cells were pre-treated with U0126 for two hours and then exposed to FGF-2 for 1 hour with the presence of U0126, cell proliferation still occurs in many cells (arrows).

J-L: When the cells were treated with FGF-2 for 1 hour but continuously exposed to U0126 for 26 hours, cell proliferation is inhibited and only a very low number of cells still proliferate (arrow).

M-O: When the cells were treated with FGF-2 for 24 hours, many cells undergo cell proliferation (arrows).

P-R: When the cells were pre-treated with U0126 for two hours and then exposed to FGF-2 for 24 hours, there are still many cells in cell division (arrows).

S-U: When the cells were pre-treated with U0126 for two hours and then exposed to FGF-2 for 24 hours with the presence of U0126, cell proliferation is effectively inhibited and the proliferating cell (arrow) number decreases.

V: The cell proliferation index increases in the cells with 1 hour and 24 hours of FGF-2 treatment. The cell proliferation is not effectively inhibited by a short time (two and three hours) of U0126 treatment, but is blocked by sustained U0126 treatment. Data are expressed as mean ± SD (n=3).

4.4.3 Phosphorylated ERK1/2 was associated with spindle poles and the spindle during the M phase of the cell cycle

The bovine lens epithelial cells on the capsule or cultured on coverslips were co-stained with phosphosrylated ERK1/2 and DAPI. The punctate phosphorylated ERK1/2 staining was only detected in the proliferating cells in the M phase (Figure 4.3). The distribution of the punctate staining was unusual, with two bright staining dots in the opposite sides and some small dots in the middle, and did not fully merge with the DAPI-stained chromosomes (Figure 4.3I-L). These two bright dots were identified as the spindle poles when the cells were co-stained with α-tubulin and phosphorylated ERK1/2 (Figure 4.8). The association of phosphorylated ERK1/2 with spindle poles was further confirmed by its colocalisation with the centrosome protein γ-tubulin (Figure 4.9). During the prophase of the M phase (Figure 4.8A-D and 4.9A-D), chromatin condensed together into highly ordered chromosomes. A proportion of phosphorylated ERK1/2 migrated to the centrosome position, which started to nucleate α-tubulin to form spindle. The rest of phosphorylated ERK1/2 staining accumulated at the chromosome position or in the vicinity of chromosomes. In the metaphase (Figure 4.8E-H and 4.9E-H), the chromosomes convened along the metaphase plate, and the two centrosomes pulled the spindle towards the two ends of the cell. Punctate phosphorylated ERK1/2 staining was localised along the spindle and at the spindle poles. As the cells progressed to the anaphase and the telophase (Figure 4.8I-P and 4.9I-P), the two sister chromatids were pulled apart by the spindle and moved toward their centrosomes. At these stages, phosphorylated ERK1/2 was diffusely distributed in the region with separating homologous chromosomes and at the spindle poles.

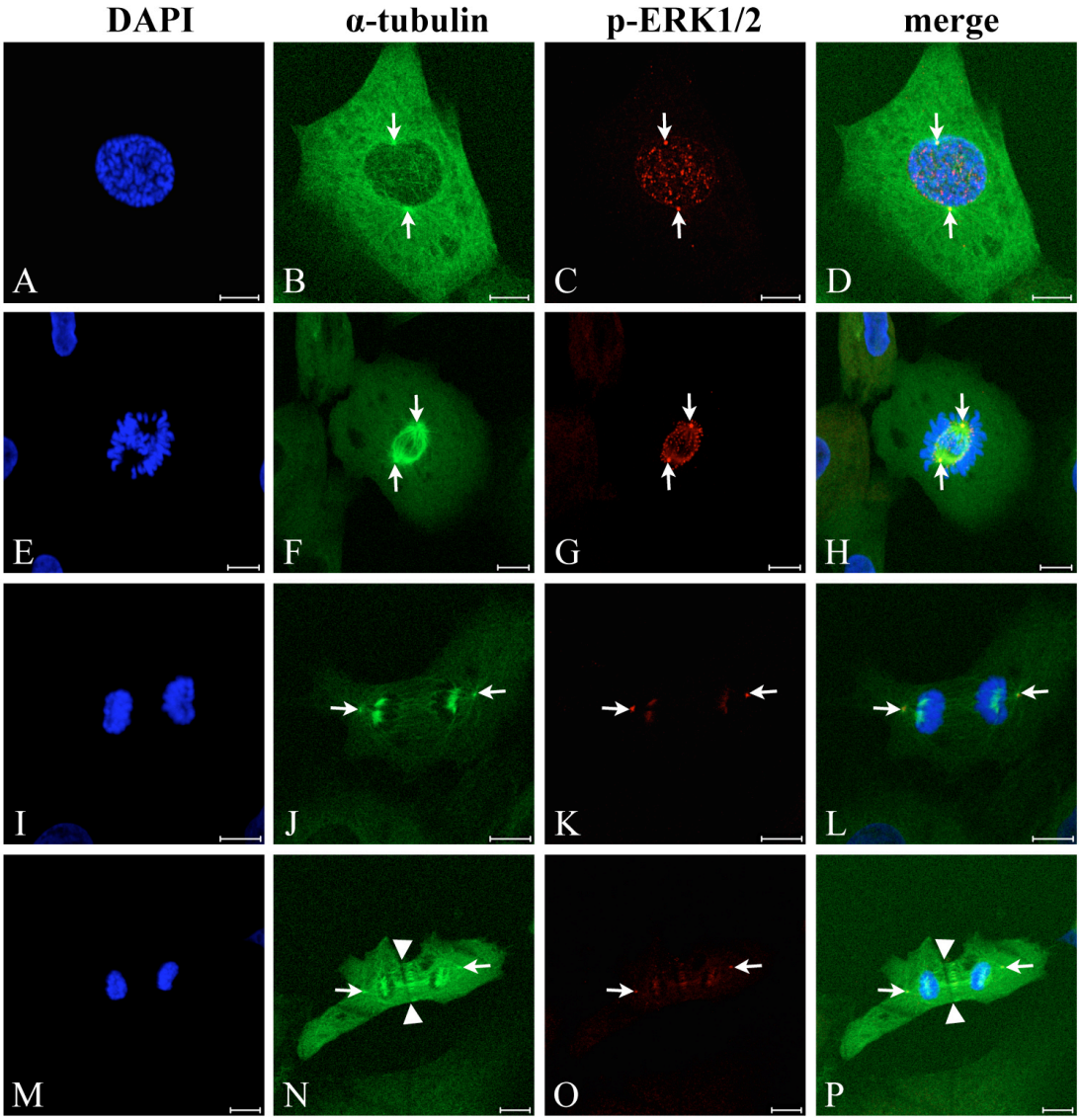
DAPI
α-tubulin
p-ERK1/2
merge
A
B
C
D
E
F
G
H
I
J
K
L
M
N
O
P

Figure 4.8. Association of phosphorylated ERK1/2 with the spindle poles and the spindle in the cells in the M phase.

The primary bovine lens epithelial cells cultured on glass coverslips were co-stained with DNA indicator DAPI (blue), microtubule filament α-tubulin (green) and MAPK signalling protein phosphorylated ERK1/2 (red). The phosphorylated ERK1/2 staining was only observed in the cells in the M phase of the cell cycle. Images of the four different phases of the M phase are shown. Scale bars = 10 μm.

A-D: At prophase, chromatin condenses into highly ordered chromosomes. α-tubulin starts to nucleate around the spindle poles (arrows). Some phosphorylated ERK1/2 staining accumulates at the spindle poles (arrows), and the rest punctate staining distributes in dots on chromosomes or in the vicinity of chromosomes.

E-H: At metaphase, the chromosomes convene along the metaphase plate. The spindle has formed. Phosphorylated ERK1/2 is localised in dots along the spindle and at the spindle poles.

I-L: At anaphase, the two sister chromatids were pulled apart by the spindle. Some phosphorylated ERK1/2 staining is still localised at the spindle poles (arrows), but the number of the staining dots along the spindle decrease.

M-P: At telophase, lengthening spindle pushes the two sister chromatids further apart. A cell pinch starts to appear (arrowheads). The phosphorylated ERK1/2 staining is still localised at the spindle poles and along the spindle microtubules.

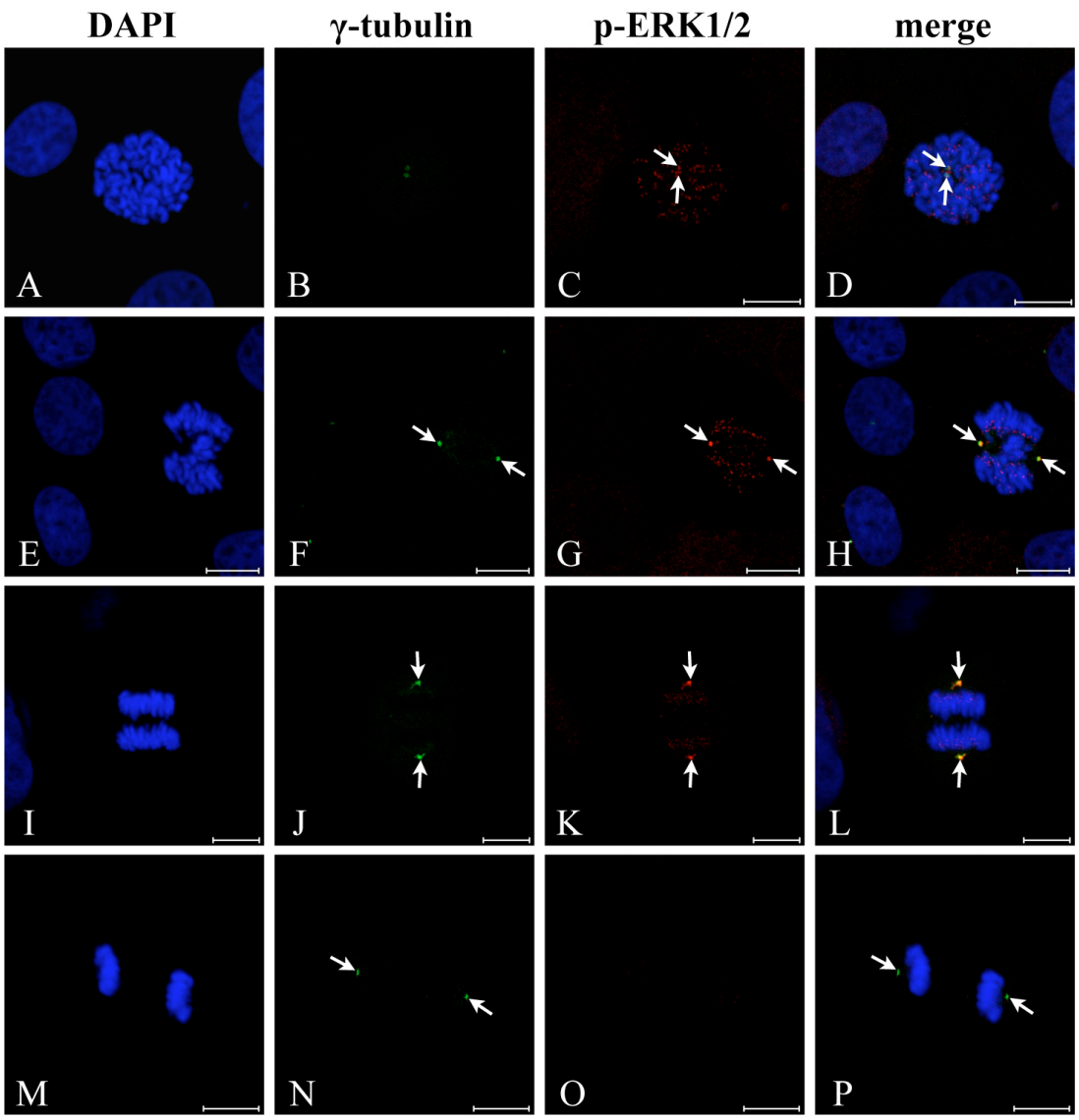
DAPI
γ-tubulin
p-ERK1/2
merge
A
B
C
D
E
F
G
H
I
J
K
L
M
N
O
P

Figure 4.9. Colocalisation of phosphorylated ERK1/2 with γ-tubulin at the centrosome position in the cells in the M phase.

Primary bovine lens epithelial cells cultured on glass coverslips were co-stained with DAPI (blue), centrosomal protein γ-tubulin (green) and MAPK signalling protein phosphorylated ERK1/2 (red). Images of the four different phases of the M phase are shown. Scale bars = 10 μm.

A-D: At prophase, chromatin condenses into highly ordered chromosomes. Two γ-tubulin foci are present at the chromosomes. Punctate phosphorylated ERK1/2 staining is localised on chromosomes or in the vicinity of chromosomes. Some phosphorylated ERK1/2 staining starts to accumulate at the centrosome position (arrows).

E-H: At metaphase, the chromosomes align in the metaphase plate. The two γ-tubulin foci are localised in the opposite sides of the cell. Two bright phosphorylated ERK1/2 staining dots co-localised with γ-tubulin at the centrosome position (arrows). The rest phosphorylated ERK1/2 staining scatters in the chromosomes as small dots.

I-L: At anaphase, the two sister chromatids were pulled apart toward their centrosomes. The phosphorylated ERK1/2 staining still colocalised with γ-tubulin at the centrosome position.

M-P: At telophase, the two sister chromatids are pulled further apart. γ-tubulin foci are still present in the opposite sides of the cells (arrows), while no phosphorylated ERK1/2 staining is detected in this cell.

4.5 Discussion

4.5.1 The levels of phosphorylated MAPK and PI3-K signalling proteins are consistent with the FGF-2 gradient

In the previous studies, the increase of cell proliferation and the fibre-specific protein expression is correlated with the increase of phosphorylated MAPK/ERK1/2 and PI3-K signalling proteins, and blocking the two signalling pathway can effectively inhibit cell proliferation and differentiation (Iyengar *et al.*, 2006; Iyengar *et al.*, 2007; Lovicu and McAvoy, 2001; Wang *et al.*, 2010; Wang *et al.*, 2009b; Weber and Menko, 2006; Zatechka and Lou, 2002). These results indicate that the MAPK/ERK1/2 and PI3-K signalling pathways regulate lens epithelial cell proliferation and differentiation. Since FGF-2 can activate these two signalling pathways and a higher level of FGF-2 was detected at the equator of the inner surface of the bovine lens capsule in chapter 3, the hypothesis was made that a higher level of phosphorylated MAPK and PI3-K signalling proteins was present in the GZ and TZ. In order to investigate this hypothesis, the lens epithelium was separated into the CZ and the GZ+TZ. The immunoblotting results indicate that these signalling pathways are activated in the periphery, which is consistent with results from other studies showing they have a role in proliferation and differentiation.

In the present study, higher levels of phosphorylated ERK1/2, p38, JNK, GSK3α/β and AKT were detected in the freshly dissected cells from the GZ+TZ where cells proliferate and prepare for fibre cell differentiation. The increase of phosphorylated GSK3α/β, AKT and p38 levels in the GZ+TZ was statistically significant compared with the CZ. The results indicate that these signalling pathways are activated in the GZ and TZ, which is consistent with results from other studies showing the MAPK/ERK1/2 and PI3-K/AKT signalling pathways play an important role in lens epithelial cell proliferation and differentiation. Although p38 and JNK are found to play a role in the regulation of cell differentiation and the cell cycle (Dong *et al.*, 2000; Dong *et al.*, 1998; Morooka and Nishida, 1998; Takenaka *et al.*, 1998), it has been reported that p38 mainly regulates normal immune and inflammatory response (Roux and Blenis, 2004) and JNK is important in regulating cell apoptosis (Kanda and Miura, 2004). This is the first time to detect the levels of phosphorylated

p38 and JNK in the lens epithelium. Their higher levels in the GZ+TZ indicate that they may play a role in regulating lens epithelial cell proliferation and differentiation.

In immunoblotting, the levels of phosphorylated ERK1/2 in the GZ+TZ were much higher than the other phosphorylated proteins in the MAPK and PI3-K signalling pathways. This suggests that ERK1/2 is the dominant protein that regulates lens epithelial cell proliferation and differentiation. This conclusion is consistent with previous results that ERK1/2 plays a crucial role in aqueous humour, vitreous humour and FGF-2-induced lens epithelial cell proliferation and differentiation (Iyengar *et al.*, 2006; Iyengar *et al.*, 2007; Lovicu and McAvoy, 2001; Wang *et al.*, 2010; Zatechka and Lou, 2002).

4.5.2 FGF-2 initiates cell proliferation by activating ERK1/2

FGF-2 plays a key role in regulating lens epithelial cell proliferation and fibre cell differentiation and it functions by ERK1/2 (Iyengar *et al.*, 2006; Lovicu and McAvoy, 2005). A higher level of FGF-2 was detected at the equator of the inner surface of the lens capsule in Chapter 3. Therefore, how it regulated lens epithelial cell proliferation was restudied in order to detect the mechanism of ERK1/2 working. In the present study, the proliferation index significantly increased with the rise of phosphorylated ERK1/2 level in the primary bovine lens epithelial cells treated with a low proliferating dose of FGF-2. Only consistent exposure to U0126 could block FGF-2-induced cell proliferation.

As a specific MEK1/2 inhibitor, U0126 can directly inhibit activated MEK1 and prevent endogenously activate MEK1/2 from phosphorylating and activating ERK1/2. It has been reported to effectively block lens epithelial cell proliferation (Iyengar *et al.*, 2006; Lovicu and McAvoy, 2001). In previous studies, U0126 was added two hours before addition of FGF-2 and present in the medium during FGF-2 treatment (Iyengar *et al.*, 2006; Lovicu and McAvoy, 2001). In the present study, the cells that were pre-treated with U0126 for two hours still proliferate as those without U0126 treatment, while cell proliferation was effectively inhibited in the cells with 26 hours of U0126 treatment. These results suggest that the inhibition of U0126 to cell proliferation is reversible. This is also found in mouse embryos, which is arrested at four-cell stage by the inhibition of U0126 and continually develop to eight-cell stage when U0126 is removed (Maekawa *et al.*, 2007). When studying the cell proliferation

inhibition of U0126 in melanoma cells, Smalley and colleagues found that U0126 blocked cell proliferation, through the up-regulation of the cyclin-dependent kinase inhibitor $p27^{Kip-1}$ (Smalley *et al.*, 2006). When U0126 is removed from the medium, the up-regulation of $p27^{Kip-1}$ stops and its block to ERK1/2 phosphorylation disappears, the epithelial cells can continue to re-enter the cell cycle.

Wang and colleagues find that lens fibre cell differentiation induced by vitreous humour or a high fibre-differentiating dose of FGF-2 (100 ng/ml) requires sustained ERK1/2 phosphorylation (Wang *et al.*, 2009b). In order to detect whether the lens epithelial cell proliferation induced by a low proliferating dose of FGF-2 (20 ng/ml) still needed sustained ERK1/2 phosphorylation, the primary bovine lens epithelial cells were exposed to FGF-2 for 1 hour and 24 hours. The statistically significant difference of in the comparison of the proliferation indexes between the control group and the one-hour-FGF-2 treated group suggests that 1 hour of FGF-2 exposure is enough to initiate cell proliferation. Moreover, the absence of significant difference in the comparison of the 1-hour-FGF-2 and 24-hour-FGF-2 groups further indicates that lens epithelial cell proliferation does not require sustained FGF-2 treatment. The immunoblotting results show that ERK1/2 phosphorylation comes to the highest level at 1-hour timepoint during FGF-2 treatment. This means that the peak activation of ERK1/2 caused by a short time of FGF-2 exposure is enough to induce lens epithelial cell proliferation.

4.5.3 Phosphorylated ERK1/2 was correlative with the spindle formation in the M phase

In order to detect how ERK1/2 regulates lens epithelial cell proliferation, the bovine lens epithelial cells on the capsule or cultured on coverslips were stained with phosphorylated ERK1/2. It was very interesting to detect some punctate staining in the proliferating cells in the GZ or on coverslips after FGF-2 treatment. DAPI and Ki-67 showed that all these proliferating cells were in the M phase of the cell cycle. The punctate staining was localised at the spindle poles and along the spindle microtubules. At the spindle poles, phosphorylated ERK1/2 co-stained with the centrosome protein γ-tubulin.

The results reported herein are quite different from previous studies. It has been reported that phosphorylated ERK1/2 translocates into the nucleus once it is activated

in the cytoplasm, and those nuclei are not specifically in the M phase (Chuderland *et al.*, 2008; Zehorai *et al.*, 2010). Iyengar and colleagues also detected the diffuse phosphorylated ERK1/2 staining in the cytoplasm of the rat lens epithelial cells after FGF-2 treatment (Iyengar *et al.*, 2006). In addition, the strong signals in immunoblotting suggest its rich expression in the bovine lens epithelial cells. The antibody works on the bovine cells in immunofluorescece according to the manufacture's instruction. It is not clear why the majority of phosphorylated ERK1/2 was not detected in the cell cytoplasm. However, the punctate phosphorylated ERK1/2 staining was found in the proliferating cells in the M phase. The reports about its special location at the spindle poles and along the spindle microtubules have not been found in the literature.

Similar location and morphology are reported in phosphorylated MEK1/2, the upstream of ERK1/2. MEK1/2 is activated during meiotic maturation of mouse oocytes and co-localised with γ-tubulin at the centrosomes to regulate microtubule organisation (Sun *et al.*, 2008; Yu *et al.*, 2007). Punctate phosphorylated MEK1/2 staining is also observed in the spindle (Yu *et al.*, 2007). The block of MEK1/2 and ERK1/2 phosphorylation by their inhibitor U0126 results in the disorganised spindle pole and spindle structure and misaligned chromosomes during mouse oocyte meiotis (Sun *et al.*, 2008; Tong *et al.*, 2003; Yu *et al.*, 2007). Similar changes were not observed in the present study because the epithelial cells did not come into cell cycle in the consistent presence of U0126. Moreover, during meiotic maturation of mouse oocytes, the activation of ERK1/2 is coinciding with the formation of bipolar spindles and phosphorylated ERK1/2 is specifically located at the centrosomes present at the spindle poles (Verlhac *et al.*, 1993; Verlhac *et al.*, 1994). It is not clear whether the special location of MEK1/2 is related to the phosphorylated ERK1/2 location in the mouse oocytes. Does ERK1/2 play similar roles in the lens epithelial cells to MEK1/2 and ERK1/2 in the mouse occytes? How does it regulate spindle organisation during the M phase? The answers are still unclear.

4.6 Summary

The aims of this chapter were to investigate the hypothesis that a higher level of FGF-2 at the equator might induce more MAPK and PI3-K signalling protein phosphorylation and how FGF-2 regulated lens epithelial cell proliferation by

ERK1/2. The results showed that higher levels of MAPK and PI3-K signalling proteins were present in the GZ+TZ than in the CZ. A pulse treatment of FGF-2 is enough to induce lens epithelial cell proliferation, and the activated ERK1/2 by FGF-2 is located at the spindle poles and along the spindle microtubules in the proliferating cells in the M phase. These results suggest that cell proliferation in the GZ of the lens epithelium is related to the higher level of FGF-2 in that region of the inner surface of the capsule, and phosphorylated ERK1/2 may play a role in the spindle formation during the M phase of the cell cycle.

5 Conclusions and future experiments

The present study was mainly to answer the following ten questions in order to better understand cell organisation in the mammalian lens epithelium and human capsular bags after cataract surgery: (1) Where does cell proliferation occur in the young mammalian lenses? Is it only in the GZ or in the GZ and the CZ? (2) How does epithelial cell proliferation change with age? (3) How many cells undergo apoptosis in the lens epithelium? (4) Is there a cell number balance existing between epithelial cell production (cell proliferation in the GZ) and epithelial cell loss (cell apoptosis and fibre cell differentiation at the end of the TZ)? (5) How does the cell density and size change across the epithelium with age? (6) Where is the epithelial cell centrosome located? (7) How do the cell characteristics above change in the human lens capsular bags after cataract surgery? (8) Does a gradient of matrix-bounded FGF-2 exist in the capsule? (9) Are higher levels of MAPK and PI3-K signalling phosphorylation present in the GZ and the TZ compared to the central zone (CZ)? (10) How does MAPK signalling pathway regulate lens epithelial cell proliferation? Furthermore, based on the location of lens epithelial cell proliferation and the function of FGF-2 and MAPK and PI3-K signalling pathways in regulating cell proliferation, two hypotheses were made: (1) FGF-2 level was higher at the equator than in the anterior and posterior lens capsule; (2) the higher level of FGF-2 induced more protein phosphorylation in the MAPK and PI3-K signalling pathways in the peripheral lens epithelium.

5.1 Summary of this study's main results

Chapter 2:

- Cell proliferation was mainly restricted to the GZ of the epithelium in the young bovine, rabbit and rat lenses, but some proliferating cells were observed in the CZ. However, the cell proliferation was only observed in the GZ of the lens epithelium in 30-90-year-old people. (Section 2.4.1.1)

- The proliferation index decreased with age in the human lens epithelium. (Section 2.4.1.1)

- In the human capsular bags with IOLs and variable degrees of PCO, cell proliferation was still mainly restricted to the periphery where the GZ used to be. (Section 2.4.1.1)

- The apoptotic cell numbers were very low in the epithelia of the young bovine, mouse and rat lenses. In addition, in the 46-81-year-old human lenses and in the human capsular bags implanted with IOLs the cell numbers were also low. (Section 2.4.1.2)

- The numbers of newly-formed cells (the number of proliferating cells) in the lens epithelium, for the 30-month-old bovine and 6-month-old rabbits, was greater than the number of lost cells (number of apoptotic cells + number of differentiating cells at the end of the TZ). However in the 30-50-year-old and 80-90-year-old human lenses, the number of the lost cells was greater than the number of newly-formed cells in the lens epithelium. (Section 2.4.1.3)

- In the young bovine, mouse, rat and rabbit lenses, the epithelial cell density remained unchanged in the CZ, increased dramatically in the GZ and decreased slowly in the TZ. In the human lenses from the 20-90-year-old donors, the epithelial cell density started to increase from the outer CZ until the end of the TZ, and cell density decreased with age in the GZ and the TZ. No significant difference was present for the lens epithelial cell density in female and male lenses. (Section 2.4.2)

- In the epithelia of the bovine, mouse, rat, rabbit and human lenses, the cell cross-sectional area decreased in the GZ, but the cell height increased quickly from the GZ to the TZ, especially in the periphery of the TZ. The cell volume of the bovine lens epithelium only decreased at the position with the highest cell density in the GZ and was similar in the rest of regions. In the human lens epithelium, the cell volume continually but slowly decreased from the CZ to the TZ. Moreover, the epithelial cell cross-sectional area and volume increased with age in the human lens. (Section 2.4.3.1 and 2.4.3.2)

- In the epithelia of the bovine, mouse, rat, rabbit and human lenses, cells became hexagonal in the meridional lines of the TZ, while they were polygonal in the other regions (Section 2.4.3.1)

- In the human capsular bags implanted with IOLs and with variable degrees of PCO, the majority of the cells still retained the original morphology and were shown as a single layer in the periphery of the anterior lens capsule. On the posterior lens capsule, the cells elongated and formed a multilayer or a monolayer sheet. The cells along the rhexis elongated dramatically and interwove into a network to surround the rhexis. (Section 2.4.3.3)

- Nuclear volume of the bovine lens epithelial cells remained stable in the CZ, decreased in the GZ and then started to increase in the TZ. Nuclear volume of the human lens epithelial cells was slightly bigger in the inner side of the CZ than in the rest of the regions. The karyoplasmic ratio (the ratio of the nucleus volume to cell volume) remained constant across the lens epithelium in bovine and human. (Section 2.4.3.4)

- In the bovine and human lens epithelial cells, immunofluorescence staining of γ-tubulin, pericentrin and ZO-1 were absent from the cells in the peripheral meridional lines in the TZ. The cytoskeleton organisation of α-tubulin and F-actin also changed in these cells. In the middle of the meridional lines, many staining foci were detected and their number was higher than the cell number there. The γ-tubulin staining was present in all the cells in the similar region in the human lens capsular bags with IOLs. (Section 2.4.4)

Chapter 3

- Gradients of FGF-2 and perlecan distribution were present on the inner surface of the bovine lens capsule, and their levels were significantly higher at the equator than in the anterior and posterior. (Section 3.4.1)

- The meshwork of the lens capsule was very dense in the inner surface but loose in the outer surface. (Section 3.4.2)

Chapter 4

- The levels of phosphorylated MAPK and PI3-K signalling proteins were higher in the GZ+TZ than in the CZ of the bovine lens epithelium. (Section 4.4.1)

- FGF-2 increased the phosphorylated ERK1/2 level and cell proliferation index. (Section 4.4.2)

- Phosphorylated ERK1/2 was associated with spindle poles and the spindle during the M phase of the cell cycle. (Section 4.4.3)

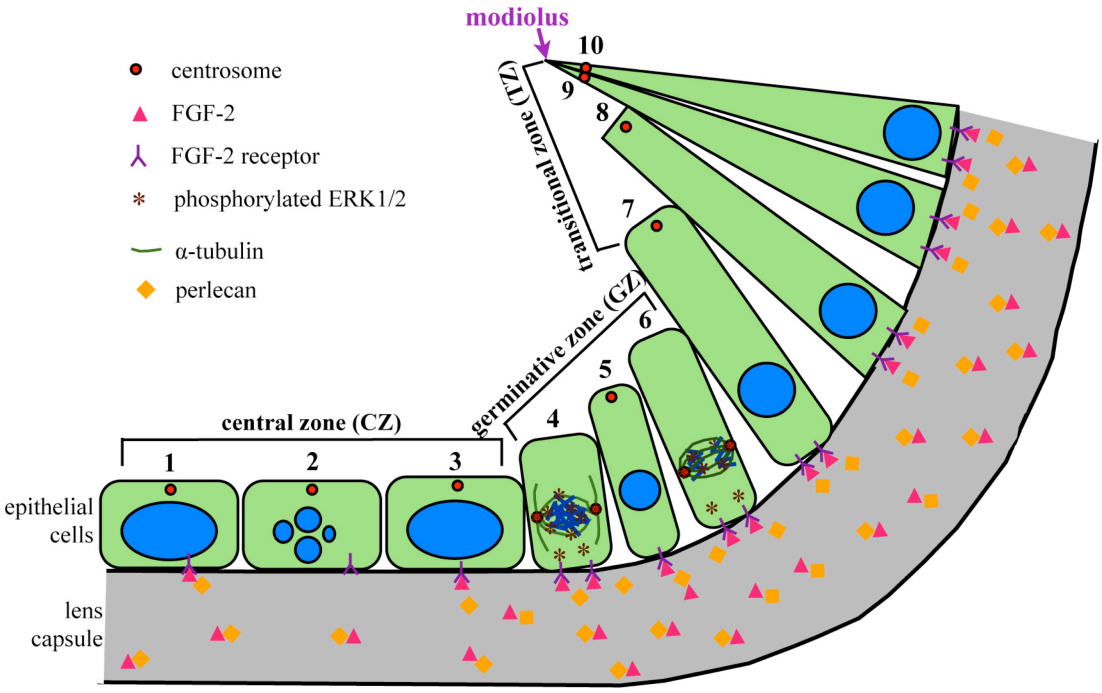

Figure 5.1 The summary diagram of this thesis's main results.

The lens epithelium is divided into three zones according to cell proliferation ability: the CZ, the GZ and the TZ. Cell proliferation mainly occurs in the GZ (section 2.4.1.1). A higher level of FGF-2 and its binding partner perlecan is detected at the equator of the inner lens capsule surface, where the GZ is located (section 3.4.1). FGF-2 induces cell proliferation by phosphorylating ERK1/2 in the cytoplasm. Phosphorylated ERK1/2 translocates to the spindle poles and the spindle during the M phase of the cell cycle (cell 4 and 6) (section 4.4). Only a very low number of cells undergo cell apoptosis in the lens epithelium (cell 2) (section 2.4.1.2). Epithelial cell density is low in the CZ, increases dramatically in the GZ, and then starts to decrease in the TZ (section 2.4.2). With the cell density change, cell cross-sectional area decreases a lot in the GZ. Cell height increases quickly from the GZ to the TZ. Cell volume does not change much across the lens epithelium, except decreasing quickly in the GZ with the highest cell density (cell 5) (section 2.4.3.1). The centrosomes are located at the apical sides of the epithelial cells. In the further half of the meridional lines in the TZ, the cell apical ends taper (cell 9 and10) and associate together to form a special structure called the modiolus, and the centrosomes also accumulate at the modiolus (section 2.4.4).

5.2 Cell organisation in the mammalian lens epithelium is specific to their functions

The crystalline lens is a transparent, biconvex structure in the eye that helps to refract light to be focused on the retina. The single layer of lens epithelium is located in the anterior portion of the lens between the lens capsule and the lens fibre cells. The main functions of the lens epithelium are to maintain the lens transparency by regulating the homeostasis of the lens and to provide new cells for lens growth (Dahm *et al.*, 2011). Cell organisation in the lens epithelium must specifically fit in with these functions. The results in the present study indicate that the ordered organisation of the polarized epithelial cells could be crucial for the solute and water transfer between the aqueous humour and the fibre mass. Moreover, by continuous proliferation in the GZ, the lens epithelium serves as the progenitor for new lens fibre cells. The results presented here also suggest that the cells in the periphery of the lens epithelium already prepare for cell migration and fibre cell differentiation. The cell organisation of the lens epithelium is unique in the mammalian epithelia. Although the other component of the eye's optical system, the cornea, has the same light refraction function, its epithelium consists of a multilayer of cells with the columnar proliferative cells at the basal layer and the flat mature squamous cells on the top (Agrawal and Tsai, 2003). This is because the corneal epithelium also acts as a barrier to protect the corneal interior from becoming infected by noxious environmental agents besides retaining cornea transparency.

Disruption of the apical junctions in the peripheral lens epithelial cells induces abnormal cell organisation and decreased cell proliferation, which ultimately result in smaller lenses and cataract in mice (Sugiyama *et al.*, 2009). In the present study, the mild nuclear cataract in the 80-90-year-old lenses may be related to the decrease of cell density and proliferation index. These suggest that changes in cell organisation can influence the functions of the lens epithelium and result in the development of cataract.

5.3 Ageing, cataract and PCO influences cell organisation in the mammalian lens epithelium

The cells in the GZ of the lens epithelium continuously proliferate throughout life, while lens volume cannot increase indefinitely because of space limitations within the eye and the need for a refractive index gradient to minimise the focal length (Augusteyn, 2008). Therefore, some lens properties such as lens dimension, fibre cell compaction and lens stiffness change with age (Augusteyn, 2008; Augusteyn, 2010). The results in the present study suggest that ageing also results in some changes in cell organisation of the lens epithelium. The decreased proliferation index could reduce the lens growth speed. The altered epithelial cell size and density might influence water and other metabolite transportation across the lens epithelium.

With lens growth, protein damage increases in the lens cells and α-crystallin continually loses its chaperone activity because of its age-related post-translational modifications (Grey and Schey, 2009; Michael and Bron, 2011; Sharma and Santhoshkumar, 2009). Furthermore, the UV filter changes and the oxidation in the lens nucleus increases (Truscott, 2005; Truscott and Zhu, 2010). All these lead to the development of age-related cataract. Previous studies show that the development of cataract is correlated with some changes in lens epithelial cell organisation, such as the increase in cell apoptosis and decrease in cell proliferation and cell density (Lee *et al.*, 2002; Liu *et al.*, 2000). Although lenses with severe cataract were not included in the present study, mild nuclear cataract was observed in those lenses from very old donors. The results about their lens epithelial cell organisation were consistent with previous density studies (Lee *et al.*, 2002; Liu *et al.*, 2000); but were slightly different from those from younger lenses without cataract. This means that cell organisation in the lens epithelium already changes at the beginning of cataract development.

Surgery is the only method to treat cataract (Asbell *et al.*, 2005). Although cataract surgery is one of the safest and most effective types of surgery, the development of PCO, which is the commonest complication of cataract surgery and also called “after cataract”, can lead to the loss of vision again and patients need to undergo a second surgery in order to restore vision (Spalton, 1999). The results in the present study showed that the majority of the cells in the periphery of the anterior capsular bags with PCO still retained their proliferation ability and original polygonal morphology and were shown as a single layer. This suggests possibilities for the

prevention of PCO and for human lens regeneration. The destruction of the peripheral lens epithelial cell organisation by some drugs during cataract surgery might decrease the proliferation ability of those residual cells. The regeneration of a new lens after removing the fibre mass has succeeded in studies on rabbits and rats (Gwon, 2006; Huang and Xie, 2010; Liu *et al.*, 2008; Lois *et al.*, 2010). The retention of cell proliferation ability and morphology in the peripheral epithelial cells suggests the possibility to regenerate a new lens instead of implanting an artificial IOL after cataract surgery. Furthermore, it is the wound-healing process, which is initiated by the cataract surgery, that leads to cell transdifferentiation, matrix deposition and contraction and cell multilayering during PCO development. Growth factors including TGFβ, FGF-2, EGF and HGF regulate those processes by Smad signalling pathway, Smad-independent signalling pathway or MAPK signalling pathway (Wormstone *et al.*, 2009). PCO is possibly suppressed or prevented if the inhibitors of these signalling pathways are safely introduced to the lens capsule after cataract surgery.

5.4 A Single model could explain the cell organisation in the mammalian lens epithelium

Computational and mathematical modelling provides a useful tool to study biological systems and has been used in the studies on lens suture formation, lens capsule biomechanics after cataract surgery and the morphogenesis of the late vertebrate lens (Kuszak *et al.*, 2004b; Marzec and Hendrix, 1997; Pedrigi and Humphrey, 2011). In the present study, the consistency of the epithelial cell organisation in different mammalian lenses suggests that a single model might explain the cell organisation in the mammalian lens epithelium. Age would be an important parameter of this model. This model could help to better understand the changes of the lens epithelial cell organisation with age. It might also be helpful in predicting cataract development in the old lenses.

5.5 Future work

With the help of some specialists who have system modelling experience, a mathematical model can be made in the future to show the cell organisation in the lens epithelium. The location of epithelial cell proliferation, the proliferation index,

the apoptotic cell number, cell density, cell size, the FGF-2 level in the lens capsule and lens age could be the main parameters of this model.

In Chapter 2, an FGF-2 gradient was detected in the inner surface of the bovine lens capsule, and a significantly higher level of FGF-2 was present at the equator. In chapter 3, the levels of phosphorylated MAPK and PI3-K signalling proteins were higher in the GZ+TZ than in the CZ of the bovine lens epithelium, and FGF-2 was found to induce lens epithelial cell proliferation by activating ERK1/2. FGF-2 acts on the lens epithelial cells by binding to its receptors (FGFRs) on the cell membrane. Therefore, a hypothesis can be made that the cells in the GZ and the TZ may have more FGFRs in order to bind the higher level of FGF-2 and lead to cell proliferation and preparation for fibre cell differentiation. Studying this hypothesis will help to further understand how FGF-2 regulates lens epithelial cell proliferation and fibre cell differentiation. Moreover, a previous study found that the expressions of FGFRs have distinct spatiotemporal patterns during lens development (de Iongh *et al.*, 1997). In embryonic and neonatal rats, FGFR3 expression has an antero-posterior increase and is strongest in the outer cortical fibres; and one pattern of FGFR2 is expressed more in the TZ than in the GZ (de Iongh *et al.*, 1997). Based on this study, the expression of FGFR2 and FGFR3 in the bovine lens epithelial cells can in the future be detected by immunoblotting and immunofluoresence.

In addition, the FGF-2 antagonists, Spry and Sef, have been found to be mainly expressed in the epithelial cells after mouse birth (Boros *et al.*, 2006). Based on the fact that cell proliferation and differentiation occur in the periphery of the lens epithelium, it is hypothesised that the levels of Spry and Sef might be lower in the GZ and the TZ than in the CZ. The study of this hypothesis will help to understand how FGF-2 regulates lens epithelial cell proliferation and fibre cell differentiation by its antagonists. The expression of Spry and Sef in the bovine lens epithelial cells can also be detected by immunoblotting and immunofluoresence in a future study.

In summary, the compact cell organisation in the lens epithelium acts as a base for the crystalline lens to retain its transparency. The continuous cell proliferation in the GZ and the low apoptosis rate ensure consistent lens growth throughout life. The dramatic increase in cell density in the GZ may result in high population pressure and push cells to migrate to the TZ. In preparation for fibre cell differentiation, a fast cell elongation process and tight apical association are apparent in the TZ of the epithelium. All these epithelial cell characteristics are specific to their function,

supporting the growth of the lens. Age and other potential risk factors influence these characteristics and result in cataract. The continuous proliferation and epithelial-mesenchymal transition of the residual epithelial cells after cataract surgery cause the development of PCO. Due to the important roles of the upstream growth factor FGF-2 and activated MAPK signalling pathway in lens epithelial cell proliferation, appropriate inhibition may prevent the occurrence of PCO and prevent the loss of restored vision.

6 References

Agrawal, V. B., and Tsai, R. J. (2003). Corneal epithelial wound healing. Indian J Ophthalmol *51*, 5-15.

Al-Ghoul, K. J., Nordgren, R. K., Kuszak, A. J., Freel, C. D., Costello, M. J., and Kuszak, J. R. (2001). Structural evidence of human nuclear fiber compaction as a function of ageing and cataractogenesis. Exp Eye Res *72*, 199-214.

Alizadeh, A., Clark, J., Seeberger, T., Hess, J., Blankenship, T., and FitzGerald, P. G. (2003). Targeted deletion of the lens fiber cell-specific intermediate filament protein filensin. Invest Ophthalmol Vis Sci *44*, 5252-5258.

Alizadeh, A., Clark, J. I., Seeberger, T., Hess, J., Blankenship, T., Spicer, A., and FitzGerald, P. G. (2002). Targeted genomic deletion of the lens-specific intermediate filament protein CP49. Invest Ophthalmol Vis Sci *43*, 3722-3727.

Andree, H. A., Reutelingsperger, C. P., Hauptmann, R., Hemker, H. C., Hermens, W. T., and Willems, G. M. (1990). Binding of vascular anticoagulant alpha (VAC alpha) to planar phospholipid bilayers. J Biol Chem *265*, 4923-4928.

Argento, C., and Zarate, J. (1990). Study of the lens epithelial cell density in cataractous eyes operated on with extracapsular and intercapsular techniques. J Cataract Refract Surg *16*, 207-210.

Arnold, D. R., Moshayedi, P., Schoen, T. J., Jones, B. E., Chader, G. J., and Waldbillig, R. J. (1993). Distribution of IGF-I and -II, IGF binding proteins (IGFBPs) and IGFBP mRNA in ocular fluids and tissues: potential sites of synthesis of IGFBPs in aqueous and vitreous. Exp Eye Res *56*, 555-565.

Asbell, P. A., Dualan, I., Mindel, J., Brocks, D., Ahmad, M., and Epstein, S. (2005). Age-related cataract. Lancet *365*, 599-609.

Ashery-Padan, R., Marquardt, T., Zhou, X., and Gruss, P. (2000). Pax6 activity in the lens primordium is required for lens formation and for correct placement of a single retina in the eye. Genes Dev *14*, 2701-2711.

Atchison, D. A., Markwell, E. L., Kasthurirangan, S., Pope, J. M., Smith, G., and Swann, P. G. (2008). Age-related changes in optical and biometric characteristics of emmetropic eyes. J Vis *8*, 1-20.

Augusteyn, R. C. (2007a). Growth of the human eye lens. Mol Vis *13*, 252-257.

Augusteyn, R. C. (2007b). On the relationship between rabbit age and lens dry weight: improved determination of the age of rabbits in the wild. Mol Vis *13*, 2030-2034.

Augusteyn, R. C. (2008). Growth of the lens: in vitro observations. Clin Exp Optom *91*, 226-239.

Augusteyn, R. C. (2010). On the growth and internal structure of the human lens. Exp Eye Res *90*, 643-654.

Augusteyn, R. C., Coulson, G., and Landman, K. A. (2003a). Determining kangaroo age from lens protein content. Australian Journal of Zoology *51*, 485-494.

Augusteyn, R. C., Coulson, G. M., and Landma, K. A. (2003b). Determining kangaroo age from lens protein content. Aust J Zool *51*, 485-494.

Augusteyn, R. C., Jones, C. E., and Pope, J. M. (2008). Age-related development of a refractive index plateau in the human lens: evidence for a distinct nucleus. Clinical & experimental optometry : journal of the Australian Optometrical Association *91*, 296-301.

Awasthi, N., and Wagner, B. J. (2006). Suppression of human lens epithelial cell proliferation by proteasome inhibition, a potential defense against posterior capsular opacification. Invest Ophthalmol Vis Sci *47*, 4482-4489.
Ayala, M., Strid, H., Jacobsson, U., and Soderberg, P. G. (2007). p53 expression and apoptosis in the lens after ultraviolet radiation exposure. Invest Ophthalmol Vis Sci *48*, 4187-4191.
Azan, G., Low, W. C., Wendelschafer-Crabb, G., Ikramuddin, S., and Kennedy, W. R. (2011). Evidence for neural progenitor cells in the human adult enteric nervous system. Cell and tissue research *334*, 217-225.
Bacskulin, A., Bergmann, U., Horoczi, Z., and Guthoff, R. (1995). Continuous ultrasound biomicroscopic imaging of accommodative changes in the human ciliary body. Klin Monbl Augenheilkd *207*, 247-252.
Bacskulin, A., Gast, R., Bergmann, U., and Guthoff, R. (1996). Ultrasound biomicroscopy imaging of accommodative configuration changes in the presbyopic ciliary body. Ophthalmologe *93*, 199-203.
Balaram, M., Tung, W. H., Kuszak, J. R., Ayaki, M., Shinohara, T., and Chylack, L. T., Jr. (2000). Noncontact specular microscopy of human lens epithelium. Invest Ophthalmol Vis Sci *41*, 474-481.
Ball, L. E., Little, M., Nowak, M. W., Garland, D. L., Crouch, R. K., and Schey, K. L. (2003). Water permeability of C-terminally truncated aquaporin 0 (AQP0 1-243) observed in the aging human lens. Invest Ophthalmol Vis Sci *44*, 4820-4828.
Banerjee, P. R., Pande, A., Patrosz, J., Thurston, G. M., and Pande, J. (2011). Cataract-associated mutant E107A of human gammaD-crystallin shows increased attraction to alpha-crystallin and enhanced light scattering. Proc Natl Acad Sci U S A *108*, 574-579.
Barker, N., van de Wetering, M., and Clevers, H. (2008). The intestinal stem cell. Genes Dev *22*, 1856-1864.
Barker, N., van Es, J. H., Kuipers, J., Kujala, P., van den Born, M., Cozijnsen, M., Haegebarth, A., Korving, J., Begthel, H., Peters, P. J., and Clevers, H. (2007). Identification of stem cells in small intestine and colon by marker gene Lgr5. Nature *449*, 1003-1007.
Bassnett, S. (2002). Lens organelle degradation. Exp Eye Res *74*, 1-6.
Bassnett, S. (2005). Three-dimensional reconstruction of cells in the living lens: the relationship between cell length and volume. Exp Eye Res *81*, 716-723.
Bassnett, S. (2009). On the mechanism of organelle degradation in the vertebrate lens. Exp Eye Res *88*, 133-139.
Bassnett, S., and Beebe, D. C. (1990). Localization of insulin-like growth factor-1 binding sites in the embryonic chicken eye. Invest Ophthalmol Vis Sci *31*, 1637-1643.
Bassnett, S., and Mataic, D. (1997). Chromatin degradation in differentiating fiber cells of the eye lens. J Cell Biol *137*, 37-49.
Bassnett, S., Missey, H., and Vucemilo, I. (1999). Molecular architecture of the lens fiber cell basal membrane complex. J Cell Sci *112 (Pt 13)*, 2155-2165.
Bassnett, S., and Winzenburger, P. A. (2003). Morphometric analysis of fibre cell growth in the developing chicken lens. Exp Eye Res *76*, 291-302.
Beebe D. C., J. M. C., Feagans D. E., Compart P. J. (1980). The mechanism of cell elongation during lens fibre cell differentiation Ocular size and shape regulation during development New York, Springer 79-98.
Beebe, D. C., Compart, P. J., Johnson, M. C., Feagans, D. E., and Feinberg, R. N. (1982). The mechanism of cell elongation during lens fiber cell differentiation. Dev Biol *92*, 54-59.

Beebe, D. C., Silver, M. H., Belcher, K. S., Van Wyk, J. J., Svoboda, M. E., and Zelenka, P. S. (1987). Lentropin, a protein that controls lens fiber formation, is related functionally and immunologically to the insulin-like growth factors. Proc Natl Acad Sci U S A *84*, 2327-2330.
Belecky-Adams, T. L., Adler, R., and Beebe, D. C. (2002). Bone morphogenetic protein signaling and the initiation of lens fiber cell differentiation. Development *129*, 3795-3802.
Ben-Levy, R., Hooper, S., Wilson, R., Paterson, H. F., and Marshall, C. J. (1998). Nuclear export of the stress-activated protein kinase p38 mediated by its substrate MAPKAP kinase-2. Curr Biol *8*, 1049-1057.
Bencic, G., Zoric-Geber, M., Saric, D., Corak, M., and Mandic, Z. (2005). Clinical importance of the lens opacities classification system III (LOCS III) in phacoemulsification. Coll Antropol *29 Suppl 1*, 91-94.
Berliner, M. L. (1949). Biomicroscopy of the Eye: slit lamp microscopy of the living eye: New York: Paul B Hoeber).
Bhat, S. P. (2001). The ocular lens epithelium. Biosci Rep *21*, 537-563.
Blanpain, C., and Fuchs, E. (2009). Epidermal homeostasis: a balancing act of stem cells in the skin. Nat Rev Mol Cell Biol *10*, 207-217.
Bornens, M. (2002). Centrosome composition and microtubule anchoring mechanisms. Curr Opin Cell Biol *14*, 25-34.
Boros, J., Newitt, P., Wang, Q., McAvoy, J. W., and Lovicu, F. J. (2006). Sef and Sprouty expression in the developing ocular lens: implications for regulating lens cell proliferation and differentiation. Semin Cell Dev Biol *17*, 741-752.
Bours, J., and Fodisch, H. J. (1986). Human fetal lens: wet and dry weight with increasing gestational age. Ophthalmic Res *18*, 363-368.
Bours, J., Wegener, A., Hofmann, D., Fodisch, H. J., and Hockwin, O. (1990). Protein profiles of microsections of the fetal and adult human lens during development and ageing. Mech Ageing Dev *54*, 13-27.
Bova, L. M., Sweeney, M. H., Jamie, J. F., and Truscott, R. J. (2001). Major changes in human ocular UV protection with age. Invest Ophthalmol Vis Sci *42*, 200-205.
Bozzola, J. J., Russell, L. D., and Russell, L. D. (1999). Electron microscopy: principles and techniques for biologists
. Sudbury, Massachusetts, USA, 49-71.
Bretscher, M. S. (1972). Asymmetrical lipid bilayer structure for biological membranes. Nat New Biol *236*, 11-12.
Bron, A. J., Vrensen, G. F., Koretz, J., Maraini, G., and Harding, J. J. (2000). The ageing lens. Ophthalmologica *214*, 86-104.
Brown, N. P. (1973). In The human lens-in relation to cataract. CIBA Foundation Symposium *19*, 65-78.
Brunet, A., Datta, S. R., and Greenberg, M. E. (2001). Transcription-dependent and -independent control of neuronal survival by the PI3K-Akt signaling pathway. Curr Opin Neurobiol *11*, 297-305.
Budtz, P. E. (1994). Epidermal homeostasis: a new model that includes apoptosis.: Cold spring harbor: cold spring harbor laboratory press).
Bursch, W., Paffe, S., Putz, B., Barthel, G., and Schulte-Hermann, R. (1990). Determination of the length of the histological stages of apoptosis in normal liver and in altered hepatic foci of rats. Carcinogenesis *11*, 847-853.
Campbell, M. C., and Hughes, A. (1981). An analytic, gradient index schematic lens and eye for the rat which predicts aberrations for finite pupils. Vision Res *21*, 1129-1148.

Carbe, C., and Zhang, X. (2011). Lens induction requires attenuation of ERK signaling by Nf1. Hum Mol Genet *20*, 1315-1323.
Catling, P. C., Corbett, L. K., and Wetcott, M. (1991). Age determination in the dingo and crossbreeds. Wildlife Res *18*, 75-83.
Cavalier-Smith, T. (2005). Economy, speed and size matter: evolutionary forces driving nuclear genome miniaturization and expansion. Ann Bot *95*, 147-175.
Center, E. M., and Polizotto, R. S. (1992). Etiology of the developing eye in myelencephalic blebs (my) mice. Histol Histopathol *7*, 231-236.
Chamberlain, C. G., and McAvoy, J. W. (1987). Evidence that fibroblast growth factor promotes lens fibre differentiation. Curr Eye Res *6*, 1165-1169.
Chamberlain, C. G., and McAvoy, J. W. (1989). Induction of lens fibre differentiation by acidic and basic fibroblast growth factor (FGF). Growth Factors *1*, 125-134.
Chamberlain, C. G., and McAvoy, J. W. (1997). Fiber differentiation and polarity in the mammalian lens: a key role for FGF. Prog Retinal Eye Res *16*, 443-478.
Chandrasekher, G., and Sailaja, D. (2003). Differential activation of phosphatidylinositol 3-kinase signaling during proliferation and differentiation of lens epithelial cells. Invest Ophthalmol Vis Sci *44*, 4400-4411.
Charakidas, A., Kalogeraki, A., Tsilimbaris, M., Koukoulomatis, P., Brouzas, D., and Delides, G. (2005). Lens epithelial apoptosis and cell proliferation in human age-related cortical cataract. Eur J Ophthalmol *15*, 213-220.
Chen, Z., Gibson, T. B., Robinson, F., Silvestro, L., Pearson, G., Xu, B., Wright, A., Vanderbilt, C., and Cobb, M. H. (2001). MAP kinases. Chemical reviews *101*, 2449-2476.
Chow, R. L., Altmann, C. R., Lang, R. A., and Hemmati-Brivanlou, A. (1999). Pax6 induces ectopic eyes in a vertebrate. Development *126*, 4213-4222.
Chowdhury, U. R., Madden, B. J., Charlesworth, M. C., and Fautsch, M. P. (2010). Proteome analysis of human aqueous humor. Invest Ophthalmol Vis Sci *51*, 4921-4931.
Christen, W. G., Glynn, R. J., Ajani, U. A., Schaumberg, D. A., Buring, J. E., Hennekens, C. H., and Manson, J. E. (2000). Smoking cessation and risk of age-related cataract in men. Jama *284*, 713-716.
Chu, C. L., Goerges, A. L., and Nugent, M. A. (2005). Identification of common and specific growth factor binding sites in heparan sulfate proteoglycans. Biochemistry *44*, 12203-12213.
Chuderland, D., Konson, A., and Seger, R. (2008). Identification and characterization of a general nuclear translocation signal in signaling proteins. Mol Cell *31*, 850-861.
Chylack, L. T., Jr., Wolfe, J. K., Singer, D. M., Leske, M. C., Bullimore, M. A., Bailey, I. L., Friend, J., McCarthy, D., and Wu, S. Y. (1993). The Lens Opacities Classification System III. The Longitudinal Study of Cataract Study Group. Arch Ophthalmol *111*, 831-836.
Coller, H. A., Grandori, C., Tamayo, P., Colbert, T., Lander, E. S., Eisenman, R. N., and Golub, T. R. (2000). Expression analysis with oligonucleotide microarrays reveals that MYC regulates genes involved in growth, cell cycle, signaling, and adhesion. Proc Natl Acad Sci U S A *97*, 3260-3265.
Conley, Y. P., Erturk, D., Keverline, A., Mah, T. S., Keravala, A., Barnes, L. R., Bruchis, A., Hess, J. F., FitzGerald, P. G., Weeks, D. E.*, et al.* (2000). A juvenile-onset, progressive cataract locus on chromosome 3q21-q22 is associated with a missense mutation in the beaded filament structural protein-2. Am J Hum Genet *66*, 1426-1431.

Connolly, G. E., Dudzinski, M. L., and Longhurst, W. M. (1969). The eye lens as an indicator of age in the blacktailed jack rabbit. J Wildlife Mgment *33*, 159-164.
Coulombre, J. L., and Coulombre, A. J. (1963). Lens Development: Fiber Elongation and Lens Orientation. Science *142*, 1489-1490.
Creutz, C. E. (1992). The annexins and exocytosis. Science *258*, 924-931.
Cross, D. A., Alessi, D. R., Cohen, P., Andjelkovich, M., and Hemmings, B. A. (1995). Inhibition of glycogen synthase kinase-3 by insulin mediated by protein kinase B. Nature *378*, 785-789.
Cruickshanks, K. J., Klein, B. E., and Klein, R. (1992). Ultraviolet light exposure and lens opacities: the Beaver Dam Eye Study. Am J Public Health *82*, 1658-1662.
Csato, W. (1989). Development and characterization of the lens capsule of mouse embryos (day 12 to day 19 of gestation). Z Mikrosk Anat Forsch *103*, 971-984.
Cui, W., Tomarev, S. I., Piatigorsky, J., Chepelinsky, A. B., and Duncan, M. K. (2004). Mafs, Prox1, and Pax6 can regulate chicken betaB1-crystallin gene expression. J Biol Chem *279*, 11088-11095.
Cui, X., Gao, L., Jin, Y., Zhang, Y., Bai, J., Feng, G., Gao, W., Liu, P., He, L., and Fu, S. (2007). The E233del mutation in BFSP2 causes a progressive autosomal dominant congenital cataract in a Chinese family. Mol Vis *13*, 2023-2029.
Dahm, R. (1999). Lens fibre cell differentiation - A link with apoptosis? Ophthalmic Res *31*, 163-183.
Dahm, R., Gribbon, C., Quinlan, R. A., and Prescott, A. R. (1998). Changes in the nucleolar and coiled body compartments precede lamina and chromatin reorganization during fibre cell denucleation in the bovine lens. Eur J Cell Biol *75*, 237-246.
Dahm, R., and Prescott, A. R. (2002). Morphological changes and nuclear pore clustering during nuclear degradation in differentiating bovine lens fibre cells. Ophthalmic Res *34*, 288-294.
Dahm, R., Procter, J. E., Ireland, M. E., Lo, W. K., Mogensen, M. M., Quinlan, R. A., and Prescott, A. R. (2007a). Reorganization of centrosomal marker proteins coincides with epithelial cell differentiation in the vertebrate lens. Exp Eye Res *85*, 696-713.
Dahm, R., Schonthaler, H. B., Soehn, A. S., van Marle, J., and Vrensen, G. F. (2007b). Development and adult morphology of the eye lens in the zebrafish. Exp Eye Res *85*, 74-89.
Dahm, R., van Marle, J., Quinlan, R. A., Prescott, A. R., and Vrensen, G. F. (2011). Homeostasis in the vertebrate lens: mechanisms of solute exchange. Philos Trans R Soc Lond B Biol Sci *366*, 1265-1277.
Dailey, L., Ambrosetti, D., Mansukhani, A., and Basilico, C. (2005). Mechanisms underlying differential responses to FGF signaling. Cytokine Growth Factor Rev *16*, 233-247.
Danysh, B. P., and Duncan, M. K. (2009). The lens capsule. Exp Eye Res *88*, 151-164.
Danysh, B. P., Patel, T. P., Czymmek, K. J., Edwards, D. A., Wang, L., Pande, J., and Duncan, M. K. (2010). Characterizing molecular diffusion in the lens capsule. Matrix Biol *29*, 228-236.
Davison, J. A., and Chylack, L. T. (2003). Clinical application of the lens opacities classification system III in the performance of phacoemulsification. J Cataract Refract Surg *29*, 138-145.
de Iongh, R. U., Gordon-Thomson, C., Chamberlain, C. G., Hales, A. M., and McAvoy, J. W. (2001a). Tgfbeta receptor expression in lens: implications for differentiation and cataractogenesis. Exp Eye Res *72*, 649-659.

de Iongh, R. U., Lovicu, F. J., Chamberlain, C. G., and McAvoy, J. W. (1997). Differential expression of fibroblast growth factor receptors during rat lens morphogenesis and growth. Invest Ophthalmol Vis Sci *38*, 1688-1699.
de Iongh, R. U., Lovicu, F. J., Overbeek, P. A., Schneider, M. D., Joya, J., Hardeman, E. D., and McAvoy, J. W. (2001b). Requirement for TGFbeta receptor signaling during terminal lens fiber differentiation. Development *128*, 3995-4010.
De Maria, A., and Bassnett, S. (2007). DNase IIbeta distribution and activity in the mouse lens. Invest Ophthalmol Vis Sci *48*, 5638-5646.
Delaval, B., and Doxsey, S. J. (2010). Pericentrin in cellular function and disease. J Cell Biol *188*, 181-190.
Delcourt, C., Cristol, J. P., Tessier, F., Leger, C. L., Michel, F., and Papoz, L. (2000). Risk factors for cortical, nuclear, and posterior subcapsular cataracts: the POLA study. Pathologies Oculaires Liees a l'Age. Am J Epidemiol *151*, 497-504.
Delcourt, C., Dupuy, A. M., Carriere, I., Lacroux, A., and Cristol, J. P. (2005). Albumin and transthyretin as risk factors for cataract: the POLA study. Arch Ophthalmol *123*, 225-232.
Devi, R. R., Yao, W., Vijayalakshmi, P., Sergeev, Y. V., Sundaresan, P., and Hejtmancik, J. F. (2008). Crystallin gene mutations in Indian families with inherited pediatric cataract. Mol Vis *14*, 1157-1170.
Diehl, J. A., Cheng, M., Roussel, M. F., and Sherr, C. J. (1998). Glycogen synthase kinase-3beta regulates cyclin D1 proteolysis and subcellular localization. Genes Dev *12*, 3499-3511.
Dilmen, G., Koktener, A., Turhan, N. O., and Tez, S. (2002). Growth of the fetal lens and orbit. Int J Gynaecol Obstet *76*, 267-271.
Dong, C., Yang, D. D., Tournier, C., Whitmarsh, A. J., Xu, J., Davis, R. J., and Flavell, R. A. (2000). JNK is required for effector T-cell function but not for T-cell activation. Nature *405*, 91-94.
Dong, C., Yang, D. D., Wysk, M., Whitmarsh, A. J., Davis, R. J., and Flavell, R. A. (1998). Defective T cell differentiation in the absence of Jnk1. Science *282*, 2092-2095.
Donner, A. L., Lachke, S. A., and Maas, R. L. (2006). Lens induction in vertebrates: variations on a conserved theme of signaling events. Semin Cell Dev Biol *17*, 676-685.
Doxsey, S., Zimmerman, W., and Mikule, K. (2005). Centrosome control of the cell cycle. Trends Cell Biol *15*, 303-311.
Doxsey, S. J., Stein, P., Evans, L., Calarco, P. D., and Kirschner, M. (1994). Pericentrin, a highly conserved centrosome protein involved in microtubule organization. Cell *76*, 639-650.
Duke-Elder, S., and Cook, C. (1963). System of ophthalmology. Vol.III. Normal and Abnormal Development.: St. Louis: CV Mosby;).
Easter, S. S., Jr., and Nicola, G. N. (1996). The development of vision in the zebrafish (Danio rerio). Dev Biol *180*, 646-663.
Endl, E., and Gerdes, J. (2000). The Ki-67 protein: fascinating forms and an unknown function. Exp Cell Res *257*, 231-237.
Evans, B. J. (2007). Monovision: a review. Ophthalmic Physiol Opt *27*, 417-439.
Faber, S. C., Dimanlig, P., Makarenkova, H. P., Shirke, S., Ko, K., and Lang, R. A. (2001). Fgf receptor signaling plays a role in lens induction. Development *128*, 4425-4438.

Faber, S. C., Robinson, M. L., Makarenkova, H. P., and Lang, R. A. (2002). Bmp signaling is required for development of primary lens fiber cells. Development *129*, 3727-3737.
Fadok, V. A., Laszlo, D. J., Noble, P. W., Weinstein, L., Riches, D. W., and Henson, P. M. (1993). Particle digestibility is required for induction of the phosphatidylserine recognition mechanism used by murine macrophages to phagocytose apoptotic cells. J Immunol *151*, 4274-4285.
Fadok, V. A., Voelker, D. R., Campbell, P. A., Cohen, J. J., Bratton, D. L., and Henson, P. M. (1992a). Exposure of phosphatidylserine on the surface of apoptotic lymphocytes triggers specific recognition and removal by macrophages. J Immunol *148*, 2207-2216.
Fadok, V. A., Voelker, D. R., Campbell, P. A., Cohen, J. J., Bratton, D. L., and Henson, P. M. (1992b). Exposure of phosphatidylserine on the surface of apoptotic lymphocytes triggers specific recognition and removal by macrophages. J Immunol *148*, 2207-2216.
Fagerholm, P. P., and Philipson, B. T. (1981). Human lens epithelium in normal and cataractous lenses. Invest Ophthalmol Vis Sci *21*, 408-414.
Farnsworth, P. N., and Shyne, S. E. (1979). Anterior zonular shifts with age. Exp Eye Res *28*, 291-297.
Favata, M. F., Horiuchi, K. Y., Manos, E. J., Daulerio, A. J., Stradley, D. A., Feeser, W. S., Van Dyk, D. E., Pitts, W. J., Earl, R. A., Hobbs, F.*, et al.* (1998). Identification of a novel inhibitor of mitogen-activated protein kinase kinase. J Biol Chem *273*, 18623-18632.
Ferrini, W., Schorderet, D. F., Othenin-Girard, P., Uffer, S., Heon, E., and Munier, F. L. (2004). CRYBA3/A1 gene mutation associated with suture-sparing autosomal dominant congenital nuclear cataract: a novel phenotype. Invest Ophthalmol Vis Sci *45*, 1436-1441.
Finch, P. W., Cunha, G. R., Rubin, J. S., Wong, J., and Ron, D. (1995). Pattern of keratinocyte growth factor and keratinocyte growth factor receptor expression during mouse fetal development suggests a role in mediating morphogenetic mesenchymal-epithelial interactions. Dev Dyn *203*, 223-240.
Fisher, M., and Grainger, R. M. (2004). Lens induction and determination. In: F.J. Lovicu and M.L. Robinson, Editors, Development of the ocular lens, Cambridge University Press, New York).
Fisher, R. F. (1977). Changes in the permeability of the lens capsule in senile cataract. Trans Ophthalmol Soc U K *97*, 100-103.
Fredriksson, L., Li, H., and Eriksson, U. (2004). The PDGF family: four gene products form five dimeric isoforms. Cytokine Growth Factor Rev *15*, 197-204.
Friend, M. (1967). A review of research concerning eye-lens mass as a criterion of age in animals. NY Fish Game J *14*, 152-165.
Fujiwara H, F. M., Donati G, Marciano DK, Linton JM, Sato Y, Hartner A, Sekiguchi K, Reichardt LF, Watt FM. (2011). The basement membrane of hair follicle stem cells is a muscle cell niche. Cell *144*, 577-589.
Galaktionov, K., Chen, X., and Beach, D. (1996). Cdc25 cell-cycle phosphatase as a target of c-myc. Nature *382*, 511-517.
Gao, D., Hui, Y., Ji, Q., Bai, J., and Liu, H. (1998). Cell density and expression of proliferating cell nuclear antigen (PCNA) in the lens epithelium of children and aging patients with cataract. Chinese journal of ophthalmology *34*, 355-357.

Garcia-Porrero, J. A., Collado, J. A., and Ojeda, J. L. (1979). Cell death during detachment of the lens rudiment from ectoderm in the chick embryo. Anat Rec *193*, 791-804.
Gavrieli, Y., Sherman, Y., and Ben-Sasson, S. A. (1992). Identification of programmed cell death in situ via specific labeling of nuclear DNA fragmentation. J Cell Biol *119*, 493-501.
Geatrell, J. C., Gan, P. M., Mansergh, F. C., Kisiswa, L., Jarrin, M., Williams, L. A., Evans, M. J., Boulton, M. E., and Wride, M. A. (2009). Apoptosis gene profiling reveals spatio-temporal regulated expression of the p53/Mdm2 pathway during lens development. Exp Eye Res *88*, 1137-1151.
Giblin, F. J. (2000). Glutathione: a vital lens antioxidant. J Ocul Pharmacol Ther *16*, 121-135.
Giessmann, D., Theiss, C., Breipohl, W., and Meller, K. (2005). Decreased gap junctional communication in neurobiotin microinjected lens epithelial cells after taxol treatment. Anatomy and Embryology (Berlin) 209, 391-400.).
Glasser, A. (2008). Restoration of accommodation: surgical options for correction of presbyopia. Clinical & experimental optometry : journal of the Australian Optometrical Association *91*, 279-295.
Glasser, A., and Campbell, M. C. (1998). Presbyopia and the optical changes in the human crystalline lens with age. Vision Res *38*, 209-229.
Glasser, A., and Campbell, M. C. (1999). Biometric, optical and physical changes in the isolated human crystalline lens with age in relation to presbyopia. Vision Res *39*, 1991-2015.
Glasser, A., and Kaufman, P. L. (1999). The mechanism of accommodation in primates. Ophthalmology *106*, 863-872.
Gloor, B. P., Rokos, L., and Kaldarar-Pedotti, S. (1985). Cell cycle time and life-span of cells in the mouse eye. Measurements during the postfetal period using repeated 3H-thymidine injections. Dev Ophthalmol *12*, 70-129.
Goldstein, I., Tamir, A., Zimmer, E. Z., and Itskovitz-Eldor, J. (1998). Growth of the fetal orbit and lens in normal pregnancies. Ultrasound Obstet Gynecol *12*, 175-179.
Gong, X., Wang, X., Han, J., Niesman, I., Huang, Q., and Horwitz, J. (2001). Development of cataractous macrophthalmia in mice expressing an active MEK1 in the lens. Invest Ophthalmol Vis Sci *42*, 539-548.
Gonzalez-Mariscal, L., Betanzos, A., and Avila-Flores, A. (2000). MAGUK proteins: structure and role in the tight junction. Semin Cell Dev Biol *11*, 315-324.
Govindarajan, V., and Overbeek, P. A. (2001). Secreted FGFR3, but not FGFR1, inhibits lens fiber differentiation. Development *128*, 1617-1627.
Graw, J. (2009). Mouse models of cataract. J Genet *88*, 469-486.
Greiling, T. M., Aose, M., and Clark, J. I. (2010). Cell fate and differentiation of the developing ocular lens. Invest Ophthalmol Vis Sci *51*, 1540-1546.
Greiling, T. M., and Clark, J. I. (2009). Early lens development in the zebrafish: a three-dimensional time-lapse analysis. Dev Dyn *238*, 2254-2265.
Grewal, D. S., Brar, G. S., and Grewal, S. P. (2009). Correlation of nuclear cataract lens density using Scheimpflug images with Lens Opacities Classification System III and visual function. Ophthalmology *116*, 1436-1443.
Grey, A. C., and Schey, K. L. (2009). Age-related changes in the spatial distribution of human lens alpha-crystallin products by MALDI imaging mass spectrometry. Invest Ophthalmol Vis Sci *50*, 4319-4329.
Gribbon, C., Dahm, R., Prescott, A. R., and Quinlan, R. A. (2002). Association of the nuclear matrix component NuMA with the Cajal body and nuclear speckle

compartments during transitions in transcriptional activity in lens cell differentiation. Eur J Cell Biol *81*, 557-566.
Grindley, J. C., Davidson, D. R., and Hill, R. E. (1995). The role of Pax-6 in eye and nasal development. Development *121*, 1433-1442.
Gruenbaum, Y., Margalit, A., Goldman, R. D., Shumaker, D. K., and Wilson, K. L. (2005). The nuclear lamina comes of age. Nat Rev Mol Cell Biol *6*, 21-31.
Gu, Z., Ji, B., Wan, C., He, G., Zhang, J., Zhang, M., Feng, G., He, L., and Gao, L. (2010). A splice site mutation in CRYBA1/A3 causing autosomal dominant posterior polar cataract in a Chinese pedigree. Mol Vis *16*, 154-160.
Guggenmoos-Holzmann, I., Engel, B., Henke, V., and Naumann, G. O. (1989). Cell density of human lens epithelium in women higher than in men. Invest Ophthalmol Vis Sci *30*, 330-332.
Gullapalli, V. K., Murthy, P. R., and Murthy, K. R. (1995). Colour of the nucleus as a marker of nuclear hardness, diameter and central thickness. Indian J Ophthalmol *43*, 181-184.
Gwon, A. (2006). Lens regeneration in mammals: a review. Surv Ophthalmol *51*, 51-62.
Hacohen, N., Kramer, S., Sutherland, D., Hiromi, Y., and Krasnow, M. A. (1998). sprouty encodes a novel antagonist of FGF signaling that patterns apical branching of the Drosophila airways. Cell *92*, 253-263.
Haddad, A., and Bennett, G. (1988). Synthesis of lens capsule and plasma membrane glycoproteins by lens epithelial cells and fibers in the rat. Am J Anat *183*, 212-225.
Hagen A, S. N., Ostbye E, Skar HJ. (1980). he eye lens as an age indicator in the root vole. Acta Theriol (Warsz) *25*, 39-50.
Halder G, C. P., Gehring WJ (1995). Induction of ectopic eyes by targeted expression of the eyeless gene in Drosophila. Science *267*, 1788-1792.
Hammond, C. J., Snieder, H., Spector, T. D., and Gilbert, C. E. (2000). Genetic and environmental factors in age-related nuclear cataracts in monozygotic and dizygotic twins. N Engl J Med *342*, 1786-1790.
Hara, T. (1988). Observations on lens epithelial cells and their removal in anterior capsule specimens. Arch Ophthalmol *106*, 1683-1687.
Harding, C. V., Donn, A., and Srinivasan, B. D. (1959). Incorporation of thymidine by injured lens epithelium. Exp Cell Res *18*, 582-585.
Harding, C. V., Reddan, J. R., Unakar, N. J., and Bagchi, M. (1971). The control of cell division in the ocular lens. Int Rev Cytol *31*, 215-300.
Harocopos, G. J., Alvares, K. M., Kolker, A. E., and Beebe, D. C. (1998). Human age-related cataract and lens epithelial cell death. Invest Ophthalmol Vis Sci *39*, 2696-2706.
Hass, C., Kohlmann, H., and Lommatzsch, P. K. (1995). Morphologic changes in the lens epithelium in patients with age-induced cataract, radiation and steroid cataract and cataract following eye contusion. Ophthalmologe *92*, 741-744.
Hendrix, R. W., and Rubinson, K. (1996). Cell growth patterns and lens geometry: a quantitative study from three-dimensional reconstructions. Tissue Cell *28*, 473-484.
Hetts, S. W. (1998). To die or not to die: an overview of apoptosis and its role in disease. Jama *279*, 300-307.
Heys, K. R., Cram, S. L., and Truscott, R. J. (2004). Massive increase in the stiffness of the human lens nucleus with age: the basis for presbyopia? Mol Vis *10*, 956-963.
Heys, K. R., Friedrich, M. G., and Truscott, R. J. (2007). Presbyopia and heat: changes associated with aging of the human lens suggest a functional role for the

small heat shock protein, alpha-crystallin, in maintaining lens flexibility. Aging Cell *6*, 807-815.
Hiraoka, M., Inoue, K., Ohtaka-Maruyama, C., Ohsako, S., Kojima, N., Senoo, H., and Takada, M. (2010). Intracapsular organization of ciliary zonules in monkey eyes. Anat Rec (Hoboken) *293*, 1797-1804.
Hocevar, B. A., and Howe, P. H. (1998). Mechanisms of TGF-beta-induced cell cycle arrest. Miner Electrolyte Metab *24*, 131-135.
Hockwin , B.-E. U., Light W, Noll I, Rast F (1971). Concerning the estimation of age of guinea pigs, rabbits, and chickens by means of determining their lens mass. Ophthalmic Res *2*, 77-85.
Huang, L., Grami, V., Marrero, Y., Tang, D., Yappert, M. C., Rasi, V., and Borchman, D. (2005). Human lens phospholipid changes with age and cataract. Invest Ophthalmol Vis Sci *46*, 1682-1689.
Huang, Y., and Xie, L. (2010). Expression of transcription factors and crystallin proteins during rat lens regeneration. Mol Vis *16*, 341-352.
Huber, M. D., and Gerace, L. (2007). The size-wise nucleus: nuclear volume control in eukaryotes. J Cell Biol *179*, 583-584.
Huizinga, A., Bot, A. C., de Mul, F. F., Vrensen, G. F., and Greve, J. (1989). Local variation in absolute water content of human and rabbit eye lenses measured by Raman microspectroscopy. Exp Eye Res *48*, 487-496.
Hunt, H. H. (1961). A study of the fine structure of the optic vesicle and lens placode of the chick embryo during induction. Dev Biol *3*, 175-209.
Hunter, T. (2000). Signaling--2000 and beyond. Cell *100*, 113-127.
Iozzo, R. V. (1998). Matrix proteoglycans: from molecular design to cellular function. Annu Rev Biochem *67*, 609-652.
Ishizaki, Y., Jacobson, M. D., and Raff, M. C. (1998). A role for caspases in lens fiber differentiation. J Cell Biol *140*, 153-158.
Ivanov, D., Dvoriantchikova, G., Pestova, A., Nathanson, L., and Shestopalov, V. I. (2005). Microarray analysis of fiber cell maturation in the lens. FEBS Lett *579*, 1213-1219.
Iyengar, L., Patkunanathan, B., Lynch, O. T., McAvoy, J. W., Rasko, J. E., and Lovicu, F. J. (2006). Aqueous humour- and growth factor-induced lens cell proliferation is dependent on MAPK/ERK1/2 and Akt/PI3-K signalling. Exp Eye Res *83*, 667-678.
Iyengar, L., Wang, Q., Rasko, J. E., McAvoy, J. W., and Lovicu, F. J. (2007). Duration of ERK1/2 phosphorylation induced by FGF or ocular media determines lens cell fate. Differentiation *75*, 662-668.
Jakobs, P. M., Hess, J. F., FitzGerald, P. G., Kramer, P., Weleber, R. G., and Litt, M. (2000). Autosomal-dominant congenital cataract associated with a deletion mutation in the human beaded filament protein gene BFSP2. Am J Hum Genet *66*, 1432-1436.
Jampel, H. D., Roche, N., Stark, W. J., and Roberts, A. B. (1990). Transforming growth factor-beta in human aqueous humor. Curr Eye Res *9*, 963-969.
Jones, C. E., Atchison, D. A., Meder, R., and Pope, J. M. (2005). Refractive index distribution and optical properties of the isolated human lens measured using magnetic resonance imaging (MRI). Vision Res *45*, 2352-2366.
Jorgensen, P., Edgington, N. P., Schneider, B. L., Rupes, I., Tyers, M., and Futcher, B. (2007). The size of the nucleus increases as yeast cells grow. Mol Biol Cell *18*, 3523-3532.
Kanda, H., and Miura, M. (2004). Regulatory roles of JNK in programmed cell death. J Biochem *136*, 1-6.

Karbassi, M., Khu, P. M., Singer, D. M., and Chylack, L. T., Jr. (1993). Evaluation of lens opacities classification system III applied at the slitlamp. Optom Vis Sci *70*, 923-928.
Karim, A. K., Jacob, T. J., and Thompson, G. M. (1987). The human anterior lens capsule: cell density, morphology and mitotic index in normal and cataractous lenses. Exp Eye Res *45*, 865-874.
Kasthurirangan, S., Markwell, E. L., Atchison, D. A., and Pope, J. M. (2008). In vivo study of changes in refractive index distribution in the human crystalline lens with age and accommodation. Invest Ophthalmol Vis Sci *49*, 2531-2540.
Kasthurirangan, S., Markwell, E. L., Atchison, D. A., and Pope, J. M. (2011). MRI study of the changes in crystalline lens shape with accommodation and aging in humans. J Vis *11*, 1-16.
Katso, R., Okkenhaug, K., Ahmadi, K., White, S., Timms, J., and Waterfield, M. D. (2001). Cellular function of phosphoinositide 3-kinases: implications for development, homeostasis, and cancer. Annu Rev Cell Dev Biol *17*, 615-675.
Kauffman, R. G., and Norton, H. W. (1966). Growth of the porcine lens during insufficiencies of dietary protein. Growth *30*, 463-470.
Keeney, A. H., Hagman, R. E., and Fratello, C. J. (1995). Dictionary of Ophthalmic Optics: Newton, MA, Butterworth-Heinemann).
Kelman, C. D. (1967). Phaco-emulsification and aspiration. A new technique of cataract removal. A preliminary report. Am J Ophthalmol *64*, 23-35.
Kenworthy, A. K., Magid, A. D., Oliver, T. N., and McIntosh, T. J. (1994). Colloid osmotic pressure of steer alpha- and beta-crystallins: possible functional roles for lens crystallin distribution and structural diversity. Exp Eye Res *59*, 11-30.
Kiernan, D. F., and Mieler, W. F. (2009). The use of intraocular corticosteroids. Expert Opin Pharmacother *10*, 2511-2525.
Kim, J., Kim, C. S., Sohn, E., Kim, H., Jeong, I. H., and Kim, J. S. (2010). Lens epithelial cell apoptosis initiates diabetic cataractogenesis in the Zucker diabetic fatty rat. Graefes Arch Clin Exp Ophthalmol *248*, 811-818.
Kim, J., Kim, C. S., Sohn, E., Kim, H., Jeong, I. H., and Kim, J. S. (2011). KIOM-79 Prevents Lens Epithelial Cell Apoptosis and Lens Opacification in Zucker Diabetic Fatty Rats. Evidence-based complementary and alternative medicine: eCAM *2011*, 1-10.
Kistler, J., Kirkland, B., Gilbert, K., and Bullivant, S. (1986). Aging of lens fibers. Mapping membrane proteins with monoclonal antibodies. Invest Ophthalmol Vis Sci *27*, 772-780.
Kitaoka, T., Aotaki-Keen, A. E., and Hjelmeland, L. M. (1994). Distribution of FGF-5 in the rhesus macaque retina. Invest Ophthalmol Vis Sci *35*, 3189-3198.
Klein, B. E., Klein, R., Lee, K. E., and Meuer, S. M. (2003). Socioeconomic and lifestyle factors and the 10-year incidence of age-related cataracts. Am J Ophthalmol *136*, 506-512.
Klein, B. E., Klein, R. E., and Lee, K. E. (1999). Incident cataract after a five-year interval and lifestyle factors: the Beaver Dam eye study. Ophthalmic Epidemiol *6*, 247-255.
Kojima, M., Hanazawa, M., Yamashiro, Y., Sasaki, H., Watanabe, S., Taki, M., Suzuki, Y., Hirata, A., Kamimura, Y., and Sasaki, K. (2009). Acute ocular injuries caused by 60-Ghz millimeter-wave exposure. Health physics *97*, 212-218.
Kok, A., Lovicu, F. J., Chamberlain, C. G., and McAvoy, J. W. (2002). Influence of platelet-derived growth factor on lens epithelial cell proliferation and differentiation. Growth Factors *20*, 27-34.

Kondoh, H., Uchikawa, M., and Kamachi, Y. (2004). Interplay of Pax6 and SOX2 in lens development as a paradigm of genetic switch mechanisms for cell differentiation. Int J Dev Biol *48*, 819-827.
Konofsky, K., Naumann, G. O., and Guggenmoos-Holzmann, I. (1987). Cell density and sex chromatin in lens epithelium of human cataracts. Quantitative studies in flat preparation. Ophthalmology *94*, 875-880.
Koretz, J. F., Kaufman, P. L., Neider, M. W., and Goeckner, P. A. (1989). Accommodation and presbyopia in the human eye--aging of the anterior segment. Vision Res *29*, 1685-1692.
Krag, S., and Andreassen, T. T. (2003a). Mechanical properties of the human lens capsule. Prog Retin Eye Res *22*, 749-767.
Krag, S., and Andreassen, T. T. (2003b). Mechanical properties of the human posterior lens capsule. Invest Ophthalmol Vis Sci *44*, 691-696.
Krag, S., Olsen, T., and Andreassen, T. T. (1997). Biomechanical characteristics of the human anterior lens capsule in relation to age. Invest Ophthalmol Vis Sci *38*, 357-363.
Kreuger, J., Jemth, P., Sanders-Lindberg, E., Eliahu, L., Ron, D., Basilico, C., Salmivirta, M., and Lindahl, U. (2005). Fibroblast growth factors share binding sites in heparan sulphate. Biochem J *389*, 145-150.
Krishna, M., and Narang, H. (2008). The complexity of mitogen-activated protein kinases (MAPKs) made simple. Cell Mol Life Sci *65*, 3525-3544.
Kumamoto, Y., Takamura, Y., Kubo, E., Tsuzuki, S., and Akagi, Y. (2007). Epithelial cell density in cataractous lenses of patients with diabetes: association with erythrocyte aldose reductase. Exp Eye Res *85*, 393-399.
Kurose, H., Bito, T., Adachi, T., Shimizu, M., Noji, S., and Ohuchi, H. (2004). Expression of Fibroblast growth factor 19 (Fgf19) during chicken embryogenesis and eye development, compared with Fgf15 expression in the mouse. Gene Expr Patterns *4*, 687-693.
Kuszak J.R., A.-g. K. J. a. C. M. J. (1998). Pathology of Age-Related Human Catarcts, (Philadelphia: Lippincott, Williams and Wilkins.).
Kuszak, J. R. (1997). A re-examination of primate lens epithelial cell size, density and structure as a function of development, growth and age. Nova Acta Leopoldina *75*, 45-66.
Kuszak, J. R., Novak, L. A., and Brown, H. G. (1995). An ultrastructural analysis of the epithelial-fiber interface (EFI) in primate lenses. Exp Eye Res *61*, 579-597.
Kuszak, J. R., Peterson, K. L., Sivak, J. G., and Herbert, K. L. (1994). The interrelationship of lens anatomy and optical quality. II. Primate lenses. Exp Eye Res *59*, 521-535.
Kuszak, J. R., and Rae, J. L. (1982). Scanning electron microscopy of the frog lens. Exp Eye Res *35*, 499-519.
Kuszak, J. R., Sivak, J. G., Herbert, K. L., Scheib, S., Garner, W., and Graff, G. (2000). The relationship between rabbit lens optical quality and sutural anatomy after vitrectomy. Exp Eye Res *71*, 267-281.
Kuszak, J. R., Zoltoski, R. K., and Sivertson, C. (2004a). Fibre cell organization in crystalline lenses. Exp Eye Res *78*, 673-687.
Kuszak, J. R., Zoltoski, R. K., and Tiedemann, C. E. (2004b). Development of lens sutures. Int J Dev Biol *48*, 889-902.
Kuwabara, T., and Imaizumi, M. (1974). Denucleation process of the lens. Invest Ophthalmol *13*, 973-981.

Kyriakis, J. M., and Avruch, J. (2001). Mammalian mitogen-activated protein kinase signal transduction pathways activated by stress and inflammation. Physiological reviews *81*, 807-869.
Ladage, P. M., Yamamoto, K., Li, L., Ren, D. H., Petroll, W. M., Jester, J. V., and Cavanagh, H. D. (2002). Corneal epithelial homeostasis following daily and overnight contact lens wear. Cont Lens Anterior Eye *25*, 11-21.
Lang, R., Lustig, M., Francois, F., Sellinger, M., and Plesken, H. (1994). Apoptosis during macrophage-dependent ocular tissue remodelling. Development *120*, 3395-3403.
Lang, R. A. (2004a). Pathways regulating lens induction in the mouse. Int J Dev Biol *48*, 783-791.
Lang, R. A., McAvoy, J.W (2004b). Growth factors in lens development. In: Lovicu, FJ, Robinson, ML (Eds), Development of the Ocular Lens Cambridge Univ Press, New York.
Latker, C. H., and Kuwabara, T. (1981). Regression of the tunica vasculosa lentis in the postnatal rat. Invest Ophthalmol Vis Sci *21*, 689-699.
Lavker, R. M., and Sun, T. T. (2003). Epithelial stem cells: the eye provides a vision. Eye (Lond) *17*, 937-942.
Lavoie, J. N., L'Allemain, G., Brunet, A., Muller, R., and Pouyssegur, J. (1996). Cyclin D1 expression is regulated positively by the p42/p44MAPK and negatively by the p38/HOGMAPK pathway. J Biol Chem *271*, 20608-20616.
Lee, C. J., Vroom, J. A., Fishman, H. A., and Bent, S. F. (2006). Determination of human lens capsule permeability and its feasibility as a replacement for Bruch's membrane. Biomaterials *27*, 1670-1678.
Lee, E. H., Wan, X. H., Song, J., Kang, J. J., Cho, J. W., Seo, K. Y., and Lee, J. H. (2002). Lens epithelial cell death and reduction of anti-apoptotic protein Bcl-2 in human anterior polar cataracts. Mol Vis *8*, 235-240.
Lenormand, P., Sardet, C., Pages, G., L'Allemain, G., Brunet, A., and Pouyssegur, J. (1993). Growth factors induce nuclear translocation of MAP kinases (p42mapk and p44mapk) but not of their activator MAP kinase kinase (p45mapkk) in fibroblasts. J Cell Biol *122*, 1079-1088.
Leonard, M., Zhang, L., Zhai, N., Cader, A., Chan, Y., Nowak, R. B., Fowler, V. M., and Menko, A. S. (2011). Modulation of N-cadherin junctions and their role as epicenters of differentiation-specific actin regulation in the developing lens. Dev Biol *349*, 363-377.
Li, L., and Xie, T. (2005). Stem cell niche: structure and function. Annu Rev Cell Dev Biol *21*, 605-631.
Li, W. C., Kuszak, J. R., Dunn, K., Wang, R. R., Ma, W., Wang, G. M., Spector, A., Leib, M., Cotliar, A. M., Weiss, M., and et al. (1995). Lens epithelial cell apoptosis appears to be a common cellular basis for non-congenital cataract development in humans and animals. J Cell Biol *130*, 169-181.
Li, Y., Corradetti, M. N., Inoki, K., and Guan, K. L. (2004). TSC2: filling the GAP in the mTOR signaling pathway. Trends Biochem Sci *29*, 32-38.
Liang, J., Zubovitz, J., Petrocelli, T., Kotchetkov, R., Connor, M. K., Han, K., Lee, J. H., Ciarallo, S., Catzavelos, C., Beniston, R.*, et al.* (2002). PKB/Akt phosphorylates p27, impairs nuclear import of p27 and opposes p27-mediated G1 arrest. Nat Med *8*, 1153-1160.
Liu, J., Chamberlain, C. G., and McAvoy, J. W. (1996). IGF enhancement of FGF-induced fibre differentiation and DNA synthesis in lens explants. Exp Eye Res *63*, 621-629.

Liu, X., Liu, Y., Zheng, J., Huang, Q., and Zheng, H. (2000). Lens epithelial cell proliferation and cell density in human age-related cataract. Yan Ke Xue Bao *16*, 184-188.
Liu, X., Zhang, M., Liu, Y., Challa, P., and Gonzalez, P. (2008). Proteomic analysis of regenerated rabbit lenses reveal crystallin expression characteristic of adult rabbits. Mol Vis *14*, 2404-2412.
Lois, N., Reid, B., Song, B., Zhao, M., Forrester, J., and McCaig, C. (2010). Electric currents and lens regeneration in the rat. Exp Eye Res *90*, 316-323.
Lovicu, F. J., Chamberlain, C. G., and McAvoy, J. W. (1995). Differential effects of aqueous and vitreous on fiber differentiation and extracellular matrix accumulation in lens epithelial explants. Invest Ophthalmol Vis Sci *36*, 1459-1469.
Lovicu, F. J., and McAvoy, J. W. (1993). Localization of acidic fibroblast growth factor, basic fibroblast growth factor, and heparan sulphate proteoglycan in rat lens: implications for lens polarity and growth patterns. Invest Ophthalmol Vis Sci *34*, 3355-3365.
Lovicu, F. J., and McAvoy, J. W. (2001). FGF-induced lens cell proliferation and differentiation is dependent on MAPK (ERK1/2) signalling. Development *128*, 5075-5084.
Lovicu, F. J., and McAvoy, J. W. (2005). Growth factor regulation of lens development. Dev Biol *280*, 1-14.
Lu, S., Zhao, C., Jiao, H., Kere, J., Tang, X., Zhao, F., Zhang, X., Zhao, K., and Larsson, C. (2007). Two Chinese families with pulverulent congenital cataracts and deltaG91 CRYBA1 mutations. Mol Vis *13*, 1154-1160.
Ma, X., Li, F. F., Wang, S. Z., Gao, C., Zhang, M., and Zhu, S. Q. (2008). A new mutation in BFSP2 (G1091A) causes autosomal dominant congenital lamellar cataracts. Mol Vis *14*, 1906-1911.
Maekawa, M., Yamamoto, T., Kohno, M., Takeichi, M., and Nishida, E. (2007). Requirement for ERK MAP kinase in mouse preimplantation development. Development *134*, 2751-2759.
Maidment, J. M., Duncan, G., Tamiya, S., Collison, D. J., Wang, L., and Wormstone, I. M. (2004). Regional differences in tyrosine kinase receptor signaling components determine differential growth patterns in the human lens. Invest Ophthalmol Vis Sci *45*, 1427-1435.
Makarenkova, H. P., Ito, M., Govindarajan, V., Faber, S. C., Sun, L., McMahon, G., Overbeek, P. A., and Lang, R. A. (2000). FGF10 is an inducer and Pax6 a competence factor for lacrimal gland development. Development *127*, 2563-2572.
Marcantonio, J. M., Rakic, J. M., Vrensen, G. F., and Duncan, G. (2000). Lens cell populations studied in human donor capsular bags with implanted intraocular lenses. Invest Ophthalmol Vis Sci *41*, 1130-1141.
Maruno, K. A., Lovicu, F. J., Chamberlain, C. G., and McAvoy, J. W. (2002). Apoptosis is a feature of TGF beta-induced cataract. Clinical & experimental optometry : journal of the Australian Optometrical Association *85*, 76-82.
Marzec, C. J., and Hendrix, R. W. (1997). A dynamic model for the morphogenesis of the late vertebrate lens. J Theor Biol *186*, 349-372.
McAvoy, J. W. (1978a). Cell division, cell elongation and distribution of alpha-, beta- and gamma-crystallins in the rat lens. J Embryol Exp Morphol *44*, 149-165.
McAvoy, J. W. (1978b). Cell division, cell elongation and the co-ordination of crystallin gene expression during lens morphogenesis in the rat. J Embryol Exp Morphol *45*, 271-281.

McAvoy, J. W. (1980a). Beta- and gamma-crystallin synthesis in rat lens epithelium explanted with neural retinal. Differentiation *17*, 85-91.
McAvoy, J. W. (1980b). Induction of the eye lens. Differentiation *17*, 137-149.
McAvoy, J. W. (1981). The spatial relationship between presumptive lens and optic vesicle/cup during early eye morphogenesis in the rat. Exp Eye Res *33*, 447-458.
McAvoy, J. W., and Chamberlain, C. G. (1989). Fibroblast growth factor (FGF) induces different responses in lens epithelial cells depending on its concentration. Development *107*, 221-228.
McAvoy, J. W., Chamberlain, C. G., de Iongh, R. U., Hales, A. M., and Lovicu, F. J. (1999). Lens development. Eye (Lond) *13 (Pt 3b)*, 425-437.
McCarty, C. A., and Taylor, H. R. (2002). A review of the epidemiologic evidence linking ultraviolet radiation and cataracts. Dev Ophthalmol *35*, 21-31.
McManus, E. J., and Alessi, D. R. (2002). TSC1-TSC2: a complex tale of PKB-mediated S6K regulation. Nat Cell Biol *4*, 214-216.
Meder, D., Shevchenko, A., Simons, K., and Fullekrug, J. (2005). Gp135/podocalyxin and NHERF-2 participate in the formation of a preapical domain during polarization of MDCK cells. J Cell Biol *168*, 303-313.
Menko, S., Philp, N., Veneziale, B., and Walker, J. (1998). Integrins and development: how might these receptors regulate differentiation of the lens. Ann N Y Acad Sci *842*, 36-41.
Messam, C. A., and Pittman, R. N. (1998). Asynchrony and commitment to die during apoptosis. Exp Cell Res *238*, 389-398.
Messina-Baas, O. M., Gonzalez-Huerta, L. M., and Cuevas-Covarrubias, S. A. (2006). Two affected siblings with nuclear cataract associated with a novel missense mutation in the CRYGD gene. Mol Vis *12*, 995-1000.
Michael, R., and Bron, A. J. (2011). The ageing lens and cataract: a model of normal and pathological ageing. Philos Trans R Soc Lond B Biol Sci *366*, 1278-1292.
Michael, R., Vrensen, G. F., van Marle, J., Gan, L., and Soderberg, P. G. (1998). Apoptosis in the rat lens after in vivo threshold dose ultraviolet irradiation. Invest Ophthalmol Vis Sci *39*, 2681-2687.
Middleton, C. A. (1977). The effects of cell-cell contact on the spreading of pigmented retina epithelial cells in culture. Exp Cell Res *109*, 349-359.
Mikulicich, A. G., and Young, R. W. (1963). Cell Proliferation and Displacement in the Lens Epithelium of Young Rats Injected with Tritiated Thymidine. Invest Ophthalmol *2*, 344-354.
Millodot, M. (1997). Dictionary of Optometry and Vision Science.: 4th Ed.. Oxford: Butterworth-Heinemann.).
Mitalipov, S., and Wolf, D. (2009). Totipotency, pluripotency and nuclear reprogramming. Adv Biochem Eng Biotechnol *114*, 185-199.
Mizukami, Y., Yoshioka, K., Morimoto, S., and Yoshida, K. (1997). A novel mechanism of JNK1 activation. Nuclear translocation and activation of JNK1 during ischemia and reperfusion. J Biol Chem *272*, 16657-16662.
Moffat, B. A., Landman, K. A., Truscott, R. J., Sweeney, M. H., and Pope, J. M. (1999). Age-related changes in the kinetics of water transport in normal human lenses. Exp Eye Res *69*, 663-669.
Moore, K. A., and Lemischka, I. R. (2006). Stem cells and their niches. Science *311*, 1880-1885.
Moritz, M., Braunfeld, M. B., Sedat, J. W., Alberts, B., and Agard, D. A. (1995). Microtubule nucleation by gamma-tubulin-containing rings in the centrosome. Nature *378*, 638-640.

Morooka, T., and Nishida, E. (1998). Requirement of p38 mitogen-activated protein kinase for neuronal differentiation in PC12 cells. J Biol Chem *273*, 24285-24288.
Muise-Helmericks, R. C., Grimes, H. L., Bellacosa, A., Malstrom, S. E., Tsichlis, P. N., and Rosen, N. (1998). Cyclin D expression is controlled post-transcriptionally via a phosphatidylinositol 3-kinase/Akt-dependent pathway. J Biol Chem *273*, 29864-29872.
Murphy, L. O., and Blenis, J. (2006). MAPK signal specificity: the right place at the right time. Trends Biochem Sci *31*, 268-275.
Murphy, L. O., Smith, S., Chen, R. H., Fingar, D. C., and Blenis, J. (2002). Molecular interpretation of ERK signal duration by immediate early gene products. Nat Cell Biol *4*, 556-564.
Musch, A. (2004). Microtubule organization and function in epithelial cells. Traffic *5*, 1-9.
Mutti, D. O., Zadnik, K., Fusaro, R. E., Friedman, N. E., Sholtz, R. I., and Adams, A. J. (1998). Optical and structural development of the crystalline lens in childhood. Invest Ophthalmol Vis Sci *39*, 120-133.
Myers, K., and Gilbert, N. (1968). Determination of age of wild rabbits in Australia. J Wildl Mgmt *32*, 841-849.
Nagata, S. (2005). DNA degradation in development and programmed cell death. Annu Rev Immunol *23*, 853-875.
Nakahara, M., Nagasaka, A., Koike, M., Uchida, K., Kawane, K., Uchiyama, Y., and Nagata, S. (2007). Degradation of nuclear DNA by DNase II-like acid DNase in cortical fiber cells of mouse eye lens. Febs J *274*, 3055-3064.
Negoescu, A., Guillermet, C., Lorimier, P., Brambilla, E., and Labat-Moleur, F. (1998). Importance of DNA fragmentation in apoptosis with regard to TUNEL specificity. Biomed Pharmacother *52*, 252-258.
Negoescu, A., Lorimier, P., Labat-Moleur, F., Drouet, C., Robert, C., Guillermet, C., Brambilla, C., and Brambilla, E. (1996). In situ apoptotic cell labeling by the TUNEL method: improvement and evaluation on cell preparations. J Histochem Cytochem *44*, 959-968.
Nejsum, L. N., and Nelson, W. J. (2009). Epithelial cell surface polarity: the early steps. Front Biosci *14*, 1088-1098.
Neumann, F. R., and Nurse, P. (2007). Nuclear size control in fission yeast. J Cell Biol *179*, 593-600.
Newitt, P., Boros, J., Madakashira, B. P., Robinson, M. L., Reneker, L. W., McAvoy, J. W., and Lovicu, F. J. (2010). Sef is a negative regulator of fiber cell differentiation in the ocular lens. Differentiation *80*, 53-67.
Newport, J. W., Wilson, K. L., and Dunphy, W. G. (1990). A lamin-independent pathway for nuclear envelope assembly. J Cell Biol *111*, 2247-2259.
Nigg, E. A. (2002). Centrosome aberrations: cause or consequence of cancer progression? Nat Rev Cancer *2*, 815-825.
Nishimoto, S., Kawane, K., Watanabe-Fukunaga, R., Fukuyama, H., Ohsawa, Y., Uchiyama, Y., Hashida, N., Ohguro, N., Tano, Y., Morimoto, T.*, et al.* (2003). Nuclear cataract caused by a lack of DNA degradation in the mouse eye lens. Nature *424*, 1071-1074.
Oakley, B. R. (1995). Cell biology. A nice ring to the centrosome. Nature *378*, 555-556.
Oharazawa, H., Ibaraki, N., Lin, L. R., and Reddy, V. N. (1999). The effects of extracellular matrix on cell attachment, proliferation and migration in a human lens epithelial cell line. Exp Eye Res *69*, 603-610.

Oharazawa, H., Ibaraki, N., Matsui, H., and Ohara, K. (2001). Age-related changes of human lens epithelial cells in vivo. Ophthalmic Res *33*, 363-366.
Oka, M., Toyoda, C., Kaneko, Y., Nakazawa, Y., Aizu-Yokota, E., and Takehana, M. (2010). Characterization and localization of side population cells in the lens. Mol Vis *16*, 945-953.
Ong, M. D., Payne, D. M., and Garner, M. H. (2003). Differential protein expression in lens epithelial whole-mounts and lens epithelial cell cultures. Exp Eye Res *77*, 35-49.
Osaki, M., Oshimura, M., and Ito, H. (2004). PI3K-Akt pathway: its functions and alterations in human cancer. Apoptosis *9*, 667-676.
Oshima, H., Rochat, A., Kedzia, C., Kobayashi, K., and Barrandon, Y. (2001). Morphogenesis and renewal of hair follicles from adult multipotent stem cells. Cell *104*, 233-245.
Palmade, F., Sechoy-Chambon, O., Coquelet, C., and Bonne, C. (1994). Insulin-like growth factor-1 (IGF-1) specifically binds to bovine lens epithelial cells and increases the number of fibronectin receptor sites. Curr Eye Res *13*, 531-537.
Parmigiani, C., and McAvoy, J. (1984). Localisation of laminin and fibronectin during rat lens morphogenesis. Differentiation *28*, 53-61.
Parmigiani, C. M., and McAvoy, J. W. (1989). A morphometric analysis of the development of the rat lens capsule. Curr Eye Res *8*, 1271-1277.
Parmigiani, C. M., and McAvoy, J. W. (1991). The roles of laminin and fibronectin in the development of the lens capsule. Curr Eye Res *10*, 501-511.
Pauli, S., Soker, T., Klopp, N., Illig, T., Engel, W., and Graw, J. (2007). Mutation analysis in a German family identified a new cataract-causing allele in the CRYBB2 gene. Mol Vis *13*, 962-967.
Pe'er, J., Muckarem, M., and Zajicek, G. (1996). Epithelial cell migration in the normal rat lens. Annals of anatomy *178*, 433-436.
Pedrigi, R. M., and Humphrey, J. D. (2011). Computational model of evolving lens capsule biomechanics following cataract-like surgery. Ann Biomed Eng *39*, 537-548.
Pei, X., Bao, Y., Chen, Y., and Li, X. (2008). Correlation of lens density measured using the Pentacam Scheimpflug system with the Lens Opacities Classification System III grading score and visual acuity in age-related nuclear cataract. Br J Ophthalmol *92*, 1471-1475.
Persons, B. J., and Modak, S. P. (1970). The pattern of DNA synthesis in the lens epithelium and the annular pad during development and growth of the chick lens. Exp Eye Res *9*, 144-151.
Pierscionek, B. K. (2005). Species variation in the refractive index of the eye lens and patterns of change with ageing. In: Ioseliani OR, ed. Focus on eye research.: New York: Nova science publishers Inc).
Pierscionek, B. K., and Augusteyn, R. C. (1992). Growth related changes to functional parameters in the bovine lens. Biochim Biophys Acta *1116*, 283-290.
Pierscionek, B. K., and Augusteyn, R. C. (1993). Species variability in optical parameters of the eye lens. Clin Exp Optom *76*, 22-25.
Pierscionek, B. K., and Chan, D. Y. (1989). Refractive index gradient of human lenses. Optom Vis Sci *66*, 822-829.
Pierscionek, B. K., Chan, D. Y., Ennis, J. P., Smith, G., and Augusteyn, R. C. (1988). Nondestructive method of constructing three-dimensional gradient index models for crystalline lenses: I. Theory and experiment. Am J Optom Physiol Opt *65*, 481-491.
Pirie, A. (1968). Color and solubility of the proteins of human cataracts. Invest Ophthalmol *7*, 634-650.

Pontoriero, G. F., Smith, A. N., Miller, L. A., Radice, G. L., West-Mays, J. A., and Lang, R. A. (2009). Co-operative roles for E-cadherin and N-cadherin during lens vesicle separation and lens epithelial cell survival. Dev Biol *326*, 403-417.
Praveen, M. R., Shah, G. D., Vasavada, A. R., Shah, A. R., Johar, K., Gami, Y., Diwan, R. P., and Shah, S. M. (2011). Posterior capsule opacification in eyes with steroid-induced cataracts: Comparison of early results. J Cataract Refract Surg *37*, 88-96.
Prescott, A. R., Webb, S. F., Rawlins, D., Shaw, P. J., and Warn, R. M. (1991). Microtubules rich in post-translationally modified alpha-tubulin form distinct arrays in frog lens epithelial cells. Exp Eye Res *52*, 743-753.
Priolo, S., Sivak, J. G., Kuszak, J. R., and Irving, E. L. (2000). Effects of experimentally induced ametropia on the morphology and optical quality of the avian crystalline lens. Invest Ophthalmol Vis Sci *41*, 3516-3522.
Qu, X., Hertzler, K., Pan, Y., Grobe, K., Robinson, M., and Zhang, X. (2011). Genetic epistasis between heparan sulfate and FGF-Ras signaling controls lens development. Dev Biol *355*, 12-20.
Quinlan, R. A., Sandilands, A., Procter, J. E., Prescott, A. R., Hutcheson, A. M., Dahm, R., Gribbon, C., Wallace, P., and Carter, J. M. (1999). The eye lens cytoskeleton. Eye (Lond) *13 (Pt 3b)*, 409-416.
Rabl, C. (1899). Uber den Bau und die entwicklung der linse. III. Die linse der sauetiere: ruckblick und schluss. Z Wiss Zool *67*, 1-138.
Rafferty, N. S. (1972). The cytoarchitecture of normal mouse lens epithelium. Anat Rec *173*, 225-228.
Rafferty, N. S. (1973). Experimental cataract and wound healing in mouse lens. Invest Ophthalmol *12*, 156-160.
Rafferty, N. S., and Rafferty, K. A., Jr. (1981a). Cell population kinetics of the mouse lens epithelium. J Cell Physiol *107*, 309-315.
Rafferty, N. S., and Rafferty, K. A., Jr. (1981b). Cell population kinetics of the mouse lens epithelium. Journal of cellular physiology *107*, 309-315.
Rafferty, N. S., and Smith, R. (1976). Analysis of cell population of normal and injured mouse lens epithelium. I: cell cycle, Vol 186).
Ramachandran, R. D., Perumalsamy, V., and Hejtmancik, J. F. (2007). Autosomal recessive juvenile onset cataract associated with mutation in BFSP1. Hum Genet *121*, 475-482.
Rampalli, A. M., and Zelenka, P. S. (1995). Insulin regulates expression of c-fos and c-jun and suppresses apoptosis of lens epithelial cells. Cell Growth Differ *6*, 945-953.
Rao, P. V., Huang, Q. L., Horwitz, J., and Zigler, J. S., Jr. (1995). Evidence that alpha-crystallin prevents non-specific protein aggregation in the intact eye lens. Biochim Biophys Acta *1245*, 439-447.
Ray, S., Gao, C., Wyatt, K., Fariss, R. N., Bundek, A., Zelenka, P., and Wistow, G. (2005). Platelet-derived growth factor D, tissue-specific expression in the eye, and a key role in control of lens epithelial cell proliferation. J Biol Chem *280*, 8494-8502.
Reddan, J. R., and Wilson-Dziedzic, D. (1983). Insulin growth factor and epidermal growth factor trigger mitosis in lenses cultured in a serum-free medium. Invest Ophthalmol Vis Sci *24*, 409-416.
Reneker L.W., O. P. A. (1996). Lens-specific expression of PDGF-A alters lens growth and development. . Dev Biol *180*, 554-565.
Richardson, J. C., and Simmons, N. L. (1979). Demonstration of protein asymmetries in the plasma membrane of cultured renal (MDCK) epithelial cells by lactoperoxidase-mediated iodination. FEBS Lett *105*, 201-204.

Richardson, N. A., Chamberlain, C. G., and McAvoy, J. W. (1993). IGF-1 enhancement of FGF-induced lens fiber differentiation in rats of different ages. Invest Ophthalmol Vis Sci *34*, 3303-3312.
Riese, D. J., 2nd, and Stern, D. F. (1998). Specificity within the EGF family/ErbB receptor family signaling network. Bioessays *20*, 41-48.
Riley, E. F., and Devi, S. K. (1967). Dynamics of cell populations in the rat lens epithelium. Exp Eye Res *6*, 383-392.
Robinson, M. L. (2006). An essential role for FGF receptor signaling in lens development. Semin Cell Dev Biol *17*, 726-740.
Roels, S., Tilmant, K., and Ducatelle, R. (1999). PCNA and Ki67 proliferation markers as criteria for prediction of clinical behaviour of melanocytic tumours in cats and dogs. J Comp Pathol *121*, 13-24.
Ron, D., Fuchs, Y., and Chorev, D. S. (2008). Know thy Sef: a novel class of feedback antagonists of receptor tyrosine kinase signaling. Int J Biochem Cell Biol *40*, 2040-2052.
Rosen, A. M., Denham, D. B., Fernandez, V., Borja, D., Ho, A., Manns, F., Parel, J. M., and Augusteyn, R. C. (2006). In vitro dimensions and curvatures of human lenses. Vision Res *46*, 1002-1009.
Rossi, M., Morita, H., Sormunen, R., Airenne, S., Kreivi, M., Wang, L., Fukai, N., Olsen, B. R., Tryggvason, K., and Soininen, R. (2003). Heparan sulfate chains of perlecan are indispensable in the lens capsule but not in the kidney. Embo J *22*, 236-245.
Roux, P. P., and Blenis, J. (2004). ERK and p38 MAPK-activated protein kinases: a family of protein kinases with diverse biological functions. Microbiology and molecular biology reviews : MMBR *68*, 320-344.
Rovasio, R. A., Delouvee, A., Yamada, K. M., Timpl, R., and Thiery, J. P. (1983). Neural crest cell migration: requirements for exogenous fibronectin and high cell density. J Cell Biol *96*, 462-473.
Sa, G., and Das, T. (1999). Basic fibroblast growth factor stimulates cytosolic phospholipase A2, phospholipase C-gamma1 and phospholipase D through distinguishable signaling mechanisms. Molecular and cellular biochemistry *198*, 19-30.
Sabanayagam, C., Wang, J. J., Mitchell, P., Tan, A. G., Tai, E. S., Aung, T., Saw, S. M., and Wong, T. Y. (2011). Metabolic syndrome components and age-related cataract: the singapore malay eye study. Invest Ophthalmol Vis Sci *52*, 2397-2404.
Saika, S., Shirai, K., Yamanaka, O., Miyazaki, K., Okada, Y., Kitano, A., Flanders, K. C., Kon, S., Uede, T., Kao, W. W.*, et al.* (2007). Loss of osteopontin perturbs the epithelial-mesenchymal transition in an injured mouse lens epithelium. Laboratory investigation; a journal of technical methods and pathology *87*, 130-138.
Saitoh, J., Nishi, O., and Hitani, H. (1990). Cell density and hexagonality of lens epithelium in human cataracts. Nippon Ganka Gakkai Zasshi *94*, 176-180.
Sanders, E. J., and Parker, E. (2002). The role of mitochondria, cytochrome c and caspase-9 in embryonic lens fibre cell denucleation. J Anat *201*, 121-135.
Sanders, E. J., and Parker, E. (2003). Retroviral overexpression of bcl-2 in the embryonic chick lens influences denucleation in differentiating lens fiber cells. Differentiation *71*, 425-433.
Sandilands, A., Prescott, A. R., Wegener, A., Zoltoski, R. K., Hutcheson, A. M., Masaki, S., Kuszak, J. R., and Quinlan, R. A. (2003). Knockout of the intermediate filament protein CP49 destabilises the lens fibre cell cytoskeleton and decreases lens optical quality, but does not induce cataract. Exp Eye Res *76*, 385-391.

Sandilands, A., Wang, X., Hutcheson, A. M., James, J., Prescott, A. R., Wegener, A., Pekny, M., Gong, X., and Quinlan, R. A. (2004). Bfsp2 mutation found in mouse 129 strains causes the loss of CP49' and induces vimentin-dependent changes in the lens fibre cell cytoskeleton. Exp Eye Res *78*, 875-889.
Sato, S., Fujita, N., and Tsuruo, T. (2004). Involvement of 3-phosphoinositide-dependent protein kinase-1 in the MEK/MAPK signal transduction pathway. J Biol Chem *279*, 33759-33767.
Scadden, D. T. (2006). The stem-cell niche as an entity of action. Nature *441*, 1075-1079.
Schaumberg, D. A., Dana, M. R., Christen, W. G., and Glynn, R. J. (1998). A systematic overview of the incidence of posterior capsule opacification. Ophthalmology *105*, 1213-1221.
Schmitt, E. A., and Dowling, J. E. (1994). Early eye morphogenesis in the zebrafish, Brachydanio rerio. J Comp Neurol *344*, 532-542.
Schook, P. (1980). Morphogenetic movements during the early development of the chick eye. An ultrastructural and spatial study. C. Obliteration of the lens stalk lumen and separation of the lens vesicle from the surface ectoderm. Acta Morphol Neerl Scand *18*, 195-201.
Schulz, M. W., Chamberlain, C. G., de Iongh, R. U., and McAvoy, J. W. (1993). Acidic and basic FGF in ocular media and lens: implications for lens polarity and growth patterns. Development *118*, 117-126.
Schulz, M. W., Chamberlain, C. G., and McAvoy, J. W. (1997). Binding of FGF-1 and FGF-2 to heparan sulphate proteoglycans of the mammalian lens capsule. Growth Factors *14*, 1-13.
Sekulic, A., Hudson, C. C., Homme, J. L., Yin, P., Otterness, D. M., Karnitz, L. M., and Abraham, R. T. (2000). A direct linkage between the phosphoinositide 3-kinase-AKT signaling pathway and the mammalian target of rapamycin in mitogen-stimulated and transformed cells. Cancer Res *60*, 3504-3513.
Servant, M. J., Giasson, E., and Meloche, S. (1996). Inhibition of growth factor-induced protein synthesis by a selective MEK inhibitor in aortic smooth muscle cells. J Biol Chem *271*, 16047-16052.
Sharma, K. K., and Santhoshkumar, P. (2009). Lens aging: effects of crystallins. Biochim Biophys Acta *1790*, 1095-1108.
Sharrocks, A. D. (2001). The ETS-domain transcription factor family. Nat Rev Mol Cell Biol *2*, 827-837.
Shin, K., Fogg, V. C., and Margolis, B. (2006). Tight junctions and cell polarity. Annu Rev Cell Dev Biol *22*, 207-235.
Shirke, S., Faber, S. C., Hallem, E., Makarenkova, H. P., Robinson, M. L., Overbeek, P. A., and Lang, R. A. (2001). Misexpression of IGF-I in the mouse lens expands the transitional zone and perturbs lens polarization. Mech Dev *101*, 167-174.
Shui, Y. B., and Beebe, D. C. (2008). Age-dependent control of lens growth by hypoxia. Invest Ophthalmol Vis Sci *49*, 1023-1029.
Siebinga, I., Vrensen, G. F., De Mul, F. F., and Greve, J. (1991). Age-related changes in local water and protein content of human eye lenses measured by Raman microspectroscopy. Exp Eye Res *53*, 233-239.
Simpsona, M. J., Landmanb, K. A., and Hughes, B. D. (2010). Cell invasion with proliferation mechanisms motivated by time-lapse data. Physica A: Statistical Mechanics and its Applications *389*, 3779-3790.
Slatter, D. H., Bradley, J. S., Vale, B., Constable, I. J., and Cullen, L. K. (1983). Hereditary cataracts in canaries. J Am Vet Med Assoc *183*, 872-874.

Smalley, K. S., Haass, N. K., Brafford, P. A., Lioni, M., Flaherty, K. T., and Herlyn, M. (2006). Multiple signaling pathways must be targeted to overcome drug resistance in cell lines derived from melanoma metastases. Mol Cancer Ther *5*, 1136-1144.
Smallwood, P. M., Munoz-Sanjuan, I., Tong, P., Macke, J. P., Hendry, S. H., Gilbert, D. J., Copeland, N. G., Jenkins, N. A., and Nathans, J. (1996). Fibroblast growth factor (FGF) homologous factors: new members of the FGF family implicated in nervous system development. Proc Natl Acad Sci U S A *93*, 9850-9857.
Smith, A. N., Radice, G., and Lang, R. A. (2010). Which FGF ligands are involved in lens induction? Dev Biol *337*, 195-198.
Snytnikova, O. A., Fursova, A., Chernyak, E. I., Vasiliev, V. G., Morozov, S. V., Kolosova, N. G., and Tsentalovich, Y. P. (2008). Deaminated UV filter 3-hydroxykynurenine O-beta-D-glucoside is found in cataractous human lenses. Exp Eye Res *86*, 951-956.
Soriano, P. (1997). The PDGF alpha receptor is required for neural crest cell development and for normal patterning of the somites. Development *124*, 2691-2700.
Soules, K. A., and Link, B. A. (2005). Morphogenesis of the anterior segment in the zebrafish eye. BMC Dev Biol *5*, 12-28.
Spalton, D. J. (1999). Posterior capsular opacification after cataract surgery. Eye (Lond) *13 (Pt 3b)*, 489-492.
Stemple, D. L., and Anderson, D. J. (1992). Isolation of a stem cell for neurons and glia from the mammalian neural crest. Cell *71*, 973-985.
Stolen, C. M., and Griep, A. E. (2000). Disruption of lens fiber cell differentiation and survival at multiple stages by region-specific expression of truncated FGF receptors. Dev Biol *217*, 205-220.
Strenk, S. A., Semmlow, J. L., Strenk, L. M., Munoz, P., Gronlund-Jacob, J., and DeMarco, J. K. (1999). Age-related changes in human ciliary muscle and lens: a magnetic resonance imaging study. Invest Ophthalmol Vis Sci *40*, 1162-1169.
Strenk, S. A., Strenk, L. M., and Guo, S. (2006). Magnetic resonance imaging of aging, accommodating, phakic, and pseudophakic ciliary muscle diameters. J Cataract Refract Surg *32*, 1792-1798.
Struck, H. G., Hammer, U., and Seydewitz, V. (1997). Effect of diabetes mellitus on anterior central lens epithelium in cataract patients. Ophthalmologe *94*, 327-331.
Sugiyama, Y., Akimoto, K., Robinson, M. L., Ohno, S., and Quinlan, R. A. (2009). A cell polarity protein aPKClambda is required for eye lens formation and growth. Dev Biol *336*, 246-256.
Sugiyama, Y., Prescott, A. R., Tholozan, F. M., Ohno, S., and Quinlan, R. A. (2008). Expression and localisation of apical junctional complex proteins in lens epithelial cells. Exp Eye Res *87*, 64-70.
Sukonpan, K., and Phupong, V. (2009). A biometric study of the fetal orbit and lens in normal pregnancies. J Clin Ultrasound *37*, 69-74.
Sun, S. C., Xiong, B., Lu, S. S., and Sun, Q. Y. (2008). MEK1/2 is a critical regulator of microtubule assembly and spindle organization during rat oocyte meiotic maturation. Mol Reprod Dev *75*, 1542-1548.
Sun, T. T., and Lavker, R. M. (2004). Corneal epithelial stem cells: past, present, and future. The journal of investigative dermatology Symposium proceedings / the Society for Investigative Dermatology, Inc [and] European Society for Dermatological Research *9*, 202-207.
Sun, T. T., Tseng, S. C., and Lavker, R. M. (2010). Location of corneal epithelial stem cells. Nature *463*, E10-11; discussion E11.

Suzuki, A., and Ohno, S. (2006). The PAR-aPKC system: lessons in polarity. J Cell Sci *119*, 979-987.
Sweeney, M. H., and Truscott, R. J. (1998). An impediment to glutathione diffusion in older normal human lenses: a possible precondition for nuclear cataract. Exp Eye Res *67*, 587-595.
Taipale, J., and Keski-Oja, J. (1997). Growth factors in the extracellular matrix. Faseb J *11*, 51-59.
Tait, J. F., Gibson, D., and Fujikawa, K. (1989). Phospholipid binding properties of human placental anticoagulant protein-I, a member of the lipocortin family. J Biol Chem *264*, 7944-7949.
Takamura, Y., Kubo, E., Tsuzuki, S., and Akagi, Y. (2003). Apoptotic cell death in the lens epithelium of rat sugar cataract. Exp Eye Res *77*, 51-57.
Takenaka, K., Moriguchi, T., and Nishida, E. (1998). Activation of the protein kinase p38 in the spindle assembly checkpoint and mitotic arrest. Science *280*, 599-602.
Tan, A. C., Loon, S. C., Choi, H., and Thean, L. (2008a). Lens Opacities Classification System III: cataract grading variability between junior and senior staff at a Singapore hospital. J Cataract Refract Surg *34*, 1948-1952.
Tan, J. S., Wang, J. J., and Mitchell, P. (2008b). Influence of diabetes and cardiovascular disease on the long-term incidence of cataract: the Blue Mountains eye study. Ophthalmic Epidemiol *15*, 317-327.
Tanaka, S., Sumioka, T., Fujita, N., Kitano, A., Okada, Y., Yamanaka, O., Flanders, K. C., Miyajima, M., and Saika, S. (2010). Suppression of injury-induced epithelial-mesenchymal transition in a mouse lens epithelium lacking tenascin-C. Mol Vis *16*, 1194-1205.
Tanaka, T., Saika, S., Ohnishi, Y., Ooshima, A., McAvoy, J. W., Liu, C. Y., Azhar, M., Doetschman, T., and Kao, W. W. (2004). Fibroblast growth factor 2: roles of regulation of lens cell proliferation and epithelial-mesenchymal transition in response to injury. Mol Vis *10*, 462-467.
Tardieu, A., Veretout, F., Krop, B., and Slingsby, C. (1992). Protein interactions in the calf eye lens: interactions between beta-crystallins are repulsive whereas in gamma-crystallins they are attractive. Eur Biophys J *21*, 1-12.
Taylor, G., Lehrer, M. S., Jensen, P. J., Sun, T. T., and Lavker, R. M. (2000). Involvement of follicular stem cells in forming not only the follicle but also the epidermis. Cell *102*, 451-461.
Taylor, H. R., West, S. K., Rosenthal, F. S., Munoz, B., Newland, H. S., Abbey, H., and Emmett, E. A. (1988). Effect of ultraviolet radiation on cataract formation. N Engl J Med *319*, 1429-1433.
Teska, W. R., and Pinder, J. E. (1986). Effects of nutrition on age determination using eye lens weights. Growth *50*, 362-370.
Tholozan, F. M., Gribbon, C., Li, Z., Goldberg, M. W., Prescott, A. R., McKie, N., and Quinlan, R. A. (2007). FGF-2 release from the lens capsule by MMP-2 maintains lens epithelial cell viability. Mol Biol Cell *18*, 4222-4231.
Thomas, L. A., and Yamada, K. M. (1992). Contact stimulation of cell migration. J Cell Sci *103 (Pt 4)*, 1211-1214.
Tkachov, S. I., Lautenschlager, C., Ehrich, D., and Struck, H. G. (2006). Changes in the lens epithelium with respect to cataractogenesis: light microscopic and Scheimpflug densitometric analysis of the cataractous and the clear lens of diabetics and non-diabetics. Graefes Arch Clin Exp Ophthalmol *244*, 596-602.

Tong, C., Fan, H. Y., Chen, D. Y., Song, X. F., Schatten, H., and Sun, Q. Y. (2003). Effects of MEK inhibitor U0126 on meiotic progression in mouse oocytes: microtuble organization, asymmetric division and metaphase II arrest. Cell Res *13*, 375-383.
Tripathi, R. C., Borisuth, N. S., Tripathi, B. J., and Fang, V. S. (1991). Analysis of human aqueous humor for epidermal growth factor. Exp Eye Res *53*, 407-409.
Troy TC, A. A., Turksen K. (2011). Re-Assessing K15 as an Epidermal Stem Cell Marker. Stem Cell Rev.
Truscott, R. J. (2005). Age-related nuclear cataract-oxidation is the key. Exp Eye Res *80*, 709-725.
Truscott, R. J., and Augusteyn, R. C. (1977). Changes in human lens proteins during nuclear cataract formation. Exp Eye Res *24*, 159-170.
Truscott, R. J., and Zhu, X. (2010). Presbyopia and cataract: a question of heat and time. Prog Retin Eye Res *29*, 487-499.
Tseng, H., Matsuzaki, K., and Lavker, R. M. (1999). Basonuclin in murine corneal and lens epithelia correlates with cellular maturation and proliferative ability. Differentiation *65*, 221-227.
Tseng, S. H., Yen, J. S., and Chien, H. L. (1994). Lens epithelium in senile cataract. J Formos Med Assoc *93*, 93-98.
Tsorbatzoglou, A., Nemeth, G., Szell, N., Biro, Z., and Berta, A. (2007). Anterior segment changes with age and during accommodation measured with partial coherence interferometry. J Cataract Refract Surg *33*, 1597-1601.
Tsujimura, A., Koikawa, Y., Salm, S., Takao, T., Coetzee, S., Moscatelli, D., Shapiro, E., Lepor, H., Sun, T. T., and Wilson, E. L. (2002). Proximal location of mouse prostate epithelial stem cells: a model of prostatic homeostasis. J Cell Biol *157*, 1257-1265.
Uga, S., Kohara, M., and Ishikawa, S. (1983). Morphological study of age-related changes in mouse lens. Jpn J Ophthalmol *27*, 157-165.
Uga, S., Obara, Y., Takehana, M., Nishigori, H., Hikida, M., and Mibu, H. (1996). Morphological study of age-related changes in Fischer rat lens. Jpn J Ophthalmol *40*, 33-41.
Ulloa-Montoya, F., Verfaillie, C. M., and Hu, W. S. (2005). Culture systems for pluripotent stem cells. J Biosci Bioeng *100*, 12-27.
Urfer, S. R., Greer, K., and Wolf, N. S. (2010). Age-related cataract in dogs: a biomarker for life span and its relation to body size. Age (Dordr), Epub ahead of print.
van der Flier, L. G., and Clevers, H. (2009). Stem cells, self-renewal, and differentiation in the intestinal epithelium. Annu Rev Physiol *71*, 241-260.
van Engeland, M., Nieland, L. J., Ramaekers, F. C., Schutte, B., and Reutelingsperger, C. P. (1998). Annexin V-affinity assay: a review on an apoptosis detection system based on phosphatidylserine exposure. Cytometry *31*, 1-9.
Varma, N. R., Janic, B., Ali, M. M., Iskander, A., and Arbab, A. S. (2011). Lentiviral Based Gene Transduction and Promoter Studies in Human Hematopoietic Stem Cells (hHSCs). J Stem Cells Regen Med *7*, 41-53.
Vasavada, A. R., Cherian, M., Yadav, S., and Rawal, U. M. (1991). Lens epithelial cell density and histomorphological study in cataractous lenses. J Cataract Refract Surg *17*, 798-804.
Vendra, V. P., and Balasubramanian, D. (2010). Structural and aggregation behavior of the human gammaD-crystallin mutant E107A, associated with congenital nuclear cataract. Mol Vis *16*, 2822-2828.
Verlhac, M. H., de Pennart, H., Maro, B., Cobb, M. H., and Clarke, H. J. (1993). MAP kinase becomes stably activated at metaphase and is associated with

microtubule-organizing centers during meiotic maturation of mouse oocytes. Dev Biol *158*, 330-340.
Verlhac, M. H., Kubiak, J. Z., Clarke, H. J., and Maro, B. (1994). Microtubule and chromatin behavior follow MAP kinase activity but not MPF activity during meiosis in mouse oocytes. Development *120*, 1017-1025.
Vermes, I., Haanen, C., Steffens-Nakken, H., and Reutelingsperger, C. (1995). A novel assay for apoptosis. Flow cytometric detection of phosphatidylserine expression on early apoptotic cells using fluorescein labelled Annexin V. J Immunol Methods *184*, 39-51.
Viglietto, G., Motti, M. L., Bruni, P., Melillo, R. M., D'Alessio, A., Califano, D., Vinci, F., Chiappetta, G., Tsichlis, P., Bellacosa, A.*, et al.* (2002). Cytoplasmic relocalization and inhibition of the cyclin-dependent kinase inhibitor p27(Kip1) by PKB/Akt-mediated phosphorylation in breast cancer. Nat Med *8*, 1136-1144.
Vogel-Hopker, A., Momose, T., Rohrer, H., Yasuda, K., Ishihara, L., and Rapaport, D. H. (2000). Multiple functions of fibroblast growth factor-8 (FGF-8) in chick eye development. Mech Dev *94*, 25-36.
Von Sallmann, L., Grimes, P., and Mc, E. N. (1962). Aspects of mitotic activity in relation to cell proliferation in the lens epithelium. Exp Eye Res *1*, 449-456.
Wade, R. H. (2009). On and around microtubules: an overview. Mol Biotechnol *43*, 177-191.
Wakida, N. M., Botvinick, E. L., Lin, J., and Berns, M. W. (2010). An intact centrosome is required for the maintenance of polarization during directional cell migration. PLoS One *5*, e15462.
Walker, J., and Menko, A. S. (2009). Integrins in lens development and disease. Exp Eye Res *88*, 216-225.
Wang, A. Z., Ojakian, G. K., and Nelson, W. J. (1990). Steps in the morphogenesis of a polarized epithelium. I. Uncoupling the roles of cell-cell and cell-substratum contact in establishing plasma membrane polarity in multicellular epithelial (MDCK) cysts. J Cell Sci *95 (Pt 1)*, 137-151.
Wang, J. J., Rochtchina, E., Tan, A. G., Cumming, R. G., Leeder, S. R., and Mitchell, P. (2009a). Use of inhaled and oral corticosteroids and the long-term risk of cataract. Ophthalmology *116*, 652-657.
Wang, K. J., Wang, B. B., Zhang, F., Zhao, Y., Ma, X., and Zhu, S. Q. (2011). Novel {beta}-Crystallin Gene Mutations in Chinese Families With Nuclear Cataracts. Arch Ophthalmol *129*, 337-343.
Wang, Q., McAvoy, J. W., and Lovicu, F. J. (2010). Growth factor signaling in vitreous humor-induced lens fiber differentiation. Invest Ophthalmol Vis Sci *51*, 3599-3610.
Wang, Q., Somwar, R., Bilan, P. J., Liu, Z., Jin, J., Woodgett, J. R., and Klip, A. (1999). Protein kinase B/Akt participates in GLUT4 translocation by insulin in L6 myoblasts. Mol Cell Biol *19*, 4008-4018.
Wang, Q., Stump, R., McAvoy, J. W., and Lovicu, F. J. (2009b). MAPK/ERK1/2 and PI3-kinase signalling pathways are required for vitreous-induced lens fibre cell differentiation. Exp Eye Res *88*, 293-306.
Wawersik, S., Purcell, P., Rauchman, M., Dudley, A. T., Robertson, E. J., and Maas, R. (1999). BMP7 acts in murine lens placode development. Dev Biol *207*, 176-188.
Weber, G. F., and Menko, A. S. (2006). Phosphatidylinositol 3-kinase is necessary for lens fiber cell differentiation and survival. Invest Ophthalmol Vis Sci *47*, 4490-4499.
Weeber, H. A., Eckert, G., Pechhold, W., and van der Heijde, R. G. (2007). Stiffness gradient in the crystalline lens. Graefes Arch Clin Exp Ophthalmol *245*, 1357-1366.

West, S., Munoz, B., Emmett, E. A., and Taylor, H. R. (1989). Cigarette smoking and risk of nuclear cataracts. Arch Ophthalmol *107*, 1166-1169.
Wheeler, S. H., and King, D. R. (1980). The use of eye-lens weights for aging wild rabbits, Oryctolagus cuniculus (L.), in Australia. Australian Wildlife Research *7*, 79-84.
Wiese, C., and Zheng, Y. (2006). Microtubule nucleation: gamma-tubulin and beyond. J Cell Sci *119*, 4143-4153.
Wiley, L. A., Shui, Y. B., and Beebe, D. C. (2010). Visualizing lens epithelial cell proliferation in whole lenses. Mol Vis *16*, 1253-1259.
Wilkinson, D. G., Bhatt, S., and McMahon, A. P. (1989). Expression pattern of the FGF-related proto-oncogene int-2 suggests multiple roles in fetal development. Development *105*, 131-136.
Williams, D. L., Heath, M. F., and Wallis, C. (2004). Prevalence of canine cataract: preliminary results of a cross-sectional study. Vet Ophthalmol *7*, 29-35.
Williams, S. E., Beronja, S., Pasolli, H. A., and Fuchs, E. (2011). Asymmetric cell divisions promote Notch-dependent epidermal differentiation. Nature *470*, 353-358.
Wilmarth, P. A., Tanner, S., Dasari, S., Nagalla, S. R., Riviere, M. A., Bafna, V., Pevzner, P. A., and David, L. L. (2006). Age-related changes in human crystallins determined from comparative analysis of post-translational modifications in young and aged lens: does deamidation contribute to crystallin insolubility? J Proteome Res *5*, 2554-2566.
Wolf, N., Penn, P., Pendergrass, W., Van Remmen, H., Bartke, A., Rabinovitch, P., and Martin, G. M. (2005). Age-related cataract progression in five mouse models for anti-oxidant protection or hormonal influence. Exp Eye Res *81*, 276-285.
Wolf, N. S., Li, Y., Pendergrass, W., Schmeider, C., and Turturro, A. (2000). Normal mouse and rat strains as models for age-related cataract and the effect of caloric restriction on its development. Exp Eye Res *70*, 683-692.
Wood, I. C., Mutti, D. O., and Zadnik, K. (1996). Crystalline lens parameters in infancy. Ophthalmic Physiol Opt *16*, 310-317.
Worgul, B. V., and Rothstein, H. (1975). Congenital cataracts associated with disorganized meridional rows in a new laboratory animal: the degu (Octodon degus). Biomedicine *23*, 1-4.
Worman, H. J., and Courvalin, J. C. (2005). Nuclear envelope, nuclear lamina, and inherited disease. Int Rev Cytol *246*, 231-279.
Wormstone, I. M., Del Rio-Tsonis, K., McMahon, G., Tamiya, S., Davies, P. D., Marcantonio, J. M., and Duncan, G. (2001). FGF: an autocrine regulator of human lens cell growth independent of added stimuli. Invest Ophthalmol Vis Sci *42*, 1305-1311.
Wormstone, I. M., Tamiya, S., Eldred, J. A., Lazaridis, K., Chantry, A., Reddan, J. R., Anderson, I., and Duncan, G. (2004). Characterisation of TGF-beta2 signalling and function in a human lens cell line. Exp Eye Res *78*, 705-714.
Wormstone, I. M., Tamiya, S., Marcantonio, J. M., and Reddan, J. R. (2000). Hepatocyte growth factor function and c-Met expression in human lens epithelial cells. Invest Ophthalmol Vis Sci *41*, 4216-4222.
Wormstone, I. M., Wang, L., and Liu, C. S. (2009). Posterior capsule opacification. Exp Eye Res *88*, 257-269.
Wride, M. A. (2011). Lens fibre cell differentiation and organelle loss: many paths lead to clarity. Philos Trans R Soc Lond B Biol Sci *366*, 1219-1233.

Wride, M. A., and Sanders, E. J. (1993). Expression of tumor necrosis factor-alpha (TNF alpha)-cross-reactive proteins during early chick embryo development. Dev Dyn *198*, 225-239.
Wride, M. A., and Sanders, E. J. (1998). Nuclear degeneration in the developing lens and its regulation by TNFalpha. Exp Eye Res *66*, 371-383.
Xie, L., Overbeek, P. A., and Reneker, L. W. (2006). Ras signaling is essential for lens cell proliferation and lens growth during development. Dev Biol *298*, 403-414.
Xiong, W., Cheng, B. H., Jia, S. B., and Tang, L. S. (2010). Involvement of the PI3K/Akt signaling pathway in platelet-derived growth factor-induced migration of human lens epithelial cells. Curr Eye Res *35*, 389-401.
Yamamoto, N., Majima, K., and Marunouchi, T. (2008a). A study of the proliferating activity in lens epithelium and the identification of tissue-type stem cells. Med Mol Morphol *41*, 83-91.
Yamamoto, N., Majima, K., and Marunouchi, T. (2008b). A study of the proliferating activity in lens epithelium and the identification of tissue-type stem cells. Medical molecular morphology *41*, 83-91.
Yang, L., Guan, T., and Gerace, L. (1997). Lamin-binding fragment of LAP2 inhibits increase in nuclear volume during the cell cycle and progression into S phase. J Cell Biol *139*, 1077-1087.
Yeaman, C., Grindstaff, K. K., and Nelson, W. J. (1999). New perspectives on mechanisms involved in generating epithelial cell polarity. Physiol Rev *79*, 73-98.
York, R. D., Yao, H., Dillon, T., Ellig, C. L., Eckert, S. P., McCleskey, E. W., and Stork, P. J. (1998). Rap1 mediates sustained MAP kinase activation induced by nerve growth factor. Nature *392*, 622-626.
Young, H. M., Bergner, A. J., Anderson, R. B., Enomoto, H., Milbrandt, J., Newgreen, D. F., and Whitington, P. M. (2004). Dynamics of neural crest-derived cell migration in the embryonic mouse gut. Dev Biol *270*, 455-473.
Young, R. W., and Ocumpaugh, D. E. (1966). Autoradiographic studies on the growth and development of the lens capsule in the rat. Invest Ophthalmol *5*, 583-589.
Yu, L. Z., Xiong, B., Gao, W. X., Wang, C. M., Zhong, Z. S., Huo, L. J., Wang, Q., Hou, Y., Liu, K., Liu, X. J.*, et al.* (2007). MEK1/2 regulates microtubule organization, spindle pole tethering and asymmetric division during mouse oocyte meiotic maturation. Cell Cycle *6*, 330-338.
Zampighi, G. A., Eskandari, S., and Kreman, M. (2000). Epithelial organization of the mammalian lens. Exp Eye Res *71*, 415-435.
Zatechka, S. D., and Lou, M. F. (2002). Studies of the mitogen-activated protein kinases and phosphatidylinositol-3 kinase in the lens. 2. The intercommunications. Exp Eye Res *75*, 177-192.
Zehorai, E., Yao, Z., Plotnikov, A., and Seger, R. (2010). The subcellular localization of MEK and ERK--a novel nuclear translocation signal (NTS) paves a way to the nucleus. Mol Cell Endocrinol *314*, 213-220.
Zhang, L., Gao, L., Li, Z., Qin, W., Gao, W., Cui, X., Feng, G., Fu, S., He, L., and Liu, P. (2006). Progressive sutural cataract associated with a BFSP2 mutation in a Chinese family. Mol Vis *12*, 1626-1631.
Zhang, Q., Guo, X., Xiao, X., Yi, J., Jia, X., and Hejtmancik, J. F. (2004). Clinical description and genome wide linkage study of Y-sutural cataract and myopia in a Chinese family. Mol Vis *10*, 890-900.
Zhao, J., Mo, V., and Nagasaki, T. (2009). Distribution of label-retaining cells in the limbal epithelium of a mouse eye. J Histochem Cytochem *57*, 177-185.

Zhao , J. R., D.M. Ornitz, D.C. Beebe and M.L. Robinson (2003). Different FGFR genes play an essential but redundant role in post-induction lens development. nvest Ophthalmol Visual Sci, Suppl *44*, 954.
Zhao, S., Hung, F. C., Colvin, J. S., White, A., Dai, W., Lovicu, F. J., Ornitz, D. M., and Overbeek, P. A. (2001). Patterning the optic neuroepithelium by FGF signaling and Ras activation. Development *128*, 5051-5060.
Zheng, Y., Wong, M. L., Alberts, B., and Mitchison, T. (1995). Nucleation of microtubule assembly by a gamma-tubulin-containing ring complex. Nature *378*, 578-583.
Zhou, M., Leiberman, J., Xu, J., and Lavker, R. M. (2006). A hierarchy of proliferative cells exists in mouse lens epithelium: implications for lens maintenance. Invest Ophthalmol Vis Sci *47*, 2997-3003.
Zhu, Y., Shentu, X., Wang, W., Li, J., Jin, C., and Yao, K. (2010). A Chinese family with progressive childhood cataracts and IVS3+1G>A CRYBA3/A1 mutations. Mol Vis *16*, 2347-2353.
Zwaan, J., and Kenyon, R. E., Jr. (1984). Cell replication and terminal differentiation in the embryonic chicken lens: normal and forced initiation of lens fibre formation. J Embryol Exp Morphol *84*, 331-349.